Computer Sciences Corporation

CSC/TM-88/6060

Advanced Tracking Systems Design and Analysis

CSC

Prepared for

National Aeronautics and Space Administration
Goddard Space Flight Center
Greenbelt, Maryland

Under

Contract NAS 5-31500
Task Assignment 39 101

September 1989

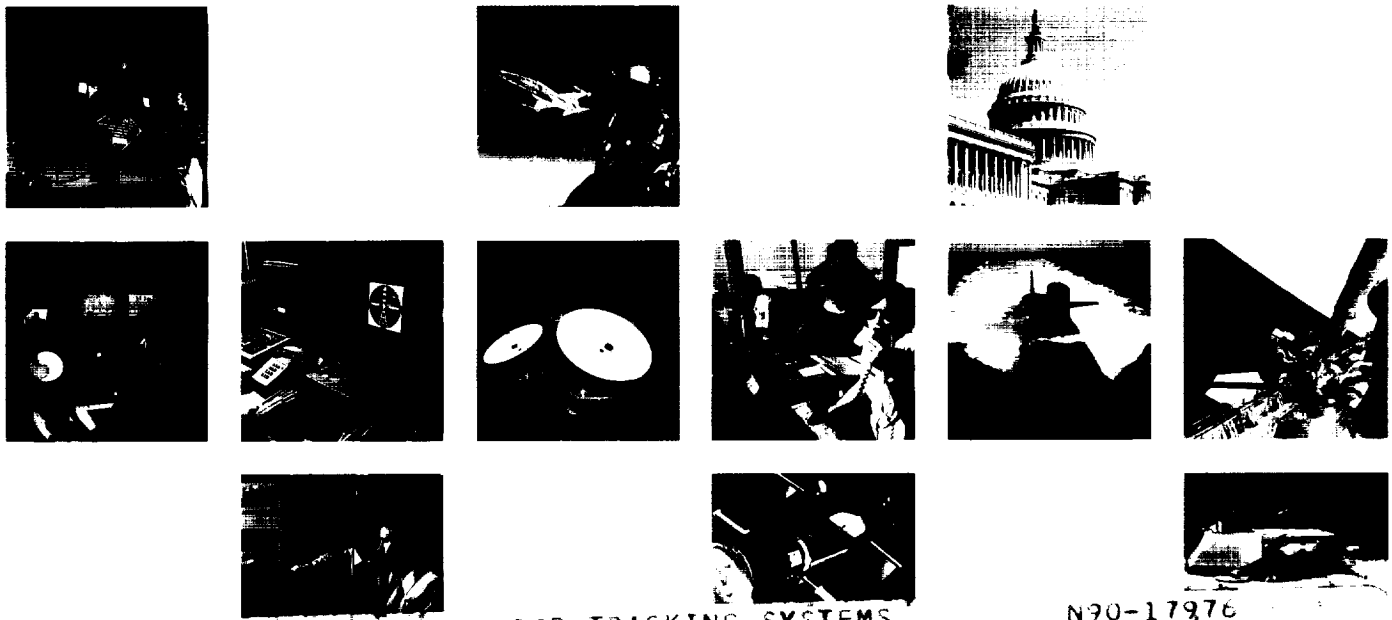

ADVANCED TRACKING SYSTEMS DESIGN AND ANALYSIS

Prepared for

GODDARD SPACE FLIGHT CENTER

By

Computer Sciences Corporation
EG&G Washington Analytical Services Center, Inc.
Interferometrics, Inc.
Stanford Telecommunications, Inc.

Under

Contract NAS 5-31500
Task Assignment 39 101

Prepared by:

R. Potash 9/26/89
(Interferometrics) Date
L. Floyd (Interferometrics)

for A. Jacobsen (STel) Date
K. Cunningham (STel)
A. Kapoor (STel)
C. Kwadrat (STel)
J. Radel (STel)
J. McCarthy (EG&G)

Approved by:

A. Long 9/24/89
Date
Senior Systems Designer

S. Liu 9/26/89
Date
Technical Manager

ABSTRACT

This report summarizes the results of an assessment of several types of high-accuracy tracking systems proposed to track the spacecraft in the National Aeronautics and Space Administration (NASA) Advanced Tracking and Data Relay Satellite System (ATDRSS). Tracking systems based on the use of interferometry and ranging are investigated. For each system, the top-level system design and operations concept are provided. A comparative system assessment is presented in terms of orbit determination performance, ATDRSS impacts, life-cycle cost, and technological risk.

TABLE OF CONTENTS

TABLE OF CONTENTS (Cont'd)

TABLE OF CONTENTS (Cont'd)

TABLE OF CONTENTS (Cont'd)

LIST OF ILLUSTRATIONS

LIST OF ILLUSTRATIONS Cont'd)

Figure

LIST OF TABLES

LIST OF TABLES (Cont'd)

SECTION 1 - INTRODUCTION AND ASSESSMENT SUMMARY

The National Aeronautics and Space Administration (NASA) Advanced Tracking and Data Relay Satellite System (ATDRSS) will be deployed after 1998 as a successor to the existing Tracking and Data Relay Satellite System (TDRSS). ATDRSS will provide greatly enhanced data relay and tracking services to user spacecraft. Current ATDRSS design activities include reevaluation and redesign of TDRSS components. As part of this activity, alternative modes for relay satellite tracking are being considered.

Currently, the Bilateration Ranging Transponder System (BRTS) is used to track the Tracking and Data Relay Satellite (TDRS) with estimated orbit accuracies of about 150 meters (m) [three standard deviations (3-σ) maximum uncertainty over the definitive period]. Because the tracking of user satellites is performed using a two-way link via TDRS, the ultimate accuracy for user orbits is limited by the quality of the BRTS-derived trajectories. For some planned NASA missions, orbital accuracies of 75 m (3-σ) are needed for the Advanced Tracking and Data Relay Satellite (ATDRS). Furthermore, BRTS is undesirable because it uses a network of ground transponder stations located outside the United States and relies on the TDRS user service antennas, thereby consuming data relay services when TDRS tracking is performed.

1.1 PURPOSE AND SCOPE

This report presents a comparative assessment of high-accuracy tracking systems for the ATDRSS satellites. Four principal alternatives to BRTS tracking are evaluated for ATDRSS: a Ku-band ranging system, variants of interferometric tracking systems, tracking systems that employ the Global Positioning System (GPS), and tracking systems that employ the Precise Ranging and Timing System (PRTS) concept. The specifications for these systems are presented in sufficient detail to characterize their properties. Orbit determination (OD) performance is evaluated using covariance analysis techniques and compared with BRTS tracking. A preliminary life-cycle cost estimate is developed for each system based on current system design and operations concepts. An assessment of these systems is provided based on the criteria identified in Section 1.3.

1.2 ATDRSS TRACKING GOALS

For this study, the following goals are defined for proposed ATDRSS tracking systems:

1. A steady-state OD accuracy of better than 75-m (3-σ) maximum uncertainty over a definitive period of 30 hours under normal conditions for all assigned ATDRS orbit locations

2. Rapid recovery of the ATDRS trajectories after maneuvers, with a steady-state performance with 2 hours of tracking data

3. All ground stations confined to the continental United States (CONUS)

4. Minimized impact on ATDRSS service functions and nontracking operations

5. Calibrated data available from tracking systems suitable for orbit analysis in near real time, with minimal personnel during normal operations

6. Minimized 10-year life-cycle cost

1.3 ASSESSMENT CRITERIA

In this comparative assessment study, each proposed ATDRSS tracking system is evaluated based on the following criteria, derived from the ATDRSS tracking goals listed in Section 1.2:

1. ATDRS Positioning Performance

- OD definitive performance criteria consist of a total position accuracy of no worse than 75 m (3 σ) during 30 hours of tracking determined at the end of that interval

- OD predictive performance criteria consist of a total position accuracy of no worse than 75 m (3 σ) during the 72 hours of prediction starting from 30 hours of previous tracking

- TR definitive performance criteria consist of a total position accuracy of no worse than 75 m (3 σ) during 2 hours of tracking determined at the end of that interval

- TR predictive performance criteria consist of a total position accuracy of no worse than 75 m (3 σ) during the 24 hours of prediction starting from 2 hours of previous tracking

- Observation staleness [defined as the processing delay between the epoch of an observation and its availability for orbit analysis at Goddard Space Flight Center (GSFC), fully calibrated)]

2. ATDRSS impacts--Weight, volume, and power requirements of any necessary spacecraft-borne payloads; signal generation and power requirements of the ground stations and their deployment inside or outside CONUS; and operational scheduling requirements

3. Cost and staffing needs--Staffing requirements of the ground stations and 10-year life-cycle cost (estimated initial development and capital costs together with projected operational and maintenance costs over a 10-year interval)

4. Technology risks--Novel hardware elements or improved capabilities required in the ground station or spacecraft equipment; new processing algorithms; untested calibration techniques; and sensitivity of the estimated tracking uncertainties to the assumed values of error sources

5. External dependencies--Reliance on other systems or facilities (e.g., data transfer requirements)

1.4 DOCUMENT ORGANIZATION

The remainder of Section 1 of this document is a summary of the assessment results presented in Sections 3 through 7 of this report. Section 2 discusses key assessment assumptions related to the ATDRSS architecture and OD error models. Sections 3, 4, 5, and 6 present high-level descriptions and assessments of the ATDRS Ku-Band Ranging System (AKuRS), PRTS and Modified PRTS (MPRTS), interferometric tracking systems based on either very long baseline interferometry (VLBI) or connected element interferometry (CEI), and the Global Positioning System (GPS), respectively. Section 7 provides a comparative assessment of each of these systems with respect to the assessment criteria defined in Section 1.3.

Appendix A contains a detailed description of the error models and OD error analysis studies performed in support of this study. Appendix B to this document provides a detailed description of the interferometric tracking systems and associated life-cycle costs summarized in Section 5. Appendix C provides a derivation of the noise levels associated with the PRTS, MPRTS, and AKuRs measurements. Appendix D provides life-cycle cost results for the ATDRS/GPS tracking system. References 1-1 through 1-5 provide the detailed descriptions and life-cycle cost results for the PRTS baseline system and a modification thereof (MPRTS), respectively, summarized in Section 4. Appendix E provides updates to these results.

1.5 ASSESSMENT SUMMARY

This section summarizes the results of the analyses presented in Sections 3 through 7 of this report. Each tracking system is briefly described and assessed in terms of the criteria presented in Section 1.3.

1.5.1 TRACKING SYSTEMS

This study addresses four alternative ATDRS tracking concepts: (1) a Ku-band ranging system similar to BRTS, (2) ATDRSS beacon-based ranging systems employing the PRTS signal structure, (3) VLBI and CEI interferometric tracking systems, and (4) GPS-based tracking systems. Table 1-1 summarizes the major characteristics of the specific tracking systems studied. Each of the tracking concepts and the associated tracking systems is briefly discussed in the following subsections.

1.5.1.1 AKuRS

AKuRS relies on observation of a Ku-band navigation beacon designed to support one-way navigation by ATDRSS users. Tracking of the ATDRSS satellites is accomplished by a network of ground stations that observe the Ku-band beacon and generate coherent return signals for transmission back to the ATDRSS Ground Terminal (AGT). Three ground tracking network configurations are evaluated: (1) a CONUS-based network, (2) an intermediate-baseline network that has two non-CONUS locations--Reykjavik, Iceland (REY), and Hawaii (HAW), and (3) a long-baseline network that has three non-CONUS locations--Ascension Island (ACN), Guam (GWM) and American Samoa (AMS).

TRACKING SYSTEM	TRACKING CONFIGURATIONS	TRACKING MEASUREMENTS	TRACKING SIGNAL	ATDRSS SERVICES
BRTS	MASTER STATION: WSGT BRTS: AUSTRALIA (AUS), ACN	TWO-WAY RANGE, TWO-WAY RANGE-RATE	S-BAND	TWO-WAY TRACKING SERVICE
AKuRS	(1) CONUS BASELINE (2) INTERMEDIATE BASELINE (3) LONG BASELINE	TWO-WAY RANGE, TWO-WAY,RANGE-RATE	Ku-BAND BEACON	Ku-BAND BEACON, DEDICATED Ku-BAND RETURN CHANNEL
PRTS	(1) CONUS BASELINE (2) INTERMEDIATE BASELINE (3) LONG BASELINE	ONE-WAY PSEUDORANGE, ONE WAY PSEUDORANGE-RATE (OPTIONAL)	S-BAND BEACON WITH PRTS SIGNAL STRUCTURE	S-BAND PRTS BEACON, RETURN CHANNEL
MPRTS	(1) CONUS BASELINE (2) INTERMEDIATE BASELINE (3) LONG BASELINE	TWO-WAY RANGE, TWO-WAY RANGE-RATE	S-BAND BEACON WITH PRTS SIGNAL STRUCTURE	S-BAND PRTS BEACON, RETURN CHANNEL
VLBI-Q	CONUS-BASED THREE-STATION NETWORK	VLBI RANGE DIFFERENCE, GT RANGE (OPTIONAL)	Ku-BAND SGL QUASAR SIGNALS	NONE
CEI-Q	THREE CONUS-BASED THREE-STATION NETWORKS	CEI RANGE DIFFERENCE, GT RANGE (OPTIONAL)	Ku-BAND SGL QUASAR SIGNALS	NONE
VLBI-2S	CONUS-BASED THREE-STATION NETWORK	VLBI RANGE DIFFERENCE GT RANGE (OPTIONAL)	Ku-BAND SGL, Ku-BAND SATELLITE SIGNAL	NONE

2055B(3)-19

Table 1-1. ATDRS Tracking System Characteristics (1 of 3)

TRACKING SYSTEM	TRACKING CONFIGURATIONS	TRACKING MEASUREMENTS	TRACKING SIGNAL	ATDRSS SERVICES
VLBI-3S	CONUS-BASED FOUR-STATION NETWORK (FOR THREE ATDRSs)	VLBI RANGE DIFFERENCE	Ku-BAND SGL FOR THREE ATDRSs	NONE
VLBI-Ku	CONUS-BASED THREE-STATION NETWORK	VLBI RANGE DIFFERENCE	Ku-BAND BEACON FROM TWO ATDRSs	Ku-BAND BEACON
VLBI-GT	CONUS-BASED THREE-STATION NETWORK	VLBI RANGE DIFFERENCE	Ku-BAND SGL GPS SIGNAL USED FOR TIME TRANSFER	NONE
VLBI-GC	CONUS-BASED THREE-STATION NETWORK	VLBI RANGE DIFFERENCE GPS ONE-WAY PSEUDORANGE DIFFERENCE	Ku-BAND SGL FOR TWO ATDRSs DECODED GPS SIGNAL	NONE
VLBI-GH	CONUS-BASED THREE-STATION NETWORK	RANGE DIFFERENCE FOR ATDRS AND GPS	Ku-BAND SGL FOR TWO ATDRSs GPS SIGNAL	NONE
GPS-D	GPS 24-SATELLITE CONSTELLATION MASTER STATION: WSGT	ONE-WAY PSEUDORANGE AND ONE-WAY PSEUDORANGE-RATE TO ATDRS	GPS SIGNALS	ONBOARD GPS RECEIVER
GPS-PD	GPS 24-SATELLITE CONSTELLATION MASTER STATION: WSGT TWO REMOTE STATIONS	SIMULTANEOUS GPS ONE-WAY PSEUDORANGE AND ATDRS ONE-WAY PSEUDO- RANGE PROVIDES DOUBLE DIFFERENTIAL MEASUREMENTS	GPS SIGNALS AND S-BAND OR Ku-BAND ATDRS BEACON	S-BAND OR Ku-BAND BEACON

2055B(3)-20

Table 1-1. ATDRS Tracking System Characteristics (2 of 3)

TRACKING SYSTEM	TRACKING CONFIGURATIONS	TRACKING MEASUREMENTS	TRACKING SIGNAL	ATDRSS SERVICES
GPS-DD	GPS 24-SATELLITE CONSTELLATION MASTER STATION: WSGT TWO REMOTE STATIONS	SIMULTANEOUS GPS ONE-WAY PSEUDORANGE TO ATDRS AND REMOTE STATIONS PROVIDES DOUBLE DIFFERENTIAL MEASUREMENTS	GPS SIGNALS	ONBOARD GPS RECEIVER

2055B(3)-21

Table 1-1. ATDRS Tracking System Characteristics (3 of 3)

Two-way range and range-rate measurements are extracted by the AGT from these signals for use in ATDRS OD. The concept is similar to BRTS; however, whereas BRTS requires scheduled two-way S-band service, Ku-band ATDRS tracking is supported by a continuously available beacon and a Ku-band dedicated return channel to avoid burdening ATDRS Ku-band single access (KSA) services. Moreover, Ku-band operation significantly diminishes the effect of ionospheric delays, thereby improving ATDRS OD performance relative to that provided by comparable S-band BRTS networks.

1.5.1.2 Precise Ranging and Timing Systems

PRTS comprises a continuously available S-band navigation beacon transmitted by each ATDRS and a network of ground tracking stations capable of making one-way pseudorange and pseudorange-rate measurements of the PRTS beacon. Periodic return ATDRSS communications from the PRTS ground stations are required for network synchronization and relay of the tracking measurements. The PRTS beacon signal structure and signal processing combine aspects of both PN and tone ranging to allow precise one-way range measurements and calibration of ionospheric and group delays. Observation of the PRTS beacon emitted by the ATDRSS satellites would support both ATDRSS OD and one-way forward navigation by ATDRSS users.

MPRTS is similar to baseline PRTS except that, for ATDRSS OD, the ground stations coherently turn around a component of the PRTS beacon signal structure to allow measurement of two-way range and range-rate at the AGT. The MPRTS ground stations, thus, transmit a return signal back to the AGT that is generated coherent in carrier phase and PN epoch with the received PRTS beacon signal. The full PRTS beacon signal structure is used by the MPRTS ground stations to measure the signal path delay due to the ionosphere; then these measurements are sent to the AGT as data on the return signal. MPRTS thereby provides a means to obtain two-way range and range-rate measurements at S-band while allowing correction of the ionospheric delay contributions. Two-way range and range-rate measurements imply that the measurements are made solely with respect to the AGT clock; system clock biases, therefore, do not contribute to the OD error. Like PRTS, MPRTS offers ATDRSS users an option for enhanced one-way navigation through precise tracking of the PRTS beacon signal.

Three ground tracking networks are evaluated for PRTS and MPRTS: (1) a CONUS-based network; (2) an intermediate baseline network that has 2 non-CONUS locations--ACN and

HAW; and (3) a long-baseline network that has 4 non-CONUS locations--ACN, REY, GWM, and AMS.

1.5.1.3 Interferometric Systems

Three distinct interferometric systems were evaluated. Each is described briefly in the following.

The quasar-calibrated very long baseline interferometry (VLBI-Q) system consists of a CONUS-based VLBI-Q tracking network that can observe signals from quasars and track ATDRS using the Ku-band space-to-ground link (SGL). By using observations of quasars lying near ATDRS in the sky, the VLBI-Q quasar system is able to reduce or eliminate clock calibration errors.

The quasar-calibrated connected element interferometry (CEI-Q) system consists of several receivers able to perform interferometric measurements on ATDRS in a manner similar to the VLBI-Q systems, except that the CEI-Q receivers are separated by relatively short baselines and are connected by cables. The direct connections between the elements essentially eliminate the clock errors of the VLBI-Q systems. One CONUS-based CEI-Q network is needed to support each ATDRS.

The two-satellite VLBI (VLBI-2S) system is a VBLI network that uses a second geostationary satellite (possibly another ATDRS satellite) positioned midway between the east ATDRS (ATDRS-E) and west ATDRS (ATDRS-W) satellites. The purpose of this second satellite is determination of the clock synchronization. The VLBI-2S system will track the two satellites and solve for the orbits of both satellites and for the clock corrections simultaneously. The three-satellite VLBI (VLBI-3S) system is an extension of the VLBI-2S system to track three ATDRS satellites and solve for the orbits of all three satellites and the clock correction simultaneously. The Ku-band beacon VLBI (VLBI-Ku) system is similar to VLBI-2S except that a Ku-band beacon on each ATDRS satellite is observed by a set of three ground stations.

Three interferometric systems were studied that make use of GPS. The GPS time transfer calibrated VLBI (VLBI-GT) system uses GPS for time synchronization of the ground stations. The coded GPS calibrated VLBI (VLBI-GC) system combines VLBI-2S measurements with GPS range difference measurements derived from the decoded GPS signal. The hybrid GPS calibrated VLBI (VLBI-GH) system combines VLBI-2S measurements with interferometric tracking of the GPS broadcast signal.

Each of these systems can be supplemented with ground terminal (GT) ranging data to improve OD performance over short tracking arcs.

1.5.1.4 GPS-Based Systems

Three GPS-based tracking systems were evaluated for ATDRS tracking. The direct ATDRS/GPS tracking system (GPS-D) uses a GPS receiver onboard the ATDRS satellite to measure pseudorange and pseudorange-rate from the broadcast GPS signal. These measurements are relayed to the master station for orbit determination processing. The passive differential ATDRS/GPS tracking system (GPS-PD) uses the differences between simultaneous ATDRS beacon pseudorange and GPS beacon pseudorange measurements obtained at the master station and two remote stations. The direct differential ATDRS/GPS tracking system (GPS-DD) uses the differences between simultaneous GPS beacon pseudorange measurements obtained onboard ATDRS with measurements obtained at the master station and two remote stations.

1.5.2 ASSESSMENT CONCLUSIONS

Each of the tracking systems described in Section 1.5.1 was evaluated against the criteria defined in Section 1.3. Assessments given here are described in more detail in Chapter 7. The overall assessment is presented in Table 1-2. A brief summary of the findings follows.

1. ATDRS Position Accuracy--The positioning accuracy goal is to provide orbit accuracies of 75 m (3 σ) for both nominal OD and TR scenarios. The nominal OD scenario consists of 30 hours of tracking and up to 3 days of prediction, whereas TR consists of 2 hours of tracking and up to 1 day of prediction. These scenarios were chosen to be representative of expected ATDRSS operational satellite tracking requirements.

Among the non-CONUS-based ranging systems, the AKuRS system showed the best performance, meeting all positioning goals. The non-CONUS PRTS and MPRTS systems fail to meet the goals only for the predictive period in the OD scenario. The CONUS-based ranging systems do not come close to meeting the goals for the TR scenario, demonstrating the importance of station position geometry for short arcs.

The GPS-D system meets the performance goal only in the definitive period for the OD scenario. The GPS-PD system looked promising; however, because of limitations of computer analysis tools, no ATDRS positioning results were estimated.

TRACKING SYSTEM	OD PERFORMANCE: 75-METER (3σ) ACCURACY MET		TR PERFORMANCE: 75-METER (3σ) ACCURACY MET		CONUS NETWORK	TOTAL 10-YEAR COST (RELATIVE TO MPRTS)
	DEFINITIVE (30 HOURS)	PREDICTIVE (3 DAYS)	DEFINITIVE (2 HOURS)	PREDICTIVE (1 DAY)		
BRTS	NEARLY[a]	NO	NEARLY[a]	NO	NO	–
AKuRS (CONUS)	YES	YES	NEARLY[a]	NO	YES	2.2
AKuRS (NON-CONUS)	YES	YES	YES	YES	NO	2.2
PRTS (CONUS)	YES	NEARLY[a,b]	NO	NO	YES	1.2
PRTS (NON-CONUS)	YES	NO	YES	YES	NO	1.2
MPRTS (CONUS)	YES	NEARLY[a, b]	NO	NO	YES	1.0
MPRTS (NON-CONUS)	YES	NO	YES	YES	NO	1.0
VLBI-Q	YES	YES	YES	NEARLY[c]	YES	2.8
CEI-Q*	YES	YES	NEARLY[a]	NO	YES	1.6
VLBI-3S*	YES	YES	YES	NEARLY[c]	YES	.80
GPS-D	YES	NO	NO	NO	YES	.18
GPS-PD	–	–	–	–	YES	.52
GPS-DD	–	–	–	–	YES	–
VLBI-Ku	YES	YES	YES	NO	YES	NA
VLBI-GT	NO	–	–	–	YES	.80
VLBI-GC	YES	NEARLY[a]	NEARLY[a]	NO	YES	.92
VLBI-GH	YES	NEARLY[a]	NEARLY[a]	NO	YES	.92

2055B(3)-018

[a] 100-METER (3σ) ACCURACY MET

[b] 75-METER (3σ) ACCURACY OBTAINED FOR A 2-DAY PREDICTION PERIOD

[c] 75-METER (3σ) ACCURACY OBTAINED FOR A 6-HOUR PREDICTION PERIOD

*PERFORMANCE LISTED IS CONTINGENT ON OPTIMISTIC GT RANGING WITH 1-METER NOISE AND 3-METER BIAS.

Table 1-2. Overall ATDRSS Tracking System Performance Comparison

The VLBI-Q tracking system meets the tracking goals for definitive and prediction periods in the OD scenarios without supplemental ranging from the AGT. However, such ranging in the TR scenario is mandatory for optimal performance that still falls short of the study goals. Conversely, the CEI-Q tracking system requires GT ranging in the OD scenario and is inadequate in the TR scenario. VLBI-3S meets the study goals in the OD scenario given troposphere height solutions as part of the OD process. However, GTR (ranging) is required to reach the TR tracking goals. VLBI-2S did not perform as well, making VLBI-3S the choice between these two systems. The VLBI-Ku system met every tracking goal except predictions in the TR scenario.

The tracking performance of the multiple GPS-assisted systems VLBI-GC and VLBI-GH were found to be similar to each other. Accurate definitive period orbits require GTR in the OD scenario and are unattainable in the TR scenario. Predictive period performance is insufficient in either scenario. The VLBI-GT system did not meet any of the tracking goals in either scenario.

2. ATDRSS Impacts--Table 1-1 identifies the primary ATDRSS services required by each tracking system. PRTS and MPRTS cause impacts on the ATDRSS due to the need to support the PRTS signal structure on the S-band navigation beacon. AKuRS requires a Ku-band beacon to be added to the ATDRS. GPS-PD requires use of either the S-band or Ku-band beacons of (M)PRTS or AKuRS. All these ranging systems require an ATDRSS return channel. GPS-D and GPS-DP require a GPS receiver be added to each ATDRS. Interferometric systems generally require GTR to support TR, a system already present but not fully utilized in the TDRS. VLBI-Ku requires a separate Ku-band beacon be added to the ATDRS.

3. Cost and Staffing Needs--The relative costs of the tracking systems studied are given in Table 1-2. The least expensive systems are the GPS-based ranging systems. Next are the PRTS-based and multiple-satellite interferometry (e.g., VLBI-2S) systems. AKuRS and the quasar-calibrated interferometric systems cost the most. Staffing for the interferometric systems is generally three times as great as for the ranging systems.

4. Technological Risks--Technological risk is believed to be low for all the tracking alternatives, with the possible exception of the multiple-satellite interferometric systems. These systems require untested troposphere height solutions during the OD process and may be subject to performance degradation during rainy weather.

5. External System Dependencies--PRTS and MPRTS have one external dependency. If the return link from the remote stations is not available, a relatively low bandwidth NASA Communications Network (Nascom) link will have to be used as a secondary command link for system reconfiguration. In addition, PRTS will use this link for the transfer of timing information. The VLBI-Q system has a requirement for a high bandwidth (32Mb/s) data link from the remote sites to the central processing facility. Because much less data is required, a much lower bandwidth connection with caching can be used for the VLBI-S system. The CEI-Q system is not constrained by data transport requirements.

GTR from each ATDRS to the AGT is required at some level for all interferometric tracking approaches. An a priori ephemeris is required for the CEI-Q system to resolve phase ambiguities encountered while processing the first data from a new orbit.

1.5.3 RECOMMENDATIONS

Summarizing the above, no system studied meets all of the study goals. There are three possible responses to this:

- Change (i.e., relax) the study goals
- Study the present systems more thoroughly (perhaps yielding a positive result)
- Consider different tracking systems

The most promising systems studied that can be used as a basis for further analysis are AKuRS, MPRTS, VLBI-3S, and VLBI-Ku. In addition, an enhanced version of the present BRTS system that also uses GTR is being considered in another study (Reference 1-5).

1.6 REFERENCES

1-1. Stanford Telecommunications, Inc., TR880106, Precise Ranging and Timing System: (PRTS) System Specifications, Preliminary, September 1988

1-2. --, TR880123, Precise Ranging and Timing System (PRTS) Life Cycle Costing, Preliminary, September 1988

1-3. --, SP880102, Modified Precise Ranging and Timing System (PRTS): System Specifications, Preliminary, September 1988

1-4. --, TR880124, Modified Precise Ranging and Timing System (PRTS): Life Cycle Costing, Preliminary, September 1988

1-5. Alan Schanzle, personal communication.

SECTION 2 - ASSESSMENT ASSUMPTIONS AND CONSIDERATIONS

ATDRSS is the proposed follow-on to the current TDRSS; its architecture and user services remain to be fully determined. This section discusses the five candidate ATDRSS architectures and identifies the configuration chosen as the baseline for this assessment study. In addition, error modeling assumptions used in the tracking performance analysis are summarized.

2.1 ATDRSS ARCHITECTURE OPTIONS

Considerations and assumptions in the development of the ATDRSS architecture include ATDRSS user and NASA Space Network perspectives. The ATDRSS architecture must support growth in the required number of communications channels with improved service access availability. Potential enhancements to user services in the Space Station era include improved link efficiency, closure of the zone-of-exclusion, direct data distribution to user terminals, support of data rates beyond 300 megabits per second (Mbps), near-real-time demand access, support of more than two users in proximity operations, and support of autonomous navigation.

At the same time, the transition to ATDRSS should be transparent to the user community and reflect the best compromise between minimum cost and risk to obtain maximum performance, flexibility, and robustness. The ATDRSS architecture should maintain spacecraft visibility to CONUS, should utilize the existing White Sands Ground Terminal (WSGT) and Second TDRSS Ground Terminal (STGT) facilities, and should retain use of Ku-band in the space-to-ground link (SGL) frequency plan, evolving to use of Ka-band only if required.

Subject to these considerations, five candidate ATDRSS architectures have been developed (Reference 2-1), providing a range of potential system capabilities with concomitant increases in cost and risk. The five options have been labeled the TDRSS/Cluster, Augmented, Augmented with Distributed Ground Terminals, X-Link [interoperability (I-O)], and X-Link [Tracking and Data Acquisition System (TDAS)] architectures. Their salient features are summarized in Table 2-1 and illustrated in Figure 2-1.

Each of these five architectures has been assessed in terms of associated user benefits and impacts, technology risk,

Table 2-1. ATDRSS Architecture Options

KEY INGREDIENTS / ARCHITECTURE			TDRSS/ CLUSTER	AUGMENTED		X-LINK	
				BASELINE	WITH DISTRIBUTED GROUND TERMINALS	I-O	TDAS
GEO ORBITAL SLOT LOCATIONS	SLOTS TO SATISFY GEOMETRIC COVERAGE REQUIREMENTS	LOCATIONS	O 171° W O 41° W	O 171° W O 41° W	O 171° W O 17° W	O 171° W O 9° W	O 136° E O 62° W
		NO. SATELLITES PER SLOT	2	1	1	1	1
	ADDITIONAL (OPTIMAL) SLOT FOR O SPARE OR O EAST/WEST PEAK-SERVICE OFFLOAD		105° W	105° W	O 94° W	91° W	143° W
GROUND TERMINAL LOCATIONS	WHITE SANDS		O WSGT O STGT	O WSGT O STGT	O WSGT O STGT	O WSGT O STGT	O WSGT O STGT
	OUTSIDE OF WHITE SANDS (FULL-OPS)		-	-	EAST COAST GROUND TERMINAL (ECGT)	-	-
	OUTSIDE OF WHITE SANDS (RGT)		-	-	-	O EUROPE (OPTION) O JAPAN (OPTION)	O ECGT O CALIFORNIA O HOUSTON O COLORADO O EUROPE OR JAPAN (OPTION)
	S-TT&C, OUTSIDE OF WHITE SANDS		-	-	-	ECGT	HAWAII
FREQUENCY PLANS	SPACE-TO-SPACE (EXISTING)		O S O Ku	O S O Ku	O S O Ku	O S O Ku	O S O Ku
	SPACE-TO-SPACE (NEW)		-	O SA OPTIONS - Ka - W - OPTICAL	O SA OPTIONS - Ka - W - OPTICAL	O OPTIONS - Ka, SA - W, SA AND/OR X-LINK - OPTICAL, SA	O OPTIONS - Ka, SA - W, SA AND/OR X-LINK - OPTICAL, SA
	SGL TO WHITE SANDS		O Ku O S (TT&C)	O Ku O S (TT&C)	O Ku O S (TT&C)	O Ka O S (TT&C)	O Ku O S (TT&C)
	SGL, NEW		-	-	Ku TO ECGT	O Ka, TO RGT'S	Ku TO RGT'S
NUMBER ATDRSS S/C REQUIRED OVER LIFE CYCLE (EXCLUDING SPARES)			12	6	6	6	6

93JM1AJ/001/5-6-88

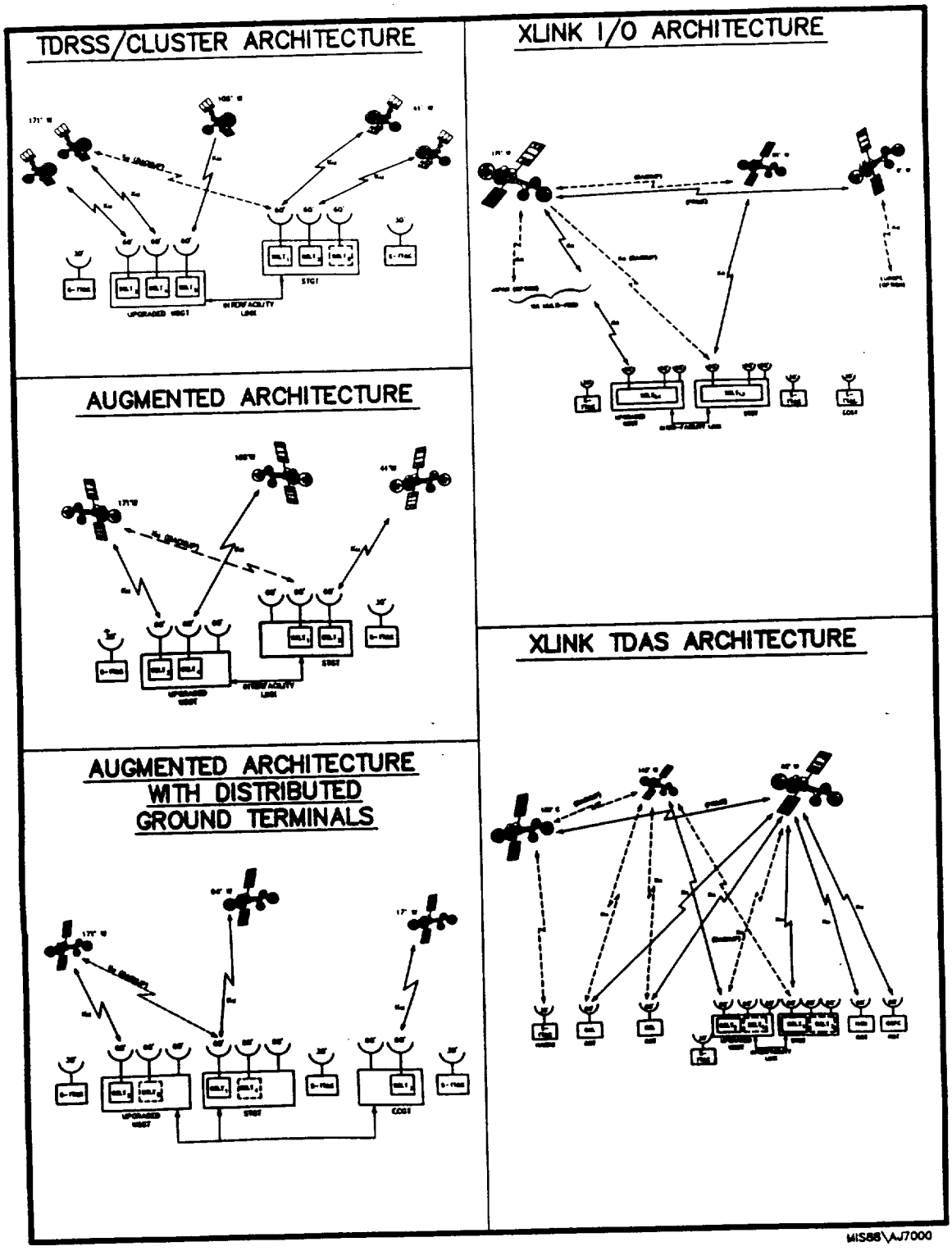

Figure 2-1. ATDRSS Architecture Options

operational risk and robustness, network operability, space and ground segment transition scenarios, and future growth flexibility and presented to NASA for consideration. Currently, the Augmented architecture has been chosen as the reference ATDRSS architecture by the ATDRSS Study Project (Reference 2-2) and is being used in the preliminary development of ATDRSS specifications.

This reference ATDRSS architecture has been selected for this advanced tracking systems study. It has been assumed that ATDRS-E and ATDRS-W are in the current TDRSS geosynchronous orbital slots of 41 and 171 degrees west longitude, respectively, with the spare ATDRS Central (ATDRS-C) satellite located at 106 degrees west longitude.

2.2 TRACKING PERFORMANCE ERROR ANALYSIS

The OD performance of candidate ATDRS tracking systems was analyzed using the Orbital Analysis (ORAN) program (Reference 2-3). The ORAN program is designed to simulate a satellite OD process and analyze the random and systematic errors involved in such a process. ORAN simulates a Bayesian least-squares data reduction for orbital trajectories. ORAN does not process measurement data but is intended to compute the accuracy of the results of a data reduction if measurements of a given accuracy are available and are processed in a least-squares data reduction program. ORAN examines the effects of unmodeled, systematic errors on the solved-for satellite position and velocity and on any other satellite parameters that are estimated in the least-squares OD process.

ORAN input consists of all the information needed to specify the geometrical and dynamic models for the OD process, such as the satellite orbital parameters, satellite area-to-mass ratio, drag and solar radiation coefficients, tracking station locations, types of tracking measurements, and their frequency and precision. The satellite parameters used in this study are shown in Table 2-2.

In addition, ORAN allows the input of systematic errors associated with numerous physical and geometrical parameters and can compute the effects of each error on the satellite position and velocity estimates. This isolation of the effects due to various systematic error sources is not possible in an actual OD run.

The force model parameters, which constitute the dynamic model for the satellite, are (1) the gravitational constant

Table 2-2. ATDRS Satellite Parameters

Epoch time	1980 March 01 0h 0m 0.0s
Keplerian elements	
Semimajor axis	42166663.000 meters
Eccentricity	0.0000245
Inclination	0.5 degree
Right ascension of the ascending node	319.00 degrees (ATDRS-E) 189.00 degrees (ATDRS-W) 254.00 degrees (ATDRS-C)
Argument of perigee	0.0 degrees
Mean anomaly	158.9252 degrees
ATDRS area/mass ratio	0.0227 [m^2/kilograms (kg)]
ATDRS coefficient of reflectivity	1.4

of the Earth (GM); (2) the geopotential coefficients and their associated errors, which measure the probable overall error in the harmonic coefficients of the Earth's gravitational field; and (3) the solar radiation pressure coefficient (C_R), which is proportional to the solar radiation force used in the satellite dynamic model. Additional parameters that are not force model parameters (i.e., they do not affect the value of the force on the satellite) but are independent of the type of measurements are the polar motion X and Y values and the difference between Atomic Time (A1) and Universal Time (UT1): A1 - UT1. All three parameters are involved in the transformations made between the satellite's inertial system of coordinates and the Earth-fixed, rotating system of coordinates in which the measurements are taken. The errors in the force model and other measurement-independent parameters used in this study, shown in Table 2-3, are representative of a performance level projected for the 1995 - 2000 timeframe.

All OD error-analysis runs in this study used the satellite and force model errors defined in Tables 2-1 and 2-2. The measurement time span for all systems ranged from 1 hour to 30 hours, with 30 hours considered the nominal data span for routine OD operations. The shorter arcs of 1 and 2 hours were used to study the capability of the tracking system for TR.

The measurement-related parameters used varied depending on the system under study, but the major parameters were the station location errors, the measurement biases, the clock synchronization errors, and atmospheric refraction effects.

Detailed discussion of these errors, the values used for each system, and the error analysis results are presented in Appendix A.

Table 2-3. Measurement Independent Errors

Model parameter	Uncertainty (3-σ)
GM	6×10^{-8} (fractional error)
Gravity model difference	135% of (GEM10 - GEM7)
C_R	2%
Polar motion X	0.015 arcsec
Polar motion Y	0.015 arcsec
A1 - UT1	0.09 arcsec

2.3 REFERENCES

2-1. Stanford Telecommunications, Inc., "ATDRSS Architecture Definition and Trades" (briefing presented to NASA/GSFC, January 15, 1988)

2-2. ATDRSS Study Project, "A Description of the Reference ATDRSS Architecture," NASA/GSFC, 15 May 1988, draft version

2-3. Martin, T. V., and J. J. McCarthy, "ORAN Descriptive Summary," EG&G Washington Analytical Services Center, Inc., July 1978

SECTION 3 - ATDRS KU-BAND TRACKING SYSTEM

The AKuRS relies on observation of a Ku-band navigation beacon designed to support one-way navigation by ATDRSS users. Tracking of the ATDRSS satellites is accomplished by a network of ground stations that observe the Ku-band beacon and generate coherent return signals for transmission back to the AGT. Two-way range and range-rate measurements are extracted by the AGT from these signals for use in ATDRS OD. The concept is similar to BRTS, which currently supports TDRS tracking. Whereas BRTS requires scheduled two-way S-band service, Ku-band ATDRS tracking is supported by a continuously available beacon and a Ku-band dedicated return channel to avoid burdening ATDRS Ku-band single access (KSA) services. Moreover, Ku-band operation significantly diminishes the effect of ionospheric delays, thereby improving ATDRS OD performance relative to that provided by comparable S-band BRTS networks.

3.1 AKuRS DEFINITION

This section provides an overview of the AKuRS architecture and operations concept, describes the Ku-Band navigation beacon and return signals and the associated ATDRS links, discusses the ground station requirements, and considers several tracking network options.

3.1.1 ARCHITECTURE AND OPERATIONS CONCEPT

The AKuRS depicted in Figure 3-1 relies on two-way range and range-rate estimates made by the AGT and a network of ground stations to track the ATDRSS satellites. The tracking system is effectively a Ku-band version of the S-band BRTS, thereby taking advantage of the minimal ionospheric delays experienced by Ku-band signals. In addition, the Ku-band signal is designed to support both one-way ATDRSS user navigation and ATDRSS tracking without affecting KSA user services.

A navigation beacon is generated by the AGT for each ATDRSS satellite and relayed via the ATDRSS uplink to each ATDRS. The beacon and return signals required by the AKuRS will be uplinked and downlinked at either Ka- or Ku-band, depending on the future allocation. To avoid potential interference among the beacons emitted by different satellites, independent beacon signals are transmitted to each of the ATDRSS satellites using different PN codes. After appropriate frequency translation and amplification onboard the satellite, the Ku-band signal is emitted by each ATDRSS

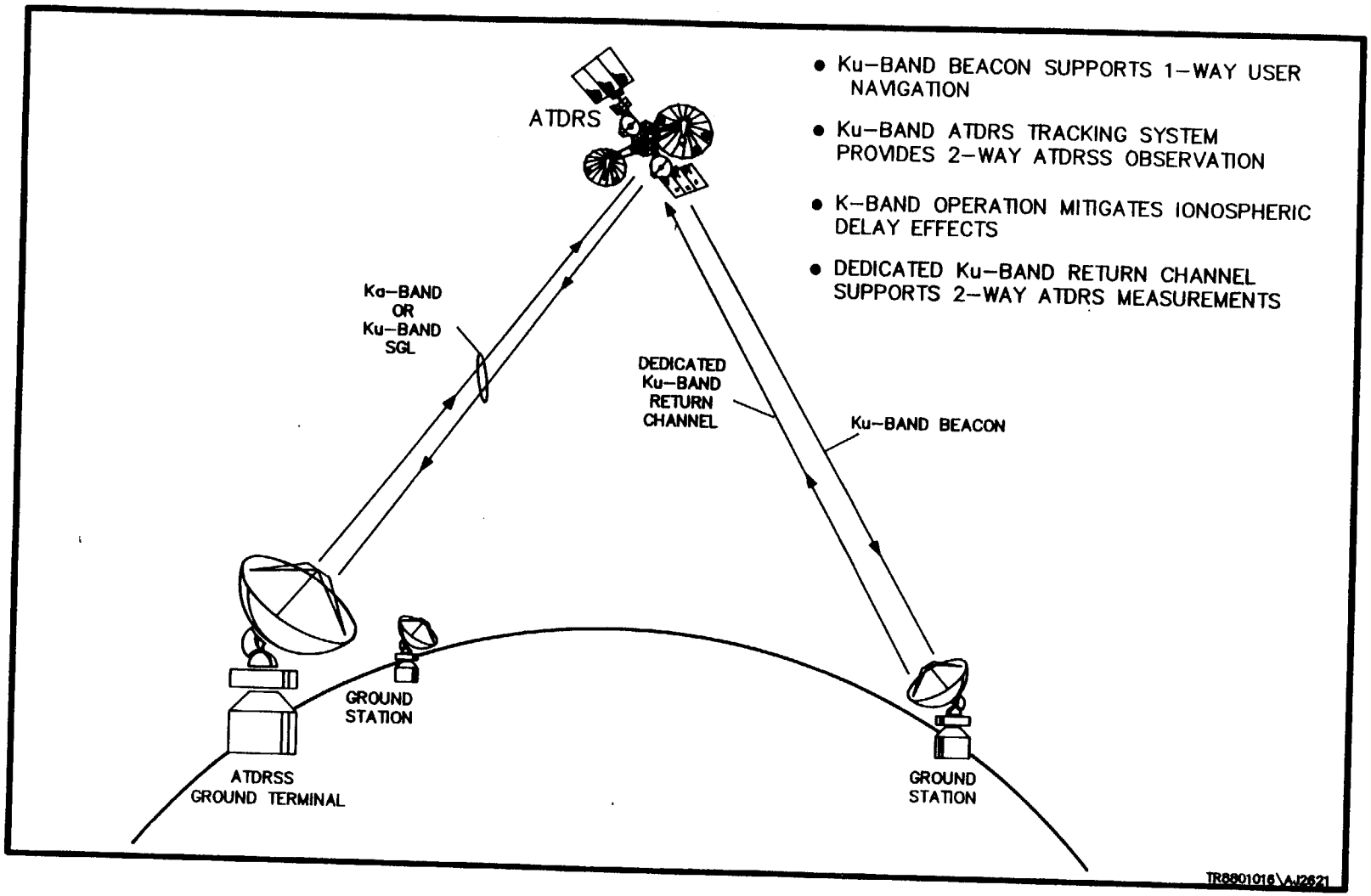

Figure 3-1. AKuRS Architecture

as a continuously available navigation beacon providing Earth and ATDRSS user coverage.

A network of AKuRS ground stations observes the Ku-band beacon. Each ground station is capable of receiving the signal and transmitting a coherent return signal back to the AGT via a dedicated Ku-band channel. Coherent turnaround of the beacon requires that the return signal use the recovered beacon carrier as its frequency reference and that the return signal's epoch be synchronized with the received beacon signal epoch. The Ku-band return signal is processed by the AGT to yield two-way range and range-rate estimates, as illustrated in Figure 3-2. Measurements are relayed to the Flight Dynamics Facility (FDF), which is responsible for ATDRSS OD. When a minimum of two ground stations are used to observe the beacon from each ATDRSS satellite, the satellite orbit may be determined through multilateration.

The beacon's navigation message includes data to support one-way navigation, ATDRSS system health, and commands to the tracking network as supplied by the Network Control Center (NCC). The station executive at each ground station monitors the beacon navigation message, extracting pertinent data and responding to commands. Return data prepared by the ground stations is time-tagged and relayed back to the ground terminal on the return path of the coherent two-way link.

The ground stations are designed to preclude the need for resident staffing by relying on computer automation to perform routine functions, with service technicians dispatched as needed to repair and maintain station elements. The station executive is programmed to diagnose station abnormalities, correct those it can, and notify the ground terminal concerning those it cannot. Should the beacon be lost, the station executive is programmed to access the ground terminal through Nascom link for further instruction. Station equipment failure and periodic maintenance are handled by trained personnel, who are dispatched to the stations as needed to perform routine maintenance, delay calibration, and station location surveys.

3.1.2 Ku-BAND NAVIGATION BEACON SIGNAL

Many different criteria might be applied in defining a Ku-band beacon, but this study has assumed that the Ku-band beacon should have the following characteristics:

- Be as compatible as possible with the current TDRSS KSA forward service

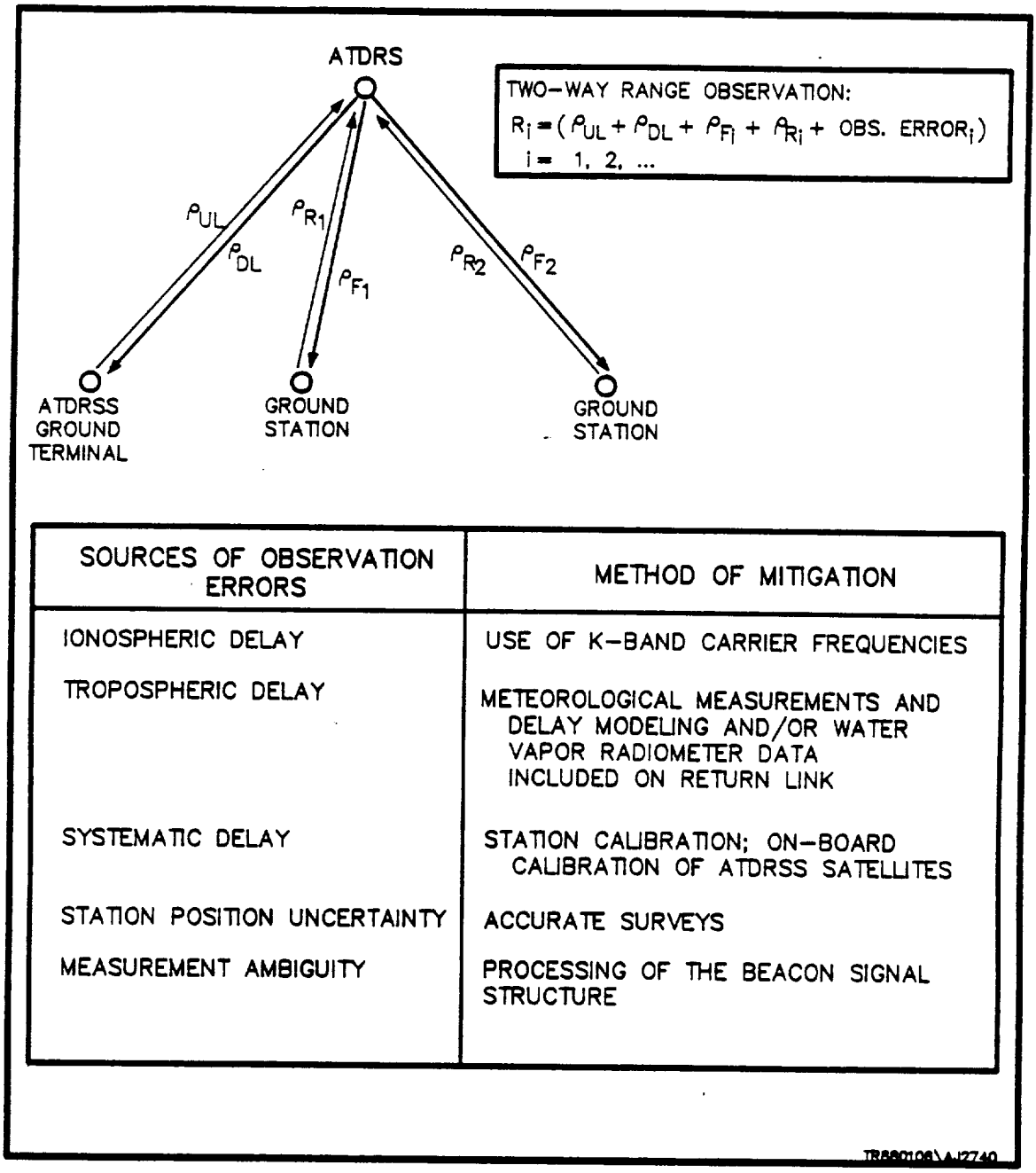

SOURCES OF OBSERVATION ERRORS	METHOD OF MITIGATION
IONOSPHERIC DELAY	USE OF K-BAND CARRIER FREQUENCIES
TROPOSPHERIC DELAY	METEOROLOGICAL MEASUREMENTS AND DELAY MODELING AND/OR WATER VAPOR RADIOMETER DATA INCLUDED ON RETURN LINK
SYSTEMATIC DELAY	STATION CALIBRATION; ON-BOARD CALIBRATION OF ATDRSS SATELLITES
STATION POSITION UNCERTAINTY	ACCURATE SURVEYS
MEASUREMENT AMBIGUITY	PROCESSING OF THE BEACON SIGNAL STRUCTURE

TR880108\AM2740

Figure 3-2. AKuRS Measurement Model

- Provide sufficient data to fully support onboard one-way orbit and time determination by ATDRSS users

- Use a fixed transmit frequency and provide a uniform and rational time base with the signal epochs referenced to calendar epochs in standard time units

The Ku-band signal structure has been developed in the same manner as the recommended ATDRSS S-band navigation beacon (Reference 3-1) to support one-way ATDRSS user navigation. If the beacon were merely to support the AKuRS alone, many of the features discussed here would not be necessary.

Consistent with TDRSS specifications, the ATDRSS navigation beacon uses a dual-channel (range and command) signal structure as outlined in Table 3-1, with a long PN code for the range channel and a short code for the data-modulated command channel. The long and short PN codes are related to assist in signal acquisition, with the range-channel long code constructed from a cyclic repetition of the command-channel short code. An unmodified version of the short code appears within the long code once per long-code period to define the all-1's epoch of the long code. Acquisition of the command-channel code phase may thus be accomplished by searching the entire 1023-chip short-code cycle, whereas the range-channel code phase may then be found by searching only the 256 long code positions corresponding to the embedded short-code epochs.

The Ku-band beacon relies on the known synchronous relationship between the signal's data and PN code to support time transfer and the resolution of range ambiguity. The command-channel data provides a coarse time reference to resolve initial range ambiguities; the range-channel pseudorandom noise (PN) code allows ambiguities to be resolved further; and the command-channel PN code phase provides fine time resolution to a few percent of the PN chip duration. Furthermore, the beacon establishes a rational and uniform time base by relating the PN code and data rates to an integer number of seconds and hours, days, and weeks.

The nominal TDRSS KSA forward transmit frequency is specified as 13.775 gigahertz (GHz), $\pm$ 0.7 megahertz (MHz) (Reference 3-2), with the command- and range-channel PN chip rates related to the carrier frequency by a factor of $31/(1469 \times 96)$. The Ku-band beacon signal parameters specified in Table 3-1 stipulate a carrier frequency offset from the TDRSS nominal value by 224320 hertz (Hz) so that

Table 3-1. Ku-Band Navigation Signal Parameters

PARAMETER	DEFINITION
TRANSMIT CARRIER FREQUENCY (Hz)	F_C = 13.77522432 GHz
CARRIER FREQUENCY ARRIVING AT USER SPACECRAFT (Hz)[1]	F_R
$\left(\frac{\text{COMMAND CHANNEL RADIATED POWER}}{\text{RANGE CHANNEL RADIATED POWER}}\right)$	+10 dB
RANGE CHANNEL	
CARRIER FREQUENCY	COMMAND CHANNEL CARRIER FREQUENCY DELAYED $\pi/2$ RADIANS
PN MODULATION	PSK, $\pm\pi/2$ RADIANS
CARRIER SUPPRESSION	30 dB MINIMUM
PN CHIP RATE	SYNCHRONIZED TO COMMAND CHANNEL PN CHIP RATE
PN CODE LENGTH (CHIPS)	$(2^{10} - 1)$ X 256 (LONG CODE)
PN CODE EPOCH REFERENCE	ALL 1'S CONDITION SYNCHRONIZED TO THE COMMAND CHANNEL PN CODE
PN CODE FAMILY	TRUNCATED 18 STAGE SHIFT REGISTER SEQUENCES
COMMAND CHANNEL	
CARRIER FREQUENCY (Hz)	TRANSMIT CARRIER FREQUENCY (F_C)
PN MODULATION	PSK, $\pm\pi/2$ RADIANS
CARRIER SUPPRESSION	30 dB MINIMUM
PN CODE LENGTH (CHIPS)	$2^{10} - 1$ (SHORT CODE)
PN CODE FAMILY	GOLD CODES
PN CHIP RATE (CHIPS/SEC.)	$\frac{31}{1469 \text{ X } 96}$ X F_C
DATA FORMAT	NRZ
DATA RATE	1 Kbps
DATA MODULATION	MODULO-2 ADDED SYNCHRONOUSLY TO PN CODE

93IM1KC/009/9-1-88

1. IF THE REFERENCE POINT FOR F_C IS THE ATDRSS GROUND TERMINAL, THEN F_R WILL INCLUDE BOTH SGL AND USER DOPPLER OFFSETS.

4625 long-code cycles equal 400 seconds (sec). The first PN epoch of a 400-sec block is thus coincident with 20-minute epochs, dividing an hour into thirds and providing users with calendar compatibility. With a 1 kilobit per second (kbps) data rate, the minimum allowed TDRSS value, 200 frames of 2000 bits define a 400-second block, as shown in Figure 3-3. The frame synch word of the leading data frame in each block of 400 sec is coincident with a long PN code epoch; for other data frames within a block, the time interval between the synch word and the next PN epoch is a known variable, depending on which data frame is under consideration. In this manner, the frame sync word provides a coarse time reference pointing to a time-tagged PN epoch.

These features of the Ku-band navigation beacon support one-way navigation by ATDRSS users. For ATDRS tracking, however, the signal is received by each ground station and a return signal coherently generated with the return signal's PN epoch synchronized to the received beacon signal's epoch. Coherent generation of the return signal requires carrier tracking of the beacon at the ground stations to provide a root mean square (rms) phase error less than, for example, 5 degrees. Such performance corresponds to a carrier loop signal-to-noise ratio (SNR) of approximately 22.6 dB (Reference 3-3).

Table 3-2 provides a representative link budget for the ATDRS-to-tracking-station link. The link budget conservatively assumes a 500° kelvin (K) noise temperature for the tracking station low noise amplifier (LNA) and a rain margin of 6 decibels (dB). Moreover, the ground station antenna gain is assumed to be 23 dB, representing a Ku-band aperture that, analogous to the S-band BRTS system, provides a two-sided beamwidth of approximately 15 degrees. The size of such a Ku-band aperture would be on the order of 10 centimeters (cm) such that the resultant beamwidth allows the ground station to receive and transmit to ATDRS under nominal conditions without antenna pointing after initial installation. If a larger ground station antenna were used, higher gain would be achieved but might require an additional tracking system to follow the ATDRSS navigation beacon.

To support ATDRSS users as well as the AKuRS network, the two-sided beamwidth of the Ku-band beacon is assumed to be 26 degrees. The ATDRS Ku-band aperture would therefore be less than 10 cm to provide a gain of approximately 18 dB along the boresight. The link budget of Table 3-2 then assumes 40 watts (W) of transmit power to illustrate how the necessary Eb/N0 and carrier loop SNR at the ground station

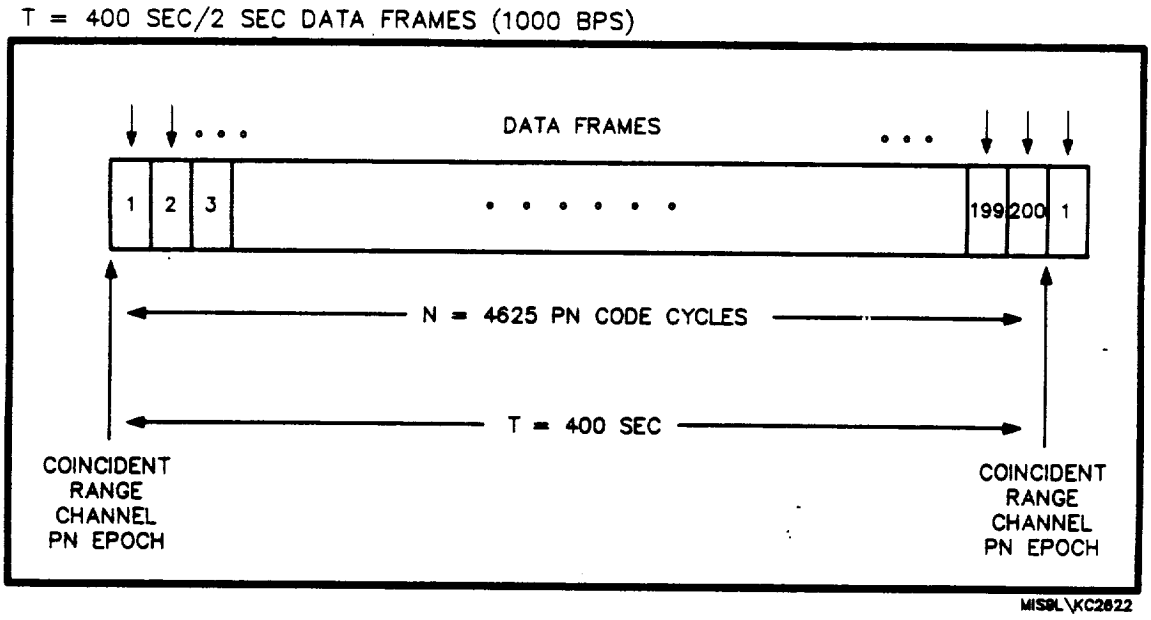

Figure 3-3. Ku-Band Beacon Data Frame Structure

Table 3-2. Ku-Band Navigation Beacon Link Budget

LINK ELEMENT	VALUE	COMMENTS
(1) ATDRS BEACON EIRP (dBW)	33.8	O 40W (16 dBW) Ku-BAND NAV BEACON XMIT POWER (REPRESENTATIVE VALUE) O ANTENNA GAIN ≈ 17.8 dB CORRESPONDING TO 26° BEAMWIDTH
(2) PATH LOSS (dB)	207.6	O Ku-BAND (~14 GHz) O RANGE ≈ 41000 KM
(3) RECEIVE ANTENNA G/T (dB/°K) AT TRACKING STATION	-4.0	O ANTENNA GAIN ≈ 23 dB CORRESPONDING TO 15° TWO-SIDED BEAMWIDTH O NOISE TEMPERATURE: 500°K
(4) BOLTZMANN's CONSTANT (dBW/Hz-°K)	-228.6	
(5) IMPLEMENTATION LOSS (dB)	3.0	ASSUMED VALUE
(6) RAIN MARGIN (dB)	6.0	ASSUMED VALUE
(7) RECEIVED C/N_0 (dB-Hz)	41.8	(1) - (2) + (3) - (4) - (5) - (6)
(8) BEACON DATA RATE (dB-Hz)	30.0	1 kbps, SUPERIMPOSED ON BEACON COMMAND CHANNEL PN CODE
(9) E_b/N_0 (dB)	11.8	O (7) - (8) O 10^{-5} BER REQUIRES $E_b/N_0 > \begin{cases} 9.6 \text{ (UNCODED)} \\ 4.6 \text{ (CODED)} \end{cases}$
(10) CARRIER LOOP SNR (dB)	24.8	O 50 Hz LOOP BANDWIDTH (17 dB-Hz) O (7) - 17 dB-Hz O RMS PHASE ERROR OF 5° REQUIRES SNR ≈ 22.6 dB

93JM1KC/011/9-1-88

may be achieved. Many trade-offs exist between the onboard and ground station requirements, but any reduction in ATDRS effective isotropic radiated power (EIRP) must also be seen in terms of the associated impact to ATDRSS users. For example, the ATDRS EIRP should be sufficient to allow users to observe the Ku-band navigation beacon successfully without requiring high-gain antennas, especially because such high-gain antennas may require a tracking system to maintain the navigation beacon in view.

3.1.3 AKuRS RETURN SIGNAL

The AKuRS return signal is intended to support two-way communications as required for ATDRS tracking. To avoid burdening the KSA return system, a dedicated Ku-band return channel is provided with the beacon emitter diplexed as a receive antenna. The signal structure is given in Table 3-3 and is meant to be as compatible as possible with the current Mode 1 TDRSS KSA return signal. The return signal is thus a dual-channel staggered quadriphase pseudonoise (SQPN) signal with transmit frequency coherently related to the beacon receive frequency by the coherent turnaround ratio. The epoch of the signal's PN code is similarly synchronized to the received PN code epoch of the beacon signal. The coherent turnaround ratio is not specified in Table 3-3, however, pending determination of an appropriate frequency allocation. The current KSA return service allocation is not employed because its use may create interference problems with ATDRSS KSA users.

Table 3-4 provides a representative link budget for the tracking-station-to-ATDRS link, assuming that the ground station receive antenna is diplexed to transmit the Ku-band return signal. The ground station transmit antenna is assumed to have a large beamwidth to avoid antenna tracking of the ATDRSS satellites, consequently providing less gain than would otherwise be achieved with a larger aperture. If the ATDRS Ku-band beacon aperture provides a gain of 17.8 dB and, conservatively, the ATDRS Ku-band dedicated channel LNA has a noise temperature of 500° K, then the ATDRS gain/noise temperature (G/T) is -9.2 dB/K. With these assumptions, the link budget demonstrates how a ground station transmit power of 17 decibel watts (dBW) (50 W) satisfies the Eb/N0 and carrier loop SNR requirements at the ATDRS, neglecting the relatively strong ATDRS-to-ground link.

Although the indicated EIRP from the Ku-band tracking station is readily achieved, this level of power over a 6 MHz bandwidth may pose interference problems for KSA

Table 3-3. AKuRS Return Signal Parameters

PARAMETERS	DEFINITION
TRANSMIT CARRIER FREQUENCY (Hz)	K_1 X F_R (NOTE 1)
PN MODULATION	SQPN
PN CHIP RATE	K_2 X F_R (NOTE 2)
PN CODE LENGTH (CHIPS)	$(2^{10} - 1)$ X 256 (LONG CODE)
PN CODE EPOCH REFERENCE	
I CHANNEL	SYNCHRONIZED TO EPOCH OF RECEIVED FORWARD LINK RANGE CHANNEL
Q CHANNEL	Q CHANNEL EPOCH DELAYED BY (X + 1/2) PN CHIPS RELATIVE TO I CHANNEL EPOCH, WHERE X ≤ 20,000 AND THE Q CHANNEL PN CODE IS IDENTICAL TO THE I CHANNEL CODE
PN CODE FAMILY	TRUNCATED 18-STAGE SHIFT REGISTER SEQUENCES
DATA FORMAT	NRZ
DATA RATE	1 kbps, IDENTICAL DATA ON BOTH CHANNELS
DATA MODULATION	MODULO-2 ADDED SYNCHRONOUSLY TO PN CODE ACCORDING TO Ku-BAND BEACON DATA FRAME FORMAT

93JM1KC/010/9-7-88

NOTES:

1. THE COHERENT TURNAROUND RATIO K_1 DEPENDS ON THE FREQUENCY ALLOCATION OF THE Ku-BAND ATDRS TRACKING RETURN SIGNAL (SEE ACCOMPANYING TEXT); FOR TDRSS KSA RETURN SIGNALS, K_1 = 1600/1469.

2. THE VALUE OF K_2 IS RELATED TO K_1; IN TDRSS, K_2 = 31/(1600 X 96).

Table 3-4. AKuRS Return Signal Link Budget

LINK ELEMENT	VALUE	COMMENTS
(1) STATION EIRP (dBW)	40.0	• 50 WATT XMIT POWER • ANTENNA GAIN≈ 23 dB CORRESPONDING TO 15° TWO-SIDED BEAMWIDTH
(2) PATH LOSS (dB)	208.8	• Ku-BAND (~16 GHz) • RANGE ≈ 41000 KM
(3) ATDRSS G/T (dB/°K)	-9.2	• ANTENNA GAIN ≈ 17.8 dB CORRESPONDING TO 26° TWO-SIDED BEAMWIDTH • NOISE TEMPERATURE: 500°K
(4) BOLTZMANN'S CONSTANT (dBW/Hz - °K)	-228.6	
(5) IMPLEMENTATION AND INTERFERENCE LOSSES (dB)	4.0	ASSUMED VALUE
(6) RAIN MARGIN (dB)	6.0	ASSUMED VALUE
(7) RECEIVED C/N_o (dB-Hz)	40.6	(1) - (2) + (3) - (4) - (5) - (6)
(8) RETURN DATA RATE (dB-Hz)	30.0	1 KBPS, SUPERIMPOSED ON 3 Mcps PN CODE
(9) E_b/N_o (dB)	10.6	• (7) - (8) • 10^{-5} BER REQUIRES $E_b/N_o >$ { 9.6 (UNCODED) / 4.6 (CODED) }
(10) CARRIER LOOP SNR (dB)	23.6	• 50 Hz LOOP BANDWIDTH (17 dB-Hz) • (7) - 17 dB-Hz • RMS PHASE ERROR OF 5° REQUIRES SNR ≈ 22.6 dB

return users operating within the transmit beamwidth. Likewise, KSA return signals could interfere with the AKuRS return signal due to the wide beamwidth of the beacon antenna. To avoid such difficulties, the coherent turnaround ratio has been specified as a variable so that the dedicated Ku-band return channel can be assigned a frequency that will not be disruptive to KSA user communications. Further analysis is required, but it may be possible to avoid a completely new Ku-band allocation with negligible user impact by placing the AKuRS return channel somewhere toward the edge of the current KSA return allocation.

3.1.4 GROUND STATION REQUIREMENTS

The AKuRS ground stations are designed to provide adequate resources to meet all performance goals while minimizing staffing and maintenance requirements. To this end, the ground stations have been designed with basic subsystems to perform specified functions and with control features that preclude the need for permanent onsite personnel. Each ground station is composed of a station executive, Ku-band transponder, station clock, antenna, and peripheral support equipment, as illustrated in Figure 3-4.

The ground station's transponder operates at Ku-band and is capable of generating a Ku-band return signal coherent with the received Ku-band beacon signal. A diplexed antenna supports both reception of the beacon and transmission of the return signal. Command, control, and navigation data are extracted by the transponder and provided to the station executive. The executive directs station operation and collects information from various sensors and monitors at the site. Peripheral sensors monitor the station health and collect meteorological information for use in tropospheric delay estimation by the station executive. Such data is then time-tagged and formatted for relay via the dedicated return channel to the AGT.

The AKuRS ground stations are designed to require minimal staffing support. Command and control messages included as part of the Ku-band beacon navigation message are used to direct operation of the tracking network and perhaps even individual stations. Routine station tasks and operations are independently directed at each station by the station executive. Routine maintenance and repair are generally scheduled operations, precluding the need for full-time station operators.

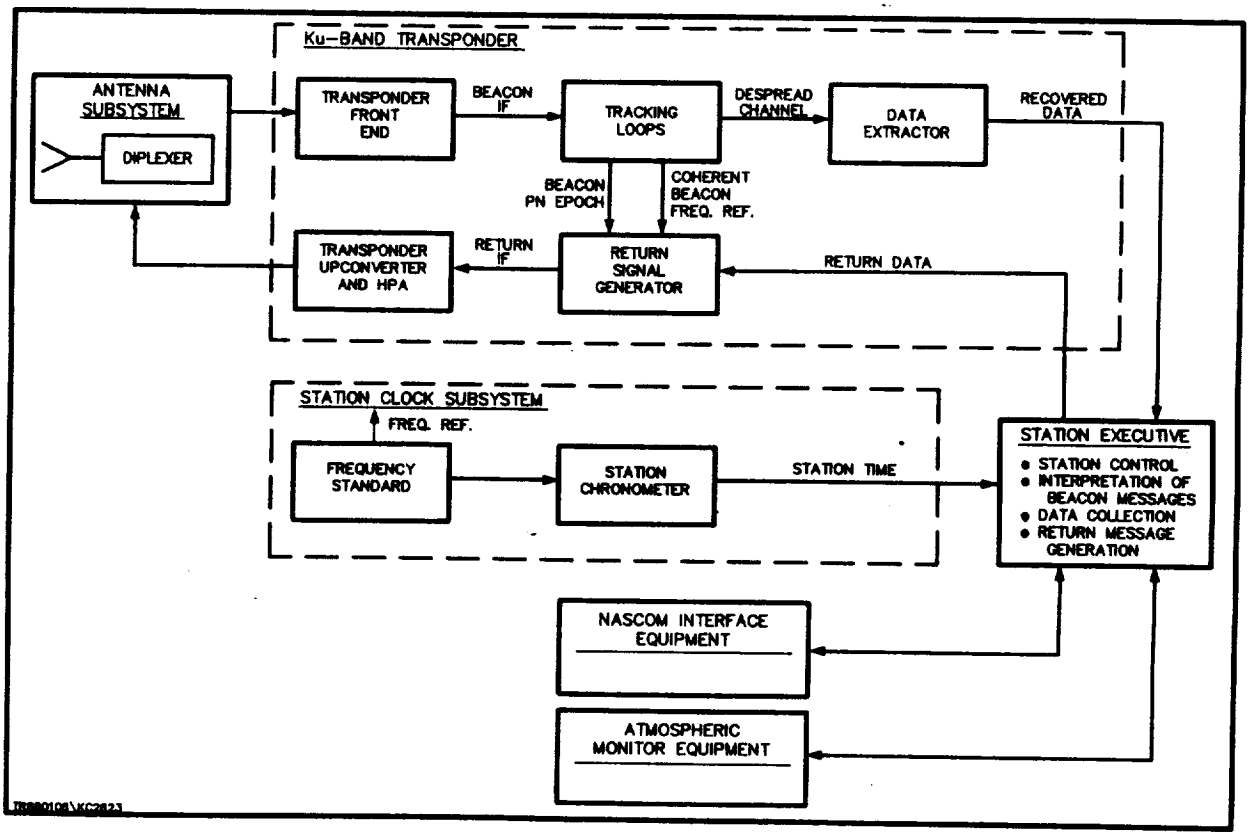

Figure 3-4. AKuRS Ground Station Architecture

3.1.4.1 Station Executive

Ground station operation is controlled by a resident computer, designated the station executive, responsible for initiating and coordinating station activities. The station executive performs routine functions to satisfy operational requirements and ensure station integrity, accepts beacon data and commands provided by the station transponder, extracts applicable information, and carries out received commands.

The station executive gathers information from other station subsystems to monitor overall system performance and support the OD process. Information such as the station health and the executive's tropospheric delay estimate and associated meteorological data are time-tagged and formatted by the executive and transmitted through the return signal for use by the ground terminal and the FDF.

Because no significant concurrent or dedicated computation is required to operate the ground station, system management and data processing tasks may be handled sequentially. The architectural requirements for the executive are thus simplified, allowing off-the-shelf microcomputer technology to be employed to implement the station executive, thereby reducing the costs associated with this subsystem.

3.1.4.2 Ku-Band Transponder

The tracking station's Ku-band transponder supports the demodulation of the Ku-band beacon and the coherent generation of the tracking system's Ku-band return signal. Currently, no standard NASA/TDRSS Ku-band transponder is available. Ideally, a standard ATDRSS Ku-band transceiver/transponder would be developed that supports both KSA user requirements, including one-way navigation using the Ku-band beacon, and the needs of the AKuRS ground stations. Such a device would possess more capabilities than would be needed solely for the purposes of the AKuRS but would encourage ATDRS users to operate at Ku-band and to take advantage of the Ku-band beacon.

Assuming a standard Ku-band transceiver/transponder were developed, it would be operated as a beacon transponder in the AKuRS ground stations. Support of both KSA user services and the Ku-band beacon by a standard Ku-band transceiver/tra..sponder may entail some additional design complexity, mainly because of the different transmit and receive frequencies involved. For example, the Ku-band beacon frequency is offset from the nominal KSA forward

service frequency, and the AKuRS return signal likely requires a different coherent turnaround ratio than used in Mode 1 KSA service. Even if such a standard Ku-band device were not developed, the requirements of the AKuRS ground station could readily be met by developing a specific Ku-band beacon transponder.

3.1.4.3 Antenna

Selection of the ground station antenna is contingent on many system parameters, as discussed earlier in the discussion of the Ku-band beacon link budget. Trade-offs among onboard power, antenna size, and satellite inclination all affect the ground station antenna design. Ideally, the subsystem would comprise a fixed antenna capable of viewing the ATDRSS satellite throughout its allowed range of orbital positions. If the inclination of the ATDRSS satellites were kept to a small value--an ATDRS inclination of 0.5 degrees, for example, has been assumed in the ORAN modeling performed in this study--it may be possible to increase the antenna gain without requiring a tracking system to follow the ATDRSS satellites' motion. Although increased ground station antenna gain would enable the onboard beacon transmit power to be reduced, the beacon EIRP must still support beacon users. Final selection of the ground station's antenna, therefore, depends on aspects of the ATDRSS design, its stationkeeping requirements, and ATDRSS user parameters and requirements, which are not fully known at this time.

3.1.4.4 Station Clock

Because the AKuRS relies on two-way measurements, timing requirements for the ground stations are relatively simple. Local time is required to tag the return signal data and to support the observation schedule. Coarse time transfer may be obtained from the Ku-band beacon itself, readily providing clock biases between the AGT standard and the local station clock to within a few hundred μsec. This level of accuracy is more than adequate for all station functions.

The ground station's reference oscillator also serves as the frequency reference for much of the transponder circuitry. Again, coherent turnaround of the received Ku-band signal implies that the required stability be comparable to that of a thermally controlled crystal oscillator. The frequency reference is, therefore, readily and inexpensively obtained.

3.1.4.5 Peripheral Support Equipment

Two subsystems provide peripheral support to the tracking stations: the Nascom interface subsystem, providing contingency communications with the ground stations, and the atmospheric monitor equipment, which supports the estimation of tropospheric delays. The Nascom interface provides backup command, control, and telemetry communications in the event that the two-way Ku-band link is lost. A more primary role is served by the atmospheric monitor equipment, which allows the two-way measurements to be corrected for the effects of tropospheric delay. The atmospheric monitor equipment obtains local meteorological data to allow modeling of the tropospheric delay or may even use a water vapor radiometer to measure the tropospheric delay directly. This data is then processed by the station executive to obtain a line-of-sight tropospheric delay estimate and relayed by means of the AKuRS return signal to the AGT and the FDF. Alternatively, the raw data might be relayed for processing by the FDF, thereby reducing the processing burden at the station executive.

3.1.5 TRACKING NETWORK OPTIONS

The AKuRS relies on the use of spatially separated stations from which two-way ATDRS range and range-rate observations are made. Several considerations influence deployment of the tracking system stations:

- Visibility with respect to each ATDRS
- Geographical, climatic, and political constraints
- OD performance as a function of the network/satellite geometry
- Conformance with existing resources to facilitate economical development and ease transition into the new system

To reduce signal degradation due to ground reflections and large uncertainties in the tropospheric delay, ground stations must view the ATDRSS satellites with an elevation angle of at least 10 degrees. Furthermore, stations are best situated in areas with dry climatic conditions and stable geological features. State-of-the-art surveying is required to allow knowledge of the absolute antenna boresight position with respect to Earth-centered coordinates accurate to within 75 cm (3 σ) in each of three dimensions.

OD accuracy depends in large measure on the tracking network geometry with respect to the observed satellite. Generally, long baselines in both N-S and E-W components are desirable to minimize the geometric dilution of precision. Geographical and political constraints necessarily limit the achievable network geometry, especially because the most desirable station locations reflecting geopolitical and NASA operations considerations are those situated within CONUS.

Due to their geosynchronous locations, the beacon footprints (depicted in Figure 3-5) of ATDRS-E and ATDRS-W do not allow a long-baseline network capable of observing both satellites; consequently, independent Ku-band tracking networks have been chosen for ATDRS-E and ATDRS-W. Three networks for each satellite have been considered; one defines an all-CONUS network, and the others achieve intermediate and long baselines by situating stations outside CONUS.

Station locations for the AKuRS have been selected to correspond with either existing NASA facilities or locations on or near property currently leased or owned by the U.S. Government. The ground stations used to define the various network options are listed in Table 3-5.

Consideration of tracking performance for ATDRS-C has not been a focus of this study and has not been specifically investigated. Because the selected station sites can support ATDRS-C and provide it with superior station geometry options, OD performance is likely to be better for ATDRS-C than for ATDRS-E or ATDRS-W.

3.1.5.1 CONUS-Based ATDRS Tracking System

The following networks of ground stations are restricted to CONUS:

- The ATDRS-E beacon is observed by ground stations at White Sands (WHS), Merritt Island (MIL), and GSFC.
- The ATDRS-W beacon is observed by ground stations at WHS; Vandenberg (VAN); and Richland, Washington (WAS).
- The ATDRS-C beacon may be observed by any of the above five stations, with the best network geometry obtained by WHS, WAS, and GSFC.

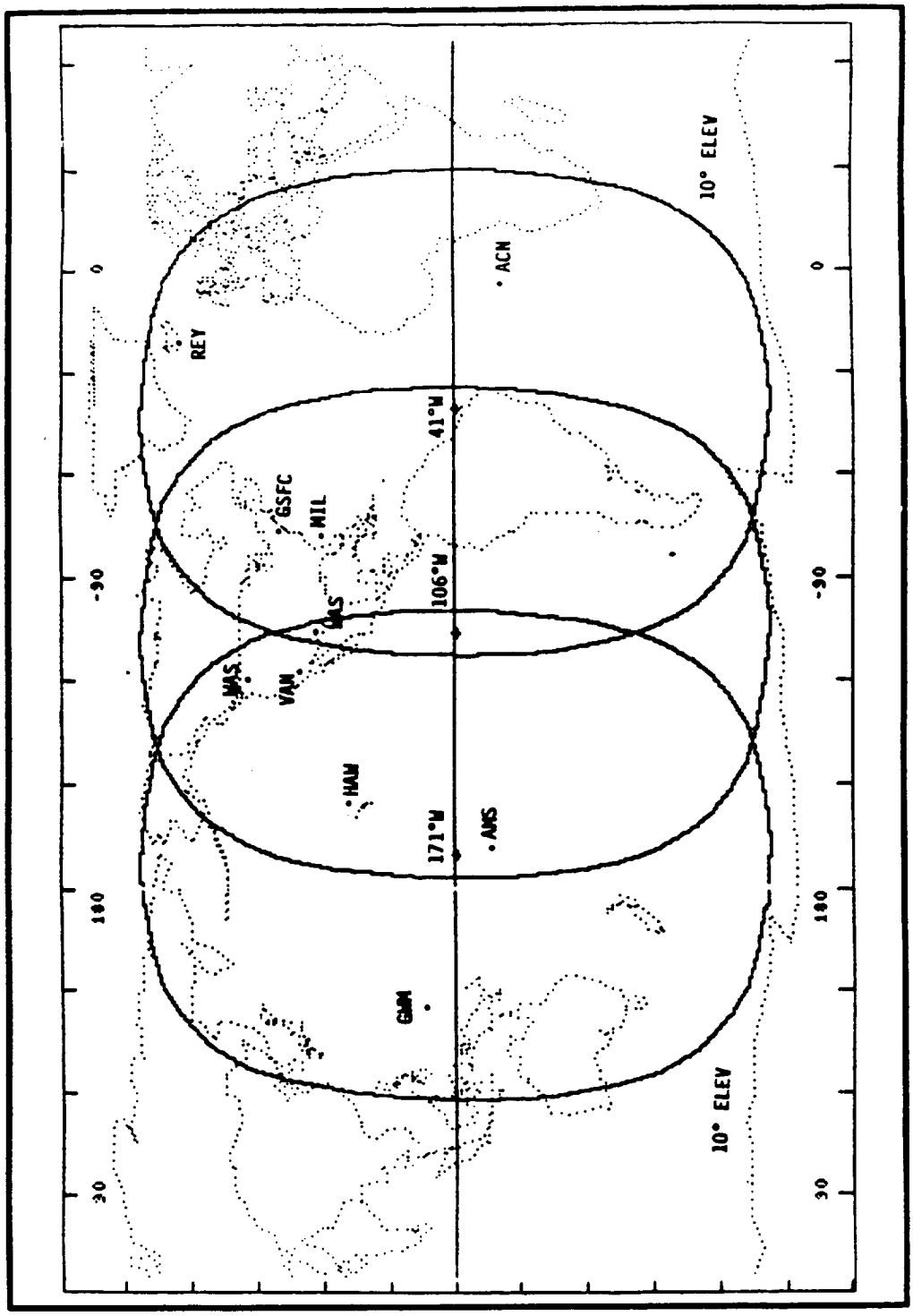

Figure 3-5. AKuRS Ground Station Options

Table 3-5. AKuRS Ground Station Sites

ACRONYM	LOCATION	VISIBILITY	REMARKS
WHSK/WHS	WHITE SANDS, NM (32° N, 107° W)	WEST, CENTRAL, EAST	ATDRSS GROUND TERMINAL
GSFC	GREENBELT, MD (39° N, 76° W)	CENTRAL, EAST	GODDARD SPACE FLIGHT CENTER
MIL	MERRITT ISLAND, FL (29° N, 81° W)	CENTRAL, EAST	EXISTING NASA FACILITY; STDN SITE
VAN	VANDENBURG AFB, CA (35° N, 121° W)	WEST, CENTRAL	STDN SITE
WAS	RICHLAND, WA (46° N, 119° W)	WEST, CENTRAL	COARSE COORDINATES NEAR HANFORD-N WEAPONS REACTOR
ACN	ASCENSION ISLAND (8° S, 14° W)	EAST	BRTS TRANSPONDER SITE
HAW	HAWAII (22° N, 159° W)	WEST, CENTRAL	STDN SITE
GWM	GUAM (13° N, 144° E)	WEST	STDN SITE
AMS	AMERICAN SAMOA (14° S, 171° W)	WEST, CENTRAL	BRTS TRANSPONDER SITE
REY	REYKJAVIK, ICELAND (64° N, 22° W)	EAST	COARSE COORDINATES NEAR NATO AIR STATION AT KEFLAVIK OPERATED BY US NAVY

MIS93JTAB

3.1.5.2 Intermediate-Baseline ATDRS Tracking System

The following networks use station locations outside CONUS, but the desire to site ground stations on U.S. territory has led to the selection of HAW as an intermediate-baseline ground station location for ATDRS-W:

- The ATDRS-E beacon is observed by WHS and REY.
- The ATDRS-W beacon is observed by WHS and HAW.
- The ATDRS-C beacon would employ the same station deployment as ATDRS-W.

3.1.5.3 Long-Baseline ATDRS Tracking System

The following networks provide the longest baselines and consequently the most advantageous geometries:

- ATDRS-E is observed by WHS and ACN.
- ATDRS-W is observed by WHS and GWM.
- ATDRS-C is observed by WHS and AMS.

Although the current TDRSS BRTS system places a BRTS transponder at Alice Springs, Australia, here the long-baseline station has been positioned in GWM to reflect geopolitical considerations.

3.2 AKuRS ASSESSMENT

This section assesses the impact of the AKuRS on ATDRS development and operations; system cost and staffing requirements; reliability, maintainability, and availability; technological risks associated with system implementation; and the ATDRS OD performance achievable with such a system.

3.2.1 ATDRS IMPACTS

Implementation of the AKuRS and its incorporation into ATDRSS affects ATDRSS development and operations in four distinct ways:

- Support of the Ku-band beacon signal
- Support of the dedicated Ku-band return signal
- AGT processing
- ATDRSS delay calibration

3.2.1.1 Support of the Ku-Band Beacon

The introduction of the Ku-band beacon as an additional ATDRSS service requires the allocation of new frequency bands to support the uplink and forward paths of the signal. Continuous use of these channels for beacon transmission precludes time sharing with any existing service. The beacon carrier frequency has been defined as 13.77522432 GHz, with the signal characteristics specified in Section 3.1.2, but the uplink channel has not been specified because its allocation depends on the ultimate ATDRSS design and the allocation of Ku- or Ka-band uplink channels.

Implementation of the Ku-band beacon requires that each ATDRS be equipped with resources capable of providing continuous wide beam forward service without affecting current KSA services. Ku-band beacon support of ATDRSS user one-way navigation further requires dedicated electronics and a beacon emitter with sufficient beamwidth to satisfy coverage requirements. An aperture on the order of 10 cm is specified to provide the 26 degree beamwidth needed to provide user coverage, with transmit power of approximately 40 W indicated to provide the necessary EIRP.

3.2.1.2 Support of the Ku-Band Return Signal

Support of the AKuRS return channel requires allocation of a dedicated Ku-band 6 MHz channel and the accompanying SGL channel. It is assumed that the Ku-band beacon emitter is diplexed to receive the return signal transmitted by the ground stations and that an onboard LNA provides sufficient amplification to establish adequate link margin. In anticipation of possible interference with KSA return services, the AKuRS return channel frequency has not been specified pending further analysis.

3.2.1.3 AGT Processing

To maintain a continuous beacon signal, the AGT must be equipped with a dedicated signal generation capability for each ATDRS. Independent beacon signals must be transmitted up to each ATDRS for broadcast. Because ground stations and users may receive more than one beacon at a time, each must be modulated with independent PN codes for identification purposes. Ground terminal resources must also include support processing to supply tracking-system control, time, and user/ground station information for transmission on the beacon.

Processing for the return signal is similar to that currently required with BRTS. Two-way range and range-rate observations, along with ground station data, must be extracted by the ground terminal and compiled for use by the FDF. The return channel is processed to yield two-way range and range-rate measurements and to extract the return data, which provides the health of the tracking stations and allows correction for tropospheric delays.

3.2.1.4 ATDRS Delay Calibration

Transmission media that affect transit time along the Ku-band beacon and return signal paths must be characterized in order to minimize the impact of range bias on ATDRS OD processing. Range bias is especially significant for ATDRSS users relying on the Ku-band beacon for one-way navigation and time transfer. Consequently, signal-path delays through the ATDRSS space segment, as well as through the AGT and ground stations, must be calibrated. The forward-path delay uncertainty, combining the effects of the uplinked beacon signal and its transit through ATDRS, has been modeled in ORAN as a range bias on the forward link of 6 m (3 σ), assuming a delay uncertainty of 20 nanoseconds (ns) (3 σ). Similarly, the return-path delay uncertainty has been modeled as a range bias on the return link of 6 m.

Calibration of the ATDRSS space segment is ideally effected through onboard measurement of a calibration signal generated locally and injected at the appropriate access points. Such calibration need not interfere with emission of the beacon or relay of the return signals if, for example, the calibration signal is a tone outside the beacon or return frequency band but within the equipment band. The time base for such differential measurements would be derived from the ATDRS frequency system, whether it be referenced to an uplinked pilot tone or to an onboard oscillator. If such local onboard measurements were not possible, the alternative would be extensive ground testing and characterization of the signal-path delays. Onboard monitoring and telemetry of component temperatures might then be used to allow modeling and estimation of the transit delay to the necessary accuracy.

3.2.2 COST AND STAFFING REQUIREMENTS

Cost and staffing requirements of the AKuRS are beyond the scope of this study. Future consideration should include investigation of this system aspect.

3.2.3 RELIABILITY/MAINTAINABILITY/AVAILABILITY

Reliability, maintainability, and availability of the AKuRS are beyond the scope of this study and should be considered in any future work.

3.2.4 TECHNOLOGICAL RISK

None of the components necessary for implementation of the Ku-band beacon concept involves the use of new technologies. The AKuRS does require appropriate enhancements to ATDRSS and the design and development of a Ku-band transponder. Ideally, the system's transponder would be one of a new generation of Ku-band user transceivers/transponders that would also support Ku-band one-way navigation.

3.2.5 EXTERNAL DEPENDENCIES

Outside ATDRSS, no external dependencies are required by this system under normal operation. As a contingency, however, dedicated telecommunications services provided by Nascom or commercial leased lines are specified to support command of the ground stations during startup or recovery periods. The cost associated with such support is dependent on the geography of the network, but the forward and return data rates could be as low as 100 bits per second (bps).

3.2.6 OBSERVATION STALENESS

Because the AKuRS relies on coherent two-way range and range-rate measurements, this data is available at the AGT with the processing of the dedicated return signal. Therefore, almost instantaneous relay of these measurements to the FDF for OD processing is possible. Outages may occur, however, during rainy periods at the stations. Ku-band links are particularly sensitive to rain outages, and degraded performance due to inclement weather is expected. The demands of tracking, however, are not as stringent as for data communications, especially because the Ku-band beacon is emitted continuously. The occasional loss of observations (for periods of less than 6 hours, for example) is acceptable for adequate tracking in most scenarios except after a spacecraft maneuver. Climatic conditions at the ground station sites must permit regular Ku-band communications throughout the year.

3.2.7 AKuRS OD PERFORMANCE

Performance of the AKuRS has been assessed using ORAN, examining OD performance with three tracking networks for each of the considered ATDRSS satellites. Solutions for definitive periods from 1 to 30 hours have been generated to provide a measure of system performance both for periods of satellite recovery following an orbital maneuver and for periods of time associated with a nominal orbital solution of 30 hours.

The error budget used with ORAN to model the AKuRS is given in Table 3-6. The table gives the values characterizing the system's two-way range and range-rate measurements and the range-bias uncertainties for each segment of the two-way signal path. The given range bias values assume an average of 3 m of uncertainty through each node in the signal path, reflecting imperfectly characterized propagation through the hardware at these points even after delay calibration. Both the AGT and the ATDRS uncertainties are combined to form a 6-m bias uncertainty along the uplink and downlink. Biases at each of the remote sites are independent of one another and modeled as 3-m biases on the forward and return links. Use of ORAN has shown that the errors due to these range biases are among the most dominant of all error contributors. Future analysis should examine the possibility of periodically estimating the biases to reduce these levels of uncertainty further. The range-rate observations, by contrast, are characterized by error due to measurement noise, with no range-rate bias assumed due to the two-way measurement type. The indicated two-way range-rate measurement noise of 0.006 cm/sec reflects typical performance corresponding to the carrier loop SNRs described in the link budgets of Tables 3-2 and 3-4.

The remaining ORAN errors are based on values specified for use by all systems in this study. The exception is ionospheric refraction error, which is assumed to be 100 percent uncertain but has minimal effect at the Ku-band and SGL frequencies. Monitoring equipment at the tracking stations has been specified to support tropospheric-delay estimation to the level of accuracy shown. Aside from errors due to A1 - UT1, all other parameters have negligible impact on the total position error.

Ku-band tracking systems are sensitive to rainfall attenuation. In order to compensate for this effect, the system must be able to change scheduled measurement times whenever weather conditions dictate. The continuous availability of the Ku-band beacon and the use of a

Table 3-6. AKuRS ORAN Error Modeling (3-σ Values)

- 2-WAY RANGE AND RANGE-RATE MEASUREMENTS
- MEASUREMENT SCHEDULE FOR EACH STATION (OVER 30-HOUR TRACKING ARC);
  - MEASUREMENTS EVERY 30 SECONDS FOR 5 MINUTES (11 OBSERVATIONS) EACH HOUR
- STATION POSITION UNCERTAINTY: 75 CM IN EACH DIRECTION
- 2-WAY RANGE MEASUREMENTS
  - RANGE MEASUREMENT NOISE: 4.0M
  - UPLINK (ATDRSS GT - ATDRS) BIAS: 6.0M
  - FORWARD (ATDRS - REMOTE STATION) BIAS: 3.0M
  - RETURN (REMOTE STATION - ATDRS) BIAS: 3.0M
  - DOWNLINK (ATDRS - ATDRSS GT) BIAS: 6.0M
- 2-WAY RANGE-RATE MEASUREMENTS
  - RANGE-RATE MEASUREMENT NOISE: 0.015 CM/SEC
  - RANGE-RATE BIAS: 0 CM/SEC
- SOLAR RADIATION: 2%
- TROPOSPHERIC REFRACTION ERROR: .045
- IONOSPHERIC REFRACTION ERROR: 1.0
- CARRIER FREQUENCY: 14,000 MHZ

dedicated return channel readily provide the AKuRS with such flexibility. Additionally, ORAN modeling shows that the OD performance is relatively insensitive to observation frequency over a 30-hour arc, with only minor OD accuracy degradations resulting from short-term outages. Further study is required to characterize the system's robustness fully in this regard.

Performance of the AKuRS is summarized in Table 3-7 for a CONUS-based network observing ATDRS-E. Appendix A provides more detailed results for all considered network options. As the results show, the system easily provides better than (less than) 75-m (3-σ) OD accuracy over a 30-hour tracking arc. For short tracking arcs, simulating the system's capability to support TR, OD accuracy is quite good, although not at the 75-m level. Nonetheless, CONUS-based tracking over a 2-hour arc provides accuracy better than (less than) 100 m (3 σ) and demonstrates the effectiveness of the AKuRS.

3.3 REFERENCES

3-1. R. Bruno and B. Elrod, TR860167, TDAS Beacon Signal Definition: Analysis and Specification, Stanford Telecommunications, Inc., October 1986

3-2. NASA/Goddard Space Flight Center, S-805-1, Performance Specification for Services via the Tracking and Data Relay Satellite System, Revision B, 4 April 1983

3-3. B. Elrod, A. Jacobsen, et al., TR25066, Tracking and Data Acquisition System (TDAS) for the 1990's: Volume VI, TDAS Navigation System Architecture, Stanford Telecommunications, Inc., May 1983

Table 3-7. AKuRS Performance

	MAXIMUM 3σ ATDRS-E POSITION ERROR OVER THE DEFINITIVE TRACKING ARC (METERS)	
	2 HR ARC	30 HR ARC
Ku-BAND ATDRS TRACKING SYSTEM (CONUS-BASED NETWORK)	77	36

7/18/89 MIS83P\AJ5645

SECTION 4 - PRECISE RANGING AND TIMING SYSTEM

The PRTS concept was initially developed by Stanford Telecommunications, Inc. (STel), as Phase I and Phase II efforts under the NASA Small Business Innovative Research (SBIR) program. Consistent with SBIR program policy, the PRTS signal structure and PRTS signal processing are considered STI proprietary. Two ATDRSS satellite tracking systems that employ the PRTS concept are presented in this section: a baseline system, termed simply "baseline PRTS," and a modification of the baseline, termed "Modified PRTS (MPRTS)." These two system options reflect the PRTS design evolution over the course of this study; ultimately, only one system will be called the Precise Ranging and Timing System. Details of proprietary system aspects of the two options are given in separate system specifications prepared in conjunction with this report (Reference 4-1, Reference 4-2). Nonproprietary system definitions and assessments of baseline PRTS and MPRTS are presented here.

In baseline PRTS, a continuously available S-band navigation beacon is transmitted by each ATDRSS satellite and observed by a network of ground tracking stations capable of making one-way pseudorange and pseudorange-rate measurements of the PRTS beacon (Reference 4-3). The PRTS beacon signal structure and signal processing combine aspects of both PN and tone ranging to allow precise one-way pseudorange measurements and calibration of ionospheric and group delays. Observation of the PRTS beacon emitted by the ATDRSS satellites would support both ATDRSS OD and one-way forward navigation by ATDRSS users. Because the PRTS signal is transmitted as a continuously available beacon, no forward link user service resources need to be scheduled for navigation support. Periodic return ATDRSS communications from the PRTS ground stations are required to allow network synchronization and relay of the measurements. This return link is supported by scheduled ATDRSS S-band multiple access (SMA) return service or, as an option, by a dedicated S-band PRTS return channel.

To support OD of the ATDRSS satellites, the PRTS beacon is observed by a network of PRTS ground stations. Ground station locations are constrained by the ATDRSS beacon footprints and other considerations, but PRTS measurements made by a ground network of two Remote Stations and a single Master Station within CONUS are capable of providing OD accuracy for each ATDRSS satellite below 75 m (3 σ), as required. Because of the orbit locations of the ATDRSS satellites, five PRTS ground stations are required: one

Master Station, visible to both ATDRS-E and ARDRS-W, and two Remote Stations for each of the two satellites. Additional equipment at a subset of these stations supports tracking of ATDRS-C. Networks involving remote stations outside CONUS provide improved geometries and further enhance ATDRSS OD accuracies.

MPRTS is similar to baseline PRTS except that, for ATDRSS OD, the ground stations coherently turn around a component of the PRTS beacon signal structure to allow measurement of two-way range and range-rate at the AGT. The MPRTS ground stations thus transmit a return signal back to the AGT that is generated coherent in carrier phase and PN epoch with the received PRTS beacon signal. The full PRTS beacon signal structure is used by the MPRTS ground stations to measure the signal path delay due to the ionosphere; these measurements are then sent to the AGT as data on the return signal. MPRTS thereby provides a means to obtain two-way range and range-rate measurements at S-band while allowing correction of the ionospheric delay contributions. Two-way range and range-rate measurements imply that the measurements are made solely with respect to the AGT clock; system clock biases, therefore, do not contribute to the OD error. Like PRTS, MPRTS offers ATDRSS users an option for enhanced one-way navigation through precise tracking of the PRTS beacon signal.

4.1 PRTS SYSTEM DEFINITION

This section provides an overview of the PRTS architecture and operations concept, describes the PRTS beacon and return signals, discusses the station architectures for both PRTS options, and outlines various potential PRTS tracking networks.

4.1.1 PRTS ARCHITECTURE AND OPERATIONS CONCEPT

Both baseline PRTS and MPRTS rely on system architectures with identical ground station deployments, channel requirements, and interfaces to the AGT. The two systems yield different observation types, however, resulting in somewhat different resource requirements. In baseline PRTS, one-way pseudorange and pseudorange-rate are measured at the PRTS ground stations, using the resolution afforded by the PRTS beacon to obtain high pseudorange precision. In MPRTS, the MPRTS ground stations coherently turn around a PRTS beacon signal component to allow two-way measurements to be made by the AGT, while the MPRTS ground stations monitor ionospheric delay using the full PRTS beacon signal structure. The following sections present the system

architectures and operational aspects of both baseline PRTS and MPRTS.

4.1.1.1 Baseline PRTS

In baseline PRTS, the PRTS beacon signal structure is employed by both the ATDRSS user spacecraft and PRTS ground stations to obtain one-way pseudorange and pseudorange-rate measurements. The measurements are termed "pseudorange" and "pseudorange-rate" to reflect the biases introduced as a result of independent transmit and receive clocks, although PRTS includes the means by which network synchronization may be established.

As illustrated in Figure 4-1, a PRTS beacon signal is generated and time-tagged by the PRTS Master Station (colocated with the AGT) and relayed via the ATDRSS uplink to the ATDRSS satellites. Depending on the ATDRSS SGL frequency allocations, the PRTS uplink may be at either Ku- or Ka-band. Independent PRTS beacon signals are transmitted to each ATDRSS satellite. After appropriate frequency translation and amplification onboard the spacecraft, the PRTS beacon is emitted by each ATDRSS satellite as a continuously available S-band navigation beacon providing Earth and ATDRSS user coverage. The beacon signals include the ATDRSS satellite ephemerides and other data needed to support one-way navigation, as provided by the NCC.

To track each ATDRSS satellite, a network of one Master and two Remote PRTS ground stations observes the PRTS beacon emitted by the satellite: each station independently estimates the one-way pseudorange and pseudorange-rate. The PRTS beacon signal structure is exploited through signal processing, allowing resolution of coarse range ambiguity, correction of ionospheric and group delay effects, and range measurement precision to the cm level. A model of the PRTS beacon measurements, presented in Figure 4-2, shows the means by which PRTS resolves the various sources of observation errors. The PRTS Remote Stations relay their observations back to the AGT via a low data rate S-band link supported by the ATDRSS satellite. Measurements are then relayed to the FDF, which is assumed to be responsible for ATDRSS OD, estimation of the Remote Station clock biases, and dissemination of the orbit solutions throughout the ATDRSS network.

Beyond merely providing a relay of the PRTS Remote Station measurements, the PRTS return signals are supported by ATDRSS as a means to estimate the Remote Station clock biases and thereby establish PRTS network synchronization.

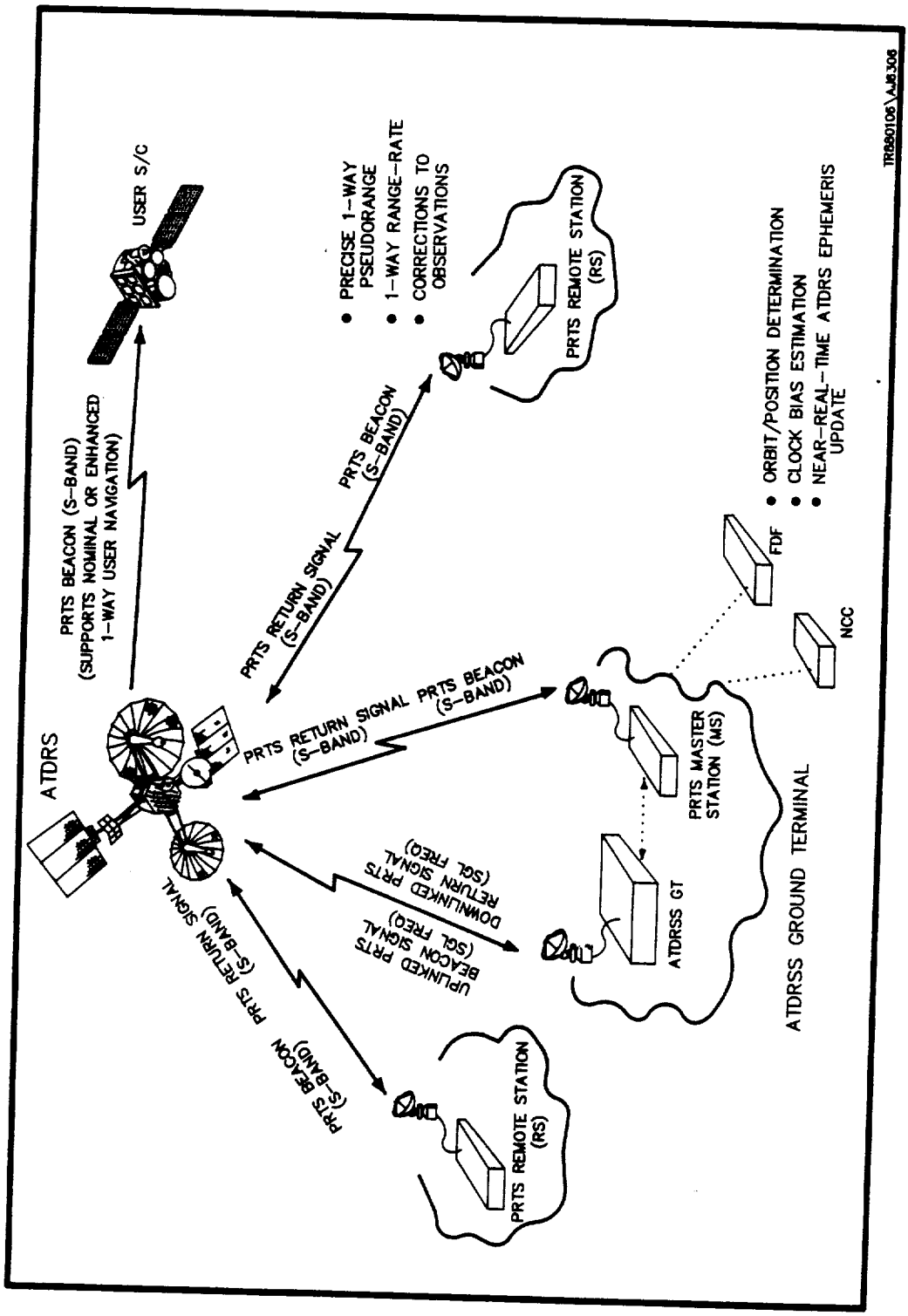

Figure 4-1. Baseline PRTS Architecture

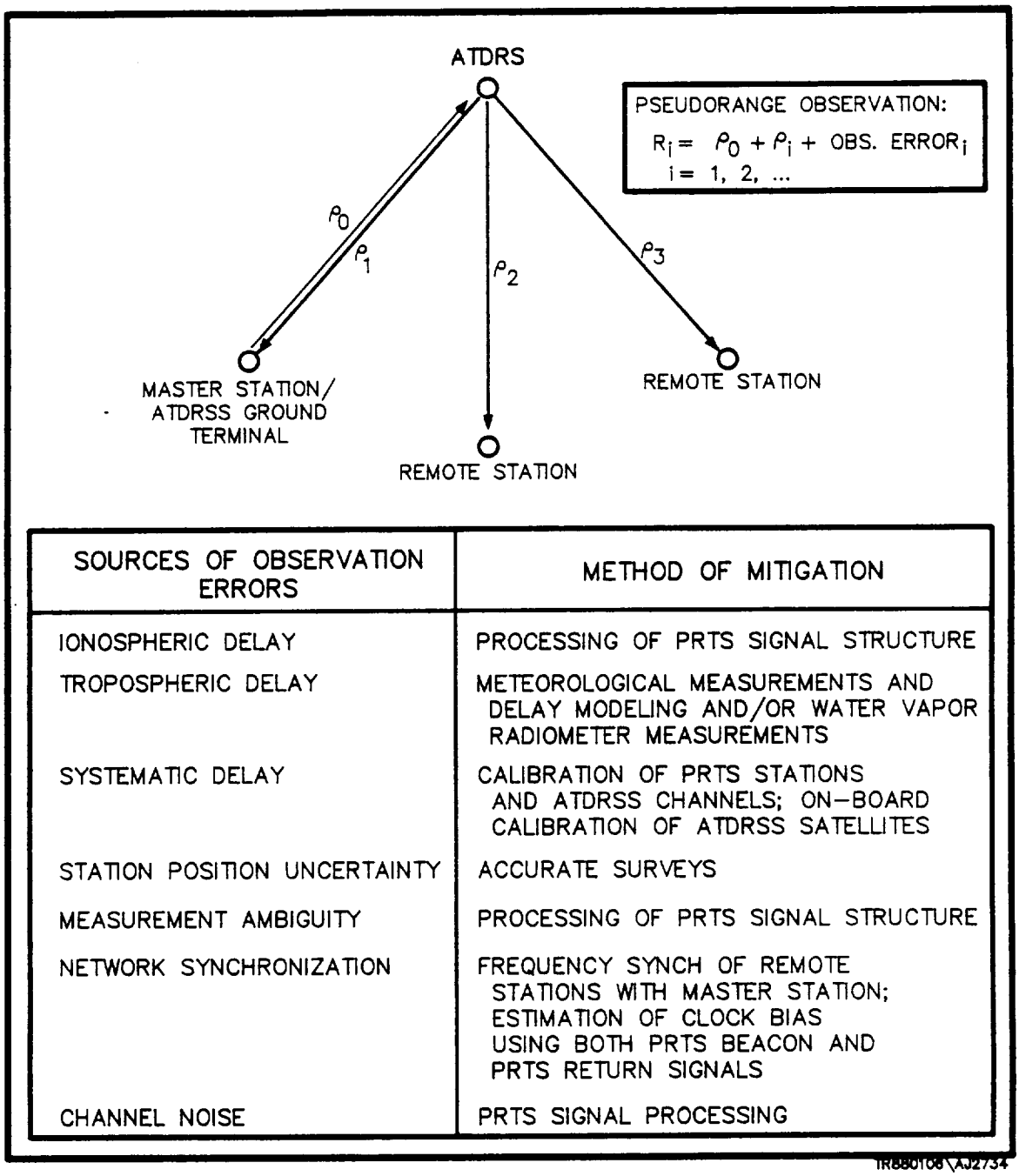

SOURCES OF OBSERVATION ERRORS	METHOD OF MITIGATION
IONOSPHERIC DELAY	PROCESSING OF PRTS SIGNAL STRUCTURE
TROPOSPHERIC DELAY	METEOROLOGICAL MEASUREMENTS AND DELAY MODELING AND/OR WATER VAPOR RADIOMETER MEASUREMENTS
SYSTEMATIC DELAY	CALIBRATION OF PRTS STATIONS AND ATDRSS CHANNELS; ON-BOARD CALIBRATION OF ATDRSS SATELLITES
STATION POSITION UNCERTAINTY	ACCURATE SURVEYS
MEASUREMENT AMBIGUITY	PROCESSING OF PRTS SIGNAL STRUCTURE
NETWORK SYNCHRONIZATION	FREQUENCY SYNCH OF REMOTE STATIONS WITH MASTER STATION; ESTIMATION OF CLOCK BIAS USING BOTH PRTS BEACON AND PRTS RETURN SIGNALS
CHANNEL NOISE	PRTS SIGNAL PROCESSING

IR880108\AJ2734

Figure 4-2. Baseline PRTS Measurement Model

The PRTS ground stations are frequency synchronized to the beacon signal but, due to signal path delays, are not phase synchronous with the Master Station clock. Range and range-rate measurement of the PRTS return signals by the AGT, in combination with the relayed PRTS beacon measurements from the Remote Stations, allows the Remote Station clock biases to be estimated either separately or as part of the ATDRSS OD solution. The PRTS return signal might be supported by any ATDRSS channel, but S-band communications using the SMA system or a dedicated PRTS return channel are the most likely options. The establishment of a dedicated return channel is especially attractive because it facilitates reduction of range biases through delay calibration and eliminates any burden to ATDRSS user services in supporting the PRTS return signal and the routine transfer of Remote Station tracking data.

Tracking network operation is directed by the NCC via the navigation message of the PRTS beacon or direct Nascom link to each of the Remote Stations. The Remote Station system executive monitors the beacon or Nascom link, extracting pertinent data and responding to commands. The Remote Stations are designed to preclude the need for resident staffing by relying on computer automation to perform routine housekeeping functions, with service technicians dispatched as necessary to repair and maintain station elements. The executive is programmed to diagnose station abnormalities, correct those it can, and continuously inform the Master Station (via the ATDRSS return data link or Nascom link) of the station health. Should a Remote Station unexpectedly lose contact with the beacon, the executive is programmed to access the ground terminal via the Nascom link for further instruction. Trained personnel, sent to the station as needed, repair or replace defective station components and perform routine maintenance and system calibration.

4.1.1.2 Modified PRTS

MPRTS, as depicted in Figure 4-3, relies on coherent turnaround of a component of the PRTS beacon signal by a network of MPRTS ground stations, with two-way range and range-rate measurements then made by the AGT. This distinction from the baseline PRTS concept does not change the way in which ATDRSS users may employ the full PRTS beacon signal for enhanced one-way navigation, but it does simplify the MPRTS ground stations in comparison to those of the baseline system.

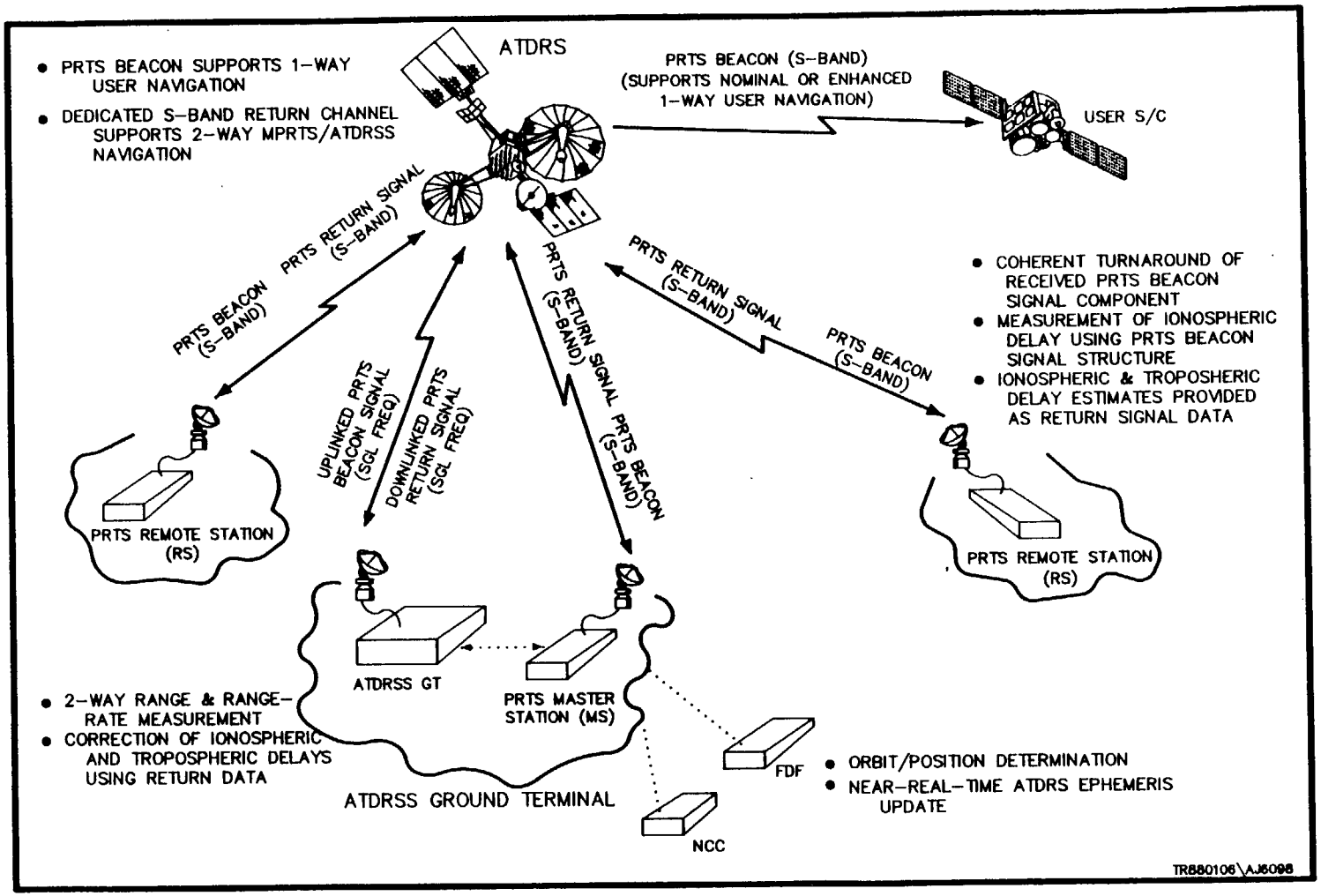

Figure 4-3. MPRTS Architecture

As in baseline PRTS, a PRTS navigation beacon is generated by the MPRTS Master Station for each ATDRSS satellite and relayed by the AGT to the designated ATDRS. To avoid potential interference at ground stations and user spacecraft exposed to multiple beacons, independent beacon signals are transmitted to each ATDRSS satellite, using different PN codes. After appropriate frequency translation and amplification onboard the satellite, the S-band signal is emitted by each ATDRSS satellite as a continuously available navigation beacon providing Earth and ATDRSS user coverage.

A network of MPRTS ground stations observes the beacon, each capable of receiving the signal and transmitting a coherent return signal back to the AGT via a dedicated channel. Coherent turnaround of the beacon requires that the return signal use the recovered beacon carrier as its frequency reference and that the return signal's epoch be synchronized with the received beacon reference channel epoch. The coherent return signal, as in baseline PRTS, could be transmitted via any ATDRSS return service; because the return channel is essential to ATDRSS OD, however, a dedicated channel is specified here to provide a level of performance comparable to that of SSA return services. The return signal is processed at the AGT to yield two-way range and range-rate measurements, as illustrated in Figure 4-4. As in baseline PRTS, the measurements obtained at the AGT are then relayed to the FDF for ATDRSS OD processing.

Besides coherently generating the return signal, the MPRTS Remote Stations monitor local atmospheric conditions to allow estimation of the tropospheric delay and process the received PRTS beacon signal to estimate the ionospheric delay. Both ionospheric and tropospheric delay data are then included in the health, status, and data messages sent to the AGT via the MPRTS return signal.

4.1.2 PRTS BEACON SIGNAL

The PRTS beacon signal supports both ATDRS and ATDRSS user navigation and both the baseline PRTS and MPRTS ATDRSS tracking networks. The unique PRTS beacon signal structure allows PRTS-specific receivers to realize fully the PRTS range measurement precision and the measurement of ionospheric delay through appropriate signal processing. The following sections treat these issues, as well as the generation and transmission of the PRTS beacon.

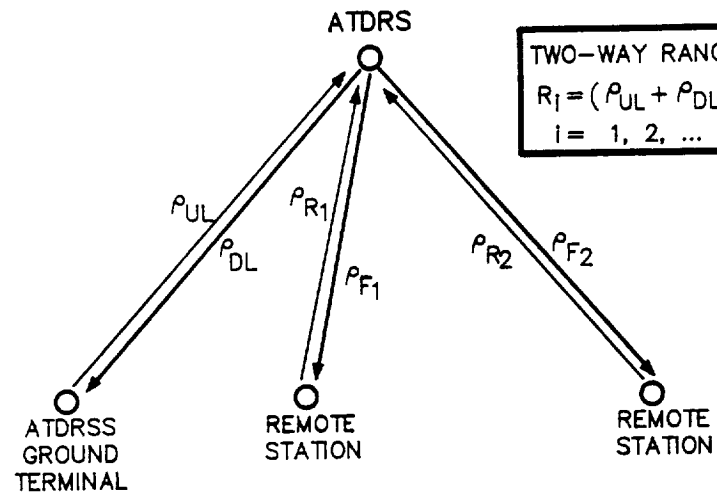

SOURCES OF OBSERVATION ERRORS	METHOD OF MITIGATION
IONOSPHERIC DELAY	ONE-WAY PROCESSING OF PRTS BEACON SIGNAL STRUCTURE
TROPOSPHERIC DELAY	METEOROLOGICAL MEASUREMENTS AND DELAY MODELING AND/OR WATER VAPOR RADIOMETER DATA INCLUDED ON RETURN LINK
SYSTEMATIC DELAY	STATION CALIBRATION; ON-BOARD CALIBRATION OF ATDRSS SATELLITES
STATION POSITION UNCERTAINTY	ACCURATE SURVEYS
MEASUREMENT AMBIGUITY	PROCESSING OF THE BEACON SIGNAL STRUCTURE
NETWORK SYNCHRONIZATION	TWO-WAY MEASUREMENT ELIMINATES CLOCK BIASES

TR880106\A.J2735

Figure 4-4. MPRTS Measurement Model

4.1.2.1 PRTS Beacon Signal Structure

The PRTS beacon signal structure is made up of several disjoint spectral components spanning a bandwidth of 78 MHz but occupying only 16.2 percent of this bandwidth. One spectral component defines the reference channel, a data-modulated signal identical to the recommended ATDRSS S-band user navigation beacon (Reference 4-4). The remaining components define auxiliary channels and are used in one-way PRTS signal processing to obtain the full PRTS range measurement precision and to allow measurement of ionospheric and group delays. The PRTS signal structure may be processed by ATDRSS users as well as the PRTS ground stations; moreover, ATDRSS users may neglect the PRTS beacon auxiliary channels and process only the reference channel to support one-way user navigation. Complete signal structure details are provided in the PRTS system specifications (Reference 4-1). The proprietary PRTS beacon signal structure inherently allows

- Measurement of both one-way pseudorange and one-way pseudorange-rate, with the pseudorange measurements exhibiting high precision as a result of the wideband time resolution provided by the spectrally efficient PRTS signal
- Calibration of ionospheric and group delays
- Range ambiguity resolution
- Generation of an Earth coverage beacon that meets signal flux density constraints
- High SNR
- Efficient coherent signal processing
- Navigation beacon support for those users who do not require PRTS measurement precision and/or are not capable of PRTS signal processing
- Broadcast of a navigation message, including ATDRSS network data for use by both the PRTS ground stations and ATDRSS users; as an option, commands and messages might be included to support user demand access, rapid service acquisition, PRTS ground station control, and notification of service schedule changes

4.1.2.2 PRTS Beacon Signal Generation and Relay

The PRTS beacon signal is generated by the PRTS Master Station and uplinked to each ATDRSS satellite for emission as an S-band navigation beacon. Due to the nature of the PRTS measurements, system delay uncertainties are a potential major source of measurement error and must be minimized. Onboard the ATDRSS satellite, the beacon signal path is a dedicated path that must have minimal delay uncertainty, either through onboard monitoring or prelaunch calibration. Similarly, delay uncertainties in the generation of the beacon signal at the ground must also be minimal so that the time-tag corresponding to the signal epoch accurately reflects the true transmit time. In this study, uncertainties in the forward path through the ground station and the ATDRSS satellite have been modeled as 6 m (3 σ) or, equivalently, 20 ns, conservatively reflecting achievable calibration precisions.

A PRTS beacon signal is generated by a Master Station and uplinked to each ATDRSS satellite by the AGT. Adequate ATDRSS SGL bandwidth for the PRTS beacon signal at either Ku- or Ka-band must be allocated for its uplink to each ATDRSS satellite. The spatial separation between satellites allows the same SGL frequency allocation for each ATDRSS satellite, with the PRTS beacon signal frequency multiplexed with the other components of each satellite's SGL uplink.

After the uplink is received by the ATDRSS satellite, it is frequency translated and amplified for emission as an S-band navigation beacon. In TDRSS, the SMA system provides a (two-sided) beamwidth of 26 degrees, thereby continuously supporting users to altitudes as great as 3122 kilometers (km). In ATDRSS, a similar beamwidth has been considered for the navigation beacon; alternatively, the beamwidth might be reduced to obtain greater antenna gain (at the loss of support to higher altitude users). The beacon antenna could be a dedicated forward element of the SMA array or a separate parabolic dish. For a parabolic dish, a 3-dB beamwidth of 26 degrees implies an antenna gain of approximately 16.5 dB and a diameter of approximately 0.4 m. The link budget of Table 4-1 focuses on the weaker ATDRS-to-ground station link and demonstrates that an EIRP of 29.0 dBW is required to ensure adequate carrier loop SNR at the PRTS receivers. With a parabolic dish of 0.4 m, an amplifier yielding 15.5 dBW (approximately 36 W) would be needed to support ATDRS transmission of the S-band PRTS beacon and provide the necessary EIRP at the 3-dB beam edges.

Table 4-1. PRTS Beacon Link Budget

LINK ELEMENT	VALUE	COMMENTS
(1) SATELLITE EIRP (dBW)	29.0	REFLECTS COMPOSITE EIRP OF PRTS SPECTRAL COMPONENTS
(2) PATH LOSS (dB)	192.0	S-BAND, ~2100 MHz
(3) RECEIVE ANTENNA G/T (dB/°K) AT PRTS STATION	-2.7	• ANTENNA GAIN: 24.3 dB - 1 METER DISH - 55% EFFICIENCY • NOISE TEMPERATURE = 500°K
(4) BOLTZMANN'S CONSTANT (dBW/Hz - °K)	-228.6	
(5) RECEIVED C/N_o (dB-Hz)	62.9	(1) - (2) + (3) - (4)
(6) C/N_o FOR REFERENCE CHANNEL (dB-Hz)	59.9	REFLECTS BASELINE ATDRSS NAVIGATION BEACON
(7) C/N_o FOR EACH AUXILIARY CHANNEL (dB-Hz)	55.1	REFLECTS EACH AUXILIARY PRTS SPECTRAL COMPONENT
(8) IMPLEMENTATION LOSS (dB)	3.0	ASSUMED VALUE
(9) NET C/N_o (dB-Hz) - REFERENCE CHANNEL - EACH AUXILIARY CHANNEL	 (a) 56.9 (b) 52.1	 (6) - (8) (7) - (8)
(10) HOUSEKEEPING DATA RATE (dB-Hz)	24.0	125 BPS, SUPERIMPOSED ON REFERENCE CHANNEL PN CODE
(11) E_b/N_o (dB)	32.9	• (9a) - (10) • PROVIDES BER << 10^{-5}
(12) CARRIER LOOP SNR (dB) - EACH AUXILIARY CHANNEL SPECTRAL COMPONENT	35.1	• 50 Hz LOOP BANDWIDTH (17 dB-Hz) • (9b) - 17 dB-Hz • YIELDS 1° - 2° RMS TRACKING ERROR • YIELDS 2.3 - 4.6 MM/SEC RMS DOPPLER ERROR, ASSUMING 10 SEC AVERAGING

NOTE: LINK MARGIN CAN BE INCREASED BY REDUCED ANTENNA TEMPERATURE AND/OR LARGER ANTENNA.

4.1.2.3 PRTS Beacon Signal Processing

Signal processing of the PRTS navigation beacon to obtain one-way pseudorange and pseudorange-rate is performed by the baseline PRTS Master Station and Remote Stations, as well as by any properly equipped ATDRSS user. Processing of the PRTS beacon in the MPRTS tracking network to estimate ionospheric delay is effectively a subset of baseline PRTS processing and is, therefore, not explicitly discussed here. Full details of the proprietary PRTS signal processing may be found in the PRTS and MPRTS system specifications (Reference 4-1, Reference 4-2).

One-way pseudorange measurement by the baseline PRTS ground stations or by ATDRSS users is made possible by the time-tag embedded in the data by the Master Station, representing the time of transmission of the signal epoch with respect to the Master Station's clock. Through processing of the received signal, a beacon receiver establishes the time of arrival of the signal's epoch with respect to the receiver's own clock. This value is then subtracted from the time-tag included in the beacon navigation message to obtain the measured path delay; multiplication by the speed of light converts the time-delay measurement to a pseudorange value.

One-way range processing of this sort may be performed on either the complete PRTS beacon signal structure or, with simpler processing and reduced measurement precision, on the reference channel alone. Both modes of operation allow resolution of range ambiguity and support one-way pseudorange and pseudorange-rate estimation. Processing of the full PRTS signal structure, however, affords improved range resolution and the means to correct for ionospheric and group delay effects. Simulation results show that processing of the reference and auxiliary channels permits estimation of ionospheric delays to subnanosecond precision (Reference 4-3).

The link budget shown in Table 4-1 reflects the analytic, simulation, and laboratory results of the Phase II SBIR effort (Reference 4-3), providing target values of the received net C/N_0 and carrier loop SNR that yield subnanosecond rms timing precision and suitably low rms phase errors. By assuming that the PRTS ground stations employ a 1-m parabolic dish to receive the PRTS beacon, thus providing sufficient beamwidth to observe the ATDRSS satellites without cracking, the necessary ATDRSS satellite EIRP to support the S-band PRTS beacon may be determined.

4.1.3 PRTS RETURN SIGNAL

Although the PRTS beacon signal just described is the same for both the baseline PRTS and MPRTS tracking networks, the return signals associated with each system are distinctly different. In baseline PRTS, a one-way return signal is generated to allow the AGT to measure one-way return pseudorange and pseudorange-rate; in MPRTS, the return signal is coherently related to the received beacon signal to allow the AGT to measure two-way range and range-rate. The following subsections provide more detailed descriptions of these two return signal types.

4.1.3.1 Baseline PRTS One-Way Return Signal

The baseline PRTS return signal supports the routine transfer of measurements and data from the PRTS Remote Stations back to the Master Station and, more important, allows the clock biases between the Remote Stations and the Master Station to be estimated. Other users of the PRTS navigation beacon (or its reference channel) need not transmit a PRTS return signal; the PRTS beacon supports one-way forward navigation without use of any return signal.

The baseline PRTS return signal is specified as a low data rate S-band signal that uses a signal structure compatible with ATDRSS SMA return service, supported by either the SMA system or a dedicated PRTS return channel. The baseline PRTS return signal structure, its generation, and its processing are discussed in the section that follows.

4.1.3.1.1 Baseline PRTS Return Signal Structure

The baseline PRTS return signal could be a one-way ATDRSS SMA, S-band single access (SSA), or even KSA return signal as long as it supports one-way return pseudorange and, less important, pseudorange-rate measurement. The only purpose of one-way pseudorange measurements using the baseline PRTS return signal is to allow estimation of the PRTS Remote Station clock biases. As demonstrated using ORAN, the PRTS return signal measurements must be available at least every 12 hours to support estimation of Remote Station clock biases. The relay of Remote Station data, however, requires more frequent return transmission, modeled here as at least a 5-minute contact every hour. Given ATDRSS resources, the PRTS return signal would be supported best by the SMA return system or by a dedicated PRTS return channel.

To consider both possible options, it has been assumed that the dedicated PRTS return channel is provided at S-band and is essentially compatible with the SMA return system. The baseline PRTS return signal is then specified as

- Modulation: SQPN
- PN code rate: 31/(240 x 96) x (carrier frequency)
- PN code length: $2^{11} - 1$
- PN code family: Gold codes
- Data format: Nonreturn to zero (NRZ)
- Data rate: 125 bps
- Carrier frequency: 2287.5832 MHz (nominal)

The cited data rate of 125 bps may be less than that supported by the SMA return system, but it can be readily raised to any minimum required data rate. Similarly, the specified carrier frequency may be changed if necessary to support a dedicated PRTS return channel.

4.1.3.1.2 Baseline PRTS Return Signal Generation and Relay

As discussed, the PRTS return signal might be supported either by the ATDRSS SMA return service or by a dedicated PRTS return channel. Because there is no requirement that the PRTS ground stations communicate simultaneously with the AGT, only a single SMA return channel might be used to support the baseline PRTS return signal, the beam being formed and directed independently to each Remote Station. If supported by a dedicated return channel, the return signal transmissions might be similarly time division multiplexed through scheduling of the return transmissions. Alternatively, if the PRTS dedicated channel is supported by an ATDRS antenna with sufficient coverage, and if the AGT can support simultaneous processing of several PRTS return signals from a single ATDRSS satellite, then distinct PN codes might be used by each PRTS ground station to provide code division multiplexing.

Although reduction of signal path delay uncertainties is necessary in the generation of the PRTS beacon signal, the PRTS return signal path does not need to be calibrated to the same level of accuracy. Using ORAN, ATDRSS OD accuracies were shown to be influenced only slightly by range biases on the PRTS return signal path, even assuming worst-case conditions. For example, in TDRSS, two-way range systematic error contributions due to the TDRSS satellite

and ground terminal are specified as ± 35 ns and ± 30 ns, respectively (Reference 4-4). Accordingly, similar values may be applied to the one-way PRTS return signal as worst case numbers by assuming a 3-σ uncertainty of 10 m (33 ns) in the return path through the PRTS ground station and ATDRSS spacecraft and an equal uncertainty through the ATDRSS spacecraft and AGT. By comparison, similar modeling of the current TDRSS BRTS has used even smaller range bias values.

Independent of whether the PRTS return signal is supported by a return SMA channel or a dedicated channel, the link budget of Table 4-2 assumes S-band return communications from the PRTS ground stations to the ATDRSS satellite and focuses on that link as typically the weaker of the two ATDRSS links. This link budget applies to both baseline PRTS and MPRTS. The link budget is parameterized by the ATDRSS G/T supporting the PRTS return signal and the transmit power at the ground station, assuming that the 1-m parabolic dish used by the PRTS ground stations to receive the beacon is diplexed to transmit the PRTS return signal.

If supported by a return SMA channel and the G/T corresponding to a formed beam, the PRTS ground stations can easily provide the necessary power to satisfy minimum signal-to-noise requirements at the AGT. If supported by a dedicated PRTS return channel that offers full Earth coverage, however, then considerably less G/T would be available. Even then, link margin requirements could be readily met simply by increasing the power of the PRTS ground station transmitters or possibly increasing the size of the antenna.

As an example, a dedicated PRTS channel might be provided through diplexing the PRTS beacon antenna. Two possible beacon antenna options have been discussed: a 0.4-m parabolic dish and use of a single element of the SMA array. If the beacon antenna were a 0.4-m parabolic dish, then, assuming a noise temperature of 170° K for the on-board S-band LNA (corresponding to a noise figure of 1.6 dB), the ATDRSS G/T would be -5.8 dB/K. Alternatively, if the beacon were supported by a single element of the SMA array, then, assuming state-of-the-art technology, the element might be diplexed (or another single element used) to support a G/T of -11 dB/K (Reference 4-5).

The reduced G/T of a dedicated PRTS return channel compared to nominal SMA return service implies that the PRTS ground

Table 4-2. PRTS Return Signal Link Budget

LINK ELEMENT	VALUE	COMMENTS
(1) PRTS STATION EIRP (dBW)	24.3 + P	• P = XMIT POWER (dBW) • ANTENNA GAIN: 24.3 dB - 1 METER DISH - 55% EFFICIENCY
(2) PATH LOSS (dB)	192.0	S-BAND, ~2100 MHz
(3) ATDRSS G/T (dB/°K)	G/T .	INCLUDING COMBINER GAIN, IF APPROPRIATE
(4) BOLTZMANN'S CONSTANT (dBW/Hz - °K)	-228.6	
(5) IMPLEMENTATION AND INTERFERENCE LOSSES	4.0	ASSUMED VALUE
(6) RECEIVED C/N_o (dB-Hz)	P + G/T + 56.9	(1) - (2) + (3) - (4) - (5)
(7) RETURN DATA RATE (dB-Hz)	24.0	125 BPS, SUPERIMPOSED ON 3 Mcps PN CODE
(8) E_b/N_o (dB)	P + G/T + 32.9	• (6) - (7) 10^{-5} BER REQUIRES E_b/N_o > { 9.6 (UNCODED) / 4.6 (CODED) }
(9) CARRIER LOOP SNR (dB)	P + G/T + 39.9	• 50 Hz LOOP BANDWIDTH (17 dB-Hz) • (6) - 17 dB-Hz

stations will provide more EIRP than do typical ATDRSS SMA users. Assuming a return SMA signal structure is supported by the PRTS dedicated channel, interference difficulties may be mitigated by using an orthogonal polarization (e.g., right-hand circular polarization rather than the TDRSS return SMA system's left-hand circular polarization) or, if necessary, by allocating a different return carrier frequency to support the PRTS dedicated return channel.

4.1.3.1.3 Baseline PRTS Return Signal Processing and Network Synchronization

Processing of the baseline PRTS return signal is performed by the AGT: the PN code and carrier phase are tracked, range and range-rate estimates are extracted, and data is demodulated. The baseline PRTS return signal is meant to provide one-way return range and range-rate measurements, although one-way return ranging is not currently supported by TDRSS and is not explicitly specified for the AGT (Reference 4-6). Ionospheric correction of the S-band return signal is achieved through the Remote Station measurements of the PRTS S-band beacon signal: the beacon's measured ionospheric delay is included as data on the return signal and, after scaling to the return S-band frequency, applied to the return signal (ionospheric delay of Ku- or Ka-band SGL is neglected). This procedure to allow ionospheric correction of the signal received at the AGT is also followed in MPRTS.

The return signal range and range-rate uncertainties have been conservatively modeled in this study as those that would correspond to dedicated one-way return S-band performance: 7.5-m (3-σ) range uncertainty, 3.5 millimeters per second (mm/sec) (3-σ) range-rate uncertainty. Such values require a received C/N_0 of at least 43.4 dB-Hz and a carrier loop SNR of at least 21.4 dB, assuming 10 sec Doppler averaging time and fairly conservative performance (Reference 4-7). Achievement of the indicated range uncertainty and C/N_0 of 43.4 dB-Hz is then the main driver. The link budget shown in Table 4-2 and the previous discussion concerning support of the dedicated PRTS return channel allow calculation of the PRTS return signal transmit power. Assuming use of a diplexed 0.4-m parabolic antenna and a 170° K LNA onboard the ATDRSS satellites (to provide G/T of -5.8 dB/K), the ground station transmit power must be -7.7 dBW or greater; assuming use of a single diplexed SMA element providing G/T of -11.0 dB/K, the ground station power must be at least -2.5 dBW.

Given a set of one-way PRTS beacon and one-way PRTS return signal measurements as obtained in baseline PRTS, the clock biases between the Remote and Master Stations may be estimated to establish PRTS network synchronization. Figure 4-5 provides a simple illustration of the concept, demonstrating how the forward and return measurements made between a single Remote Station and the Master Station may be differenced to yield an estimate of the constant offset between their respective clocks.

The key element of Figure 4-5 is the manner in which time is referenced to the Master Station's clock. Because the PRTS Remote Stations are frequency synchronized to the Master Station via the PRTS beacon signal, only the offset in phase between clocks is significant. The error in the bias estimate of Figure 4-5 is dominated by those elements of the forward and return signal paths that are not identical: differences in path delay due to nonsimultaneity of the forward and return measurements that have not been adequately corrected, uncorrected differences in the path delay due to non-identical forward and return path delays, and so forth. In assessing PRTS/ATDRSS OD performance, these errors have been modeled in ORAN as range biases in the forward and return signal paths with a 3-m (3-σ) uncertainty at each node.

4.1.3.2 MPRTS Return Signal

In MPRTS, the S-band return signal is intended to support the two-way communications required by MPRTS. To avoid burdening the SSA return system, a dedicated S-band return channel is provided with the ATDRS beacon emitter diplexed as a receive antenna. The signal structure is defined in the MPRTS system specifications (Reference 4-2) and is designed to be compatible with the reference channel of the beacon to allow its coherent turnaround. The return signal, thus, has a transmit frequency coherently related to the beacon's reference channel receive frequency and the epoch of the signal's PN code is synchronized to the received PN code epoch of the beacon reference channel.

4.1.3.2.1 MPRTS Return Signal Structure

The MPRTS return signal is a PN-spread low data rate signal coherently related to the received PRTS beacon reference channel. The return carrier frequency and PN code rate are thus related to the received beacon reference channel frequency, whereas the PN code length is the same as that of the reference channel. The return channel is 6 MHz wide to provide measurement resolution comparable to current two-way

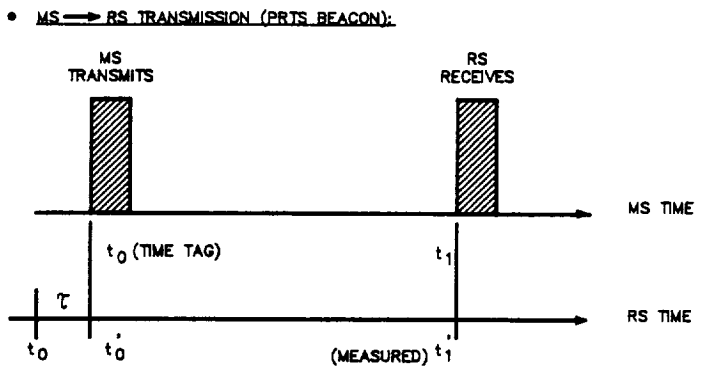

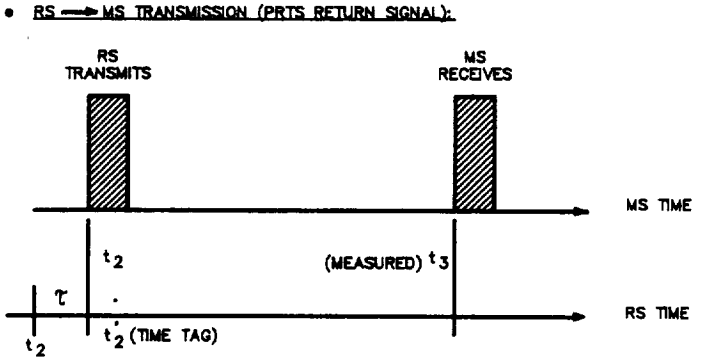

MEASUREMENTS	FWD	$T_F = (t_1' - t_0) = (t_1 - t_0) + \tau + \varepsilon_F$
	RTN	$T_R = (t_3 - t_2') = (t_3 - t_2) - \tau + \varepsilon_R$
CLOCK BIAS ESTIMATE		$\hat{\tau} = (T_F - T_R)/2$
BIAS ESTIMATE ERROR		$\tilde{\tau} = \Delta T_{FR} + (\varepsilon_F - \varepsilon_R)/2$
ΔT_{FR}		RESIDUAL SYSTEMATIC ERROR BETWEEN FWD & RTN PROPAGATION PATHS
$\varepsilon_F, \varepsilon_R$		RANDOM ERRORS IN FWD & RTN TIMING MEASUREMENTS

TR880106\AJ8288

Figure 4-5. Baseline PRTS Network Synchronization

TDRSS navigation services. More complete discussion of the MPRTS return signal is provided in the MPRTS system specification (Reference 4-2).

4.1.3.2.2 MPRTS Return Signal Generation and Relay

Much of the discussion concerning baseline PRTS return signal generation applies to MPRTS, with the distinction that the MPRTS return signal is coherently related to the received PRTS beacon signal. Because ATDRSS OD using MPRTS relies on the return signal, a dedicated channel is required to avoid dependence on ATDRSS user services. The link budget of Table 4-2 and the accompanying discussion surrounding use of a dedicated PRTS return channel then apply directly to MPRTS.

4.1.3.2.3 MPRTS Return Signal Processing

Processing of the MPRTS return signal is performed by the ATDRS Ground Terminal in the same manner as any two-way signal: the PN code and carrier phase are tracked, range and range-rate estimates are extracted, and data is demodulated. The MPRTS ground station estimates of the beacon's ionospheric delay are included as part of the return signal data and are used to correct the forward and return S-band range measurements. Range and range-rate uncertainties are otherwise similar to those obtained in nominal ATDRSS S-band two-way navigation; there is no need to estimate Remote Station clock biases with two-way measurements.

4.1.4 PRTS STATION ARCHITECTURE

The ground station design depends in part on which system--baseline PRTS or MPRTS--is employed, with the MPRTS station architecture representing a simplification of the baseline PRTS design. In general, the PRTS ground stations are envisioned to be relatively compact facilities, capable of operating untended for extended periods. Many of the system's functions may be implemented at the circuit-board level and would be incorporated into thermally controlled units suitable for ready deployment. The usual requirements of any ground station apply, e.g., adequate shelter, power, and environmental control. Moreover, to minimize the effects of station position uncertainty, the station sites must be surveyed using state-of-the-art techniques to locate the absolute antenna boresight position with respect to Earth-centered coordinates accurate to within 75 cm (3 σ) in each of three dimensions.

The following discussion treats the station architectures of both baseline PRTS and MPRTS system options, covering the baseline PRTS station architecture and then highlighting the differences involved in MPRTS.

4.1.4.1 Baseline PRTS Station Architecture

Elements of the baseline PRTS Master and Remote Stations are treated in detail in the baseline PRTS system specifications (Reference 4-1) and are summarized in Figure 4-6, which depicts common attributes of both the baseline PRTS Master and Remote Stations. Those stations that observe more than one ATDRSS satellite, such as the Master Station and those Remote Stations supporting ATDRS-C as well as ATDRS-W or ATDRS-E, must be equipped with distinct and independent equipment chains to support each observed satellite. The distinctions between the Master and Remote PRTS Stations are relatively minor and are noted in the following discussion of the seven station components: the station executive, PRTS transmitter subsystem, antenna subsystem, PRTS receiver subsystem, station clock subsystem, atmospheric monitor equipment, and Nascom interface equipment.

4.1.4.1.1 Station Executive

The station executive provides the highest level of control of the PRTS tracking station and would be implemented as one or more mini- and/or microcomputers. Functions include control of all processing of the received PRTS beacon signal, calibration of the station's equipment, final calculation of the station's range and range-rate measurements after correction for various error sources, and preparation of the data to be relayed back to the Master Station via the PRTS return signal. A distributed control strategy is envisioned in the design of the PRTS ground stations so that corrections established by the station executive are made available to other elements of the station as required. In the case of the Master Station, the station executive must support the generation of the beacon signal and interface with NASA's FDF and/or the NCC to obtain updates to the beacon's navigation message. Many of the functions of the station executive are identical in both the baseline PRTS and MPRTS options.

4.1.4.1.2 Baseline PRTS Transmitter Subsystem

In each Remote Station, the baseline PRTS transmitter subsystem comprises the upconverter, S-band high-power amplifier (HPA), and signal generator necessary to produce the baseline PRTS one-way return signal. In addition, the

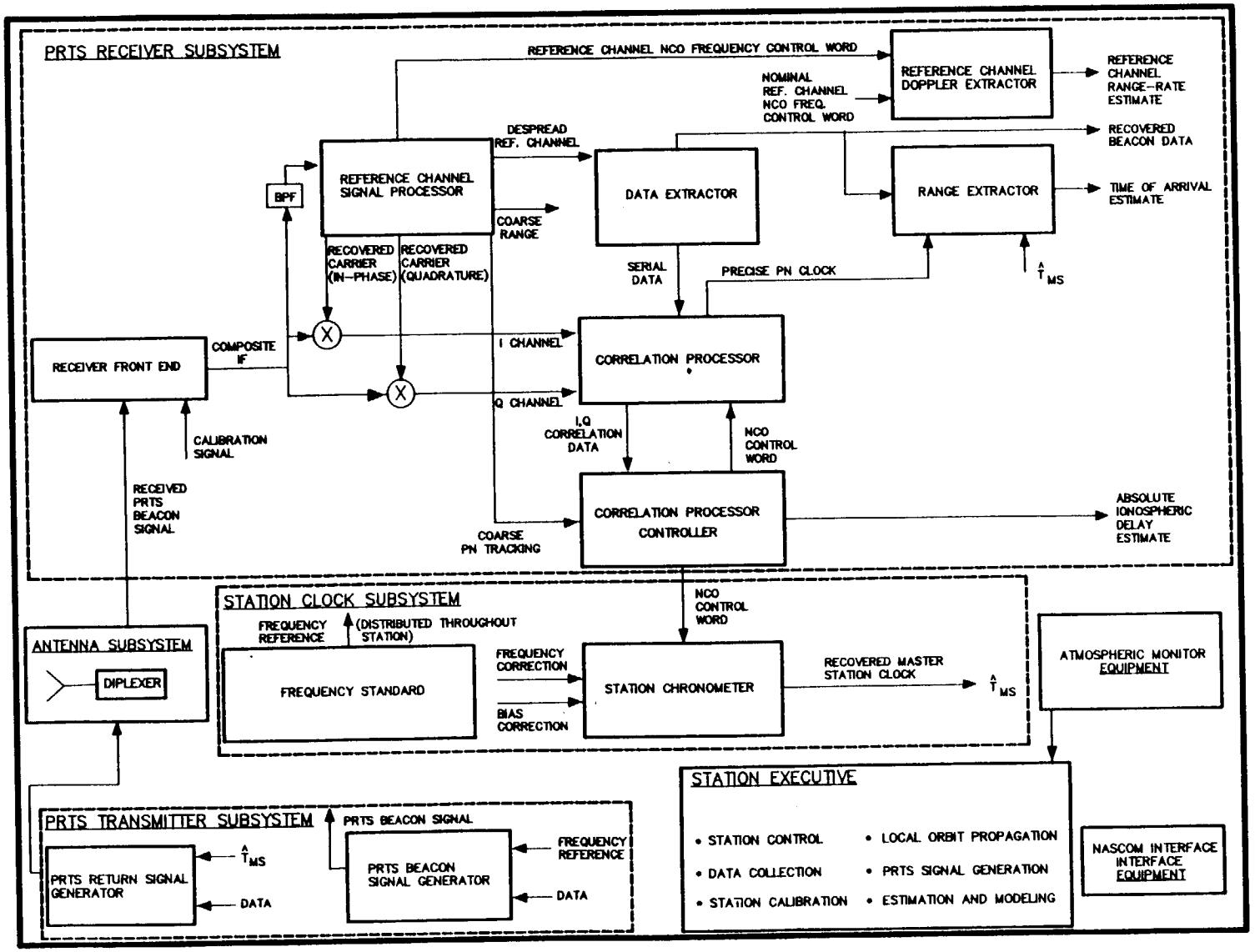

Figure 4-6. Baseline PRTS Ground Station Architecture

transmitter subsystem supports calibration of the Remote Station by generating a PRTS beacon signal to calibrate the PRTS receiver subsystem and local calibration signals for estimation of system delays.

In the Master Station, a beacon signal generator for each supported ATDRSS satellite must also support continuous generation of the PRTS beacon signal, providing an intermediate frequency (IF) output to the AGT for uplink to each satellite.

4.1.4.1.3 Antenna Subsystem

At the PRTS ground stations, a 1-m diplexed parabolic dish supports both reception of the PRTS beacon and transmission of the PRTS return signal for each observed ATDRSS satellite. This subsystem is identical in both the baseline PRTS and MPRTS options. Because the ATDRSS satellites are in geosynchronous orbits, antenna pointing is not a required capability unless non-nominal tracking, such as during orbit insertion, must be supported. In the PRTS Master Station, three 1-m antennas and their associated equipment chains are required to support observation of the beacons transmitted by the three ATDRSS satellites.

The choice of antenna size is dependent on trade-offs among the beacon EIRP, the ATDRS G/T for the return channel, and the ATDRS inclination. Given the potential that the ATDRSS satellites would be maintained within a 0.5-degree inclination as assumed in this report, it may be possible to increase antenna gain further (by increasing the antenna size, thereby reducing the beamwidth) without imposing the need for antenna steering. Adequate link margin might then be achieved with further reductions in the PRTS beacon transmit power, although the beacon EIRP must be maintained at a level adequate to support the ATDRS user community without significant burden. Final selection of the PRTS ground station's antenna thus depends on aspects of the ATDRSS design, its stationkeeping requirements, and ATDRSS user parameters and requirements that are not fully known as of now.

4.1.4.1.4 Baseline PRTS Receiver Subsystem

All baseline PRTS stations, Remote and Master, must be capable of receiving and processing the PRTS beacon signal to obtain one-way pseudorange and pseudorange-rate measurements as well as ionospheric delay estimates. A digital implementation has been assumed in Figure 4-6 and is explained in detail in the PRTS system specifications

(Reference 4-1). The baseline PRTS receiver subsystem effectively processes the reference channel separately to extract the beacon navigation message, a coarse PN range measurement, and a range-rate measurement. This processing of the reference channel is also used by the station executive to estimate any variation with time of the ionospheric delay. Processing of all the PRTS beacon channels then yields a precise time-of-arrival measurement and measurement of the absolute ionospheric delay, while allowing the Remote Stations to frequency synchronize their local clocks to the beacon and to the Master Station clock.

The baseline PRTS receiver subsystem is not responsible for data recovery and range and range-rate extraction of the PRTS return signal, however, because these functions are assumed to be performed by the AGT.

4.1.4.1.5 Baseline PRTS Station Clock Subsystem

The baseline PRTS station clock subsystem includes the frequency standard used throughout the ground station as a reference for the many ground station digital circuit elements. Because the Remote Stations are held frequency synchronous with the Master Station through the beacon, a high-quality crystal oscillator would suffice as the Remote Station frequency standard. Measurement of one-way range-rate, however, requires an independent frequency standard to measure the shift in receive frequency from the nominal transmit frequency due to the Doppler effect. Furthermore, because worst-case scenarios may involve loss of the beacon for hours or even days, a superior frequency standard such as a cesium-beam oscillator is indicated. Cesium standards exhibit the low drift rate desired and have been field tested for years in similar applications.

Similarly, the Master Station must use a cesium-beam standard in its generation of the PRTS beacon signal to minimize frequency deviations from nominal. The needs of ATDRSS are best served if the PRTS beacon and all other ATDRSS services share a common frequency reference in the same manner that the Common Time and Frequency Standard is used in TDRSS. The Master Station is, therefore, assumed to be referenced to the AGT's frequency standard.

4.1.4.1.6 Atmospheric Monitor Equipment

Atmospheric monitor equipment accompanies each PRTS ground station and provides atmospheric and meteorological measurements to the station executive. Surface meteorological measurements are used with mathematical

models of the troposphere to estimate the tropospheric delay contributions to the measured pseudorange. Tropospheric delays might also be inferred through use of water vapor radiometer line-of-sight measurements to each observed ATDRSS satellite, but such measurements, although precise, are of uncertain accuracy for many local weather conditions.

4.1.4.1.7 Nascom Interface Equipment

As a contingency, Nascom interface equipment is provided at each PRTS station to allow the exchange of commands and data among the PRTS Remote Stations, the Master Station, and other NASA facilities. Although Nascom support could allow relay of PRTS Remote Station measurements in the event of loss of the dedicated PRTS return channel, the availability of only one-way forward pseudorange and pseudorange-rate measurements would not permit estimation of the clock biases to establish baseline PRTS network synchronization.

4.1.4.2 MPRTS Station Architecture

The MPRTS ground stations are designed to provide adequate resources to meet all performance goals and minimize staffing and maintenance requirements. To this end, the ground stations comprise the basic subsystems required to perform coherent signal turnaround with autonomous control features that preclude the need for on-site personnel, except for periodic maintenance and repair.

Each MPRTS ground station is composed of a station executive, MPRTS S-band transponder, station clock subsystem, antenna subsystem, atmospheric monitor equipment, and Nascom interface equipment, as illustrated in Figure 4-7. The last three MPRTS subsystems are identical to those of the baseline PRTS option and are not discussed further; the other subsystems are somewhat different from their baseline PRTS counterparts. For example, the MPRTS station executive, although similar in many functions, prepares a different return data stream than in the baseline PRTS option. In the same manner, the MPRTS transponder combines aspects of the baseline PRTS receiver and transmitter subsystems to allow two-way coherent turnaround and one-way ionospheric delay estimation to support MPRTS ATDRSS tracking as well as allowing one-way PRTS processing for those ATDRSS users desiring the full PRTS range-measurement precision. Furthermore, because MPRTS does not rely on one-way pseudorange and pseudorange-rate measurements, the MPRTS clock subsystem requirements are less stringent than in the baseline PRTS option.

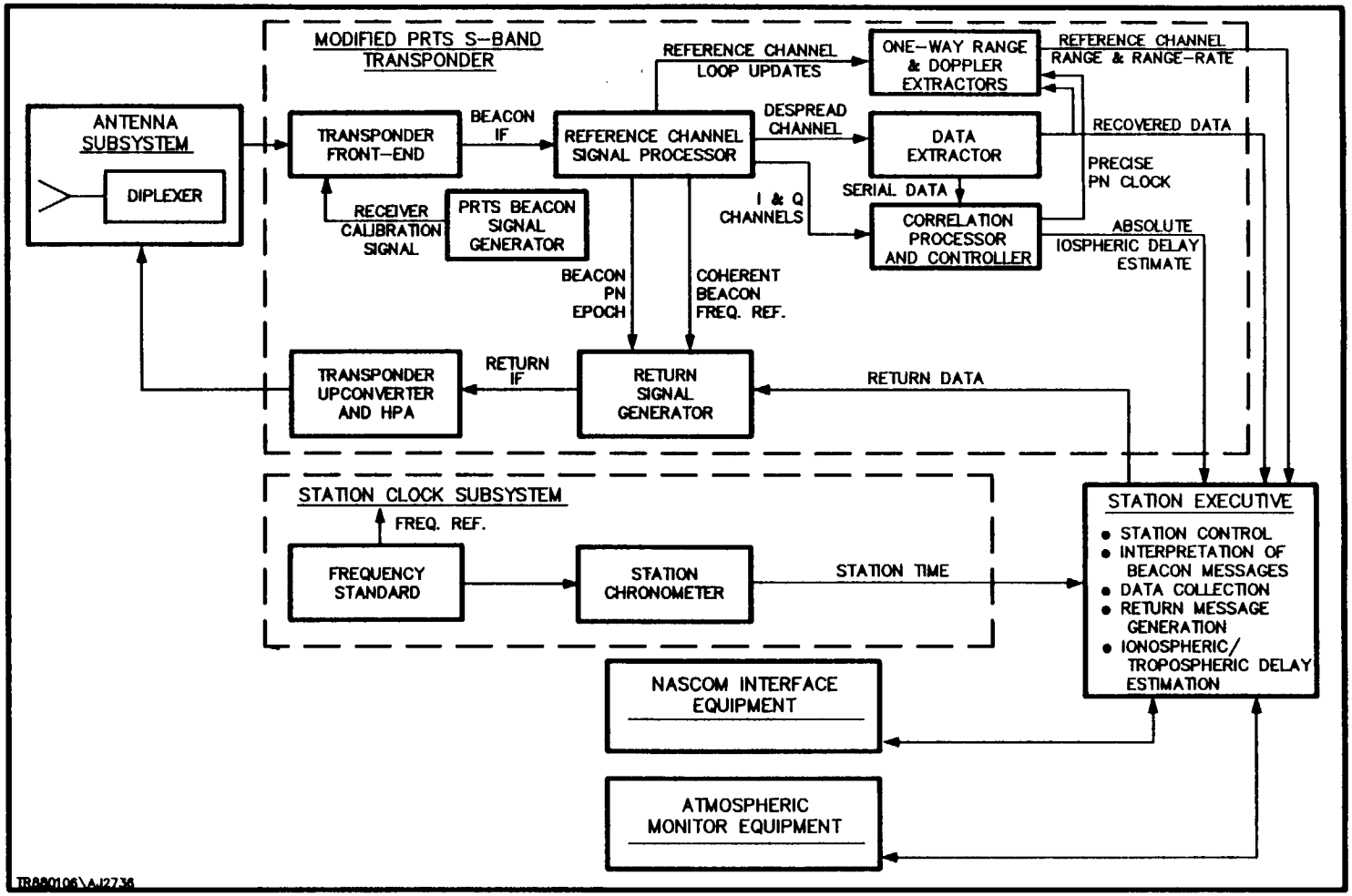

Figure 4-7. MPRTS Ground Station Architecture

4.1.4.2.1 MPRTS Station Executive

As in baseline PRTS, MPRTS ground station operation is controlled by a resident computer, designated the station executive, which is responsible for initiating and coordinating station activities. The station executive performs routine operations to satisfy operational requirements and ensure station integrity; it processes the recovered beacon data stream to extract necessary data and then respond to received commands; and it gathers information from station subsystems and sensors to monitor overall system performance and prepare data to be relayed back to the AGT via the MPRTS return signal.

Compared to the station executive functions in baseline PRTS, no significant concurrent or dedicated computation is required to operate an MPRTS ground station, permitting system management and data processing tasks to be handled sequentially. The architectural requirements for the station executive are thereby simplified so that off-the-shelf microcomputer technology can be employed. Use of such standard computer technology greatly reduces costs that would otherwise be incurred with larger, more complex systems.

4.1.4.2.2 MPRTS Transponder

The MPRTS ground station transponder combines elements of the baseline PRTS receiver and transmitter subsystems in order to support both two-way coherent turnaround, as needed for MPRTS ATDRSS tracking, and one-way pseudorange and pseudorange-rate estimation for those ATDRSS users desiring to take full advantage of the measurement precision of the PRTS beacon. The MPRTS transponder design concept detailed in the MPRTS system specifications (Reference 4-2) is thus very similar to the baseline PRTS transceiver, except that the generated MPRTS return signal is coherently related to the received PRTS beacon.

4.1.4.2.3 Modified PRTS Station Clock

Timing requirements for the MPRTS Remote Stations are relatively simple because one-way pseudorange is not used for ATDRSS OD. Local time is required to tag ionospheric and meteorological data and to support scheduling for routine housekeeping. The clock used by the station may be periodically corrected by extracting time information from the beacon, implying clock offsets between the AGT and the ground stations of up to a few hundred μsec. This

relatively low level of synchronization, however, is more than adequate for all station functions.

The station clock's reference oscillator serves as the frequency source for supporting signal turnaround within the transponder. Stability here requires a source comparable to a thermally controlled crystal oscillator. The exact oscillator frequency remains a design issue and is contingent on synthesizer requirements within the transponder.

4.1.5 PRTS NETWORK OPTIONS

The location of each of the Master and Remote Stations, for both baseline PRTS and MPRTS, depends on

- Visibility with respect to each of the ATDRSS satellites
- Geographical, climatic, and political constraints
- OD performance as a function of the network/satellite geometry

To reduce signal degradation due to ground reflections, dispersive effects through the atmosphere, and large uncertainties in the tropospheric delay, the PRTS ground stations must view the ATDRSS satellite with an elevation angle of at least 10 degrees. The stations are best situated in areas with dry climatic conditions and stable geological features. State-of-the-art surveying (e.g., periodic long-term integration of differential Global Positioning System (GPS) measurements or mobile radio interferometric measurements) is required to determine the absolute antenna boresight position with respect to Earth-centered coordinates accurate to within 75 cm (3 σ) in each of three dimensions.

Satellite OD accuracy depends in large measure on the tracking network geometry with respect to the observed satellite. Generally, long baselines in both N-S and E-W components are desirable to minimize the geometric dilution of precision. Geographical and political constraints necessarily limit the achievable network geometry, especially because the most desirable station locations reflecting geopolitical and NASA operations considerations are those situated within CONUS.

Due to their locations, the beacon footprints of ATDRS-E and ATDRS-W do not allow a long-baseline network capable of observing both satellites; consequently, independent PRTS networks have been chosen for ATDRS-E and ATDRS-W. Three networks for each satellite have been considered, one defining an all-CONUS network, the others achieving intermediate and long baselines by situating stations outside CONUS.

Station locations for the PRTS network have been selected to correspond to existing NASA facilities and possible station locations on or near property currently leased, owned, or used by the U.S. Government. The sites selected are in no way intended to be final but were simply chosen to provide concrete examples of PRTS tracking performance. The ground stations used to define the various PRTS networks are indicated in Table 4-3 and shown in Figure 4-8.

PRTS observations of ATDRS-C have not been a focus of this study because ATDRS-C is considered a spare and does not support operations. Moreover, with the selected PRTS tracking sites, the network geometries supporting OD of ATDRS-C are, in general, superior to those supporting OD of ATDRS-E and ATDRS-W. Consequently, PRTS/ATDRSS OD performance is likely to be better for the ATDRS-C than for ATDRS-E or ATDRS-W and has not been specifically investigated in this study.

4.1.5.1 CONUS-Based PRTS Network

The following networks of ground stations are restricted to CONUS:

- ATDRS-E is observed by WHS, MIL, and GSFC.
- ATDRS-W is observed by WHS, VAN, and WAS.
- ATDRS-C may be observed by any of these five stations, with WHS being the Master Station and the best network geometry obtained by WHS, WAS, and GSFC.

4.1.5.2 Intermediate-Baseline PRTS Network

The following networks of ground stations are primarily restricted to CONUS, but each includes one outlying station:

- ATDRS-E is observed by WHS, GSFC, and ACN.
- ATDRS-W is observed by WHS, WAS, and HAW.
- ATDRS-C may be observed by WHS, HAW, and GSFC.

Table 4-3. PRTS Ground Station Sites

ACRONYM	LOCATION	VISIBILITY	APPLICABLE PRTS NETWORKS	REMARKS
WHSK/WHS	WHITE SANDS, NM (32° N, 107° W)	WEST, CENTRAL, EAST	ALL	ATDRSS GROUND TERMINAL
GSFC	GREENBELT, MD (39° N, 76° W)	CENTRAL EAST	ALL CONUS, INTER.	GODDARD SPACE FLIGHT CENTER
MIL	MERRITT ISLAND, FL (29° N, 81° W)	CENTRAL EAST	--- CONUS	EXISTING NASA FACILITY; STDN SITE
VAN	VANDENBURG AFB, CA (35° N, 121° W)	WEST CENTRAL	CONUS ---	STDN SITE
WAS	RICHLAND, WA (46° N, 119° W)	WEST CENTRAL	CONUS, INTER. CONUS	COARSE COORDINATES NEAR HANFORD-N WEAPONS REACTOR
ACN	ASCENSION ISLAND (8° S, 14° W)	EAST	INTER., LONG	BRTS TRANSPONDER SITE
HAW	HAWAII (22° N, 159° W)	WEST CENTRAL	INTER. INTER.	STDN SITE
GWM	GUAM (13° N, 144° E)	WEST	LONG	STDN SITE
AMS	AMERICAN SAMOA (14° S, 171° W)	WEST CENTRAL	LONG LONG	BRTS TRANSPONDER SITE
REY	REYKJAVIK, ICELAND (64° N, 22° W)	EAST	LONG	COARSE COORDINATES NEAR NATO AIR STATION AT KEFLAVIK OPERATED BY U.S. NAVY

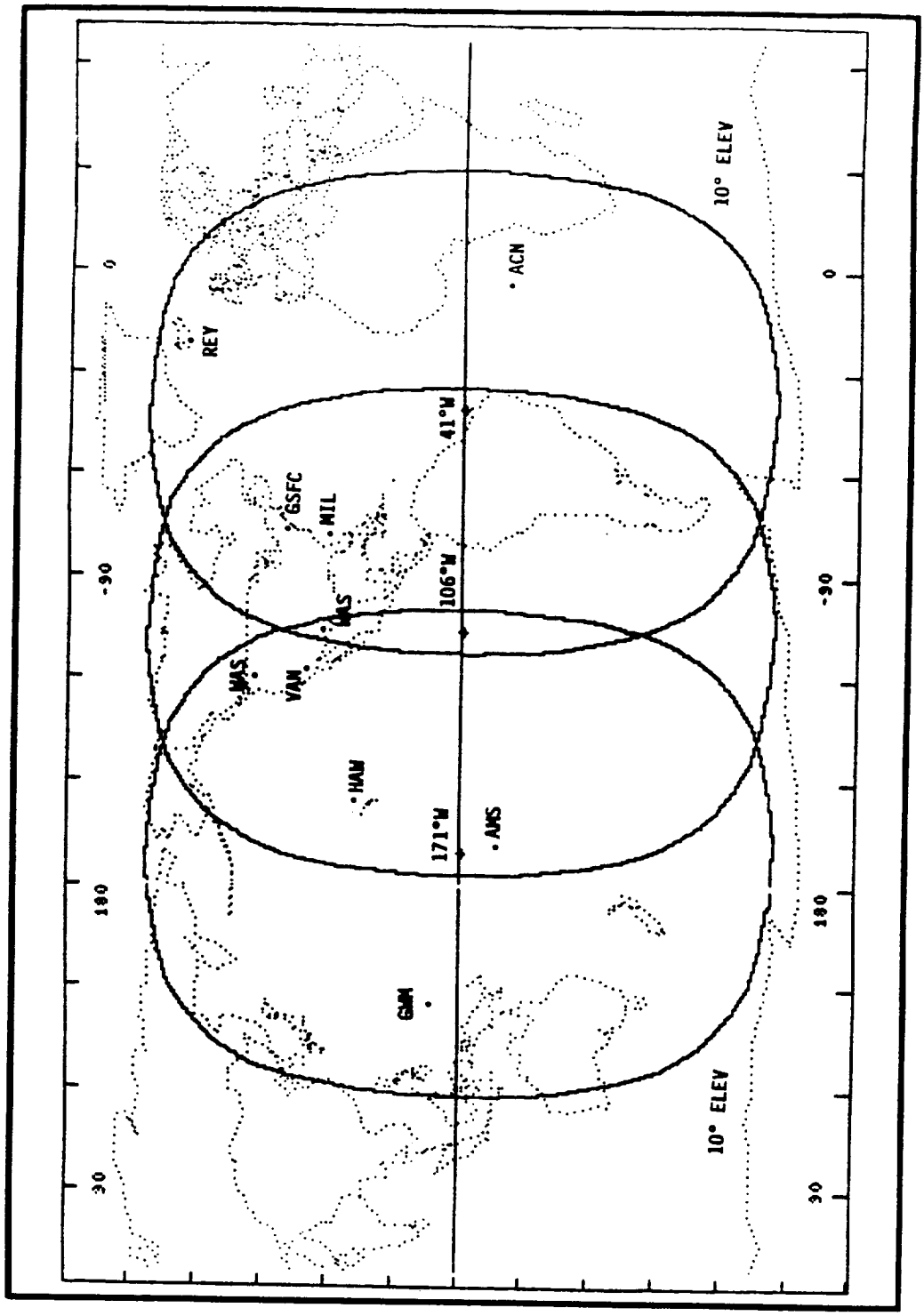

Figure 4-8. PRTS Ground Station Options

4.1.5.3 Long-Baseline PRTS Network

The following networks of ground stations provide the longest baselines and generally the most advantageous geometries:

- ATDRS-E is observed by WHS, ACN, and REY.
- ATDRS-W is observed by WHS, GWM, and AMS.
- ATDRS-C may be observed by WHS, GSFC, and AMS.

4.2 PRTS SYSTEM ASSESSMENT

For both the baseline PRTS and MPRTS options, the following sections assess the impact on ATDRSS development and operations; cost and staffing requirements; reliability, maintainability, and availability; the technological risks associated with implementation of PRTS and MPRTS; and the ATDRSS OD performance achievable with both options.

4.2.1 ATDRSS IMPACTS

Integration of ATDRSS and either baseline PRTS or MPRTS imposes several direct requirements on the ATDRSS space and ground segments. In general, baseline PRTS and MPRTS affect ATDRSS similarly, the only difference being in the return signal types that must be supported for the two system options. The following subsections discuss the ATDRSS impacts common to both systems, with any distinctions between baseline and MPRTS indicated in the text.

Implementation of baseline PRTS or MPRTS and its incorporation into ATDRSS affect ATDRSS development and operations in three distinct ways:

- Support of the PRTS signal structure as the ATDRSS navigation beacon
- Determination of ATDRSS ground and space segment signal path delays
- Support of the baseline PRTS or MPRTS return signal

4.2.1.1 Support of the PRTS Beacon

Both baseline PRTS and MPRTS assume that a PRTS signal is transmitted as the ATDRSS S-band navigation beacon. Such a beacon is part of the current ATDRSS architecture, and a navigation beacon signal structure has been recommended (Reference 4-4). In itself, any ATDRSS navigation beacon

requires appropriate SGL and S-band frequency allocations and an onboard emitter to provide the necessary beacon EIRP and ATDRSS user coverage. An element of the SMA array or a dedicated antenna may be used to support the navigation beacon, as has been discussed.

The PRTS signal structure incorporates the recommended S-band navigation beacon as one of its spectral components in order to support non-PRTS navigation. The PRTS signal structure, however, imposes some additional requirements:

- Bandwidth for the four PRTS spectral components must be allocated at S-band and in the ATDRSS uplink, where the PRTS beacon signal occupies 16.2 percent of a span of 78 MHz (compared to the single 6.138 MHz channel required by the recommended S-band beacon)

- An EIRP of at least 29.0 dBW must be provided (compared to the recommended beacon's minimum EIRP of 22.8 dBW), although this requirement might be reduced if the PRTS ground stations are enhanced accordingly

Finally, not all PRTS processing is performed by the PRTS Master and Remote Stations; specifically, uplink of the PRTS beacon signals to the ATDRSS satellites and the processing of either the baseline PRTS or MPRTS return signal are handled by the AGT. The major issue in both cases is the necessary calibration of forward and return system delays to minimize the impact of unknown range biases on ATDRSS OD.

4.2.1.2 ATDRSS Delay Calibration

Transit time of the PRTS beacon signal path must be known to minimize the impact of range bias on user navigation and ATDRSS OD processing. Consequently, signal-path delays through the ATDRSS space and ground segments as well as through the PRTS Master Station and Remote Stations are assumed to be calibrated. The forward-path delay uncertainty, combining the effects of the uplinked beacon signal and its transit through the ATDRSS satellite, has been modeled in ORAN as a range bias on the forward Master Station-ATDRS link of 6 m (3 σ), assuming a delay uncertainty of 20 ns (3 σ).

Similarly, uncertainties in the baseline PRTS or MPRTS return signal path must be reduced through delay calibration. In baseline PRTS, because the return signal is used to estimate clock biases and is not explicitly used in ATDRSS OD, the return-path delay uncertainty has been shown through ORAN runs to be less critical than the forward

uncertainty. As a result, the baseline PRTS return signal may be successfully supported by a nondedicated channel, where, accordingly, the return-path delay uncertainty due to the ATDRSS satellite and its processing by the AGT has been modeled with a 3-σ range bias uncertainty of 10 m (33 ns) to reflect the biases present in the current TDRSS BRTS tracking system.

In MPRTS, and as an option in baseline PRTS, the return signal is supported by a dedicated return channel. In such cases, the return path delay uncertainty has been modeled as a 3-σ range bias on the return ATDRS-Master Station link of 6 m.

Measurement of path delays at the PRTS Master and Remote Stations is provided by the PRTS station architecture; measurement of the PRTS forward and return signal path delays through the ATDRSS space and ground segments, however, requires additional ATDRSS capabilities. Those ground segment elements responsible for the AGT uplink of the PRTS beacon signals to each of the ATDRSS satellites and its processing of the downlinked PRTS return signals must support delay calibration.

The beacon signal path through the ATDRSS satellites must be calibrated to allow support of one-way navigation and time transfer. In the case of the ATDRSS space segment, the best solution is onboard measurement of a calibration signal generated locally and injected at the appropriate access point(s). Such calibration need not interfere with emission of the beacon signal if, for example, the calibration signal is a tone outside the beacon or return frequency band but within the equipment bandwidth. The time base for such differential measurements would be derived from the ATDRSS satellite frequency system, whether referenced to an uplinked pilot tone or an onboard oscillator. If such local onboard measurements were not possible, the alternative would be extensive ground testing and characterization of the signal-path delays. Onboard monitoring and telemetry of component temperatures might then be used to allow modeling and estimation of the transit delays to the necessary accuracy.

4.2.1.3 Support of the Baseline PRTS or MPRTS Return Signal

In baseline PRTS, the return signal permits synchronization of the ground stations while allowing the relay of the one-way ground station observations; in MPRTS, the return signal from the ground stations directly supports ATDRSS OD

by providing the means to make two-way range and range-rate measurements. The different significance of the return signals in the two system options results in two distinct approaches: in baseline PRTS, the return signal may be supported by nominal ATDRSS return services or by a dedicated channel; in MPRTS, the return signal must be supported by a dedicated return channel to ensure ATDRSS OD performance.

In baseline PRTS, where the ground stations maintain independent time standards to obtain one-way measurements, clock synchronization between each PRTS Remote Station and the Master Station is estimated as part of the PRTS/ATDRSS OD processing. The one-way forward beacon measurements alone, however, do not provide sufficient information for estimation of the Remote Station clock biases. To supplement those measurements, return signals from each of the PRTS Remote Stations are transmitted via ATDRSS back to the AGT, thereby relaying the Remote Station measurements and allowing one-way return range and range-rate measurements to be made by the AGT.

The return signal of baseline PRTS is envisioned as an S-band signal using essentially the same signal structure as a TDRSS Mode 2 return SMA signal to support low-data-rate communications and one-way return range and range-rate measurement. The return signal may be supported by a variety of ATDRSS resources, but the two most likely options are use of SMA return services or use of a dedicated PRTS return channel. If supported by SMA return service, PRTS return signals from each of the ground stations would require scheduled return service at least once an hour; if supported by a dedicated return channel, unscheduled communications from a PRTS ground station would be permitted through code division multiplexing or even through scheduling of ground station contacts. At this time, however, one-way return ranging is not specified as a function supported by the AGT (Reference 4-6), even though PN despreading of S-band return signals is required. The additional Ground Terminal processing to recover one-way return range is not likely to be extensive and may be implicit in the required ATDRSS support of time transfer (Reference 4-6).

In MPRTS, ATDRSS OD requires that a component of the PRTS beacon received by the MPRTS ground stations be coherently turned around to permit two-way range and range-rate measurements by the AGT. The MPRTS return signal is envisioned as an S-band signal using essentially the same signal structure as a TDRSS Mode 1 return SMA signal. To

avoid interference with other SMA users, however, a separate frequency channel may be required, using a non-nominal coherent turnaround ratio. At this time, further investigation is needed fully to determine the exact characteristics of the MPRTS return dedicated channel. AGT processing of the MPRTS return signal is virtually the same as for any ATDRSS user (i.e., data and two-way range and range-rate are extracted), except that the MPRTS return signal data includes information used to correct the measured two-way range for ionospheric delays.

In both MPRTS and baseline PRTS, a possible means to support a dedicated return channel would be to diplex the beacon emitter, thereby achieving full coverage of the PRTS network of ground stations. Interference with other ATDRSS S-band users would be avoided by use of an orthogonal polarization or, as a last resort, a distinct frequency allocation. The advantage of a dedicated return channel is that it supports the relay of PRTS ground station measurements and PRTS network synchronization without burdening ATDRSS user services, although the provision of such a channel represents a significant impact to the ATDRSS design, affecting both the space and ground segments.

4.2.2 COST AND STAFFING REQUIREMENTS

Estimates of the expenses required to field either baseline PRTS or MPRTS and operate the system over a 10-year period have been made, based on the level of system detail presented here and in the corresponding system specifications. The cost estimates assume that complete system specifications (as opposed to conceptual designs) would be available at the start of the design and development cycle. For either system option, given the current level of development, it is estimated that an additional $2.5 million study phase would be required to produce adequate system specifications, with such funds supporting further system analysis and the development of an engineering model for field testing. Results from these tests would then be used to complete a specification suitable for use in implementing an ultimate PRTS network.

4.2.2.1 Baseline PRTS Life-Cycle Costs

Based on the requirements presented in the associated baseline PRTS documentation, the price for the system has been estimated at approximately $25.6 million in 1988 dollars (Reference 4-8). This cost estimate reflects deployment of a system of nine stations to support ATDRSS satellites in three geostationary orbital slots.

Development and deployment of the system is estimated to cost $19.5 million; the remaining $6.1 million is allocated for operations and maintenance over a 10-year period. Additional options to enhance performance might also be included, including the use of water vapor radiometers for precise troposphere-delay estimation and data-coding/decoding capabilities. Such options would increase the system cost by roughly $1 million.

Several assumptions have been made in forming this estimate. First, it is presumed that a beacon capability, estimated to cost in itself $12 million, is included as part of the baseline ATDRSS satellite architecture independent of the cost of baseline PRTS. Second, no attempt has been made to assess system reliability, although system redundancy would certainly affect both network complexity and cost. Next, operation, maintenance, and repair of the ground facilities over a 10-year period are included in the cost model, with a seven-member staff specified to perform these functions. Finally, the cost estimates have emphasized the system design and development required to field baseline PRTS successfully. Although no new technology is required, a conservative implementation process has been assumed in developing new system modules.

4.2.2.2 MPRTS Life-Cycle Costs

As with the PRTS cost estimate, the MPRTS cost estimate relies on the current level of specification as a basis for pricing. The costs for MPRTS have been estimated to be $19.1 million (Reference 4-9). This cost reflects the use of a system with nine stations to support satellites in three geostationary orbital slots and assumptions similar to those used to assess baseline PRTS. Development and deployment of the system is estimated to cost $15.3 million; the remaining $3.8 million is allocated to support a five-member staff and to operate and maintain the system over a 10-year period. As with baseline PRTS, the use of water vapor radiometers at the ground stations to enhance estimation of tropospheric delays would increase the total cost by approximately $1 million.

4.2.3 RELIABILITY/MAINTAINABILITY/AVAILABILITY

Reliability, maintainability, and availability of baseline PRTS or MPRTS is beyond the scope of this report but should be considered as part of future efforts.

4.2.4 TECHNOLOGICAL RISK

None of the components necessary for implementation of the PRTS concept--baseline PRTS or MPRTS--involves new technologies; the PRTS transmitter and receiver designs reflect complexity comparable to conventional PN systems. Risks in the actual hardware/software implementations and in the processing algorithms may be resolved through a development schedule that emphasizes systematic resolution of any design uncertainties. Proof-of-concept PRTS hardware has already been demonstrated under the Phase II SBIR effort.

4.2.5 EXTERNAL DEPENDENCIES

Outside ATDRSS, no external dependencies are required by PRTS in its normal operation. As a contingency, however, dedicated telecommunications services provided by Nascom or commercial leased lines may be desired to support command of the PRTS Remote Stations and recovery of their observations, especially in baseline PRTS where one-way measurements are used for ATDRSS OD. Such a scenario presumes the PRTS beacon is still available but that either the navigation message provided as part of the PRTS beacon is insufficient to relay Remote Station commands or the ATDRSS channel that supports PRTS return signals has failed in some way. In the latter event, the ability to estimate the clock biases between the Master and Remote Stations and, in baseline PRTS, to estimate the ATDRS orbits accurately degrades considerably. In MPRTS, of course, if either the PRTS beacon or the return channel is lost, then no two-way measurements are possible; therefore, external telecommunications services in MPRTS are used solely to supplement Remote Station command and telemetry. The cost associated with external telecommunications support is dependent on the geography of the PRTS network, but the forward and return data rates could be as low as 100 bps.

4.2.6 OBSERVATION STALENESS

The PRTS beacon is available continuously, allowing observations by the PRTS ground stations at any time. Processing of the received PRTS signal occurs in real time, with either the baseline PRTS one-way pseudorange and pseudorange-rate measurements or the MPRTS two-way measurements available almost immediately. In baseline PRTS, data formatting of the return signal and its transmission to the AGT are the only latencies incurred. If the baseline PRTS return signal were supported by ATDRSS SMA return service, then contact times would require scheduling; if the PRTS return signals were supported by a dedicated

return channel, it is possible that no scheduling delays would be involved. In the latter case, the baseline PRTS return signals could be transmitted continually by the PRTS ground stations, with the AGT selecting a particular signal through the choice of PN code used for despreading.

4.2.7 PRTS/ATDRSS OD PERFORMANCE

The efficacy of both PRTS system options in supporting ATDRSS OD has been modeled in this study through use of the covariance analysis tool ORAN. Performance of the three network configurations--CONUS-based, intermediate-baseline, and long-baseline--has been assessed for ATDRS-E and ATDRS-W, investigating both definitive tracking performance over a finite tracking arc and TR performance after a satellite maneuver. Modeling of baseline PRTS and MPRTS is discussed, and representative results for the two systems are compared in this section.

Baseline PRTS forward beacon and return signal pseudorange measurement errors have been modeled as shown in Table 4-4. The range-bias values chosen are intended to represent the use of calibrated dedicated forward and return signal paths, although other ORAN runs not discussed in this section have been performed using greater range biases on the return signal to model use of SMA return service. Ionospheric refraction errors are shown as zero, reflecting measurement of ionospheric delay using the PRTS beacon signal structure; residual ionospheric correction errors are assumed to be included in the range-measurement noise. Although baseline PRTS measures one-way pseudorange-rate of both the PRTS beacon and the PRTS return signal in addition to pseudorange, only the beacon pseudorange-rate measurement has been modeled with ORAN. The omission of return range-rate measurements, however, is not likely to have a significant impact on the OD results shown here.

As indicated in Table 4-4, the forward beacon measurements possess greater accuracies than the return measurements as a result of one-way PRTS beacon signal processing. In baseline PRTS, however, the return measurements are not intended to assist in OD of the ATDRSS satellites; rather, the return measurements allow the clock biases between the PRTS Master Station and the Remote Stations to be determined. OD and clock-bias estimation are thus effectively decoupled and might be operationally separated. Accordingly, the baseline PRTS forward and return measurements have been partitioned in ORAN so that only the forward and return measurements, which are paired every 12 hours, are used to estimate the clock biases; all forward

Table 4-4. Baseline PRTS ORAN Error Modeling (3-σ Values)

- PRTS RANGE-RATE MEASUREMENTS HAVE NOT BEEN MODELLED
- MEASUREMENT SCHEDULE (OVER 30-HOUR TRACKING ARC):
  - FORWARD MEASUREMENTS EVERY 30 SECONDS FOR 5 MINUTES (11 OBSERVATIONS) EACH HOUR
  - RETURN MEASUREMENTS EVERY 30 SECONDS FOR 5 MINUTES (11 OBSERVATIONS) EVERY 12TH HOUR
- STATION POSITION UNCERTAINTY: 75 CM IN EACH DIMENSION
- 1-WAY FORWARD PRTS BEACON MEASUREMENTS
  - RANGE MEASUREMENT NOISE: 1.5M
  - UPLINK (MS-ATDRS) BIAS: 6.0M
  - DOWNLINK (ATDRS-RS) BIAS: 3.0M
  - RANGE-RATE NOISE: 0.131 CM/SEC
  - RANGE-RATE BIAS: 0 MM/S
  - REMOTE STATION CLOCK BIAS:
    - WITH ALL FORWARD MEASUREMENTS: .25M CONSIDER PARAMETER
    - WITH ALL FWD AND RET MEASUREMENT PAIRS: SOLVE-FOR PARAMETER
  - REMOTE STATION CLOCK DRIFT, DRIFT-RATE: 0.0
  - TROPOSPHERIC REFRACTION ERROR: .045 OF TOTAL TROPOSPHERIC DELAY
  - IONOSPHERIC REFRACTION ERROR: 0.0
- 1-WAY RETURN PRTS SIGNAL
  - RANGE MEASUREMENT NOISE: 7.5M
  - UPLINK (RS-ATDRS) BIAS: 3.0M
  - DOWNLINK (ATDRS-MS) BIAS: 6.0M
  - TROPOSPHERIC REFRACTION ERROR: .045 OF TOTAL TROPOSPHERIC DELAY
  - IONOSPHERIC REFRACTION ERROR: 0.0

MIS93JTAB

and return measurements used to solve for the ATDRSS satellite's orbit assume an unmodeled clock-bias uncertainty. Because estimation of the clock biases over a 30-hour tracking arc reduces the uncertainty in the clock biases to less than 0.25 m, that value is applied to the forward measurements for use in ATDRSS OD as a given uncertainty in the clock biases.

The rationale for partitioning clock bias and orbit estimation stems from the need to support ATDRSS TR. After a satellite maneuver, use of short tracking arcs in recovering the orbit does not allow both clock bias and orbit estimation without severely affecting their accuracy. Because the PRTS station clocks undergo limited drift over the recovery period, the most recent clock-bias estimates obtained from complete tracking arcs may continue to serve until sufficient data has been collected to estimate the clock biases again.

To model baseline PRTS ATDRSS TR with ORAN, the PRTS beacon forward measurements are used during the recovery arc to solve for the ATDRSS orbit, with the uncertainty in the clock bias estimate assumed to be that corresponding to the uncertainty estimated during the immediately preceding 30-hour tracking arc. This procedure has been used for arc lengths of 1 and 2 hours, applying a consider clock bias of 0.25 m, typical of the accuracy obtained in clock-bias estimation over a 30-hour arc, at the PRTS Remote Stations; for longer tracking arc lengths, the Remote Station clock biases have been estimated.

Similar modeling is used for MPRTS, except that there are no clock biases to be estimated. The MPRTS error budget is shown in Table 4-5, and the associated ORAN model employs two-way range and range-rate measurements, assuming dedicated forward and return channels with 3-m range-bias uncertainties in each direction at the three nodes of the signal path. The absence of ionospheric uncertainty reflects the use of the PRTS beacon signal structure at the MPRTS Remote Stations to measure the ionospheric delay.

The distinction between baseline PRTS and MPRTS is clearly modeled in ORAN: whereas MPRTS uses two-way range and range-rate measurements from between the AGT and the system's ground stations to estimate the ATDRS orbits, baseline PRTS uses one-way measurements at each of the Remote and Master Stations as well as one-way measurements back to the AGT to estimate both the ATDRS orbits and the ground station clock biases. Because the number of states

Table 4-5. MPRTS ORAN Error Modeling (3-σ Values)

- 2-WAY RANGE AND RANGE-RATE MEASUREMENTS
- MEASUREMENT SCHEDULE FOR EACH STATION (OVER 30-HOUR TRACKING ARC);
  - MEASUREMENTS EVERY 30 SECONDS FOR 5 MINUTES (11 OBSERVATION) EACH HOUR
- STATION POSITION UNCERTAINTY: 75 CM IN EACH DIRECTION
- 2-WAY RANGE MEASUREMENTS
  - RANGE MEASUREMENT NOISE: 2.2M
  - UPLINK (ATDRSS GT - ATDRS) BIAS: 6.0M
  - FORWARD (ATDRS - REMOTE STATION) BIAS: 3.0M
  - RETURN (REMOTE STATION - ATDRS) BIAS: 3.0M
  - DOWNLINK (ATDRS - ATDRSS GT) BIAS: 6.0M
- 2-WAY RANGE-RATE MEASUREMENTS
  - RANGE-RATE MEASUREMENT NOISE: 0.075 CM/SEC
  - RANGE-RATE BIAS: 0 CM/SEC
- SOLAR RADIATION: 2%
- TROPOSPHERIC REFRACTION ERROR: .045
- IONOSPHERIC REFRACTION ERROR: 0.0

MIS93Jtab

that must be solved is reduced with MPRTS, OD performance of MPRTS is generally superior to that of baseline PRTS.

Comprehensive ORAN results are not shown in this section, but, as expected, the larger tracking networks evidence improved OD accuracies compared to the CONUS-based networks. Using the maximum position error over the definitive tracking period as a figure of merit, all networks provide better than (less than) 75-m (3-σ) accuracy for tracking arcs of 30 hours. For shorter arcs, however, the differences in network geometries become significant.

The most interesting case is the PRTS network constrained to CONUS. OD performance is then less than ideal, yet, for other reasons, such a CONUS-based network is likely to be the most attractive network option. A comparison of ATDRSS OD performance for baseline PRTS and MPRTS is presented in Table 4-6, illustrating the results obtained using identical CONUS station sites to track ATDRS-E. For a tracking arc of 30 hours, both systems meet the goal of 75-m (3-σ) accuracy; for a tracking arc of 2 hours, simulating TR, both systems fail to meet the 75-m goal.

In both baseline PRTS and MPRTS, the range biases are the dominant error sources, motivating the use of dedicated forward and return channels. The effect of residual range biases in such calibrated dedicated channels might be further reduced if these biases were estimated as part of the OD processing. With dedicated channels, the range biases are likely to be constant or to vary slowly with time so that periodic estimation may reduce the range biases and permit still further improvements to ATDRS OD accuracy. This aspect of OD processing requires still further investigation.

4.3 REFERENCES

4-1. Stanford Telecommunications, Inc., TR880106, Precise Ranging and Timing System (PRTS): System Specifications, Preliminary, September 1988

4-2. --, TR880102, Modified Precise Ranging and Timing System (MPRTS): System Specifications, Preliminary, September 1988

Table 4-6. Performance Comparison of PRTS Options

ATDRSS TRACKING SYSTEM OPTIONS (CONUS-BASED NETWORK)	MAXIMUM 3 σ ATDRS-E POSITION ERROR OVER THE DEFINITIVE TRACKING ARC (METERS)	
	2 HR ARC	30 HR ARC
BASELINE PRTS	271	58
MODIFIED PRTS	215	43

7/18/89 MIS83P\AJ5646

4-3. --, TR870105, A Novel, Precise Ranging and Timing System Concept Using Pseudo-Noise Bandwidth Synthesis: Final Report, April 1987

4-4. R. Bruno and B. Elrod, TR860167, TDAS Beacon Signal Definition: Analysis and Specification, Stanford Telecommunications, Inc., October 1986

4-5. A. Jacobsen, TR870122, Phased Array Support of TDRSS S-Band Services, Stanford Telecommunications, Inc., July 1987

4-6. NASA/GSFC, S-530-A, Preliminary Draft, Advanced Tracking and Data Relay Satellite System (ATDRSS) Requirements Document: Vol. 4, Ground Segment Requirements, June 1988

4-7. B. Elrod, A. Jacobsen, et al., TR25066, Tracking and Data Acquisition System (TDAS) for the 1990's: Volume VI, TDAS Navigation System Architecture, Stanford Telecommunications, Inc., May 1983.

4-8. Stanford Telecommunications, Inc., TR880123, Precise Ranging and Timing System (PRTS): Life Cycle Costing, Preliminary, September 1988

4-9. Stanford Telecommunications, Inc., TR880124, Modified Precise Ranging and Timing System (MPRTS): Life Cycle Costing, Preliminary, September 1988

SECTION 5 - INTERFEROMETRIC TRACKING SYSTEMS ASSESSMENT

5.1 SYSTEM DEFINITIONS

The information presented in Section 5 is based on much previous work in developing systems based on interferometry for the specific purpose of tracking geosynchronous satellites. The interferometric tracking systems are considered, most of which has been specified and evaluated in previous documents (References 5-1, 5-2, 5-3, 5-4, and 5-5). This work differs from those studies in three respects. First, the error model has been updated, mostly in a more conservative direction. Second, TR performance is evaluated as well as OD performance. Third, the use of range data from the ATDRS Ground Terminal is considered to evaluate its utility to aid in OD and TR.

References 5-6 and 5-7 describe validation experiments in which the TDRS satellite was observed with existing CEI and VLBI arrays. In related work, substantial efforts are in progress at the Jet Propulsion Laboratory to develop systems based on VLBI for tracking of interplanetary probes.

This section describes radio interferometric techniques, defines proposed systems using these techniques for tracking ATDRS, and discusses factors affecting system capability and performance.

5.1.1 BASIC PRINCIPLES

5.1.1.1 Principles of Interferometry

The radio interferometer determines the phase of a signal at some remote site relative to the phase of the same signal source at a reference site. These are determined by direct cross-correlation of the undecoded signals received at the two sites. The phase offset is a measure of the delay difference between the source and each of the two receiver antennas. This principle is illustrated in Figure 5-1.

For a distant radio source such as ATDRS or celestial objects, each delay difference effectively measures the angular position of the object in the sky. With three antennas, a two-dimensional position fix can be obtained. A succession of such measurements, supplemented by the laws of orbital mechanics, can be used to determine a satellite orbit. Alternatively, the three-dimensional position measurement may be derived by the two angle measurements and

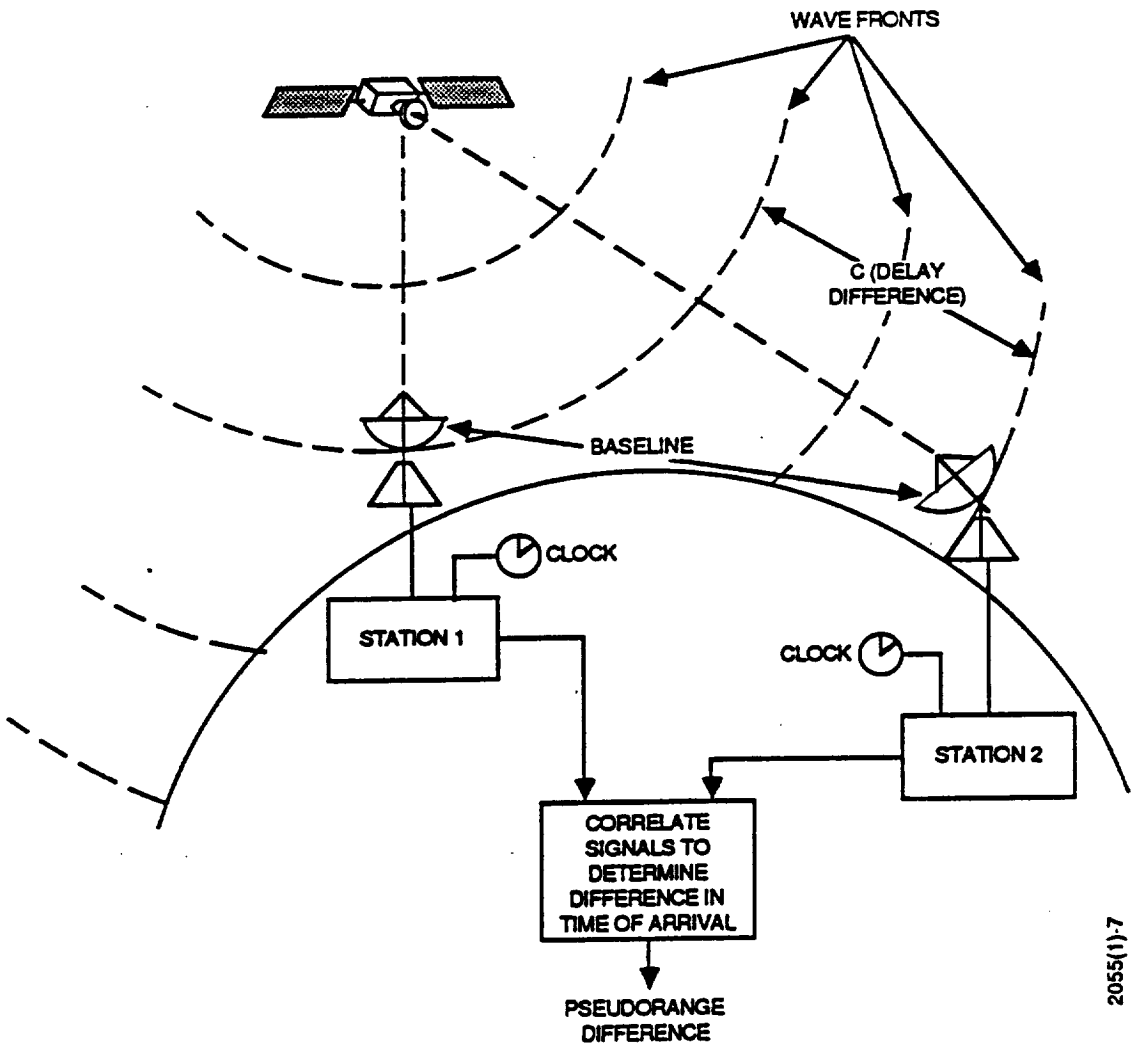

Figure 5-1. Schematic Interferometer for Satellite Tracking

a supplemental range measurement. Use of ranging measurements may improve the accuracy of the orbital solution and may require less real time to determine satellite orbits than interferometry alone.

The basic radio interferometer requires two antenna receivers and associated electronics to sample, digitize, and time-tag the signals. The receivers add noise with typically much larger rms power than the signal itself. Clocks at each receiver may be either slaved to a common master clock or independent. If the antenna sites are spaced sufficiently closely, the signals are brought together in real time using cables, waveguides, fiberoptics, or radio links. Because the antennas are physically connected, such an array is known as a connected element interferometry (CEI). If the sites are far apart, the signals are recorded, shipped, or transmitted to a central location for processing at a later time. Because of the large size of such an array, it is known as very long baseline interferometry (VLBI).

5.1.1.2 Phase Delay Versus Group Delay

There are two fundamentally different measures of the delay between the arrival times of the radiation at the two antennas. A phase delay measurement uses a nearly monochromatic component of the radio signal to determine the difference in phase. Because only a single frequency, f, is used, there is an ambiguity in the delay measurement equal to n/f where n is any integer. This is referred to as phase ambiguity. In observing the ATDRS SGL at 14 GHz, this delay ambiguity is an integer multiple of 70 picoseconds (ps). For two antennas separated by 10 km, the satellite line of position measurement would be ambiguous by integer multiples of 0.08 km.

One way to alleviate this ambiguity problem is to add more antennas at shorter separations. For shorter antenna spacings, the ambiguity distance is proportionately increased.

The group delay technique is a method of avoiding this ambiguity problem by observing the source radio signal at several different frequencies. Because there is a different constraint for each frequency band observed, the overall spacing between ambiguous solutions is increased. The ambiguity spacing is given by the reciprocal frequency spacing, or $1/\delta f$, where δf is the smallest difference in frequencies. The satellite observing system postulated in this report would make phase measurements in eight different frequency channels, of which the closest differ in frequency by 10 MHz. The group delay ambiguity will be increased to

100 ns, compared to 70 picoseconds for the phase delay. Moreover, the group delay ambiguity can be resolved by examination of correlation amplitudes at different ambiguity values.

5.1.1.3 VLBI Versus CEI

CEI arrays distribute timing signals from a single master clock to each receiver antenna. Time-tagged observations are transported in real time to a processing center and are correlated. Time and signal transport may be via cable, waveguide, phase-stabilized radio link, or, as proposed here, fiberoptic link. CEI arrays are limited in size by the physical links required to interconnect the component stations.

In VLBI arrays, signals are time-tagged using local clocks. Correlation of recorded signals can be performed offline, or signals can be transmitted to the correlator facility for processing in real time. VLBI arrays are unlimited in size.

CEI arrays have the advantage over VLBI in that the more accurate phase delay observable may be used. In addition, because wide bandwidths are more easily transported, more frequent or more sensitive observations can be obtained. Further, because CEI array component antennas are necessarily constrained to be relatively close together, systematic errors introduced by the troposphere and ionosphere very nearly cancel out. VLBI systems need to address clock synchronization; for CEI, the clocks are synchronized by real-time link to one reference clock. The longer baselines possible in a VLBI system can sometimes overcome the larger absolute errors, relative to that of a CEI system.

5.1.1.4 Signal Processing

Signal processing for all systems consists of cross-correlating the data streams from the separate antennas and determining the delay offset. For any of the systems, the first step is to clip and sample the signals, using 1-bit coding. The bit streams are delayed for approximate synchronization in accordance with an a priori estimate of the delay, multiplied, and accumulated at short intervals.

To find the phase delay, used by CEI arrays, an amplitude, phase, and time derivative is fitted to the accumulated data series. The group delay, used in VLBI arrays, is determined by fitting a phase, its time derivative, and its frequency

derivative (the group delay) globally to the data in all the frequency channels. Group delay solution is complicated by the need to detect the phase calibration signal, find its phase and rate, and apply it as a calibration prior to the global fit. In either case, the initial correlation is performed by special-purpose processors (integrated circuits). The fringe fitting is then performed by Fourier transform techniques, finding the peak in a power spectrum.

5.1.2 TRACKING SYSTEM ARCHITECTURES AND OPERATIONS CONCEPT

Several system architectures are described that use interferometric observables to track ATDRS. These interferometric tracking systems are listed below:

- CEI-Q - Quasar Calibrated Connected Element Interferometry
- VLBI-Q - Quasar Calibrated Very Long Baseline Interferometry
- VLBI-2S - Two Satellite Very Long Baseline Interferometry
- VLBI-3S - Three Satellite Very Long Baseline Interferometry
- VLBI-Ku - Ku-band Beacon Very Long Baseline Interferometry
- VLBI-GT - GPS Time Transfer Calibrated Very Long Baseline Interferometry
- VLBI-GC - Coded GPS Calibrated Very Long Baseline Interferometry
- VLBI-GH - Hybrid GPS Calibrated Very Long Baseline Interferometry

Each architecture is specified as a conceptual system for which OD performance levels are determined (Section 5.2.1).

The operation of each system is also described. When required by the level of tracking accuracy, each system would be supplemented by a ranging system to the AGT. That ranging system is not described here, but requirements for it will be derived from results of orbit simulations described in Section 5.2.1. Table 5-1 summarizes salient features of the different systems.

Table 5-1. Interferometric System Architecture at a Glance

	VLBI-Q	CEI-Q	VLBI-2S VLBI-3S	VLBI-Ku	VLBI-GT	VLBI-GH	VLBI-GC
OBSERVABLE	GROUP DELAY	PHASE DELAY (GROUP-OPTIONAL)	GROUP DELAY	GROUP DELAY	GROUP DELAY	GROUP DELAY; GROUP/PHASE DELAY	GROUP DELAY AND CODED RANGE DIFFERENCES
BASELINE LENGTH	1000 km	10 km	1000 km	~2000 km	~1000 km	~1000 km	~1000 km
TIME STANDARD	HYDROGEN MASER	CRYSTAL	HYDROGEN MASER	HYDROGEN MASER	GPS TIME TRANSFER	HYDROGEN MASER	HYDROGEN MASER
NUMBER OF SITES	4 -5	2-3	4-5	4*	4-5	4-5	4-5
NUMBER OF ANTENNAS PER SITE	1-2 ATDRS 1 QUASAR	3-5 ATDRS 3-5 QUASAR	1 ATDRS	1 ATDRS	1 ATDRS 1 GPS RECEIVER	1 ATDRS 1 GPS S-BAND ANTENNA	1 ATDRS 1 GPS RECEIVER
ATDRS ANTENNA DIAMETER RECEIVER TYPE	 2 m UNCOOLED	 2 m UNCOOLED	 2 m UNCOOLED	 2 m UNCOOLED	 2 m UNCOOLED	 2 m UNCOOLED	 2 m UNCOOLED
CALIBRATOR ANTENNA DIAMETER RECEIVER TYPE	 12 m COOLED	 12 m COOLED	 --	 --	 .6 m STD RECEIVER	 2 m UNCOOLED	 .6 m

2055B(3)-9

5.1.2.1 Signal Characteristics

The ATDRSS satellites are assumed to be located in the current orbital slots for ATDRS-E and ATDRS-W. The ATDRS signal source to be observed for all of the systems except for VLBI-Ku is the Ku-band SGL, which in this report is assumed to have the same characteristics as the current TDRS. This downlink signal is beamed toward WHS and is continuously available for tracking purposes. The beam has an intensity of about -201 dBW/Hz/m^2 over a bandwidth of about 225 MHz centered about 13.9825 GHz. The main lobe subtends a cone about 500 km in diameter, the radiation footprint of which is highly elongated for the assumed low elevations of the satellites. The proposed arrays would lie entirely within this main lobe when possible.

It should be emphasized that although it is necessary to detect and record radiation from the source of interest, it is not necessary to decode the signal. On the contrary, it is assumed that the signal resembles noise in a statistical sense. All that is required is that the signal be present in the frequency band of interest, available for passive use.

The quasar sources are highly compact, are noise-like, and have positions determined with extremely high accuracy (5-10 nanoradians). The quasar antennas are designed to observe objects down to a limiting flux density of -260 dBW/Hz/m**2. It is estimated that there will be about 45 such sources in the band of sky that passes within 10 degrees of the ATDRS positions.

The GPS satellites are assumed to be the full constellation of 24 satellites. At any time, at least four satellites are visible. The median angular distance between the ATDRS and the closest GPS is about 25 degrees. The GPS satellites transmit pseudorandom noise-like signals at two L-band frequencies. Signal strength and spectra are assumed to be as described in Reference 5-9.

In the hybrid system, the signals may be treated as noise-like (no cross-spectral correlations) for measurement of group delay, and the signal when squared yields an undithered carrier frequency tone.

5.1.2.2 VLBI-Q

System I uses VLBI observations of ATDRS and simultaneous observations of natural radio sources (quasars). The quasar observations calibrate for the effects of independent clocks

at different sites. Stations would normally be operated and monitored remotely.

Specifications for System I are described in prior reports (Reference 5-8) and in Appendix B. The array would consist of four sites, as shown in Figure 5-2. All sites are located in the SGL main footprint.

The station architecture is illustrated in Figure 5-3. Each site will have a 2-m antenna observing ATDRS and a 12-m antenna with a cryogenically cooled receiver observing quasars. A hydrogen maser time standard at each site allows coherent integration over the course of a 5-minute scan required for the quasar observations. Each antenna signal is sampled at eight narrow (2 MHz) frequency bands. The signals are converted to baseband, sampled, digitized, and multiplexed onto a data relay link to the central correlation facility. Additional modules calibrate cable delays and provide partial tropospheric calibration.

The data flow overview for a VLBI-Q system is summarized in Figure 5-4. The central processing facility instructs the sites regarding the calibration sources to observe, where ATDRS is expected to be, and when to observe. At each site, signals are detected simultaneously from the quasar and ATDRS. The signals recorded include the signal from the satellite or quasar, the calibration signals, and a large contribution from receiver noise. These signals are, without decoding, sampled, clipped, and transmitted to the central processing site for correlation and further processing.

At the central processing site, the signals from all antennas are delayed to bring all into approximate synchrony and are then correlated in real time. The correlation consists of 1-bit multiplications, results of which are dumped onto disk at short intervals for further processing, that is, determination of fringe phase, its time derivative, the single band delay (delay for maximum power), detection of the calibration signals, and fitting of the multiband or group delay. The group delay is an accurate measurement of the difference in time delays of the signals arriving at the two stations.

The remaining processing consists of several calibrations: (1) calculation of tropospheric delays from local meteorological data; (2) correction for (measured) changes in cable lengths; (3) correction for several known geometrical effects, such as Earth tides, and relativistic effects; (4) correction for Earth orientation offsets;

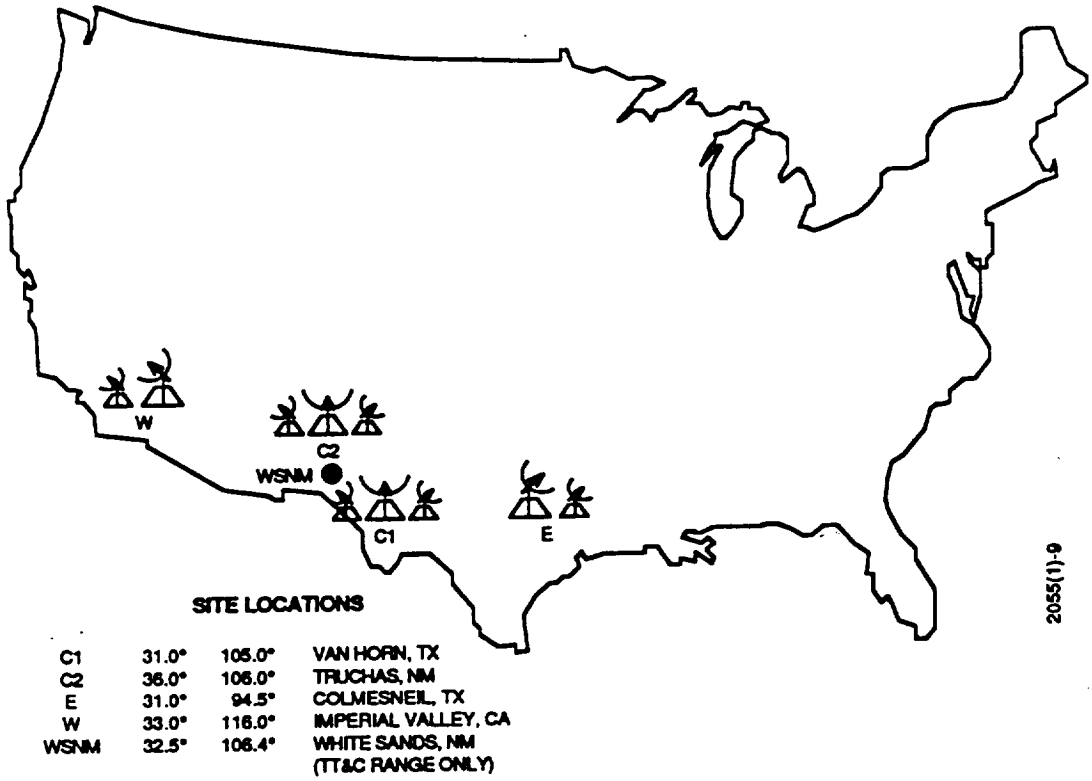

Figure 5-2. VLBI-Q Array Geometry

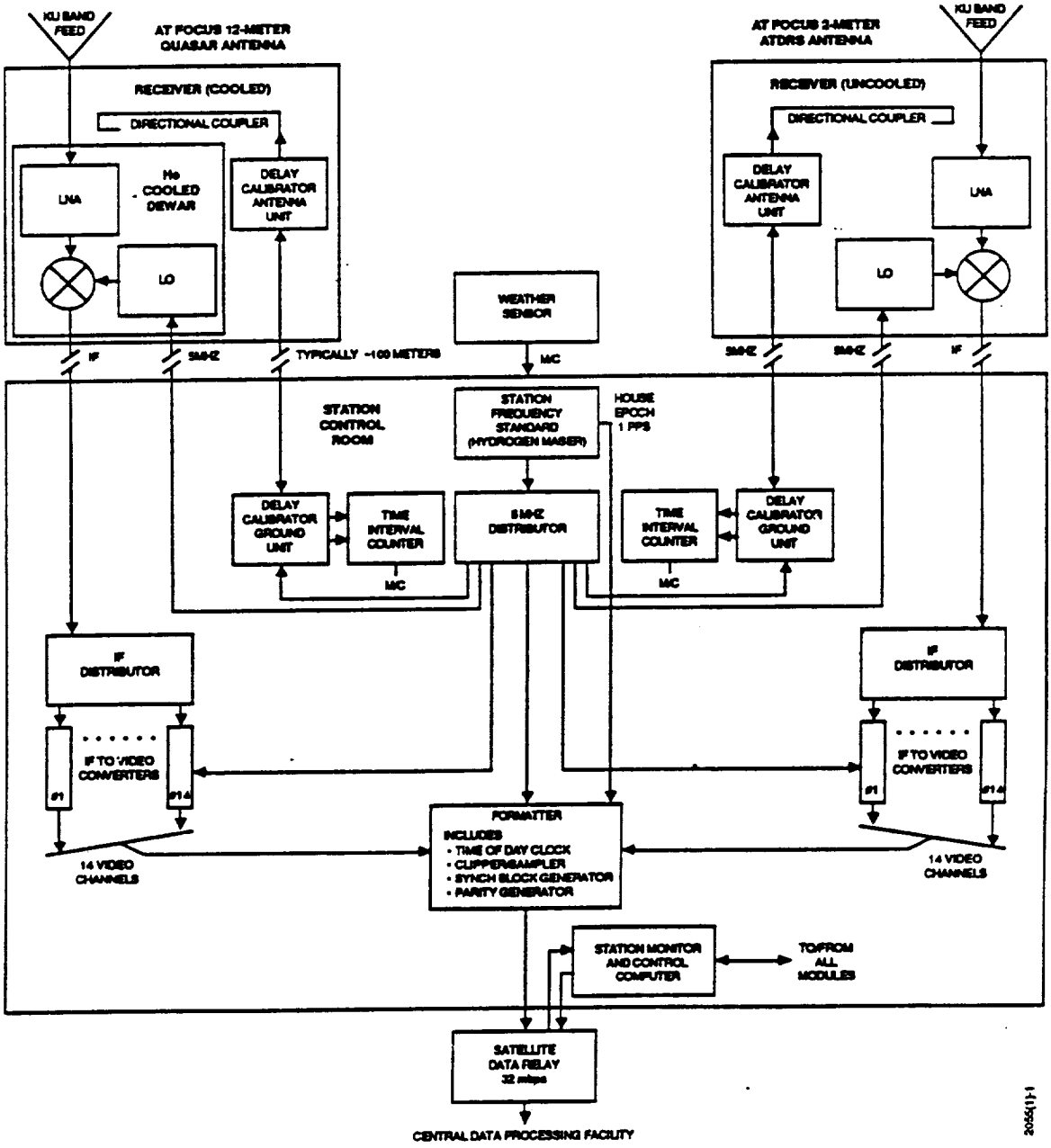

Figure 5-3. VLBI-Q Station Block Diagram

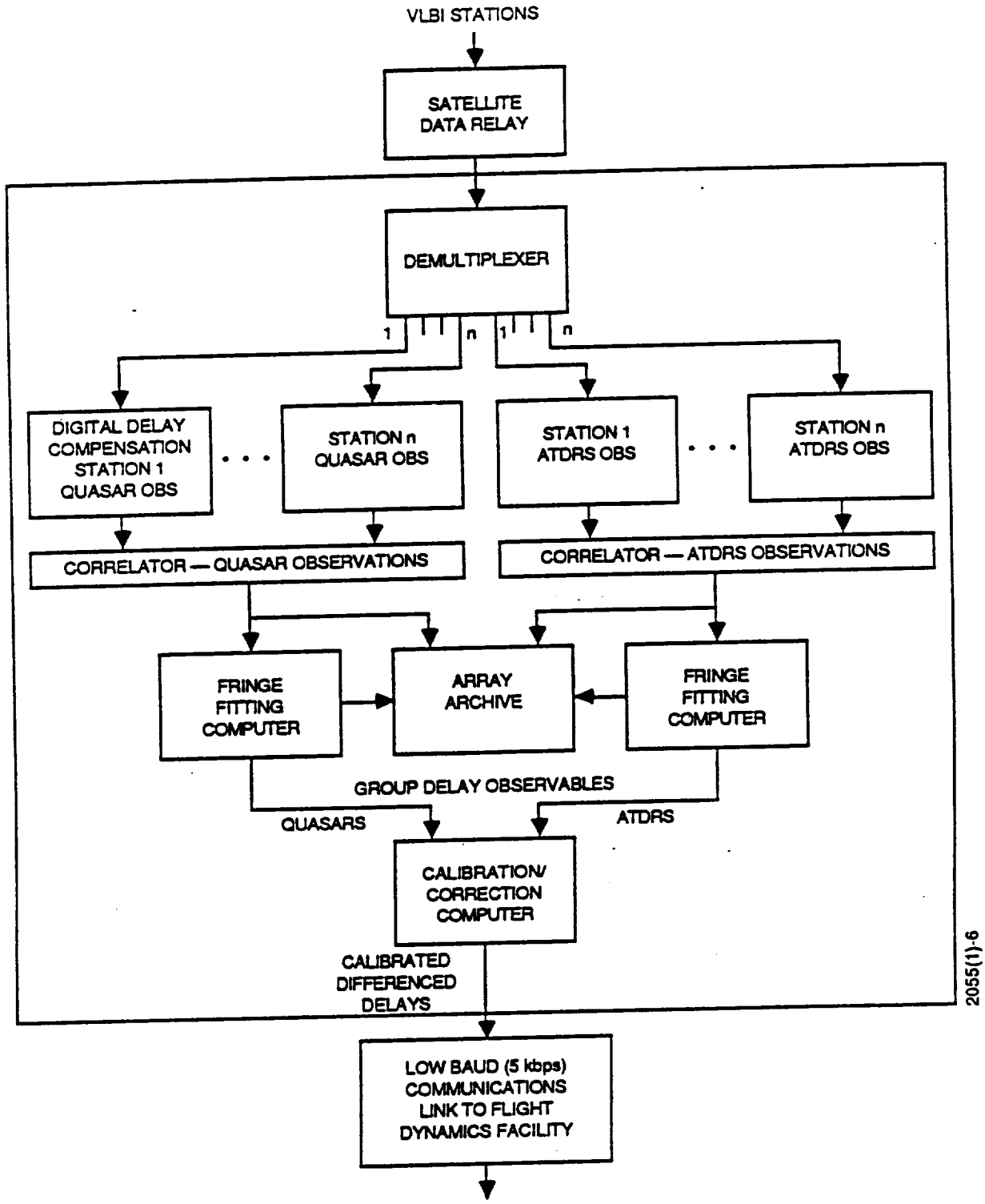

Figure 5-4. VLBI-Q Central Data Processing Facility

(5) subtraction of the satellite observation and the quasar observation; and (6) reincorporation of the known delay to the quasar. This provides the calibrated delay difference.

In order to perform the correlation, it is necessary to delay the incoming bit streams to within approximately the reciprocal single channel bandwidth, or about 0.5 μsec. This can be calculated using a priori knowledge of the satellite position, accurate to about 10 km. Without such knowledge, it is necessary to search through several delay values. This procedure, called a fringe search, requires storage of satellite observation data for multiple processings. This problem does not arise for observations of quasars, whose positions are well known.

Correlator systems to do the type of processing required, at about the speed required, are currently operating at the U.S. Naval Observatory (USNO) and at other locations. Correlation of VLBI data relayed by satellite in real time was demonstrated in 1976 (Reference 5-10). Detection and correlation of satellite sources through such a system has also been demonstrated (Reference 5-6). In sum, the elements of the proposed processing system exist today.

5.1.2.3 CEI-Q

System option II has a CEI array for each of the eastern and western orbital slots. These arrays consist of three or more antennas observing ATDRS, each paired with a 12-m antenna observing natural radio sources. The most important function of the quasar observations is reduction of errors due to tropospheric fluctuations, a dominant error source for this system. Figure 5-5 shows the location of the proposed arrays. Location outside the SGL main footprint is required for the east array because, within the main beam, the satellite elevations are very low and the tropospheric fluctuations preclude adequate measurement precision. An allowance of 28 dB is made for off-axis attenuation of the ATDRS signal toward the eastern array.

Hydrogen maser clocks are not required because clocks at all antennas are slaved in near real time to one array master oscillator. Figure 5-6 shows the geometry of each array: a triangle 10 km on a side. Additional stations at shorter spacings are included for phase ambiguity resolution but are not included in OD simulations because they are less accurate than the longer baselines.

Equipping a CEI system to perform group delay observations would eliminate the problem of phase delay ambiguity

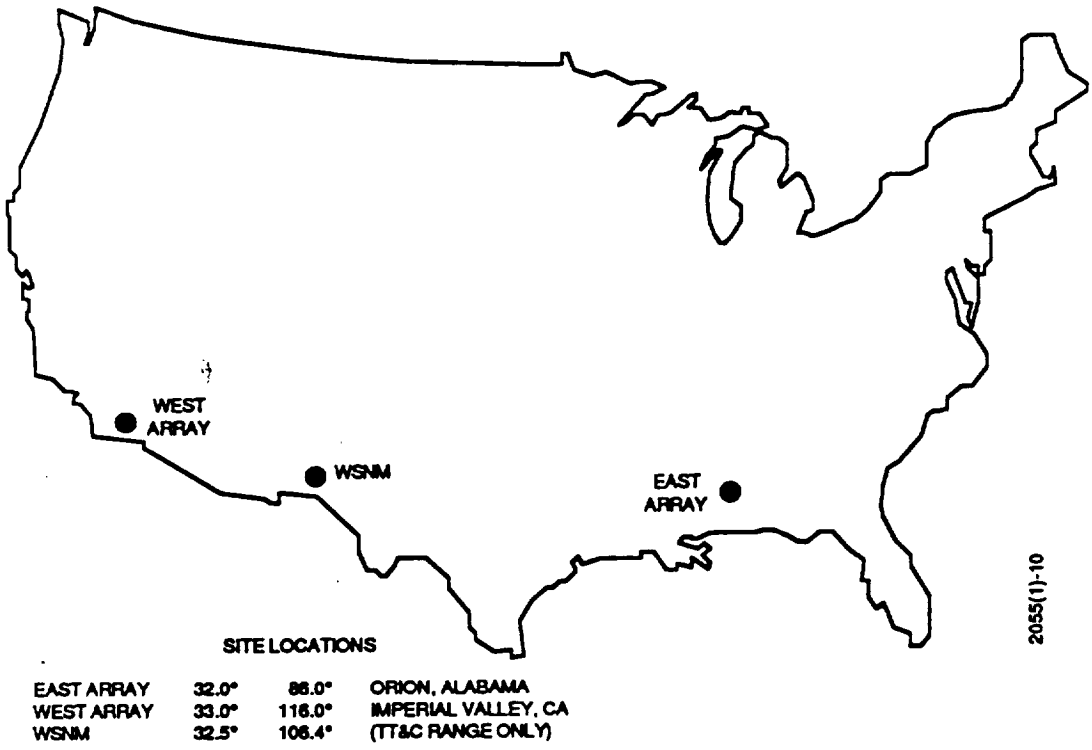

Figure 5-5. CEI-Q Array Locations

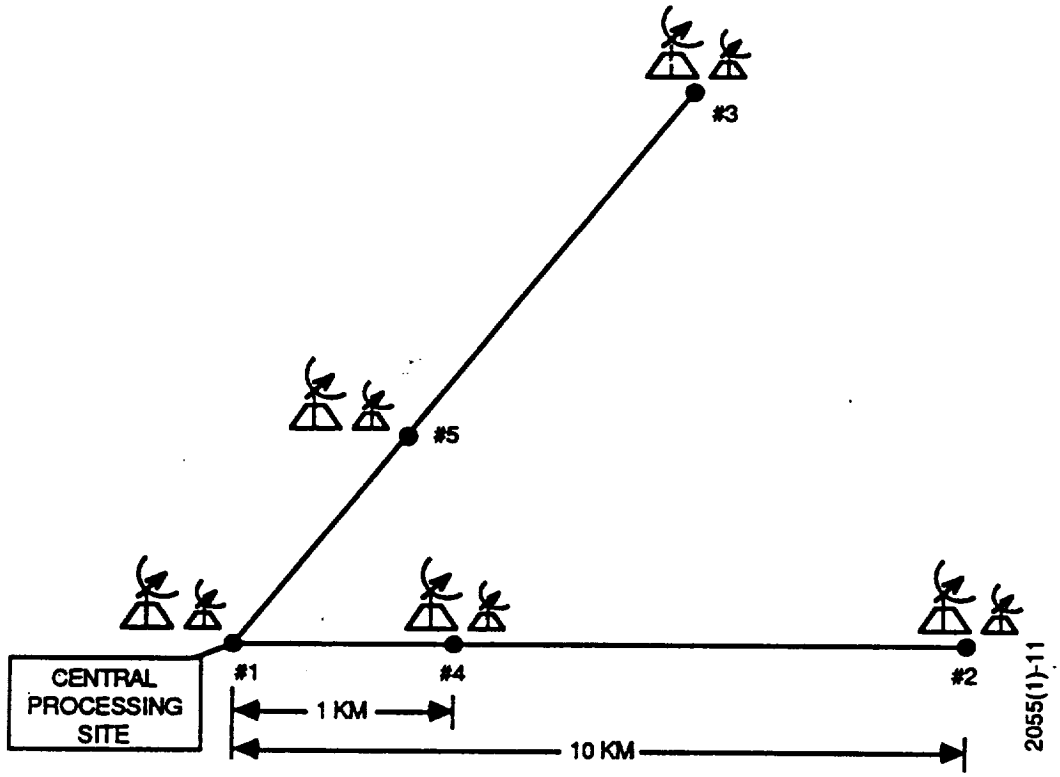

Figure 5-6. CEI-Q Array Geometry

resolution. New requirements for such a system would be (1) increasing receiver bandwidth to 1 GHz, (2) increasing data flow through fiber optic link to 1 gigabit (Gbit)/s, and (3) equipping the correlator to find group delay as well as phase delay. These all are feasible. An ancillary benefit is elimination of the need for inner stations on each arm of the array.

Operation of the proposed CEI array is summarized in Figure 5-7. Overall scheduling, and an approximate ATDRS ephemeris, are downloaded from a central processing site. Simultaneous observations are made of the satellite source and of the quasar calibration source. An optical fiber link carries instructions and timing signals out to each antenna, and carries data (receiver output) and return timing data back to the correlator, 1-10 km away. The signal bandwidths are about 50 MHz per channel, for Ku-band and possibly S-band, for quasar antenna and satellite antenna, for each site in the array. (In the group delay option, the bandwidths are 1 GHz per channel.) The data streams are sampled, clipped, and correlated (multiplied) at the central control building and the fringe phase fitted immediately by a synchronously running minicomputer. Correction for small but complicated effects, such as relativistic aberration, and corrections based on local weather data are made later. The measurement of differenced phase delay for both quasar and satellite is ready for shipment virtually as soon as the data have been taken.

At the analysis facility, the known corrections are applied to the data, the measured delays to the satellite and to the quasar are subtracted, and the theoretical delay to the quasar is added back in. The result is the calibrated delay difference to the satellite.

For TR, when the satellite position has a large a priori error, making the observation is still straightforward. The satellite position accuracy required for observation of the satellite is about 200 km (for 50-MHz bandwidth, 1-km baseline). There is, however, a possible difficulty in resolving phase ambiguities. The ambiguities can be resolved, given enough measurements, by trying values until finding that which fits best. Alternatively, the array can be built adding antennas at very short spacings (50 and 200 m), with the very short spacings used to resolve those ambiguities. Such short spacings may not necessarily require quasar calibration. The group delay alternative probably resolves the phase ambiguity problems without added antennas.

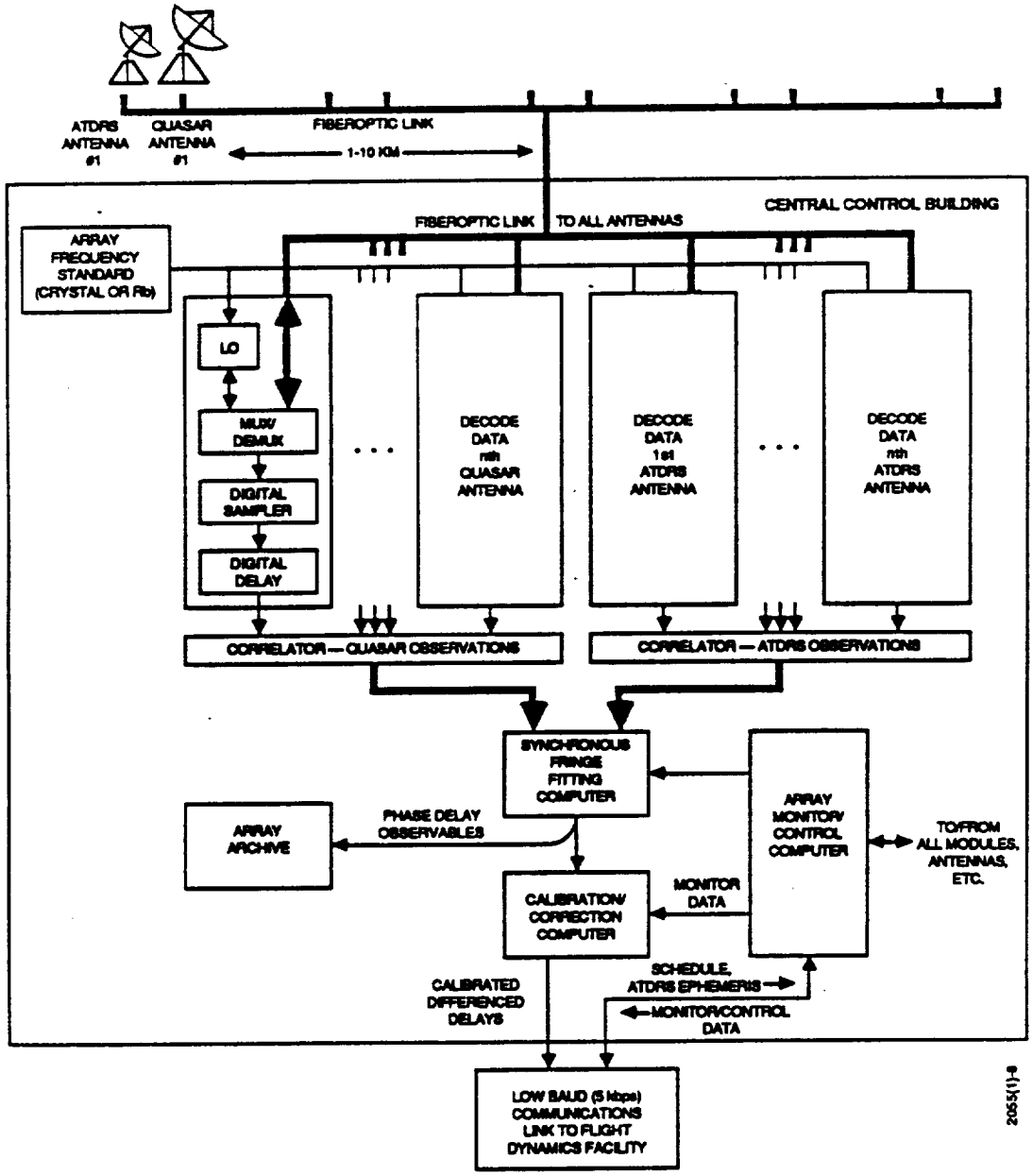

Figure 5-7. CEI-Q System Block Diagram

5.1.2.4 VLBI-2S, VLBI-3S, VLBI-Ku

Another system option is a VLBI system in which two satellites are observed by the same array: ATDRS at either location and an ATDRS-like satellite in an overhead slot. "ATDRS-like" means that signal characteristics (power, frequency, bandwidth) are assumed to be the same as that for ATDRS. The system is considered identical to the VLBI-Q except that everything related solely to quasar observations is eliminated. This eliminates the 12-m antenna with cooled receiver, some IF hardware, most data transmission volume (99.6 percent), and a large portion of the correlator load. The array geometry would be identical to the VLBI with quasar calibration.

Figure 5-8 shows the station architecture of the system. It differs from the quasar-calibrated system by omission of the large antenna, half the hardware, and most of the data transmission capacity. Figure 5-9 diagrams the central processing facility. It differs from the quasar system correlation by omission of half the correlation hardware and a large reduction in communications capacity.

Unlike the quasar-calibrated case, for which the calibrator source position and, thus, the geometric delay are accurately known, long-term clock variations must be modeled. Therefore, observations are used to determine the orbital parameters of both satellites and to fit parameters modeling clock variations.

Operation of a VLBI-2S tracking system is, at this level of description, nearly identical to that of the VLBI-Q system described earlier. The ways in which the systems differ are as follows:

- Observations of the two satellites are not simultaneous.
- The data volume is much smaller.
- The range differences still contain clock errors, which must be determined.

The VLBI-3S system uses the same hardware tracking configuration as that of VLBI-2S. It differs from the former system only in that the orbits of ATDRS-E, ATDRS-W, and ATDRS-C are solved for in one solution rather than separate solutions for the ATDRS-E and ATDRS-W satellites.

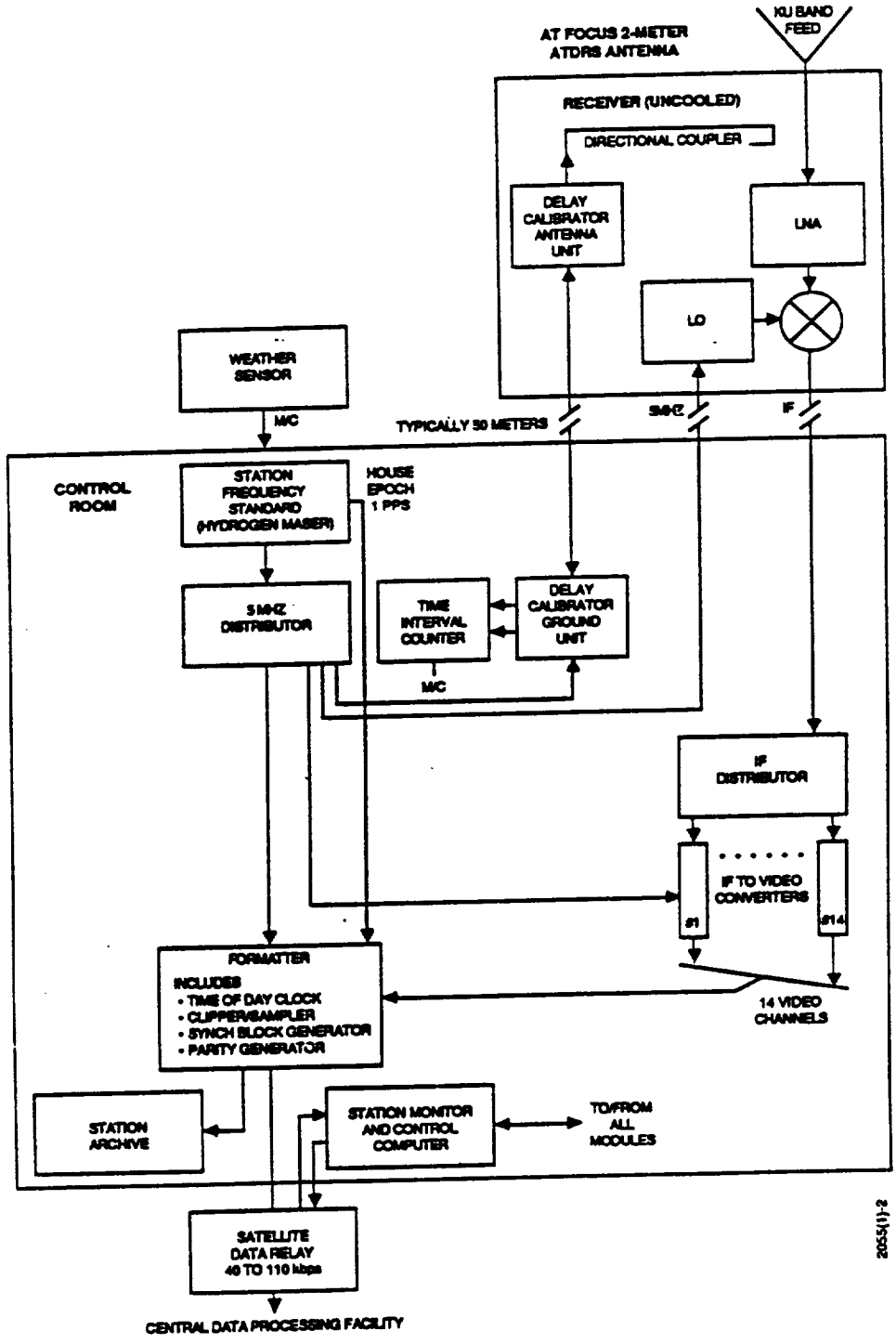

Figure 5-8. VLBI-2S Station Block Diagram

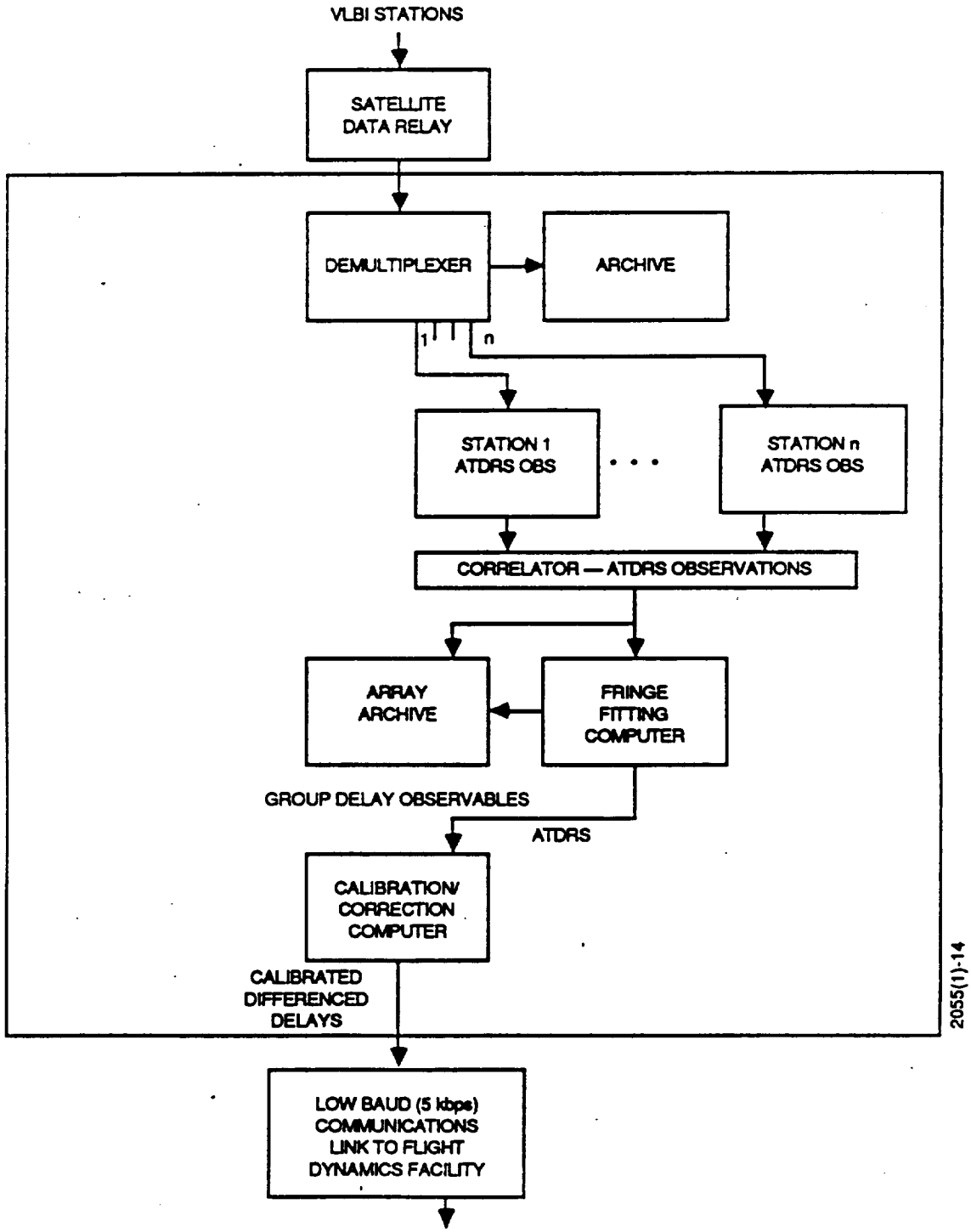

Figure 5-9. VLBI-2S Central Data Processing Facility

The Ku-band beacon based VLBI system (VLBI-Ku) operates on the same principle as the VLBI-2S system except that observables are derived from observation of a hypothetical Ku-band beacon located on the ATDRS. Use of such a beacon allows use of longer baselines and hence better measurements of the ATDRS. Unless otherwise noted, strengths and limitations ascribed to the VLBI-2S system in the following may also be ascribed to the VLBI-Ku system.

5.1.2.5 GPS-Calibrated VLBI

The fourth system option consists of a VLBI array calibrated by observations of GPS satellites. The system is similar to VLBI-2S in that the calibration objects are strong satellite sources. However, separate antennas are required to observe the GPS due to the wide difference in frequencies between the GPS (L-band) and the ATDRS SGL (Ku-band).

Three versions of the GPS-calibrated VLBI are considered for orbit determination. In the first system, GPS is a means of time transfer, VLBI-GT. The only reason for observing the GPS is for the transfer of time; the only figure of merit is its accuracy. In the second system, VLBI-GC, the GPS is observed by decoding precise positioning code. In the third, VLBI-GH, the GPS is observed by a combination of group delay and phase tracking observations.

5.1.2.5.1 GPS for Time Transfer

The first and simplest way to use the GPS is as a device for time transfer. In this system the interferometric observations of range difference to ATRS are referenced to separate clocks, which are synchronized by conventional GPS time transfer techniques. The system architecture is the same as for VLBI-2S, with the addition of a GPS timing receiver at each site. Tracking of more than one ATDRS is not required. Clock modelling is not required.

Exploratory ORAN simulations for this system (see 5.2.1.4) show this system to perform far below requirements. More detailed specification and analysis have not been performed. We note however in passing that if a suitable beacon allowed VLBI over considerably longer baselines then GPS time transfer should be reevaluated.

5.1.2.5.2 GPS Tracked by VLBI Observations

The second option is use GPS for both time transfer and troposphere calibration, doing so by VLBI observations of the GPS satellites themselves. This may be thought of as a

variant of the VLBI-2S system where the 24 GPS satellites replace the second reference ATDRS.

Figure 5-10 shows the station architecture for the system. It replaces the 12-m quasar antenna used in VLBI-Q with a 2-m L-band GPS antenna and an ominidirectional GPS phase-tracking antenna. The data transmission requirements are approximately 100 times smaller than those for VLBI-Q. Array geometry is still the conceptual network considered before.

As with VLBI-2S, knowledge of GPS satellite positions is not available, a priori. Therefore, GPS observations are used both to model clock variations and to determine GPS orbital elements. In contrast to VLBI-2S, position variations of the GPS allow more effective simultaneous determination of tropospheric zenith delay. In fact, it is possible to solve for several other systematic errors from these data (Reference 5-11).

The system operates as follows: Group delay observations of the ATDRS satellite provide precise measurements of delay difference, contaminated clock differences, mismodeling of tropospheric delay, and other smaller effects. During each pass of each GPS satellite, one group delay measurement is made to determine its delay difference, referenced to the same clock. This group delay measurement is immune to any kind of signal dithering. A separate ominidirectional antenna tracks the phase of the carrier signal from each satellite, propagating the delay difference measurement over the entire orbital pass.

These observations do not require decoding of the GPS signal. Resulting observations are then used to solve for GPS orbits, clock variations, and other factors (e.g., troposphere delay). Numerous group delay observations, a more robust and accurate method, are not used because they require greatly increased data volume.

5.1.2.5.3 GPS Tracked by Coded GPS Observations

The third option, like the second, uses GPS observations for both time transfer and tropospheric calibration. A coded GPS receiver observes the GPS satellites in place of the interferometric measurements. A system block diagram would look identical to that of the hybrid system (Figure 5-10) with the replacement of the 2m directional GPS antenna with an ominidirectional coded GPS receiver. The assumption that range difference is the observable used for tracking allows us to model this system identically to the hybrid system,

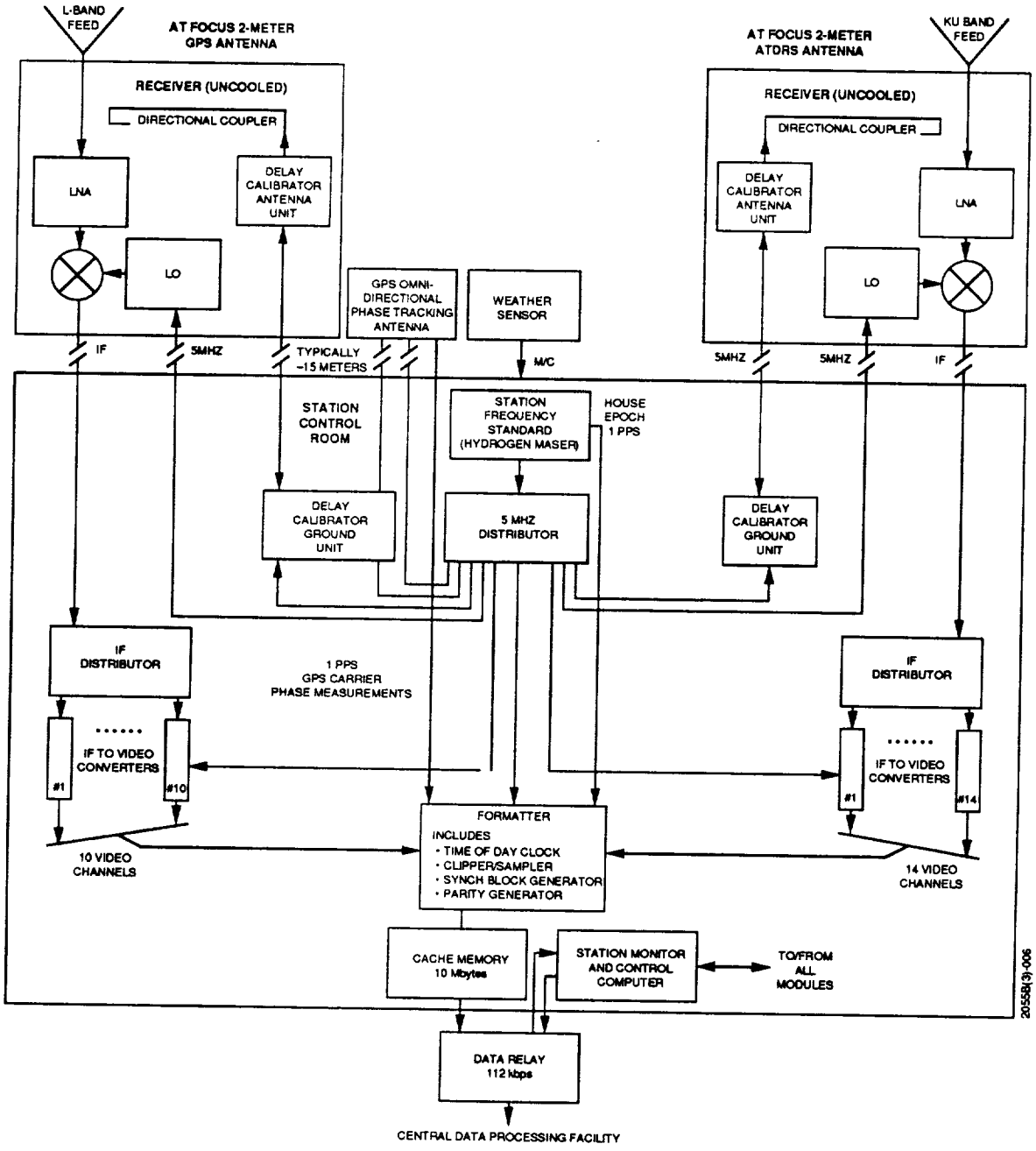

Figure 5-10. GPS-Calibrated VLBI Hybrid System Station Block Diagram

solely with the replacement of the applicable observation error levels.

5.1.2.6 Additional Comments

The specifications here are for conceptual networks, without detailed optimization for performance. In addition, some system redundancy is likely on grounds of reliability, maintainability and availability considerations. It is not, however, expected that optimization or redundancy would produce any striking differences from the simulation results that follow.

5.1.3 INTERFEROMETRY MEASUREMENT SENSITIVITY, ACCURACY, AND PRECISION

The precision of the interferometric phase measurement is directly proportional to the measurement SNR. The angular sensitivity of an interferometer can be expressed as the position error, $\delta\Theta$, of a distant radio source resulting from a given phase measurement error, $\delta\alpha$:

$$\delta\Theta = \frac{c\ \delta\alpha}{2\pi f\ b\ \sin\ \Theta}$$

where c is the speed of light, f is the frequency (phase delay) or bandwidth (group delay), b is the baseline length, and Θ is the angle between the baseline vector and the position vector from the interferometer to the source. This shows that the precision with which the source position Θ is measured increases with SNR (precision of $\delta\alpha$), frequency (or bandwidth), and baseline length, and it is most sensitive for sources at large elevation angles, where the source vector is perpendicular to the baseline vector.

5.1.3.1 Systematic Errors

Systematic errors occur whenever there are additional nongeometric contributions to the delay difference measurement. Such errors may occur due to propagation delays through refractive media (ionosphere, troposphere), propagation delays through electronics, errors in time-tagging, and errors in modeling the a priori delay (e.g., station position errors). The major expected contributors to systematic errors and a description of the estimation of their magnitude are provided in Appendix A.

The troposphere delays an incoming signal by about 7 ns (at zenith), and the ionosphere by about 0.2 ns. The former can be estimated with fair accuracy; the latter is highly variable and cannot. Mismodeling of the troposphere and ionosphere is a main contributor to systematic delay error.

In the case of CEI, most of these errors cancel out when the delay is computed because the paths to the satellite through the atmosphere are nearly the same. Antenna station position uncertainties also contribute to the overall systematic error.

Clock synchronization to the subnanosecond level is required for tracking accuracies that are less than 50 m. Therefore, calibration of the independent clocks in a VLBI system is a necessity.

5.1.3.2 Noise Effects

Noise limits the precision of both group and phase delay measurements. In either case, precision is proportional to the coherent SNR (CSNR). The measurement precision of the phase delay observable is inversely proportional to observing frequency, whereas the measurement precision of the group delay observable is inversely proportional to the effective (rms) observing bandwidth. Because bandwidth coverage is limited, VLBI measurements are less precise than CEI measurements for the same SNR.

The SNR depends on the source signal strength, antenna size, receiver noise, and the number of bits of source signal collected. Other sources of measurement noise include atmospheric (tropospheric) fluctuations, ionospheric fluctuations, phase calibration, time standard, and solar wind scintillations. For the systems considered here, these other noise-like effects are comparable to or larger than noise due to SNR limitations. More complete descriptions of these noise contributions are given in Reference 5-8.

5.1.3.3 Measurement Error Due to System Noise

Measurement precision for a digitally sampled correlation interferometer can be expressed in terms of three quantities: the instantaneous SNR, the number of independent samples of data collected, and the observing frequency (phase delay) or rms bandwidth (group delay). Instantaneous SNR depends on the source strength, the collecting area of the antenna, the aperture efficiency (here assumed to be 50 percent), and the receiver noise temperature. The number of data samples is the sampling rate (Nyquist) times the length of an observation. Digitization (clipping and sampling) degrades precision by a factor of $\pi/2$.

5.1.3.4 Summary - Assumptions Used in Calculating Interferometric Measurement Noise

This section presents a summary of all factors used to determine noise-like errors for interferometric measurements. These inputs determine the resultant measurement noise values listed in the appendix.

5.1.3.4.1 Receiver Noise

Equivalent system noise (Sequiv) depends on antenna gain and receiver noise temperature. All satellite group delay antennas are assumed to have

d = 2m; efficiency = 0.5; T = 200 degrees kelvin (k)

=> Sequiv = 2kT/A = 3.5e-21 W/Hz/m**2

For quasar antennas

d = 12m; T = 100k => Sequiv = 4.9e-23 W/Hz/m**2

The signal strength from the satellite is assumed to be

S(ATDRS) = 9e-21 W/Hz/m**2
S(quasar) = 1e-26 W/Hz/m**2
I(GPS) = -163 dBW-IC (L1)
I(GPS) = -166 dBW-IC (L2)

The signal attenuation for off boresite locations is

G(ATDRS) = -10 dB in main lobe (C1,C2,CE,CW,Austin)
G(ATDRS) = -35 dB far off axis (Westford, Richmond)
G(quasar) = 0 dB
G(GPS) = 0 dB

These parameters determine the instantaneous ratio of signal power density to noise power density. To determine the system noise contribution to group delay error, it is necessary to know the rms bandwidth and the number of bits collected:

ATDRS:	Bmax=225 MHz	Brms=90 MHz	Nbits=32e6
ATDRS*:	Bmax= 20 MHz	Brms=5.8 MHz	Nbits= 1e6
GPS:	Bmax= 20 MHz	Brms=2.9 MHz	Nbits=40e6
Quasar:	Bmax=500 MHz	Brms=200 MHz	Nbits= 1e9

The ATDRS* entry refers to a stripped-down demonstration system to be used in a proof-of-concept experiment. The GPS entry refers to each of the two bands.

5.1.3.4.2 Phase Calibration System Noise

Errors in the phase calibration system (phasecal) also cause noise-like errors in the data. The phasecal signal power is assumed to be 1 percent of receiver noise, in rails spaced 5 MHz apart. A floor of 0.5 degrees of phase error per rail, irrespective of SNR, is also assumed. Phasecal error dominates when instantaneous signal power is greater than phasecal power or when the SNR of the coherently averaged observation is greater than 300.

5.1.3.4.3 Troposphere Noise

Tropospheric fluctuations cause noise-like fluctuations in the signal path. The model used (described in Reference 5-2) predicts rms noise of differenced observations for various atmospheric states. For all systems, observers assumed median atmospheric conditions, calculated the corresponding atmospheric noise, and multiplied by three. The atmosphere on the worst possible days was not considered; those noise values would be approximately three times worse.

For VLBI-2S and similar systems, the noise values for the low elevation satellite were computed for a difference observation between it and the satellite at WHS longitude. The noise for the WHS satellite was computed for a differenced observation between the WHS satellite and one directly at zenith. Such an assumption may be somewhat optimistic. For the GPS satellites, noise on ATDRS observations is taken between ATDRS and a GPS satellite at zenith. Noise on GPS satellites is taken between one at 20 degrees elevation (the cutoff) and one at zenith. For quasar calibration, the calibrator is assumed located 10 degrees off in azimuth, at the same elevation.

Tropospheric noise applies equally to each observation at a site. Observing between one site and several others does serve to reduce true system noise errors but not the propagation errors. Therefore, for a system in which troposphere is the dominant error source (such as VLBI-2S) the system is properly simulated by including baselines from all sites to one central site and omitting observations on baselines between remote sites. Inclusion of those observations would incorrectly imply that atmospheric noise is reduced by correlating against other sites.

5.1.3.4.4 Ionosphere Noise

Ionosphere error is estimated to be four times smaller than troposphere error and is neglected.

Table 5-2 shows the detailed calculation of delay measurement precision for interferometric observations of ATDRS and quasars. Table 5-3 shows the analogous calculation for group delay observations of GPS satellites.

5.1.4 CALIBRATION OF THE INTERFEROMETRIC OBSERVABLES

Whatever the choice of interferometric tracking system, the calibration method is critical. Calibration is required to render the interferometric data meaningful in the face of systematic errors, phase ambiguity (for phase delay), and clock synchronization (for VLBI).

5.1.4.1 Calibration by Signal Subtraction

One approach to calibration is observation of natural celestial radio sources (quasars). In such a system, each antenna observing ATDRS is supplemented by an adjacent antenna observing quasars. The delay to ATDRS and the delay to the quasar will have many errors in common such as station location, atmosphere, ionosphere, and, for VLBI systems, the clock.

Subtracting the ATDRS delay from the quasar delay provides a highly accurate delay difference, giving an accurate angular offset from the quasar, the precise position of which is known. This process is described in Figure 5-11.

For VLBI systems, the most important benefit of quasar calibration is the elimination of clock offsets as an error source. An ancillary benefit is reduction of systematic error from mismodeling tropospheric delay. For a CEI system, the major benefit is the reduction of the error due to tropospheric noise, which otherwise dominates. With differencing, atmospheric effects are diminished to the extent the rays traverse the same fluctuations.

5.1.4.2 Dual-Satellite Calibration

Quasar calibration adds considerable cost and complexity to the ATDRS tracking system. This derives ultimately from the weakness of the quasar signals (about 60 dB lower than the ATDRS signals) which require large antennas and large data quantities.

An alternative is the use of a second satellite as the reference object. Unlike the quasars, the other satellite would not have an accurately known a priori position, so direct subtraction to remove clock errors does not work. Rather, using successive observations of both satellites,

Table 5-2. Gain Budget and Measurement Precision

Parameter	VLBI*--Group Delay		CEI--Phase Delay	
	Quasar	ATDRS	Quasar	ATDRS
Source intensity (dBW/HZ/m**2)	-260	-200.5	-260	-200.5
Off-axis attenuation (dB)	0	-10	0	-30
System temperature (k)	100	200	100	200
Antenna diameter (m)	12	2	12	2
Equivalent noise (2kT/A)	-223.1	-204.5	-223.1	-204.5
Instantaneous SNR (dB)	-36.9	-5.9	-36.9	-25.9
Center frequency (GHz)	13.93	13.93	13.93	13.93
Transmitter bandwidth (MHz)	unlimited	260	unlimited	260
Receiver bandwidth (MHz)	500	225	50	50
RMS BW (MHz)	200	90	14	14
Sampled bandwidth (MHz)	16	16	50	50
Scan length (s)	300	1	120	1
# Gbits/scan	9.6	0.032	12.0	0.10
Scan SNR (CSNR)	12.8	950	14.2	16.4
Measurement precision 1/(2pi CSNR Brms) or 1/(2pi CSNR freq)	62 ps	2 ps	0.8 ps	0.7 ps
Satellite position error (m) c*error * Dsat/B B = 500km, VLB B = 10 km, CEI	1.6	0.05	1.0	0.9

* except VLBI-Ku

Table 5-3. Gain Budget and Measurement Precision for GPS Group Delay

Parameter	L1 Channel	L2 Channel
Signal power (dBW)	-163	-166
Antenna gain (2m, e=.5) (dBi)	27.4	25.2
Bandwidth (dB-Hz)	73	73
Noise power density (2KT; T=200K)	-202.5	-202.5
Noise power PN = 2KT/B (dBW)	-129.5	-129.5
Received signal power (dBW)	-135.6	-140.8
$Pr/(P_N + P_R)$ (dB)	-7.1	-11.6
Observation length - 1s Nbits - 4E7 Noise reduction Nbits x $2/\pi$	36	36
Uneven bandpass loss (dB)	-3	-3
Net SNR (coherent) (dB)	25.9	21.4
RMS bandwidth (Hz)	67.6	67.6
$1/2\pi$ Brms	27.6 ns	27.6 ns
Observation error	71 ps	200 ps
Ionosphere corrected error	359 ps	

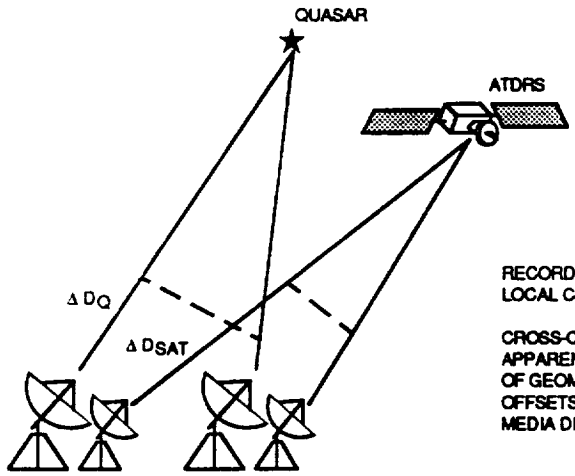

RECORD INCOMING E-FIELD, LOCAL CLOCK SIGNALS.

CROSS-CORRELATE TO FIND APPARENT LAG, CONSISTING OF GEOMETRIC DELAY, CLOCK OFFSETS, AND PROPAGATION MEDIA DELAYS.

$$\tau_Q = \frac{1}{C}\Delta D_Q + (\tau_{C1} - \tau_{C2}) + (\tau_{A1Q} - \tau_{A2Q})$$

$$\tau_S = \frac{1}{C}\Delta D_S + (\tau_{C1} - \tau_{C2}) + (\tau_{A1S} - \tau_{A2S})$$

SUBTRACT AND REARRANGE:

$$\frac{1}{C}\Delta D_S = \tau_S + \left(\frac{1}{C}\Delta D_Q - \tau_Q\right) + (\tau_{A1Q} - \tau_{A1S}) - (\tau_{A2Q} - \tau_{A2S})$$

THUS,

(1) CLOCK OFFSET ERRORS ARE ELIMINATED.

(2) ΔD_Q IS KNOWN FROM QUASAR POSITION, AND τ_Q IS MEASURED BY QUASAR OBSERVATION.

(3) IF ATDRS AND QUASAR LIE CLOSE IN THE SKY, THEN PROPAGATION DELAY ERRORS $(\tau_{A1Q} - \tau_{A1S})$, $(\tau_{A2Q} - \tau_{A2S})$ ARE SMALL AND LARGELY OFFSETTING.

RESULT: ACCURATE SATELLITE RANGE DIFFERENCE ΔD_S

BENEFITS OF CALIBRATION BY SUBTRACTION

	CLOCK OFFSETS CANCEL	SYSTEMATIC PROPAGATION DELAY ERRORS REDUCED	RANDOM PROPAGATION DELAY ERRORS REDUCED
VLBI-Q	✓	✓	(✓)
VLBI-2S	✓	—	—
CEI-Q	—	✓	✓
VLBI-GH	✓	✓	—

2055(1)-13

Figure 5-11. Calibration by Subtraction

the force model for both, and the equations of orbital mechanics, one solves for six orbital elements for each satellite as well as parameters to model the clock offsets between antenna sites.

5.1.4.3 Calibration by GPS

The U.S. Navy GPS will comprise a network of at least 18 satellites orbiting the Earth, carrying atomic clocks, and transmitting precise ephemerides and timing information. Calibration of an interferometric network with GPS may take many forms: observation of the coded navigation messages, tracking of the carrier phase, and treatment of the signal as noise-like to observe the group delay. One may use the broadcast ephemerides or solve for them. One may use the observations solely to accomplish clock syntonization, or may control other systematic error sources as well.

The GPS-calibrated system considered here combines many of the possibilities just mentioned. Group delay observations of the GPS, supplemented by carrier phase tracking, provide adequate data to solve for the GPS orbits. Collaterally, clock offset parameters can be calculated. The wide range of positions also makes it possible to solve accurately for tropospheric zenith delay. Two other possible systems are examined in less detail.

Calibration by GPS is more cumbersome than the two-TDRS technique because GPS, transmitting at a much lower frequency, requires separate antennas and receivers. Furthermore, 25 orbits must be solved for. However, the larger number of satellites and their motion make GPS well suited for solving for clock errors and other systematic biases. The advantage compared with quasars is signal strength: the GPS antenna, even for group delay measurements, would be 2 m or less in diameter, and would have uncooled receivers.

5.1.5 DESIGN TRADEOFFS

This section discusses some of the considerations in system design.

5.1.5.1 Station Locations; SGL Versus Higher Elevation

The interferometric observations will passively observe the Ku-band space-ground link, without requiring a special transmitter or signal. This signal is centered on the AGT

in White Sands, New Mexico. The footprint of the signal is a cone roughly 500 km in diameter but elongated due to the high zenith angle of the satellite in the assumed architecture.

Station locations within the main footprint are advantageous due to the relatively high signal intensity. Proximity to White Sands is also advantageous for communications and maintenance purposes. Location outside the main beam entails, besides the much weaker signal strength (typically 25-30 dB), the possibility of siting in a beam null and the possibility of nongeometric group delays caused by phase gradients across the frequency band due to small differential beam characteristics. (See Reference 5-12.)

Location outside the main beam has several advantages. Foremost is observation of ATDRS closer to the zenith. The smaller air path decreases errors caused by systematic misestimates of the effective air thickness and noise-like errors due to tropospheric fluctuations. In addition, larger station separations are possible for VLBI stations, and CEI arrays will have larger effective baselines because of less baseline foreshortening. The longer effective baseline dilutes effects of measurement error, both random and systematic, on inferred satellite position.

5.1.5.2 Choice of Calibration Objects

Absolute instrumental calibration of interferometers is difficult. Therefore, calibration sources are observed and, by subtraction, part or all of many errors are controlled. Three choices considered here are natural radio sources, GPS satellites, and a second ATDRS-like object in another orbit. The relative advantages of each are listed in the table contained in Figure 5-11.

5.1.5.3 Baseline Length

Satellite position uncertainty depends on the measurement errors, the separation between the stations, and the data arc length. Baseline length for the VLBI conceptual array is maximized subject to the boundaries of the main Ku-band footprint. The baseline lengths are about 500 to 1000 km. Station locations are specified in Figure 5-2. Baseline length for the CEI array is limited by the need for phase coherency, which requires that rms delay fluctuations be less than 5 mm over the course of a scan. Atmospheric fluctuations make this more difficult for longer baselines. The CEI arrays considered have maximum baseline lengths of 10 km.

5.1.5.4 Antenna Size, Data Transfer, Receiver Type

For either a phase delay measurement or a group delay measurement, a CSNR of about 10 is required for the measurement to be deemed reliable. A larger SNR may be needed for measurement precision adequate to the OD requirements. The 2-m ATDRS antenna meets these criteria easily. (See References 5-1 and 5-2 and Table 5-1.)

To observe natural radio sources, because quasar sources are so weak, much larger antennas are required. Integration time is limited by clock and other instrumental instabilities. Sampled bandwidth is limited by the requirement of real-time signal transmission. Receiver noise is the current (1988) state of the art for commercial, cryogenically cooled field effect transistor (FET) receivers. Antenna diameters of 12 m are required for a secure detection. For the parameters assumed (see Table 5-1), the CSNR is 12.8, for a typical quasar of flux density -260 dBW/Hz/m^2.

The most expensive part of a VLBI-Q system is data transmission. Adequate SNR requires approximately 9 Gbits of data for each observation at each site. Development of systems with improved system temperatures would reduce data volume proportional to the second power of the system temperature. Conversely, uncooled receivers would have system temperatures roughly double that of cooled receivers and would require four times as much data transfer. Use of larger antennas would reduce data volume proportional to the fourth power of the diameter. Tradeoffs between antenna size and data transfer requirements, therefore, need consideration.

For CEI systems, the quasar antennas were simply specified to be the same as chosen for the VLBI systems. Integration times are somewhat more limited due to greater sensitivity to atmospheric fluctuations. For the CEI systems, it is possible to ship much more than the specified 50 MHz down the fiber optic links. It is possible and perhaps economical to trade increased bandwidth for reduced antenna size or for use of uncooled receivers.

5.1.5.5 Operations (Remote Versus Manned)

Unmanned station operations are obviously preferred when possible. Based on concepts already developed for the more complex VLBI-based systems, unmanned operations should be feasible. However, 12-m antennas and helium-cooled receivers would require constant monitoring and periodic

maintenance. It would be necessary at least to have a traveling crew visit each site regularly and to have full-time monitoring of all stations from the central control facility. Near-site on-call personnel are necessary for certain conditions that may be diagnosed but not repaired remotely.

The CEI arrays proposed would have maintenance requirements similar to the VLBI sites, as they too consist of 12-m antennas with cooled receivers. As each site would have five or more such antennas, and as the two sites are quite distant from each other, separate support staffs are needed; however, remote monitoring can enable operation without around-the-clock staffing.

The satellite-calibrated techniques are much simpler systems than the others. The antennas are 2 m in diameter, the receivers are uncooled, and the data rates may not even require satellite communications capability. Even the most complex component, the hydrogen maser time standard, can be monitored remotely.

5.2 SYSTEM ASSESSMENT

This section describes factors to be used in assessment of interferometric systems.

5.2.1 INTERFEROMETRIC ORBIT DETERMINATION

Position accuracies for both ATDRS-E and ATDRS-W for various scenarios for the interferometric tracking systems listed in section 5.1.2 are evaluated. The first phase of this study examined the VLBI-Q and CEI-Q systems in great detail.[1] The remaining systems were evaluated in the second phase. Resources prevented complete parameter studies of these latter systems as done for the first two. During the second study, two tracking scenarios were emphasized: orbit determination (OD) and trajectory recovery (TR).

The ATDRS tracking accuracy results are divided in the following into the two scenarios, OD and TR. OD is the normal scenario for which the ATDRS tracked. In the present TDRS practice, 30 hours of data are used to determine orbits. The TR scenario simulates the post maneuver ATDRS

[1]The VLBI-2S system was studied in both phases; the definitive results shown here were derived in the second phase.

scenario. Tracking begins after the maneuver begins and accurate orbits must be determined from as little as 2 hours of data.

Performance is evaluated for both the definitive and predictive periods. In the case of OD, the predictive period of particular interest is 3 days. For TR, predictive periods of 6 hours to 1 day are emphasized.

The assumed errors used in the simulation results that follow are displayed in Tables 5-4 through 5-11. Errors listed are the three sigma values. Displayed in Tables 5-12 and 5-13 are summaries of the OD results using interferometric techniques for ATDRS-E and ATDRS-W, respectively. For each tracking alternative, the maximum total error for the definitive period, the source of the maximum error, and the number of hours that each has maintained ATDRS positions within the desired (75m) accuracy goal are shown. Tables 5-14 and 5-15 show the same for the TR scenario.

A more complete accounting of the simulation results may be found in Appendix A.

5.2.1.1 Definitive Period OD

Most of the interferometric tracking alternatives satisfy the goals of this study during the definitive period in the OD scenario. The systems that exhibit the highest level of accuracy, VLBI-Q and VLBI-Ku, achieve a performance of under 40m, 3 σ. The only systems that do not meet the study goal for ATDRS-E in this scenario are VLBI-2S system without GTR to White Sands and the VLBI-GT system. The performance of the latter system was so disappointing here that no further performance studies were made on this system.

In general, there is little difference between the performance of ATDRS-E and ATDRS-W in this scenario except that the determinations of ATDRS-E are usually better than ATDRS-W. This is principally due to better geometry in the case of the ATDRS-E.

Use of the three ATDRS satellites in VLBI-3S alternative shows improves the tracking performance by about 33% over the similar VLBI-2S system. Similarly, the use of longer baselines in the VLBI-Ku system makes this system the most accurate at OD despite its higher measurement noise value than its counterpart, VLBI-2S. As one would expect, the GPS calibrated systems, VLBI-GC and VLBI-GH, have similar performance. These results indicate that GTR is required to meet the tracking goal with a high level of confidence.

Table 5-4. Error Budget: VLBI-Q

Parameter	Estimated Uncertainty
Relative station location	0.06 m horizontal coordinates 0.18 m vertical
Troposphere - Systematic	2% of total delay on second station 0% on first station
Ionosphere	12% of total delay on second station 0% on first station
Clock offset	150 ps
Noise	
Quasar observation	(0.056 m)
ATDRSS observation	(<0.008 m)
Troposphere	(0.045 m)
Ionosphere	(0.008 m)
Total (rms)	0.073 m

Table 5-5. Error Budget: CEI-Q

Parameter		Estimated Uncertainty
Relative station location		0.006 m per coordinate (x,y,z)
Troposphere - Systematic		
East:	baseline 1-2	0.0034%
	baseline 2-3	0.0035%
	baseline 3-1	0.00014%
West:	baseline 1-2	0.0052%
	baseline 2-3	0.260%
	baseline 3-1	0.0210%
Ionosphere		0.0012% (apply as for troposphere)
		0.0012%
		0.0006%
Clock offset		0 ps
Noise: Instrumental		0.073 m
Noise: Tropospheric		
East; West		
Average day		0.014 m; 0.020 m
(Poor day)		(0.050 m); (0.077 m)

Table 5-6. Error Budget: VLBI-2S Phase I

Parameter	Estimated Uncertainty		
Relative station location (Local X, Y, Z)			
Baseline C1-C2	.076 m	.076 m	.228 m
Baseline C1-E	.154 m	.154 m	.462 m
Baseline C2-E	.186 m	.186 m	.558 m
Baseline C1-W	.168 m	.168 m	.504 m
Baseline C2-W	.156 m	.156 m	.468 m
Troposphere - Systematic	4.5% (of total delay on 2nd site)		
Ionosphere - Systematic	100% (of delay difference)		
Clock errors - Systematic	Solve for		
Noise: Instrumental (3σ)	.01 m		
Noise: Tropospheric (3σ)	East	West	Overhead
Average day			
Baseline C1-C2	.076 m	.064 m	.039 m
Baseline C1-E	.065 m	--	.039 m
Baseline C2-E	.068 m	--	.039 m
Baseline C1-W	--	.068 m	.039 m
Baseline C2-W	--	.068 m	.039 m

Table 5-7. Error Budget: VLBI-2S Phase II

Parameter	Estimated Uncertainty		
Relative station location (Local X, Y, Z)			
Baseline C1-C2	.076 m	.076 m	.228 m
Baseline C1-E	.154 m	.154 m	.462 m
Baseline C2-E	.186 m	.186 m	.558 m
Baseline C1-W	.168 m	.168 m	.504 m
Baseline C2-W	.156 m	.156 m	.468 m
Troposphere - Systematic	4.5% (of total delay on 2nd site)		
Ionosphere - Systematic	100% (of delay difference)		
Clock errors - Systematic	Solve for		
Noise: Instrumental (3σ)	.01 m		
Noise: Tropospheric (3σ)	East	West	Center
Average day			
Baseline C1-C2	.072 m	.076 m	.021 m
Baseline C1-E	.054 m	--	.020 m
Baseline C2-E	.058 m	--	.021 m
Baseline C1-W	--	.059 m	.020 m
Baseline C2-W	--	.060 m	.021 m

Table 5-8. Error Budget: VLBI-Ku (Ku-Band Beacon VLBI)

Parameter	Estimated Uncertainty
Relative station location	(Local x,y,z) Baseline WST-FTD .06 m .06 m .24 m WST-RCH .06 m .06 m .24 m FTD-RCH .06 m .06 m .24 m
Troposphere - Systematic	4.5% of total delay (if not solved for)
Ionosphere - Systematic	ATDRS: 100% of delay difference GPS: Calibrated
Clock errors - Systematic	Solve for
Noise: Instrumental	ATDRS 0.010 m
Noise: Tropospheric	ATDRS .099 for all stations and both satellites

Table 5-9. Error Budget: VLBI-GH (Hybrid System)

Parameter	Estimated Uncertainty
Relative station location	Same as VLBI-2S
Troposphere - Systematic	Solved for
Ionosphere - Systematic	ATDRS: 100% of delay difference GPS: Calibrated
Clock errors - Systematic	Solve for
Instrumental offsets (3σ)	ATDRS 0 GPS 15 cm/satellite
Noise: Instrumental (3σ)	ATDRS 0.010 m GPS 0.020
Noise: Tropospheric (3σ)	ATDRS Same as VLBI-2S GPS 0.048

Table 5-10. Error Budget: VLBI-GC (Coded System)

Parameter	Estimated Uncertainty
Relative station location	Same as VLBI-2S
Troposphere - Systematic	Solved for
Ionosphere - Systematic	ATDRS: 100% of delay difference GPS: Calibrated
Clock errors - Systematic	Solve for
Instrumental offsets (3σ)	ATDRS 0 GPS 9 cm/satellite
Noise: Instrumental (3σ)	ATDRS 0.010 m GPS .074
Noise: Tropospheric (3σ)	ATDRS Same as VLBI-2S GPS 0.048

Table 5-11. Error Budget: VLBI-GT (GPS Time Transfer)

Parameter	Estimated Uncertainty
Relative station location	Same as VLBI-2S
Troposphere - Systematic	Solved for
Ionosphere - Systematic	ATDRS: 100% of delay difference GPS: Calibrated
Clock errors - Systematic	Solve for
Instrumental offsets (3σ)	ATDRS 0
Noise: Instrumental (3σ)	ATDRS 0.010 m
Noise: Tropospheric (3σ)	ATDRS Same as VLBI-2S

Table 5-12. Summary of OD Accuracies for ATDRS-E

System	Tracking or Solution Type	Total OD Error (meters)	Largest OD Error Source	Duration of <75 m Predictions (hours)
VLBI-Q	R	35	Troposhere	45
VLBI-Q	N	33	Troposhere	>72
VLBI-Q	S	32	Troposhere	>72
CEI-Q	R	40	Range bias	>72
CEI-Q	N	71	Noise	2
VLBI-2S	RT	62	Solar Rad.	68
VLBI-2S	N	106	Troposhere	0
VLBI-3S	R	44	Range bias	>72
VLBI-3S	N	67	Ionosphere	54
VLBI-GC	NT	75	Ionosphere	19
VLBI-GC	RT	56	Ionosphere	22
VLBI-GH	NT	77	Ionosphere	0
VLBI-GH	RT	53	Ionosphere	43
VLBI-GT	N	185	Clocks	0
VLBI-Ku	N	23	Earth Orientation	>72

NOTE: Errors are all 3σ.

N = No Range Data
R = Range Data
S = R+ Solve Range bias
T = Solve Troposphere Height

Table 5-13. Summary of OD Accuracies for ATDRS-W

System	Tracking or Solution Type	Total OD Error (meters)	Largest OD Error Source	Duration of <75 m Predictions (hours)
VLBI-Q	R	36	Troposhere	>72
VLBI-Q	N	34	Troposhere	>72
CEI-Q	R	59	Solar rad. Press.	65
CEI-Q	N	87	Station Position	0
VLBI-2S	RT	121	Ionosphere	0
VLBI-2S	N	104	Troposhere	0
VLBI-3S	R	72	Troposhere	39
VLBI-3S	R	50	Ionosphere	>72
VLBI-3S	R	70	Ionosphere	51
VLBI-GC	NT	80	Ionosphere	0
VLBI-GC	RT	51	Ionosphere	56
VLBI-GH	NT	82	Ionosphere	0
VLBI-GH	RT	48	Ionosphere	0

NOTE: Errors are all 3σ.

N = No Range Data
R = Range Data
S = R+ Solve Range bias
T = Solve Troposphere Height

Table 5-14. Summary of TR Accuracies for ATDRS-E

System	Tracking or Solution Type	Total TR Error (meters)	Largest TR Error Source	Duration of <75 m Predictions (hours)
VLBI-Q	R	43	Troposhere	8
VLBI-Q	N	647	Noise	0
CEI-Q	R	100	Station position	0
CEI-Q	N	8132	Noise	0
VLBI-2S	RT	47	Range bias	9
VLBI-2S	N	1055	Noise	0
VLBI-3S	R	42	Range bias	8
VLBI-GC	RT	80	Ionosphere	0
VLBI-GH	RT	89	Ionosphere	0
VLBI-Ku	N	36	Noise	4

NOTE: Errors are all 3σ.

N = No (GTR) Range Data
R = Range (GTR) Data
T = Solve Troposphere Height

Table 5-15. Summary of TR Accuracies for ATDRS-W

System	Tracking or Solution Type	Total TR Error (meters)	Largest TR Error Source	Duration of <75 m Predictions (hours)
VLBI-Q	R	53	Troposhere	7
VLBI-Q	N	909	Noise	0
CEI-Q	R	131	Station position	0
CEI-Q	N	9741	Noise	0
VLBI-2S	RT	127	Ionosphere	0
VLBI-2S	N	1086	Noise	0
VLBI-2S	R	99	Trosphere	0
VLBI-3S	R	68	Solar rad. press.	7
VLBI-GC	RT	130	Ionosphere	0
VLBI-GH	RT	140	Ionosphere	0

NOTE: Errors are all 3σ.

N = No Ranging (GTR) Data
R = Range Data
T = Solve Troposphere Height

5.2.1.2 Predictive Period OD

Only three systems were able to maintain orbits of study goal accuracy for 3 days after tracking: VLBI-Q, VLBI-3S, VLBI-Ku. GTR is required for this performance only in the case of VLBI-3S although this system accurately tracks both ATDRSS satellites in excess of 2 days without GTR. Again, solving for the orbits of the three satellites simultaneously improves the determination for VLBI-3S over that for VLBI-2S. The remaining GPS calibrated systems, VLBI-GC and VLBI-GH, predict accurately usually between 1 and 2 days and never for 3 even when supplemented by GTR.

5.2.1.3 Definitive Period TR

The TR scenario (2 hours of tracking) is a difficult scenario for tracking systems to handle accurately. Only the VLBI-Q, VLBI-3S, and the VLBI-Ku systems maintain the study's tracking accuracy goals for both satellites. Of these, only VLBI-Ku can maintain this without GTR to White Sands. The quasar calibrated systems perform very badly without GTR for the short, 2-hour spans of data. Parameter studies given in the appendix, show that approximately 6 hours of data are needed by the VLBI-Q system for GTR not to be needed and the full 30 hours of data is needed by the CEI-Q system.

5.2.1.4 Predictive Period TR

Prediction of ATDRS orbits from only 2 hours of tracking data is the most stringent test of the various tracking alternatives. Of the systems that met the tracking goals for TR definitive, none accurately predicts for more than nine hours and all require GTR. The VLBI-Q and VLBI-3S systems show accurate predictions of more than 6 hours. The VLBI-Ku system was not simulated with GTR due to lack of time and resources.

5.2.1.5 Effect of Range Noise and Bias Levels

For the results presented here, the somewhat optimistic value of 1 m (3 σ) was used as the noise level for the ATDRSS ground station range data. To determine the impact of relaxing this constraint, VLBI-Q results for a 2-hour TR were obtained for varying levels of range noise. The results are shown in Figure A3-3 of Appendix A. Noise levels in excess of 30 m did not significantly affect TR definitive period orbit accuracy. Further, because the component of the total error due to unmodeled range bias

never exceeds 3 m, this bias can be as large as 20 m without causing the total error to exceed the performance criteria.

Due to resource and time constraints, studies of the effect of range noise and bias levels were not conducted for systems other than VLBI-Q. For several of these systems, e.g., VLBI-2S, the bias level will have a significant effect on the orbit and trajectory accuracies. If further studies of interferometric tracking alternatives are to be conducted, this is an area that merits further investigation.

5.2.1.6 Discussion

The only tracking systems that show the most acceptable level of performance for both OD and TR and during definitive and predictive periods. These are VLBI-Q, VLBI-3S, and VLBI-Ku.

5.2.2 OBSERVATION STALENESS

Table 5-16 summarizes the steps in deriving the calibrated delay difference and gives estimates of the time involved in performing each step. The first item, initial fringe search, applies only when the a priori satellite position is highly uncertain. The 5-minute data transmission for multiple-satellite and GPS-calibrated systems assumes a narrow communications channel (105 kbits/s); a wider channel would reduce this time proportionately. In the GPS hybrid system, GPS group delay observations can be multiplexed onto the same channel between ATDRS observations.

5.2.3 ATDRS IMPACTS

The signal source used in all of the systems except VLBI-Ku is the Ku-band downlink. This signal source is available for passive observation and has no impact on design or operation of ATDRS. Adequate TR performance will require AGT ranging data. Because this ranging system would probably be included in the terminal design, there may be no additional impact. Such a conclusion depends on the ranging accuracy required.

Communication of data may impose a substantial impact for a VLBI-Q system. Large data rates are required (at least 32 Mbits/sec from each remote station). Although communications need not be through ATDRS itself, some means of transport is required. The time-averaged data load for the network is about one-sixth of the above, per site, in normal OD tasks. This problem does not arise in the VLBI-2S or CEI-Q system because the data rates are at least 100 times smaller.

Table 5-16. Time Required To Derive Calibrated Delay Difference

System	VLBI-Q	CEI-Q	All Other VLBI Systems
(Fringe search)	(1 min)	(1 min)	(1 min)
Data taking	5 min	2 min	1 sec
Data transmission	1 sec	-	5 min
Correlation	(real time)	(real time)	(real time)
Fringe fitting	3 min	5 sec	20 sec
Corrections and calibrations	20 sec	20 sec	20 sec
Transmission to FDF	1 sec	1 sec	1 sec
TOTAL	10 min	3.5 min	7 min

5.2.4 TECHNOLOGY RISKS

Technology involved in building these interferometric systems is all within present-day state of the art, with minor exceptions. The performance estimates also depend on the detailed error budget, parts of which are uncertain. These aspects will be discussed in turn.

5.2.4.1 CEI System Risks

The CEI system may be compared with the Very Large Array (VLA), which has operated regularly at Ku-band for more than 10 years. At the VLA, the antennas are larger, the baselines longer, the total data transmission greater, and the number of stations greater than for the system proposed here.

This system would use optical fiber links for data transmission, as a less expensive alternative to waveguide.

Data rates of 10 GHz-km are within current capabilities. So too are receiver bandwidths of 1 GHz at Ku-band. The correlator system can employ the Haystack correlator system architecture, using the new 20 MHz correlator chips now being tested. Alternatively, for a phase-delay-only system, the VLA correlator system is adequate, scaled down and with software modifications for improved tracking of nonsidereal sources.

Modification of the CEI system to produce group delay measurements goes beyond current CEI systems but does not require any new technology. The required receiver bandwidth is about 1 GHz, well within current capabilities for cooled Ku-band receiver design. Fiber optic links, capable of transmitting the entire 1 GHz signal 10 km, are commercially available today. Correlation may be performed by a series of chips processing smaller bandwidths.

Design of a CEI system to produce group-delay measurements goes beyond current CEI systems. The hardware elements do not extend current capabilities. The required receiver bandwidth is about 1 GHz, under 10 percent of the center frequency, which is within current capabilities for cooled Ku-band receiver design. Fiberoptic lines capable of transmitting the 1-GHz-wide signal over 10 km are commercially available at present. The new NASA GSFC Crustal Dynamics Project phase-calibration system is probably adequate. Correlation may be performed by a series of chips processing smaller bandwidths. Such a system would require a new design; however, the individual processor chips required have already been developed for use in radio astronomy.

5.2.4.2 VLBI Systems Risks

VLBI arrays have operated at Ku-band for many years now and have recently operated at up to 90 GHz. The possibility of real-time data correlation was demonstrated more than 10 years ago (Reference 5-10). The present version of the phase calibration unit would perform inadequately at Ku-band. However, that phase calibration system has been redesigned, and a prototype is now being tested (summer 1988).

The major change to the correlator system would be the addition of large buffers, to allow synchronization of data being transmitted in real time from remote stations. Such buffers have been used (Reference 5-10).

5.2.4.3 GPS Error Budget Risks

For the GPS/Hybrid calibrated system, most elements are already extant. This includes the phase tracking receivers to propagate group delay measurements, and software (GEODYN) for producing GPS ephemerides. The software for utilizing the interferometric observable is not yet implemented in the commercially available PC version of GEODYN, but it has been implemented in a mainframe version.

One technical uncertainty is control of multipath effects in GPS observations. The hybrid system may be less susceptible than some others because (1) an elevation cutoff of 20 degrees is assumed; (2) group delay observations are made with a 2-m directional antenna; and (3) the carrier phase tracking observations are less susceptible to multipath effects than group delay or pseudorange measurements.

The other area of technical uncertainty is tying the GPS and ATDRS observations to the same coordinate frame. Unlike in the quasar-calibrated system, there is no way to calibrate the difference in electrical reference points by observation. That uncertainty should be added into the baseline vector uncertainty, but it has not yet been evaluated.

5.2.4.4 Error Budget Risks

The OD and TR results derived here depend critically on the error budget assumed. This error budget, described in Appendix A, was carefully considered and comprises best estimates of the true error contributions from each error source. Some of these estimates are themselves uncertain.

Errors estimates from solar radiation pressure, ionosphere, and troposphere are least firm. Solar radiation pressure depends on the orientation and reflectivity of the satellite and on the variability of solar flux. The ionospheric error depends on the ionospheric excitation level (systematic error) and the level fluctuations (noise-like error); however, neither of these are dominant error sources. Errors due to troposphere are the largest source of uncertainty in the OD/TR results.

The systematic error is based on detailed studies of how accurately tropospheric delay can be predicted. The estimated errors are global averages and neglect effects of meteorological measurement errors. Such effects cause substantial errors in delay estimates at certain times.

Tropospheric fluctuations are another major uncertainty. The equivalent delay noise assumed in based on a model of substantial uncertainty and on average weather conditions. Under severe conditions, the equivalent noise can be three to five times worse. The statistics on how often the noise is how large are particularly uncertain and probably highly site dependent. For the CEI systems, which are substantially limited by measurement noise, this poses significant uncertainties.

5.2.5 EXTERNAL DEPENDENCIES

The VLBI systems are dependent on data links to transmit observations for real-time correlation. These links may be through ATDRS (see Section 5.2.3) or may be external. The systems also rely on Earth orientation information from external sources, although VLBI-Q could, at increased operational cost, obtain that information independently.

The GPS-calibrated VLBI systems require that the Navy's GPS satellites be deployed and operational. Different versions have different requirements.

The VLBI-GT system (GPS for time transfer) requires that time transfer through GPS be accurate to at least 1 nanosecond (1E-9S). This requires at least one satellite to be visible at any given time and broadcasting its position with sufficient accuracy. It also requires decoding the secure (P-code) signal.

A subset of the satellites may have accurate, undithered, unencrypted signals available for the time-transfer community. In that event, the facility would not need to be secured. In any case, the ephemerides would have to be exceedingly accurate.

The VLBI-GC system uses GPS for calibration by observations of the coded signal, and fitting orbits. This requires signal decoding, with associated security requirements. Because GPS orbits would be fitted, the broadcast ephemeris need not be highly accurate.

The VLBI-GH system involves group delay and carrier phase observations of the GPS. The P-code signals are not decoded; therefore, secure facilities are not necessary. Broadcast GPS ephemeris need not be highly accurate because they are required only for antenna pointing.

5.2.6 OTHER FEATURES

Implementation of any of the interferometric tracking systems described here would provide time synchronization at the sites from which the ATDRS is observed. Therefore, the opportunity arises to track other satellites from these same sites using interferometric measurements. The observations might be made with the same equipment, at very little additional expense.

5.2.7 DISCUSSION

The major advantage of the interferometric observable is that no satellite cooperation is required. Passive observation of the ATDRS SGL can provide the delay difference measurement with no use of satellite resources. The proposed systems are all based on current state-of-the-art radio astronomical technology. None (excepting VLBI-Ku) requires development of new hardware systems. (See Section 5.2.7.)

The VLBI-Q and VLBI-3S system options meet normal OD requirements by these passive interferometric observations alone. The CEI-Q system does not quite meet the OD specification (25-m 1-σ error). The GPS calibrated systems, VLBI-GC and VLBI-GH, require GTR (ranging) to achieve the OD study goal.

The VLBI-Q and VLBI-3S systems require supplemental accurate range measurements to the AGT for adequate, timely TR performance. The CEI-Q system does not quite meet TR needs (25-m 1-σ uncertainty in 2 hours), even with supplemental range measurements. The VLBI-GC and VLBI-GH systems do not meet the study goals for TR.

The OD results for VLBI-Q and VLBI-3S are slightly more pessimistic than before (References 5-4, 5-5) as a result of revision of the error model. Improved atmospheric modeling, measurement, or water vapor radiometers would substantially improve all OD and TR results. For the CEI option, longer baselines may also yield better orbits.

5.3 REFERENCES

5-1. R. Potash, J. Ray, N. Zelinsky, C Knight, K. Way, and B. Schupler, Specifications for a TDRS Tracking System Using Interferometry: I: CEI Using Natural Radio Sources As Calibrators, report prepared under contract NAS 5-27600, GSFC/ NASA, Greenbelt, MD, 1987

5-2. --, Specifications for a TDRS Tracking System Using Interferometry: III: VLBI Using Natural Radio Sources As Calibrators, report prepared under contract NAS 5-27600, GSFC/NASA, Greenbelt, MD, 1987

5-3. J. Ray, Clock Calibration for Interferometric Tracking of Multiple TDRS Satellites, report prepared under contract NAS 5-27600, GSFC/NASA, Greenbelt, MD, 1987

5-4. J. Ray, A. Au, N. Zelinsky, C. Knight, K. Way, and B. Schupler, Specifications for a TDRS Tracking System Using Interferometry: II: CEI Using GPS Radio Sources As Calibrators, report prepared under contract NAS 5-27600, GSFC/NASA, Greenbelt, MD, 1987

5-5. --, Specifications for a TDRS Tracking System Using Interferometry: IV: VLBI Using GPS Radio Sources As Calibrators, report prepared under contract NAS 5-27600, GSFC/NASA, Greenbelt, MD, 1987

5-6. J. Ray and C. Knight, VLBI Experiment To Track NASA's Tracking and Data Relay Satellite (TDRS): Final Report, prepared under contract NAS 5-27600, GSFC/NASA, Greenbelt, MD, 1987

5-7. J. Ray, C. Knight, and D. Shaffer, Experiment To Track NASA's Tracking and Data Relay Satellite (TDRS) Using the VLA: Final Report, prepared under contract NAS 5-27600, GSFC/NASA, Greenbelt, MD, 1987

5-8. J. Ray and C. Knight, Interferometric Tracking of TDRS: Constraints Imposed by the Use of Natural Radio Sources As Calibrators, Interferometrics, Inc., report prepared under contract NAS 5-27600, GSFC/NASA, Greenbelt, MD, 1985

5-9. J. J. Spilker, "GPS Signal Structure and Performance Characteristics," Navigation, 25, 1978, p. 121

5-10. J. L. Yen, K. I. Kellerman, B. Raygrer, N. W. Broten, D. N. Fort, S. Knowles, and W. B. Waltman, "Real-Time, Very-Long-Baseline Interferometry Based on the Use of a Communications Satellite," Science, 1977, pp. 198, 289

5-11. N. Zelinsky, J. Ray, and P. Liebricht, Error Analysis for Earth Orientation Recovery From GPS Data, submitted to Proceedings, IUGG, Vancouver, BC, 1987

5-12. R. Potash, TDRS Beam Structure: Its Effect on Interferometric Tracking Systems, Interferometrics, Inc., report, prepared under contract NAS 5-27600, GSFC/NASA, Greenbelt, MD, 1986

SECTION 6 - ATDRS/GPS TRACKING SYSTEMS

The NAVSTAR GPS, administered by the Department of Defense (DoD), permits several techniques to determine ATDRS orbits. GPS comprises a network of as many as 24 low Earth-orbiting satellites, each emitting L-band ranging signals, and allows a GPS user equipped with a GPS receiver to observe a subset of the network at any instant and, on the basis of the emitted GPS signals, compute the user's instantaneous position and time. Use of GPS to track the ATDRSS satellites, however, is complicated by the ATDRS geosynchronous orbits. This section provides a brief introduction to GPS and presents three potential ATDRS/GPS tracking systems, termed direct, passive differential, and direct differential.

The Direct ATDRS/GPS Tracking System requires that a GPS receiver be placed onboard the ATDRSS satellites and relies on line-of-sight signal propagation between the GPS satellites and ATDRS. ATDRS measurement of the visible GPS signals and relay of the observations to the AGT then permits ATDRS OD. In the Passive Differential ATDRS/GPS Tracking System, GPS receivers are not placed onboard the ATDRS satellites; rather, the ATDRSS satellites are assumed to emit a ranging signal such as an S-band, PRTS, or Ku-band beacon. Ground tracking stations measure ranging signals from a single ATDRSS satellite and a single GPS satellite. The ATDRS and GPS measurements are differenced at each station; then the measurements of pairs of ground stations are double differenced to form the observations used for ATDRSS OD. Finally, the Direct Differential ATDRS/GPS Tracking System involves a GPS receiver onboard the ATDRSS satellites. To eliminate common mode errors, however, measurements of two GPS satellites made simultaneously by the ATDRS and a ground tracking station are differenced and then double differenced to form the ATDRSS OD observation.

6.1 GPS OVERVIEW

The NAVSTAR GPS is a worldwide precise navigation system in which a constellation of up to 24 GPS satellites provides a spatial and temporal reference system for GPS users equipped with appropriate receivers. Instantaneous position, velocity, and time may all be determined by Earth- or near-Earth-based GPS users. However, limited visibility of the GPS network requires that geosynchronous altitude users employ dynamic OD methods, which use measurements between the geosynchronous user and the GPS satellites to correct a dynamical model of the user's orbit.

Aspects of the GPS satellite constellation and system architecture, the GPS signal structure and navigation message, typical GPS receiver characteristics, selective availability of the system, and GPS visibility, especially to geosynchronous GPS users, are discussed in the sections that follow.

6.1.1 GPS SYSTEM ARCHITECTURE

GPS is divided into three segments: the Space Segment, the Control Segment, and the User Segment. The GPS Space Segment, supported by the GPS Control Segment, is designed to provide the User Segment with precise instantaneous position, velocity, and time at the GPS user's location. As shown in Figure 6-1, precise position, velocity, and time determination is made possible by satellite navigation information incorporated as data on the signal each GPS satellite emits. Each GPS satellite broadcasts its position and time as part of the GPS navigation message. Measurement of the range to four GPS satellites in simultaneous view of the GPS user provides enough information to determine the user instantaneous spatial coordinates and velocity and to eliminate the clock bias of the user's receiver with respect to the GPS system clock.

Current plans the GPS Joint Program Office has adopted call for deployment of two phases of the GPS satellite constellation (Reference 6-1) that constitutes the GPS Space Segment. The first phase requires implementation of an Optimal 21-Satellite Constellation (OSC) composed of 18 GPS satellites and 3 active spares to be placed in orbit by fall of 1989. The second phase then requires implementation by the mid-1990s of a Primary Satellite Constellation (PSC) composed of 21 GPS satellites and 3 active spares. Both the OSC and the PSC consist of 6 orbital planes inclined at 55 degrees. The longitudes of the ascending nodes of the orbital planes are separated by 60 degrees for both the OSC and PSC, with three and four satellites per plane, respectively. Positioning of the GPS satellites is not uniform within an orbital plane. The orbital radius of each satellite is 26,609 km, and the orbital period is 11 hours, 59 minutes, and 57 seconds. All references to the GPS constellation in Section 6 will refer to the 24-satellite PSC, in keeping with the likely implementation date of any ATDRS tracking system.

The GPS Control Segment performs GPS satellite tracking, monitoring, and control functions. Three types of ground stations constitute the Control Segment: remote monitor

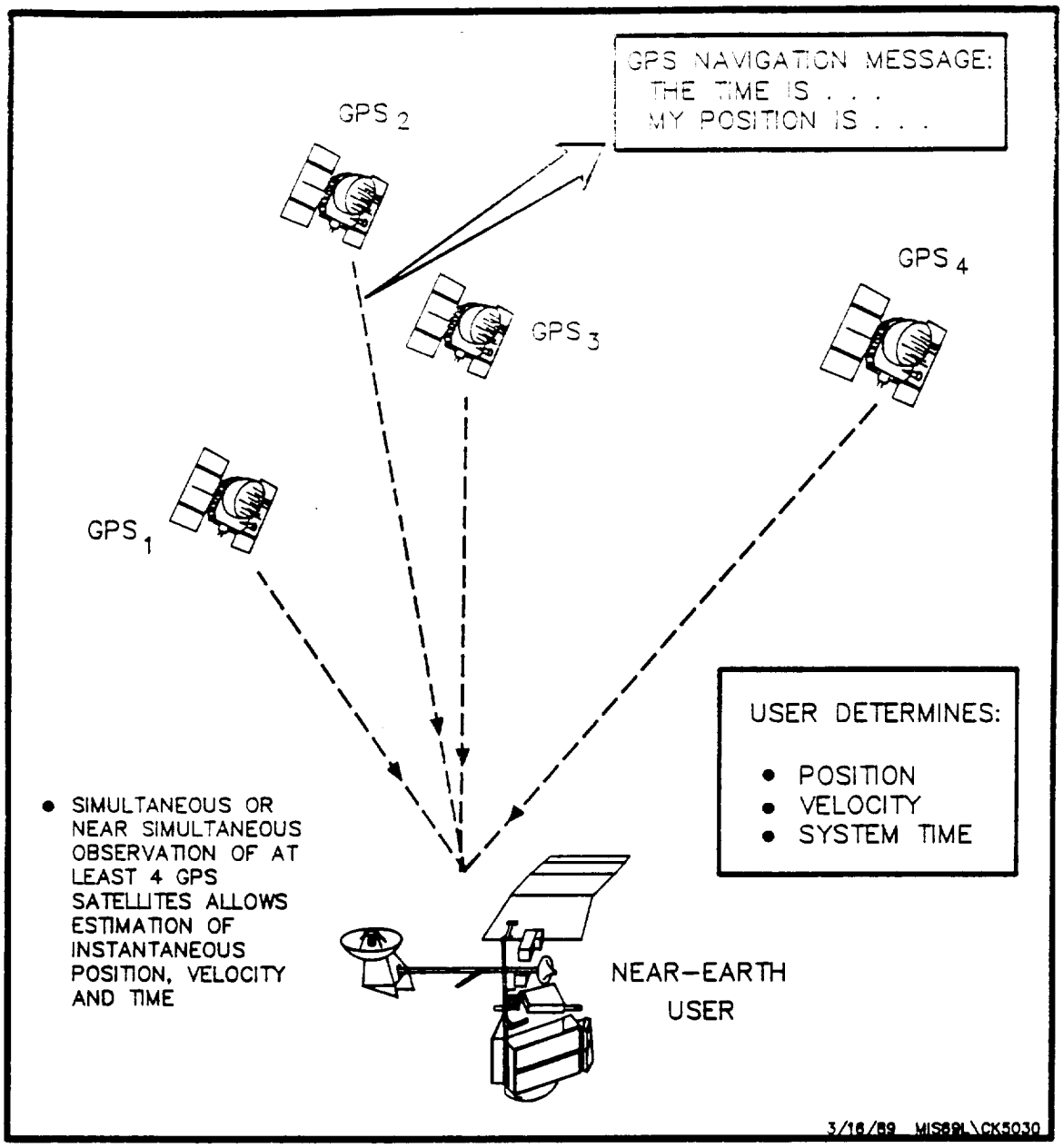

Figure 6-1. Instantaneous Navigation Using GPS

stations derive Space Segment tracking data from broadcast GPS signals; a master control station processes the tracking data and develops navigational message parameters for each GPS satellite; and an uploading station supports the relay of control commands to the elements of the Space Segment, updating the navigation message data every 8 hours. The GPS Space Segment is synchronized to the master control station's cesium clock to establish GPS system time. Knowledge of the difference between GPS system time and UTC is maintained to within 100 μsec, and the corrections are published regularly for the benefit of GPS users.

The GPS User Segment comprises the receiver/processor equipment of GPS users, both Earth-based and space-based. Users typically determine their instantaneous position and velocity through use of pseudorange and pseudorange-rate measurements of four GPS satellites in simultaneous view. GPS time transfer to GPS users may be made with the same equipment.

6.1.2 GPS SIGNAL STRUCTURE AND NAVIGATION MESSAGE

The GPS signal structure and navigation message allows GPS users to measure pseudorange and pseudorange-rate to each GPS satellite. The GPS signal each GPS satellite emits is composed of two L-band spread spectrum signals with frequencies centered at 1227.6 and 1575.42 MHz. These center frequencies are referred to as L1 and L2, respectively. Their signal characteristics are summarized in Table 6-1 (References 6-2 and 6-3). Each center frequency is a coherently selected multiple of a 10.23 MHz clock, and the frequency separation between the L1 and L2 signals provides an ionospheric error correction capability to the GPS User Segment. The L1 signal is QPSK modulated, where the in-phase component is PN-modulated by the Precise Positioning Code at 10.23 MHz to form the precise (P-code) signal and the quadrature component is modulated by the Standard Positioning Code at 1.023 MHz to form the clear acquisition (C/A-code) signal. The L2 signal is BPSK modulated by the P-code. The 1500-bit GPS navigation message is encoded on both carriers at a data rate of 50 bps. The GPS signal structure is designed to support user position, velocity, and time determination through processing of either the full signal structure or the C/A-code signal alone. Users authorized to obtain the full position determination accuracy permitted by GPS are provided access to the set of GPS P-codes for use in their GPS receivers.

Table 6-1. GPS Signal Parameters

PARAMETERS	DEFINITION
L_1 SIGNAL	
RF FREQUENCY	1575.42 MHz (154 x 10.23 MHz)
MODULATION	QPSK
IN-PHASE SIGNAL (P-CODE)	
PN CHIP RATE	10.23 Mcps
PN CODE LENGTH	- 6 x 10^{12} CHIPS (EXACTLY ONE WEEK)
CODE TYPE	PRODUCT CODE (X1 AND X2)
EPOCH	RELATED TO SUBFRAME EPOCH AND HANDOVER WORD
QUADRATURE SIGNAL (C/A CODE)	
PN CHIP RATE	1.023 Mcps
PN CODE LENGTH	1023 CHIPS
CODE TYPE	GOLD CODE
EPOCH	SYNCHRONOUS WITH 50 BPS DATA CLOCK AND X1 (P-CODE ELEMENT)
L_2 SIGNAL	
RF FREQUENCY	1227.6 MHz (120 x 10.23 MHz)
MODULATION TYPE	BPSK
PN MODULATION	P CODE (AS DESCRIBED ABOVE)
DATA MODULATION	GPS NAVIGATION MESSAGE; MODULATES L_1 IN-PHASE AND QUADRATURE CHANNELS AND L_2 SIGNAL
DATA FORMAT	NRZ
DATA RATE	50 BPS

MIS69L

The GPS navigation message is a data stream common to both the P-code and C/A-code signals on both the L1 and L2 frequencies. The information contained in the message allows the GPS user to obtain the GPS satellite ephemerides, system time, satellite clock behavior data, transmitter status information, the GPS constellation almanac, ionospheric propagation delay parameters, and C/A- to P-code handover information (References 6-3 and 6-4).

The navigation message, as shown in Figure 6-2, is contained in frames of 1500 bits, with each frame divided into five subframes of 300 bits. Each subframe contains system time and C/A to P-code handover information. Subframes are further divided into 10 words of equal length, with all subframes prefaced by a telemetry word (designated TLM) and a handover word (HOW). The TLM and HOW are generated by the GPS satellite; the remaining information in the message is generated by the GPS Control Segment and uploaded to the satellite.

The TLM contains an 8-bit preamble, 14 bits of TLM message data, 6 parity bits, and 2 extra bits. The TLM message contains status information for the GPS user regarding the GPS satellite transmitting the signal; for example, an indicator designating when an upload message is being received by the satellite, diagnostic messages, and other messages reflecting the status of the GPS satellite at the time of transmission of the navigation message.

The HOW contains a 17-bit counter that indicates the transmitting GPS satellite's time at the leading edge of the next subframe relative to the GPS system time P-code epoch. In addition, a 1-bit synchronization flag, a 3-bit subframe identifier, 6 parity bits, and 2 extra bits are contained within the HOW. When combined with the C/A-code epoch and the navigation message subframe time, the HOW provides the user equipment with enough information to make a transition from C/A-code tracking to P-code tracking at the next subframe.

In addition to the TLM and HOW, the navigation message provides uploaded data from the GPS Control Segment. The first subframe contains frequency standard corrections, an associated age-of-data word, and ionospheric propagation delay model coefficients. The second and third subframes contain a representation of the satellite's ephemeris and age-of-data words. The fourth subframe contains alphanumeric messages generated by the GPS Control Segment intended for conveying information to GPS users. The fifth subframe contains almanac data that provides enough

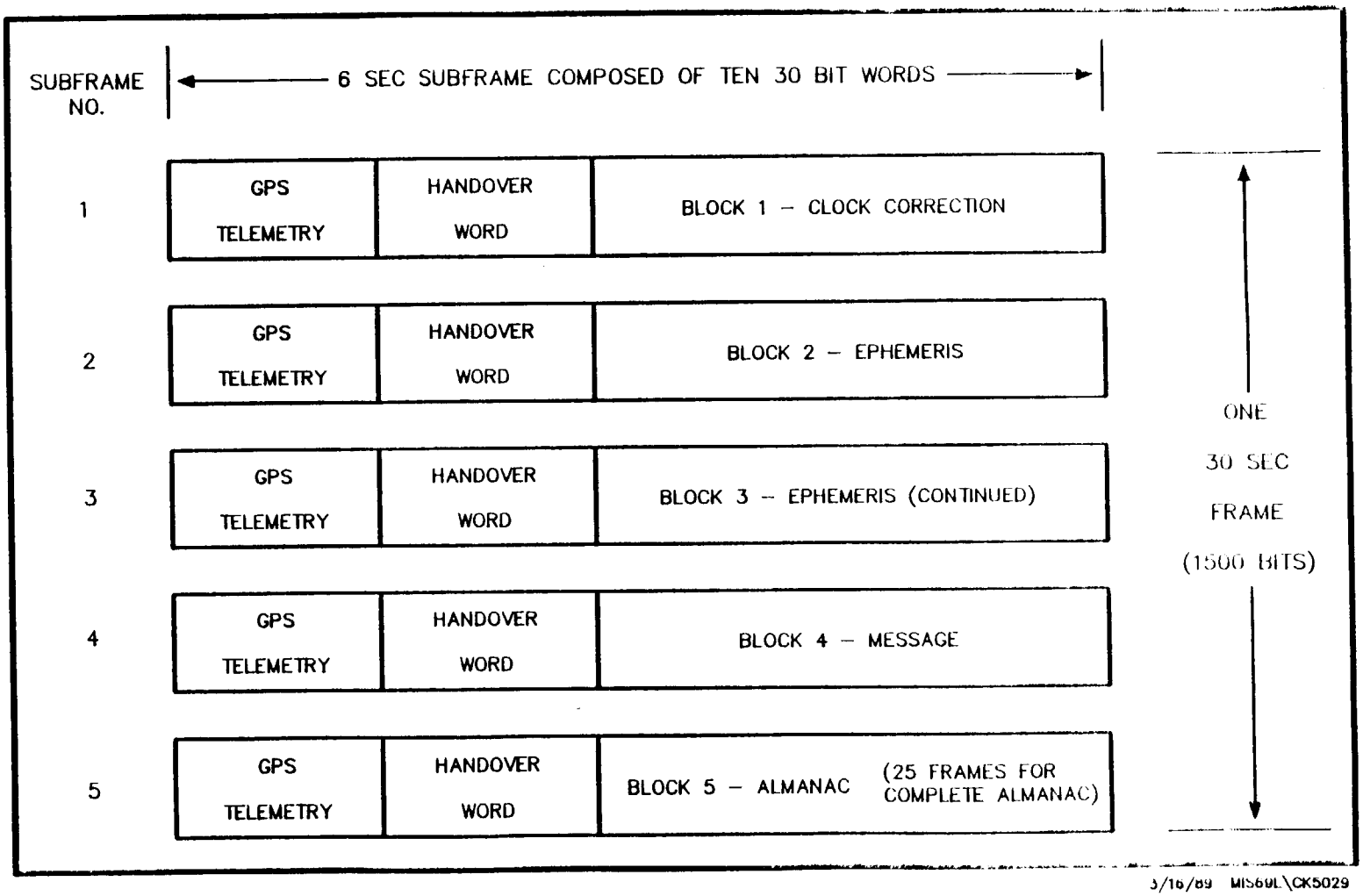

Figure 6-2. GPS Data Format Frame and Substructure

time-dependent positional information, operational status, and clock correction data on all the members of the GPS constellation to allow the GPS user to develop acquisition schedules independently. Twenty-five frames of data are required to construct the almanac.

By the mid-1990s, the GPS satellites will use cesium clocks (or possibly hydrogen masers) as their onboard time standard. Cesium clocks provide frequency stability of one part in 10^{14} per day. The master control station monitors each satellite's clock daily and compares its behavior to the ground-based GPS system time standard. The master control station generates clock correction parameters for each satellite to characterize the departure of a satellite's clock from the system time standard. The satellite's clock parameters are uploaded by the upload station for transmission to GPS users as part of the GPS navigation message.

Users with accurate a priori knowledge of their own position can effect time transfer using GPS. In its simplest form, GPS time transfer may be achieved by using the GPS satellite position (included in the navigation message) to estimate the propagation delay between a GPS satellite and the user and then adding this value to the time the signal was transmitted. Deviation of each satellite's clock from GPS system time may be corrected using data included in the navigation message. Differential GPS time transfer techniques (Reference 6-5), especially the common-mode/common-view technique, can provide time transfer accuracies on the order of one ns.

6.1.3 TYPICAL GPS RECEIVER CAPABILITIES

Figure 6-3 contains a block diagram of a typical GPS receiver for Earth- or near-Earth-based users. Inputs are the GPS signals as received by the antenna subsystem and user commands needed to initialize and control receiver operation. The GPS receiver acquires and tracks each selected GPS satellite signal to determine the GPS signal epoch and relative frequency offset; extracts the time of signal transmission from the GPS navigation message; and through comparison with the receiver's own clock and frequency reference, determines the pseudorange and pseudorange-rate. After observation of at least four GPS satellites, outputs from the receiver include the computed user position, velocity, and time bias as well as whatever intermediate data the user may require for error checking or further processing. As the figure shows, there are three

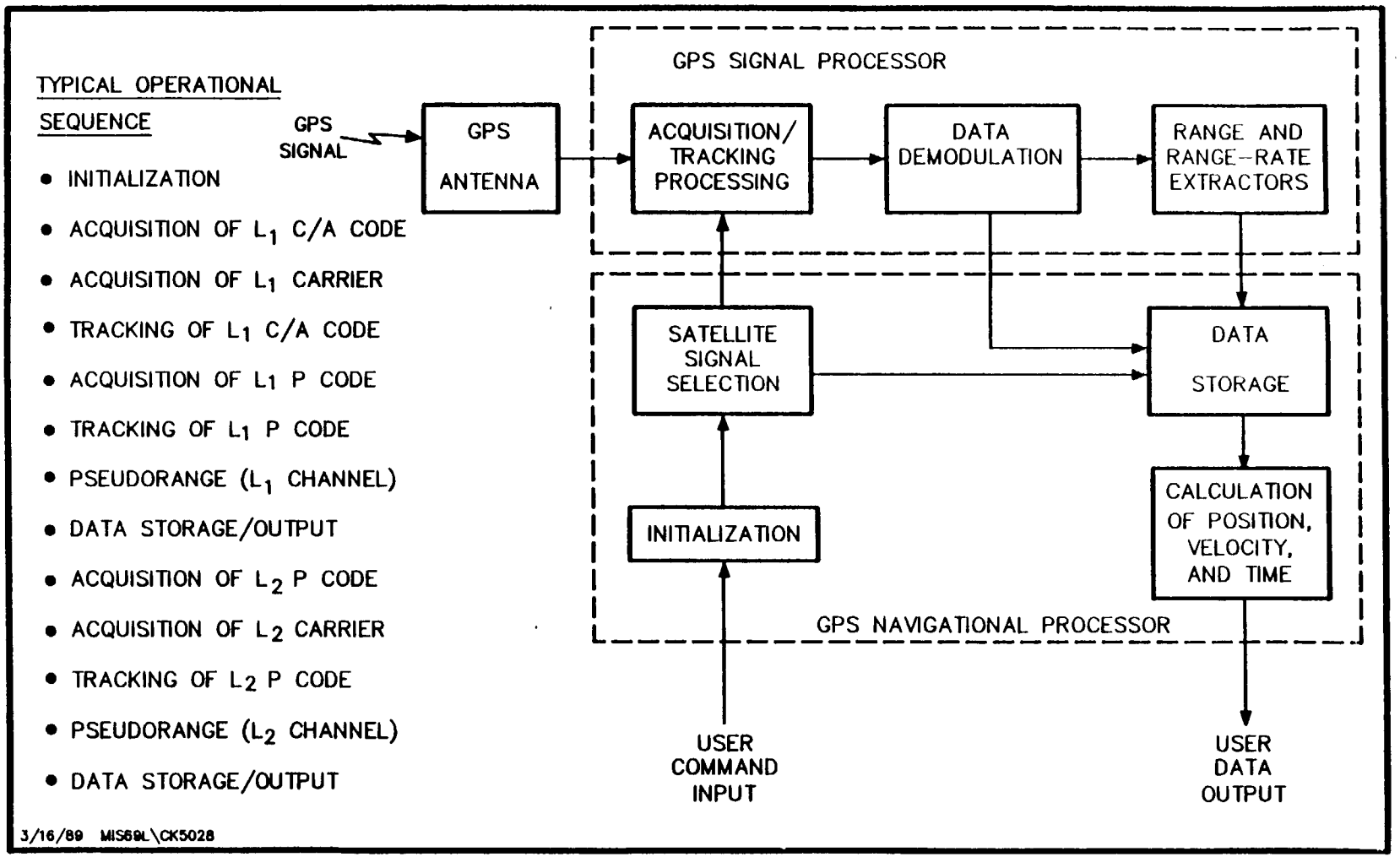

Figure 6-3. Typical GPS Receiver Functional Diagram

distinct major subsystems of a typical GPS receiver: the GPS antenna, the GPS signal processor, and the GPS navigation processor.

Upon initialization, the navigation processor of the receiver must be bootstrapped with a priori information of the positions of the GPS satellites as a function of time so that the visibility of the GPS satellites can be determined based on approximate knowledge of the user location. When the user has loaded this a priori almanac of GPS satellite positions, the receiver determines which satellites are visible and begins to acquire their signals. Ultimately, the almanac is updated automatically from data contained in the GPS navigation message. The GPS satellites to be viewed are typically selected for observation based on their angular separation: greater angular separation reduces the geometrical dilution of precision of the measurement, thereby optimizing the position/velocity/time solution.

The receiver's signal processor performs signal acquisition and tracking. Depending on the design, the receiver may acquire and track four or more satellites in parallel or sequentially. Parallel processing implies a multichannel receiver, whereas sequential processing implies a single-channel receiver that time shares its operation among the observed GPS satellites. After a GPS signal has been acquired, it is tracked either continuously by a multichannel tracking receiver or in turn by a sequential receiver. A sequential tracking scheme is controlled by the navigation processor and is typically applied as a round-robin algorithm to repeat observations of the selected GPS satellites. Therefore, a sequential receiver thus must track a particular GPS satellite's signal over a period of time sufficient to allow demodulation and message data extraction by the signal processor before switching to acquire and track the next selected GPS signal.

Independent of the specific receiver signal processor design, acquisition and tracking of each GPS satellite's signal requires a succession of operations. First, the C/A code signal is acquired at the L1 frequency. This signal, modulated by a relatively slow and short PN code, can be acquired rapidly and is used as a reference to transition to the precise P-code signal at the same frequency. After the C/A signal is tracked and the navigation message has been extracted, the HOW in the navigation message is used to acquire and track the P-code signal. The combination of the C/A code epoch, the navigation subframe epoch, and the HOW provides the signal processor with enough information to

acquire the P-code at the next subframe epoch. When the P-code signal has been acquired and is tracked, precise pseudorange and pseudorange-rate measurements may be made at the L1 frequency. This facilitates acquisition and tracking of the L2 P-code signal because the L2 signal is clocked in synchrony with the L1 signal codes. The navigation processor may use the difference between P-code pseudorange measurements made at the L1 and L2 frequencies to determine the correction for the ionospheric delay encountered in the measurement.

The time and frequency offsets of the receiver with respect to GPS system time and frequency are not critical because pseudorange measurements made to four GPS satellites provide the navigation processor with enough information to solve for the time offset as part of the navigation solution. For sequential receivers, however, the stability of the receiver's oscillator over the time required to process four GPS satellites sequentially is significant. The typical sequential GPS receiver uses a crystal quartz oscillator with a frequency stability of one part in 10^{10} per day.

Raw pseudorange and pseudorange-rate data extracted from the GPS signals by the signal processor are provided as inputs to the navigation processor. Offsets between the GPS system time and the time-of-transmission indicated by a specific GPS satellite signal are calculated by the navigation processor on the basis of clock data included in the navigation message and applied as an adjustment to the pseudorange measurements. Ionospheric corrections derived from data included in the navigation message and the L1 and L2 signal measurements are also used to adjust the raw GPS measurements. The navigation processor then uses the GPS ephemeris data in the GPS navigation message to compute the position of the user satellite. The combination of the four pseudoranges and satellite positions is sufficient information for the navigation processor to solve for the user position. Typically, a Kalman filter is implemented in the navigation processor to provide an optimized estimate of the receiver's position based on a continuing time series of GPS satellite observations.

6.1.4 GPS SELECTIVE AVAILABILITY

Selective availability refers to the intentional degradation of the GPS navigational accuracy by the GPS Control Segment. Selective availability is accomplished by the controlled dithering of the GPS satellite clocks and/or the controlled alteration of the GPS ephemerides in the GPS

navigational message. Authorized users may correct both methods of accuracy degradation.

Selective availability will be invoked at times of national emergency to deny real-time use of GPS at the nominal levels of performance. When selective availability has not been invoked, the Standard Positioning Service (SPS) provided by the C/A-code signal on the L1 carrier frequency will yield nominal performance levels equal-to-or-better-than 50 m (1 σ), and the Precise Positioning Service (PPS) provided by the P-code signal on the L1 and L2 carrier frequencies will achieve performance levels at 16 m for near-Earth users (Reference 6-6). When selective availability is invoked, these levels of performance are reduced significantly unless the GPS receiver possesses supplementary description capability to counteract the effects of selective availability. For those users without access to the correction algorithms, the accuracy of the instantaneous position determination process using the P-code may be reduced to several hundred meters.

6.1.5 GPS VISIBILITY AND ATDRS/GPS TRACKING

The simultaneous visibility of four or more GPS satellites is ensured for GPS users at or near the Earth's surface as a result of the number of GPS satellites forming the GPS satellite constellation and each satellite's broadcast coverage of the Earth. The geometry that optimizes GPS visibility to near-Earth or Earth-based GPS users, however, restricts its visibility to high-altitude space-based users desiring instantaneous navigation solutions.

Figure 6-4 illustrates the effect of the GPS user's altitude in terms of GPS satellite visibility. As indicated, each GPS provides a nadir pointing beam whose mainlobe possesses a beamwidth of $\pm$24 degrees. Visibility of four GPS satellites by high altitude space-based users is consequently not guaranteed: the further removed the GPS user is from the surface of the Earth, the less likely it is to remain within the $\pm$24-degree beamwidth of a given GPS satellite.

Because the GPS beam is nadir-directed, only a small percentage of a GPS satellite's mainlobe radiation passes by the Earth's limb to the space beyond the Earth. At geosynchronous altitude, the radiation that the Earth does not intercept is the only direct mainlobe radiation that a geosynchronous GPS user receives from a GPS satellite. As shown in Figure 6-5, the GPS satellites that illuminate a

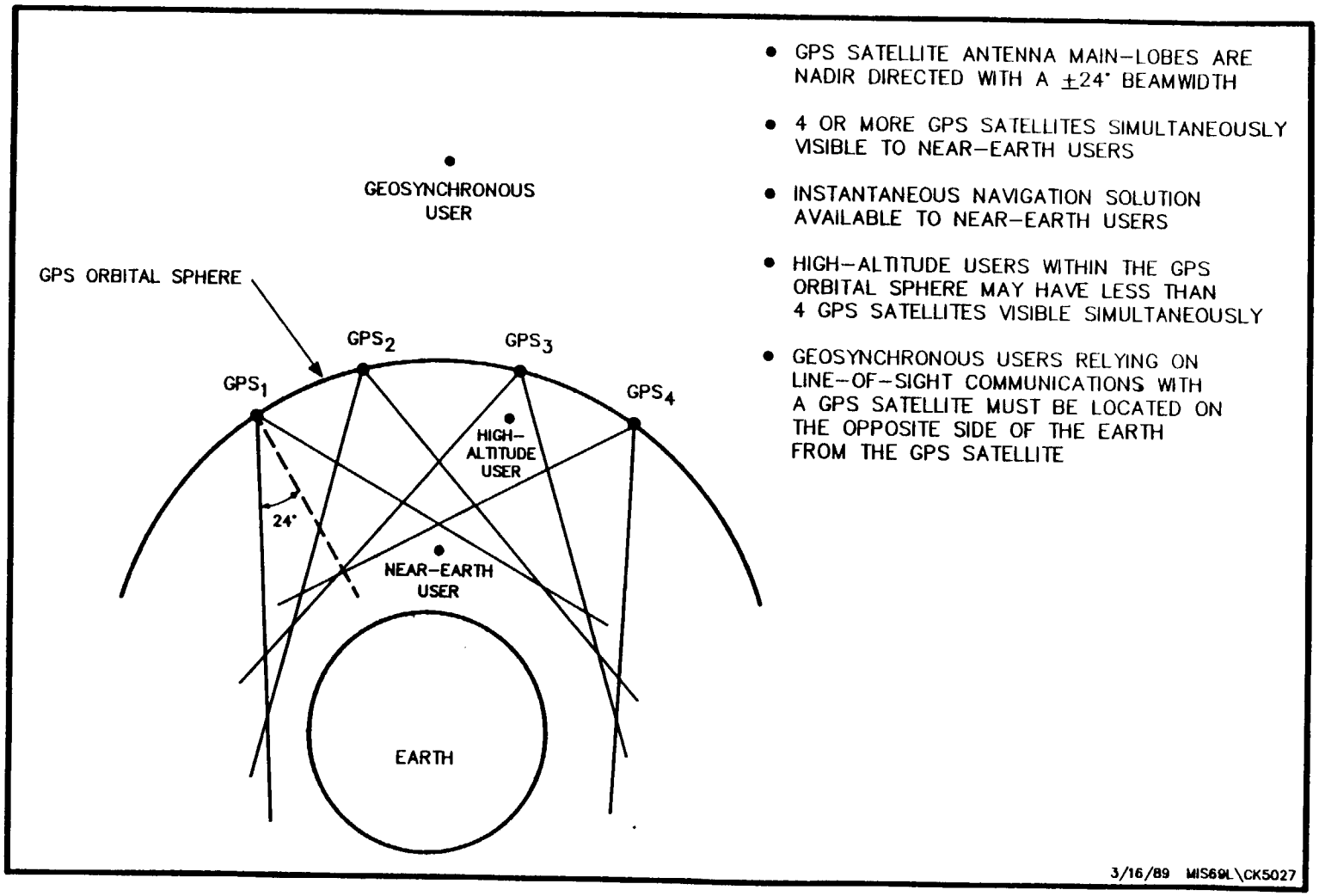

Figure 6-4. Altitude Limitations on GPS Users

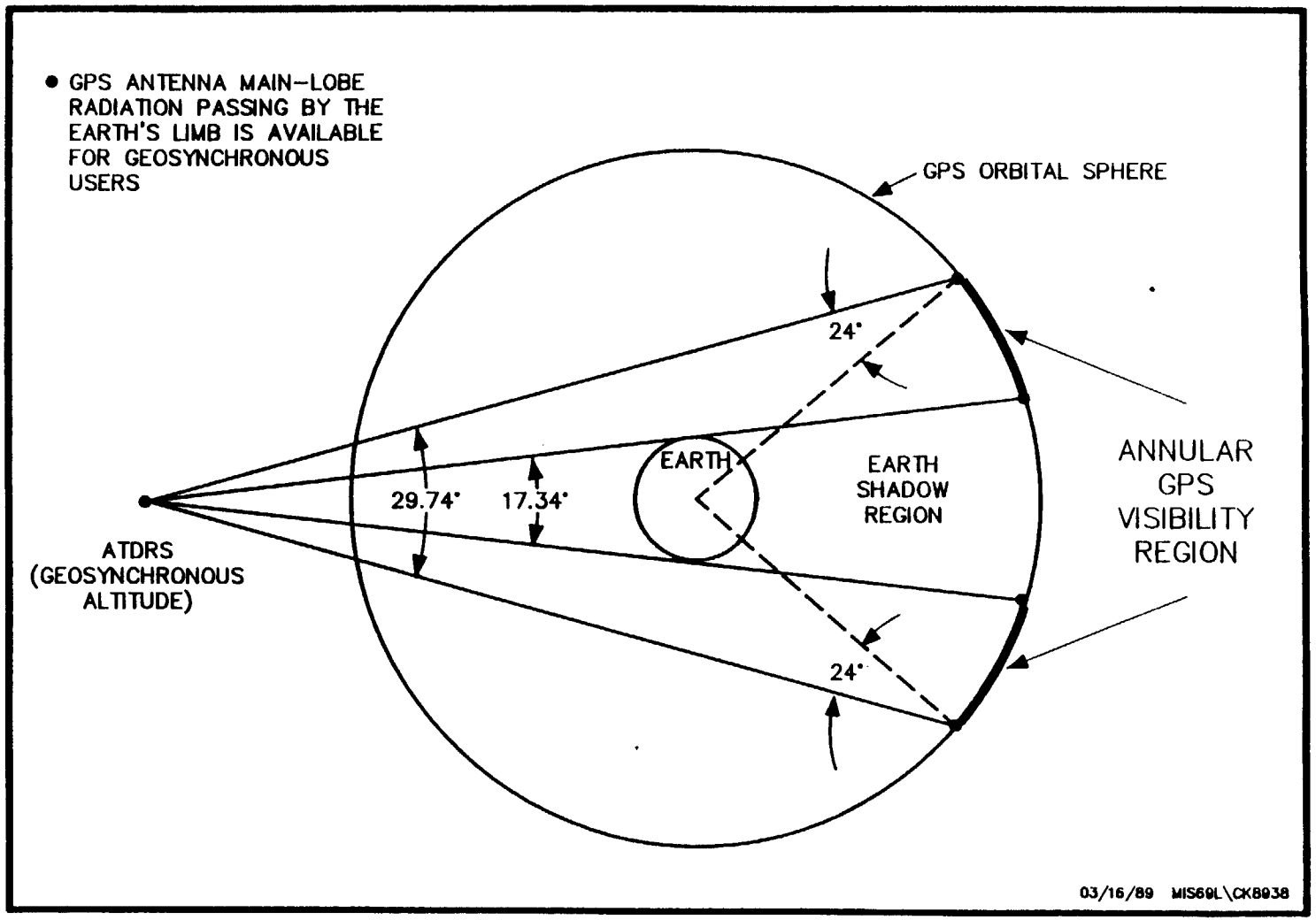

Figure 6-5. Constraints on GPS Visibility for ATDRS

geosynchronous user such as ATDRS with mainlobe radiation reside in an annular region of the GPS orbital sphere. At geosynchronous altitude, the probability of a GPS user spacecraft being within the mainlobe of four GPS satellites simultaneously is approximately 2 percent over a typical 24-hour period. The low probability of a geosynchronous user simultaneously viewing at least four GPS satellites thus limits the capability of adequately tracking such a user through GPS instantaneous position and time determination.

Pseudorange and pseudorange-rate measurements from a geosynchronous user to individual GPS satellites, however, can be employed over long tracking intervals to support dynamic OD. For this type of direct dynamic tracking, GPS measurements are collected by the user and batch or filter OD processed. Alternatively, pseudorange and pseudorange-rate measurements between the geosynchronous user, the GPS satellites, and participating ground stations can be differenced in various ways to eliminate common biases and provide differential measurement types for dynamic batch or filter OD processing.

Accordingly, three distinct methods of dynamic tracking for the ATDRSS satellites have been investigated and are treated in the remainder of this section:

- Direct ATDRS/GPS Tracking System
- Passive Differential ATDRS/GPS Tracking System
- Direct Differential ATDRS/GPS Tracking System

6.2 DIRECT ATDRS/GPS TRACKING SYSTEM

The Direct ATDRS/GPS Tracking System relies on GPS pseudorange and pseudorange-rate measurements by an ATDRSS onboard GPS receiver in order to support ATDRS OD. The large number of GPS satellites and their positions with respect to those of the ATDRSS satellites provides longer baseline geometries than can be provided by a ground-based tracking system, potentially improving the resulting ATDRS orbit solution. The signal paths between the low Earth orbit GPS satellites and the geosynchronous ATDRSS satellites minimize atmospheric effects; therefore, the dominant measurement errors are due to clock biases between the GPS and ATDRSS system times and uncertainties in the GPS ephemerides. The limited visibility of the GPS satellites from the ATDRS orbits, however, somewhat restricts the utility of the Direct ATDRS/GPS Tracking System.

6.2.1 DIRECT ATDRS/GPS TRACKING SYSTEM DEFINITION

This section provides an overview of the Direct ATDRS/GPS Tracking System architecture and operations concept, the ATDRSS onboard GPS receiver capabilities, and the GPS visibility constraints associated with the system.

6.2.1.1 Architecture and Operations Concept

As shown in Figure 6-6, in the Direct ATDRS/GPS Tracking System, ATDRS uses an onboard GPS receiver to make pseudorange and pseudorange-rate measurements of the GPS satellites. As the measurement model in Figure 6-7 shows, the direct ATDRS/GPS tracking measurements are one-way range measurements involving only the ATDRS and GPS satellites.

The GPS satellites to be observed by the ATDRSS onboard GPS receiver are chosen on the basis of visibility to ATDRS. The schedule of GPS observations may be determined on the ground by NASA's FDF and relayed to ATDRS using TT&C command from the AGT. Alternatively, the GPS satellite observation schedule might be autonomously developed onboard ATDRS on the basis of a priori data and information obtained from demodulation of the GPS navigation message. Periods when no GPS satellites are visible to ATDRS may be supplemented by ranging measurements made between ATDRS and the AGT using the ATDRS TT&C signal.

The measurements and associated navigation data for each observed GPS satellite are relayed via TT&C telemetry to the AGT and forwarded to the FDF. The ATDRSS onboard GPS receiver does not perform the determination of instantaneous position, velocity, and time, however, because four GPS satellites are rarely simultaneously visible from geosynchronous altitude; rather, ATDRS relays raw GPS pseudorange and pseudorange-rate measurements to the AGT, then to the FDF to form a time sequence of GPS measurements and navigation data as input to dynamic ATDRS OD processing.

6.2.1.2 ATDRSS Onboard GPS Receiver Capabilities

The ATDRSS onboard GPS receiver possesses many of the capabilities of the typical GPS receiver discussed in Section 6.1.3. The major exception is that the navigation processor does not attempt to solve for the ATDRS instantaneous position, velocity, and time. Unlike a typical GPS receiver, the onboard GPS receiver will forward the pseudorange and pseudorange-rate data extracted from the

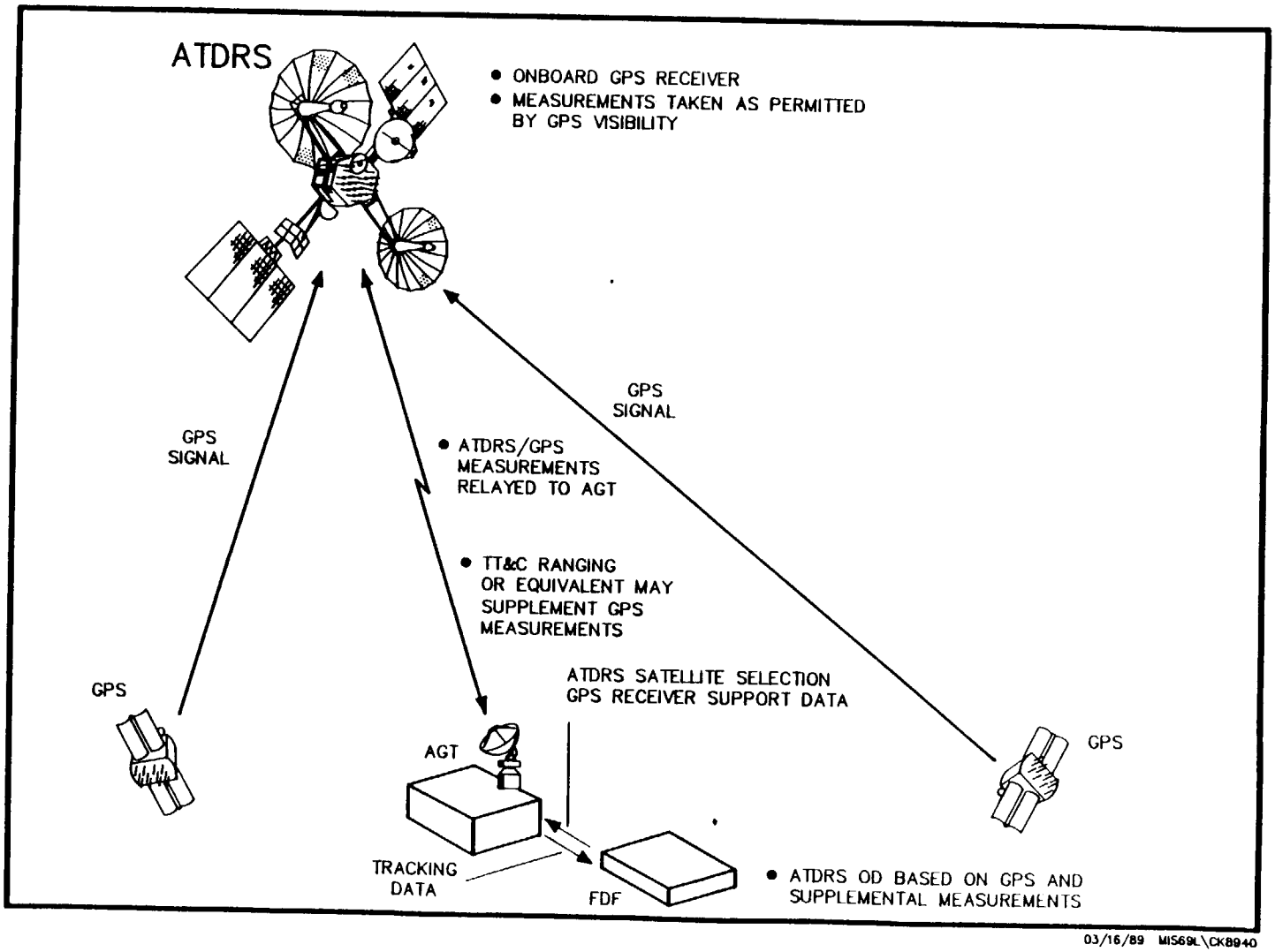

Figure 6-6. Direct ATDRS/GPS Tracking System Architecture

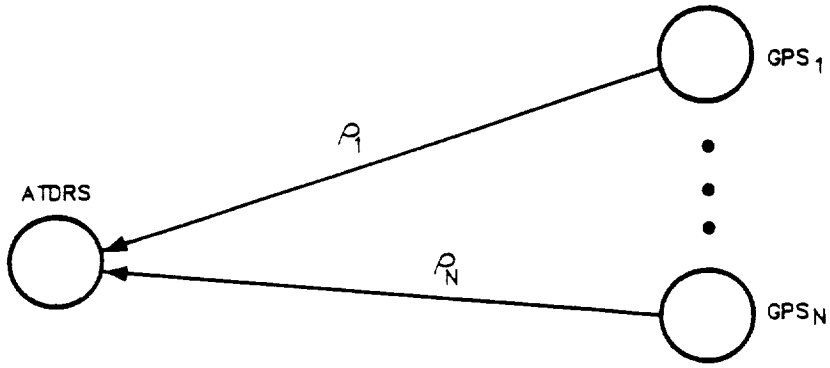

ONE-WAY RANGE OBSERVATION

$R_i = \rho_i$ + OBSERVATION ERROR

i = 1, 2, .. N (NUMBER OF VISIBLE GPS SATELLITES)

SOURCES OF OBSERVATION ERROR	METHOD OF MITIGATION
GPS CLOCK BIAS AND EQUIPMENT GROUP DELAY	CORRECTIONS FOR GPS SYSTEM TIME INCLUDED IN THE GPS NAVIGATION MESSAGE
GPS EPHEMERIS ERROR	GPS CONTROL SEGMENT PROVIDES 8 HOUR UPDATES OF SATELLITE EPHEMERIDES IN THE NAVIGATION MESSAGE
ATDRS CLOCK BIAS	DIFFERENCES BETWEEN GPS SYSTEM TIME AND ATDRS SYSTEM TIME ESTIMATED AS PART OF OD SOLUTION
ATDRSS ONBOARD GPS RECEIVER GROUP DELAY	CALIBRATION OF GPS RECEIVER SYSTEM PRIOR TO ATDRS LAUNCH
TROPOSPHERIC DELAY	MINIMAL EFFECT DUE TO LIMITED TROPOSPHERIC SIGNAL PATH
IONOSPHERIC DELAY	MINIMAL EFFECT DUE TO LIMITED IONOSPHERIC SIGNAL PATH; CAN BE CORRECTED VIA GPS SIGNAL STRUCTURE
CHANNEL NOISE	ATDRSS ONBOARD GPS RECEIVER DESIGN

3/16/89 MIS89L\CK5031

Figure 6-7. Direct ATDRS/GPS Tracking System Measurement Model

GPS signal to the FDF for input to ATDRS OD processing. The receiver's navigation processor, as noted previously, may develop the GPS satellite observation schedule autonomously or may rely on uploaded data from the AGT and FDF. Command inputs to the onboard GPS receiver will be maintained through an interface with the ATDRS command processor and TT&C commands from the AGT; data outputs from the receiver will similarly require interfaces to the ATDRS telemetry processor and the TT&C telemetry stream to the AGT. It is possible that space-qualified, commercially produced GPS receivers designed for low Earth orbit users might be modified and adapted for the functions and interfaces required for use onboard the ATDRSS satellites.

In general, the accuracy of pseudorange and pseudorange-rate measurements depends on the degree of synchronization between the time/frequency standards at the transmitting and receiving sides. For most GPS applications, the calculation of an instantaneous navigation solution eliminates the receiver clock bias from the solution, and the typical GPS receiver described in Section 6.1.3 uses a stable crystal oscillator of modest capability as its frequency reference. However, in the ATDRSS onboard GPS receiver, simultaneous measurements to four distinct GPS satellites are not available; therefore, an instantaneous solution is not obtained and the receiver clock bias is not eliminated. As a result, the clock requirements for the ATDRSS onboard GPS receiver will be at least as stringent as those for a typical sequential GPS receiver.

The ATDRSS onboard GPS receiver might use its own frequency standard or might be referenced to ATDRS frequency system. At this stage in the development of ATDRSS, its frequency system has not yet been determined. The most likely options are the use of a forward pilot tone generated by the AGT and uplinked to ATDRS (as done in the current TDRSS) or the use of an onboard independent oscillator. In either case, the ATDRS frequency reference would be used by an onboard frequency synthesizer to generate the various frequencies required, possibly including that needed by the onboard GPS receiver.

As a result of ATDRS altitude and the limited width of the GPS beams, the range between ATDRS and those GPS satellites in the ATDRS/GPS annular visibility region is greater than that for typical ground-based or low Earth orbit GPS users. Simple worst-case calculations show that the ATDRS-GPS range is approximately 67,530 km, as compared to the worst-case ground user-GPS range of approximately 24,750 km. The

incremental ATDRS-GPS range represents an additional 8.7-dB path loss (for the L2 channel) that must be in some way compensated by the ATDRS onboard GPS receiver and antenna subsystems.

GPS measurement performance may be seen as a function of the received signal-to-noise ratio (C/N0) and the code and carrier tracking loop bandwidths, where the received C/N0 value is in turn dependent on the GPS transmit EIRP and the ATDRS receive G/T. Performance must be considered over the range of both ATDRS and GPS look angles, where the worst case, as seen from Figure 6-5, would involve a GPS look angle of 24 degrees and an ATDRS look angle of 14.9 degrees. The respective beam patterns and gains of the GPS transmit antenna and the ATDRSS onboard GPS receive antenna for these look angles play decisive roles in determining the C/N0 received at ATDRS, especially if a nadir-directed fixed ATDRS GPS antenna is employed.

Typical GPS receivers are designed to operate for C/N0 values ranging from, say, 32 to 42 dB-Hz for the L1 C/A-code channel or L2 P-code channel. Previous analysis (Reference 6-9) has shown that a C/N0 value of 35 dB-Hz may be readily obtained at the ATDRS by using high or even moderate gain helix antennas with as few as 10 turns. Such a fixed antenna would be considerably cheaper than any steerable antenna and might also be integrated into the existing ATDRS MA array to minimize its impact on the ATDRS physical configuration.

6.2.1.3 GPS Visibility Constraints

Operation of the Direct ATDRS/GPS Tracking System relies on direct ATDRS observation of the GPS satellites, requiring that line-of-sight visibility between ATDRS and the members of the GPS constellation under observation be maintained for several minutes. Visibility restrictions due to Earth blockage, atmospheric grazing, and the GPS satellites' antenna beam patterns limit the line-of-sight opportunities between ATDRS and the GPS satellites.

Visibility of the GPS satellites from ATDRS is primarily constrained by the nadir-directed (Earth-center-directed) boresights of the GPS antenna beams. As previously illustrated in Figure 6-5, the ±24-degree beamwidth of the mainlobe restricts the location of those GPS satellites visible to ATDRS to the side of the Earth opposite ATDRS. As seen from an ATDRS, visible mainlobe radiation from the GPS satellites is restricted to a viewing angle of 29.74 degrees, where the Earth subtends an angle of 17.34 degrees in the center of this field of view, eclipsing the GPS radiation directed toward ATDRS. Only those GPS

satellites that fall within the annular region of the GPS orbital sphere delimited by the Earth's shadow region and the 29.74 viewing angle are visible to ATDRS.

The ATDRS/GPS annular visibility regions associated with ATDRS-E and ATDRS-W are shown as shaded areas in Figure 6-8. This figure is a planar projection of the entire GPS orbital sphere, similar to a Mercator global projection. The GPS orbital sphere is at rest in inertial space, and the Earth rotates concentrically within the sphere, maintaining alignment between their equatorial planes. In the figure, the equator of the GPS orbital sphere, marked by the horizontal center line, is coincident with the Earth's equatorial plane. The outer edge of each annular region is defined by the loss of line-of-sight contact with the ATDRS due to the GPS satellite's antenna beamwidth; the inner edge of each annular region is defined by the line-of-sight blockage due to the Earth, assuming an additional 1000 km to account for the Earth's atmosphere. The angular spacing between the centroids of the annular regions for ATDRS-E and ATDRS-W remains fixed at 130 degrees, reflecting the longitudinal separation between the ATDRSS satellites.

The ATDRS/GPS annular visibility regions are not fixed on the surface of the GPS orbital sphere. Because ATDRS maintains a fixed position relative to the rotating Earth, each ATDRS and its associated ATDRS/GPS annular visibility region are in motion relative to the GPS orbital sphere. The ATDRS/GPS annular visibility regions rotate from west to east on the surface of the GPS orbital sphere at a rate of 15 degrees per hour in synchronization with the motion of ATDRS on the celestial sphere but 180 degrees out of positional phase. The daily period of an annular region on the GPS orbital sphere is, thus, 23 hours, 56 minutes and 4 seconds. This 4-minute difference between the solar day and the periodicity of each annular region causes the daily starting point of the annular region to drift eastward on the orbital sphere by about 1 degree relative to the fixed GPS satellite constellation.

The centroids of the ATDRS/GPS annular visibility regions shown in Figure 6-8 are located in the equatorial plane of the GPS orbital sphere to represent the mean daily position of the annular region. Any inclination in the ATDRS orbit causes ATDRS to undergo a daily figure-eight motion as viewed from a mean suborbital equatorial point on the Earth's surface. Because the centroid of the ATDRS/GPS annular visibility region is always directly opposite its associated ATDRS, the centroid of the annular region

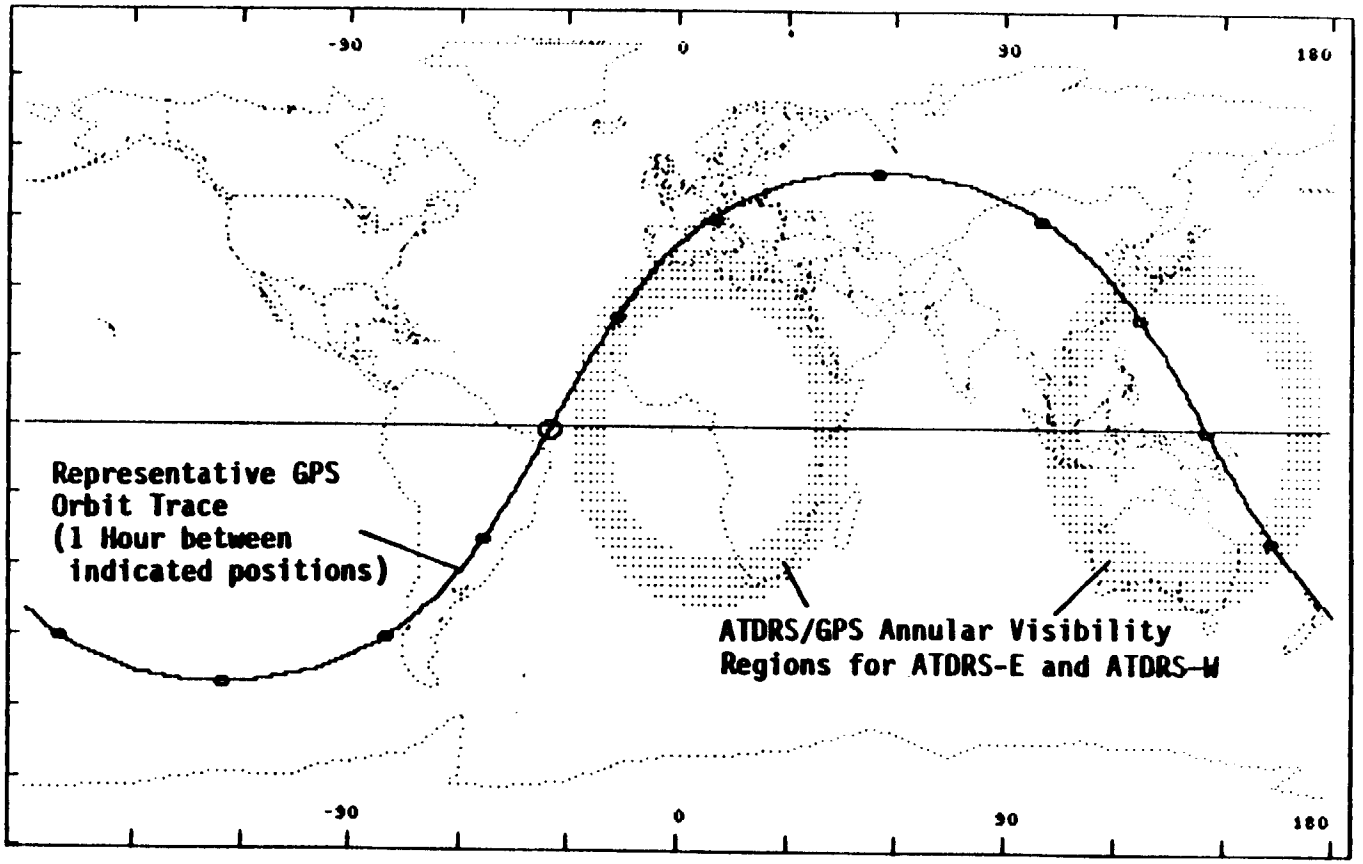

Figure 6-8. ATDRS/GPS Annular Visibility Regions

consequently traces a sinusoid on the inertial GPS orbital sphere with a period of 23 hours, 56 minutes, and 4 seconds. The angular amplitude of the centroid's sinusoidal trace with respect to the equatorial plane is equal to the inclination of the ATDRS orbit.

Figure 6-8 illustrates a typical path of a GPS satellite on the surface of the GPS orbital sphere. The GPS orbital planes are fixed in inertial space and on the GPS orbital sphere. A GPS satellite completes one orbit of the Earth in 11 hours, 59 minutes, and 57 seconds and two orbits in 23 hours, 59 minutes, and 54 seconds. This periodicity places a GPS satellite at nearly the same location on the orbital sphere twice a day, while the ATDRS/GPS annular visibility regions, as discussed above, are in relative motion. Therefore, a GPS satellite will be within an ATDRS/GPS annular visibility region at least once each day for most of the year. The daily 1-degree eastward drift of the annular visibility regions ensures that the time of entry and exit of a GPS satellite to and from an annular region is always changing.

When a GPS satellite enters an ATDRS/GPS annular visibility region, the corresponding ATDRS is then able to observe the emitted GPS signal. The amount of time that a GPS satellite spends in an ATDRS/GPS annular visibility region determines the interval of visibility for that satellite by the particular ATDRS. The relative motion of the GPS satellites and annular visibility regions, which is not indicated fully in the figure, lengthens the period during which a GPS satellite can remain within an annular region. The distance between uniformly spaced tick marks on the GPS orbital path shown in Figure 6-8 represents an interval of 1 hour and serves as a visual indicator of a GPS satellite's transit through the ATDRS/GPS annular visibility regions. The maximum interval of time that a GPS satellite spends in an annular visibility region can be shown to be several hours, whereas the combined motion of the GPS satellites can place more than one in a particular annular visibility region at any instant. Figure 6-9 shows a typical 10-day ATDRS/GPS visibility profile, revealing that occasional periods of 1 hour or more are possible when no GPS satellites are visible from an ATDRS. Time integration of these visibility profiles shows that, on average, 1.4 GPS satellites are visible from an ATDRS.

6.2.2 DIRECT ATDRS/GPS TRACKING SYSTEM ASSESSMENT

The following sections assess the impact on ATDRSS development and operations; cost and staffing requirements;

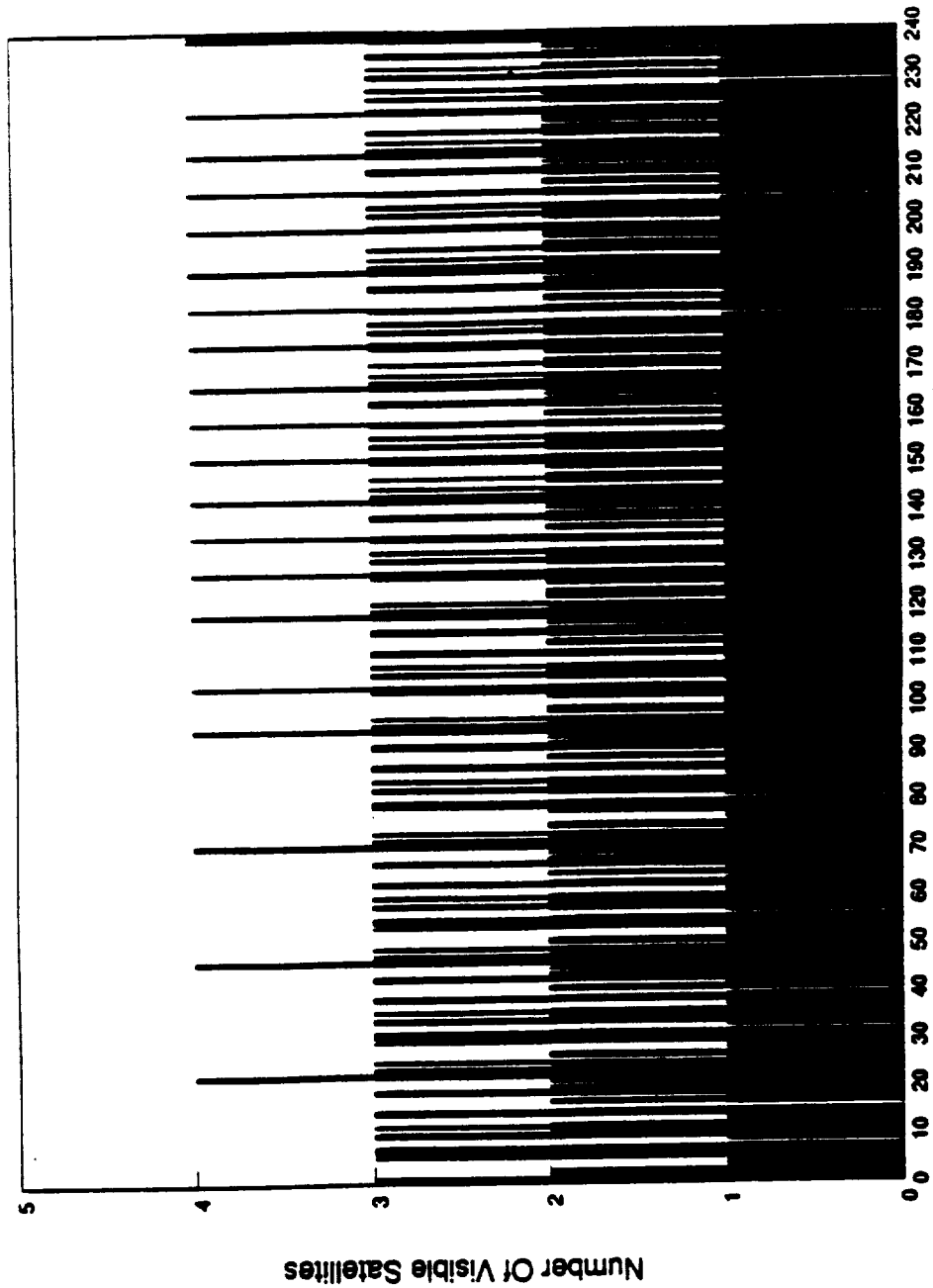

Figure 6-9. Representative Primary GPS Satellite Constellation Visibility From an ATDRS

reliability, maintainability, and availability; the technological risks associated with the implementation of the Direct ATDRS/GPS Tracking System; and the system's ATDRSS OD performance.

6.2.2.1 Cost and Staffing Requirements

Because no ground segment stations are required for the Direct ATDRS/GPS Tracking System, the costs for this system are divided into the system engineering study phase and the space segment hardware costs. The systems engineering study phase would be required to produce the necessary detailed systems specifications, supporting further analysis and the development of an engineering model to test system performance prior to full-scale system deployment. An estimate of the costs of the study phase is $1.5 million.

The major portion of the hardware costs of the space segment is associated with the ATDRS onboard GPS receiver and antenna. Although spaceborne GPS receivers have been developed to demonstrate the feasibility of autonomous spacecraft navigation, production versions are not currently available. A cost of $1.0 million is estimated for production of a radiation-hardened, space-qualified ATDRSS onboard GPS receiver, based on the current costs of a prototype receiver and antenna. The space segment costs for three ATDRSS satellites, each with a primary and secondary onboard GPS receiver, would, therefore, be about $6.0 million.

Additional space segment costs would be associated with the interface of the ATDRSS onboard GPS receiver to the ATDRS command processor. The costs of developing and implementing an ATDRSS GPS command processor executive function and the communications software required for the interface to the command processor are nonrecurring costs. By contrast, the costs of implementing the hardware interface between the GPS receiver and the command processor represent a recurring expense associated with the installation of each ATDRSS GPS receiver. These costs would be a relatively small portion of the overall system costs and are estimated to total about $0.5 million from development through test and integration.

A total cost of $8.0 million is estimated for the Direct ATDRS/GPS Tracking System, including both the study phase and the space segment hardware costs just discussed. The estimate does not include the costs of the FDF ATDRS/GPS tracking schedule support or the OD data processing aspects of this system; these costs have not been considered for any

of the systems in this study. Because there are no surface stations associated with the Direct ATDRS/GPS Tracking System, staffing requirements are restricted to any additional manpower needed by the AGT or FDF to support this tracking system. Again, these additional costs are considered to be outside the scope of this study.

6.2.2.2 Reliability/Maintainability/Availability

Reliability, maintainability, and availability of the Direct ATDRS/GPS Tracking System are beyond the scope of this study and should be considered in any future work. Because the system depends completely on the ATDRSS onboard GPS receiver, however, it is clear that maintainability and availability of the system are directly related to maintainability and availability of the entire ATDRSS Space Segment. In all likelihood, failure of both primary and secondary onboard GPS receivers or the TT&C relay of ATDRS/GPS data will result in complete failure of the tracking system unless the ATDRSS Space Segment includes provision for on-orbit repair and replacement.

6.2.2.3 Technological Risks

There are no technological risks associated with the Direct ATDRS/GPS Tracking System. The only new hardware component to be introduced into the ATDRSS to support the collection of tracking data is the GPS receiver. The technology for the implementation of the ATDRS GPS receiver exists in current GPS receiver design.

6.2.2.4 External Dependencies

The Direct ATDRS/GPS Tracking System is dependent on the navigation information embodied in the GPS signal. As discussed previously, GPS users are subject to the restrictions of selective availability. During times of national emergency, the accuracy of GPS may be intentionally degraded for the general GPS user through encryption. Only selected users will then be provided with the information necessary to employ the P-code signal with the same level of accuracy normally achieved. As a result, the ATDRSS onboard GPS receiver will be subject to a loss in range measurement precision whenever the GPS Control Segment invokes selective availability, unless the ATDRSS onboard GPS receiver has been authorized and designed to operate during periods of selective availability.

6.2.2.5 ATDRSS Impacts

Implementation of the Direct ATDRS/GPS Tracking System requires that the ATDRSS space segment include primary and secondary onboard GPS receiver and antenna subsystems for each ATDRS. Operation of the GPS receiver then requires that commands be input and navigation data retrieved from the receiver, implying support of an interface between the onboard GPS receiver and the ATDRS command processor. Receiver initialization commands and GPS satellite selection schedules originating in the ground segment and uplinked to the ATDRS would be passed to the onboard GPS receiver via this interface. Similarly, GPS measurement data derived by the onboard GPS receiver would be passed to the ATDRS command processor for relay to the ATDRSS ground segment. The introduction of this interface imposes additional but relatively minor hardware and software requirements on the ATDRSS space segment.

The inclusion of primary and secondary onboard GPS receivers and GPS antenna for each ATDRS introduces added weight, volume, and power consumption requirements. Quantitative estimates of these requirements may be derived from comparison with the specifications of a prototype GPS spaceborne receiver recently developed for JPL by Motorola. Each Motorola Monarch GPS Spaceborne User Receiver weighs 9 pounds, requires 35 Watts of DC power, and has dimensions of 5.5" x 5.5" x 8.0". The GPS antenna, as discussed previously, might be a small helix or possibly a parabolic omnidirectional antenna, where the antenna weight is unlikely to exceed 5 pounds and the volume depends on the antenna type chosen. As a conservative estimate, ATDRS support of the onboard GPS receiver imposes additional payload requirements of 23 pounds, 0.7 cubic feet, and 70 W for each ATDRSS satellite.

6.2.2.6 OD Performance

OD performance of the Direct ATDRS/GPS Tracking System has been assessed for the ATDRS-E and ATDRS-W satellites by using ORAN. As for all other systems considered in this study, performance has been determined for both a nominal 30-hour tracking arc and a 2-hour trajectory recovery arc. The 30-hour arc corresponds to routine OD operation, while the 2-hour arc corresponds to the need to quickly determine the ATDRS orbit after a maneuver.

ORAN modeling of the direct ATDRS/GPS Tracking System, however, has not been completely straightforward due to constraints and limitations imposed by the ORAN program. In particular, ATDRS-GPS visibility constraints cannot be directly modeled with ORAN, nor can the GPS ephemeris uncertainty be directly specified. Visibility of the GPS satellites from ATDRS has been established by off-line preprocessing and generation of an ATDRS/GPS observation schedule; modeling of the GPS ephemeris uncertainty has been accomplished by using a hypothetical ground GPS tracking network in ORAN.

The accuracy of ATDRS OD in the Direct ATDRS/GPS Tracking System depends in part upon the accuracy of ATDRSS knowledge of the GPS orbits. Specifications for GPS indicate that the GPS navigation message provides a GPS ephemeris error of 6 m in range and 6 mm/s in range-rate (3 σ). ORAN, however, does not allow the GPS ephemeris errors to be directly specified; instead, the ORAN runs used to model the Direct ATDRS/GPS Tracking System have included tracking of the GPS satellites in order to establish the nominal GPS ephemeris errors. In effect, the operation of the GPS Control Segment has been modeled in ORAN, simulating the tracking of the GPS satellites over a 30-hour tracking arc. Six ground GPS tracking stations were evenly distributed over the Earth to form a hypothetical GPS tracking network, where the stations monitored one satellite from each of the six GPS orbital planes over the tracking arc. The resultant GPS OD accuracy was adjusted by fine turning the bias and noise parameters for the hypothetical GPS ground station measurements until an average 6 m (3 σ) three-dimensional position error was obtained over the arc for each of the GPS satellites. The ORAN solution for the ATDRS orbit was then decoupled from the solution for the GPS orbits by adjusting the weights accordingly.

The ORAN error budget used to model the Direct ATDRS/GPS Tracking System is summarized in Table 6-2. The one-way pseudorange and pseudorange-rate measurement noise values and biases indicated in Table 6-2 assume that the ATDRS onboard GPS receiver performs P-code signal processing. The ATDRS/GPS pseudorange and pseudorange-rate measurement noise values have been derived from consideration of likely GPS receiver implementations (Reference 6-9). In particular, it is assumed that the ATDRS onboard GPS receiver and antenna will allow achievement of a received C/NO value of 35 dB-Hz. As discussed previously, ATDRS use of a moderate or high gain helix antenna as the GPS antenna would be

Table 6-2. Direct ATDRS/GPS Tracking System ORAN Error Modeling (3-σ Values)

- MEASUREMENT SCHEDULE (OVER 30 HOUR AND 2 HOUR TRACKING ARCS):
  - ATDRS/GPS PSEUDORANGE AND PSEUDORANGE-RATE MEASUREMENTS EVERY 30 SECONDS FOR ALL GPS SATELLITES IN THE ATDRS/GPS ANNULAR VISIBILITY REGION
  - GPS SATELLITE TRACKING MEASUREMENTS EVERY 900 SECONDS (OVER 30 HOUR TRACKING ARC REGARDLESS OF ATDRS TRACKING ARC)
- GPS SATELLITE EPHEMERIS ERROR
  - UNCERTAINTY IN POSITION: 6.0 m
  - UNCERTAINTY IN VELOCITY: 6.0 mm/s
- ATDRS/GPS PSEUDORANGE MEASUREMENTS (PER MEASUREMENT)
  - NOISE: 9.0 m
  - BIAS: 13.4 m
- ATDRS/GPS PSEUDORANGE-RATE MEASUREMENTS (PER MEASUREMENT)
  - NOISE: 10.5 mm/s
  - BIAS: 1/5 mm/s
- SOLAR RADIATION: 2%
- TROPOSPHERIC REFRACTION ERROR: 0
- IONOSPHERIC REFRACTION ERROR: 0
- ATDRS/GPS CLOCK BIAS
  - SOLVED-FOR OVER 30 HOUR TRACKING ARC
  - 10.0 m OVER 2 HOUR TRACKING ARC

MIS65Q-a

adequate. The P-code pseudorange error for a C/NO value of 35 dB-Hz then mostly depends on the IF bandwidth and noise bandwidth of the receiver's delay locked tracking loop. Conservatively assuming a fairly wide IF bandwidth of 100 Hz and a delay locked loop noise bandwidth of 6 Hz implies a P-code pseudorange error of 4.0 meters (3 σ).

Multipath errors depend upon the ATDRS GPS antenna design and its placement with respect to reflective surfaces of the satellite structure. Multipath may be considered to be a noiselike measurement error with typical errors from 3.6 to 8.1 meters (3 σ) (Reference 6-11). Assuming the worst case multipath value, the ATDRS/GPS pseudorange measurement noise value has been calculated to be 9.0 meters (3 σ).

Pseudorange-rate measurement error has similarly been determined based on likely GPS receiver implementations and an assumed C/NO value of 35 dB-Hz (Reference 6-9). Assuming a Doppler averaging time of 1 second and a conservatively selected phase locked loop noise bandwidth of 20 Hz, the pseudorange-rate noise value for the GPS L1 channel can be calculated to be 10.5 mm/s (3 sigma).

The bias terms for the ATDRS/GPS pseudorange measurements arise primarily from the following sources:

- GPS and ATDRS oscillator drift
- GPS ephemeris prediction errors
- Predictability of GPS satellite perturbations
- GPS and ATDRS equipment group delay uncertainty

Values for each of these bias contributors have been conservatively derived from the GPS specifications or existing analyses (References 6-3, 6-9, and 6-10). Assuming an eight-hour interval between GPS uploads and GPS satellite oscillator drift of one part in 10^{13} as indicated in the current GPS specifications, then the 3 σ bias contribution due to GPS oscillator drift is 2.6 meters. This bias has been combined with the ATDRS drift contribution to form a total clock bias value in ORAN. Assuming ATDRS GPS receiver clock stability of one part in 10^{13}, which is comparable to assuming that, as in TDRSS, a ground-based cesium frequency standard provides the onboard receiver's frequency reference through a forward pilot tone, then over a 30-hour tracking arc the drift in the ATDRS clock contributes 9.7 meters (3 σ). The total clock bias has therefore been modeled in ORAN as approximately 10.0 meters (3 σ) and is applied to each GPS satellite.

The contribution due to inaccuracies in the GPS satellite ephemeris predictions is assumed to be 12.9 meters (3 σ); the contribution due to predictability of the GPS satellite perturbations is 3.0 meters (3 σ); and the GPS group delay uncertainty contributes 1.5 meters (3 σ). Assuming a similar ATDRS group delay uncertainty of 1.5 meters (3 σ), these four contributors have been combined in ORAN to form a total bias of 13.4 meters (3 σ) on each ATDRS GPS pseudorange measurement.

The sources of bias errors for the pseudorange-rate measurements are:

- GPS and ATDRS oscillator drift
- GPS ephemeris prediction errors
- Predictability of GPS satellite perturbations

GPS oscillator drift is specified to be less than one part in 10^{13} in the 8-hour interval between uploads, resulting in a pseudorange-rate bias of 0.09 mm/sec (3 σ). GPS ephemeris error similarly yields a pseudorange-rate bias: the 12.9 meter bias due to GPS ephemeris prediction corresponds to a velocity error of at most 8.6 m/s over 6 hours (half the GPS orbital period), implying a Doppler error of 1.2 mm/sec (3 σ). Finally, unpredicted GPS satellite perturbations are specified to give an acceleration of less than 3×10^{-10} mm/sec^2, resulting in a pseudorange-rate bias of approximately 0.03 mm/sec (3 σ) over eight hours. The GPS contribution to the pseudorange-rate bias may then be calculated to be approximately 1.5 mm/sec (3 σ). Assuming ATDRS oscillator drift of one part in 10^{13}, the ATDRS contribution to the pseudorange-rate bias is 0.09 mm/sec (3 σ), and the total pseudorange-rate measurement bias is approximately 1.5 mm/sec (3 σ).

Tropospheric and ionospheric error sources have been considered negligible in the modeling of errors for the Direct ATDRS/GPS Tracking System. Tropospheric errors have been eliminated by assuming that the ATDRS-to-GPS line-of-sight is constrained to be above the Earth's atmosphere. Approximately 0.7 percent of the ATDRS/GPS annular visibility region is masked by the troposphere as seen from ATDRS, assuming a maximum troposphere height of 19 km above sea level. Restricting ATDRS GPS measurements in this way is therefore negligible in comparison to the total visibility afforded by the ATDRS/GPS annular visibility region. Ionospheric refraction errors, however,

are considered negligible since the ATDRS onboard GPS receiver is assumed to use the GPS L1 and L2 channels to correct the ionospheric delay. Additionally, the ionosphere masks only about 9.0 percent of the ATDRS/GPS annular visibility region assuming a maximum ionosphere height of 500 km,

The remaining error sources used to model to ATDRS/GPS Direct Tracking System are attributed to the standard sources specified for use by all the systems in this study, employing the same error values. Appendix A discusses at length the use of ORAN to simulate the OD performance of the Direct ATDRS/GPS Tracking System and provides the performance results. Ultimately, definitive period performance over a 30-hour tracking arc is better than (less than) the goal of 75 m (3 σ), but performance over a 2-hour arc does not meet this goal. Table 6-3 shows representative results for Direct ATDRS/GPS Tracking System OD performance and the ATDRS-E satellite.

6.3 PASSIVE DIFFERENTIAL ATDRS/GPS TRACKING SYSTEM

The Passive Differential ATDRS/GPS Tracking System relies on ground station pseudorange and pseudorange-rate measurements of both GPS and ATDRS signals to form a differential measurement for use in ATDRS OD. The ATDRSs and the GPS satellites are passive members of the tracking system; that is, they only emit ranging signals and do not actively make the tracking measurements. Multiple ground stations simultaneously observe an ATDRS ranging signal and a specific GPS satellite's signal; the measurements are differenced at each station and, on relay to a central processing facility, double differenced to remove clock biases. This double differential data is then used for ATDRS OD. The separation of the ground stations and the distribution of the jointly visible GPS satellites enhances the geometry for ATDRS tracking. Compared to the Direct ATDRS/GPS Tracking System, however, atmospheric effects introduce additional errors to the tracking measurements.

6.3.1 PASSIVE DIFFERENTIAL ATDRS/GPS TRACKING SYSTEM DEFINITION

This section provides an overview of the Passive Differential ATDRS/GPS Tracking System architecture and operations concept, describes possible options for the ATDRS ranging signal, discusses the ATDRSS ground station GPS receiver architecture, and outlines various potential tracking networks.

Table 6-3. Direct ATDRS/GPS Tracking System Performance

	MAXIMUM 3σ ATDRS-E POSITION ERROR OVER THE DEFINITIVE TRACKING ARC (METERS)	
	2 HR ARC	30 HR ARC
DIRECT ATDRS/GPS TRACKING SYSTEM	208	58

7/31/89 MIS83P\AJ5645

6.3.1.1 Architecture and Operations Concept

As Figure 6-10 shows, the Passive Differential ATDRS/GPS Tracking System comprises pairs of ground stations, each capable of simultaneously receiving ranging signals from an ATDRS and a specific GPS satellite. One ground station, the master station, is collocated with the AGT; all station pairs, where at least two pairs are needed, are then formed using the master station and a remote station.

The ATDRS ranging signal is assumed to be a user navigation beacon to provide the desired broad region of Earth coverage without burdening ATDRSS forward user services; the GPS satellite, of course, emits the GPS signal. Each ground station independently makes simultaneous pseudorange and pseudorange-rate measurements with respect to ATDRS and to a GPS satellite to form differential measurements; ground station data are then relayed via Nascom facilities to the master station where the measurements are again differenced. This second differencing operation, illustrated in Figure 6-11, effectively removes the ATDRS and GPS clock biases from the double differential pseudorange measurement. A time sequence of double differential pseudorange and pseudorange-rate measurements is then relayed from the master station to the FDF and used as the basis for dynamic ATDRS OD.

The Passive Differential ATDRS/GPS tracking system ground stations are designed to operate automatically with no resident staffing. The station executive is programmed to diagnose station abnormalities, correct those it can, and notify maintenance personnel of those abnormalities that cannot be automatically corrected. Station equipment failure and periodic maintenance are handled by trained personnel who are dispatched to the stations as needed to perform routine maintenance and update subsystem calibration and station location surveys.

The master station and the remote stations possess identical capabilities and need not be differentiated. To fully separate operation of the Passive Differential ATDRS/GPS Tracking System from that of ATDRSS and other existing NASA facilities for purposes of this initial study, however, here the master station additionally

- Controls the remote stations, issuing GPS and ATDRSS satellite observation schedules and reconfiguring station capabilities as necessary

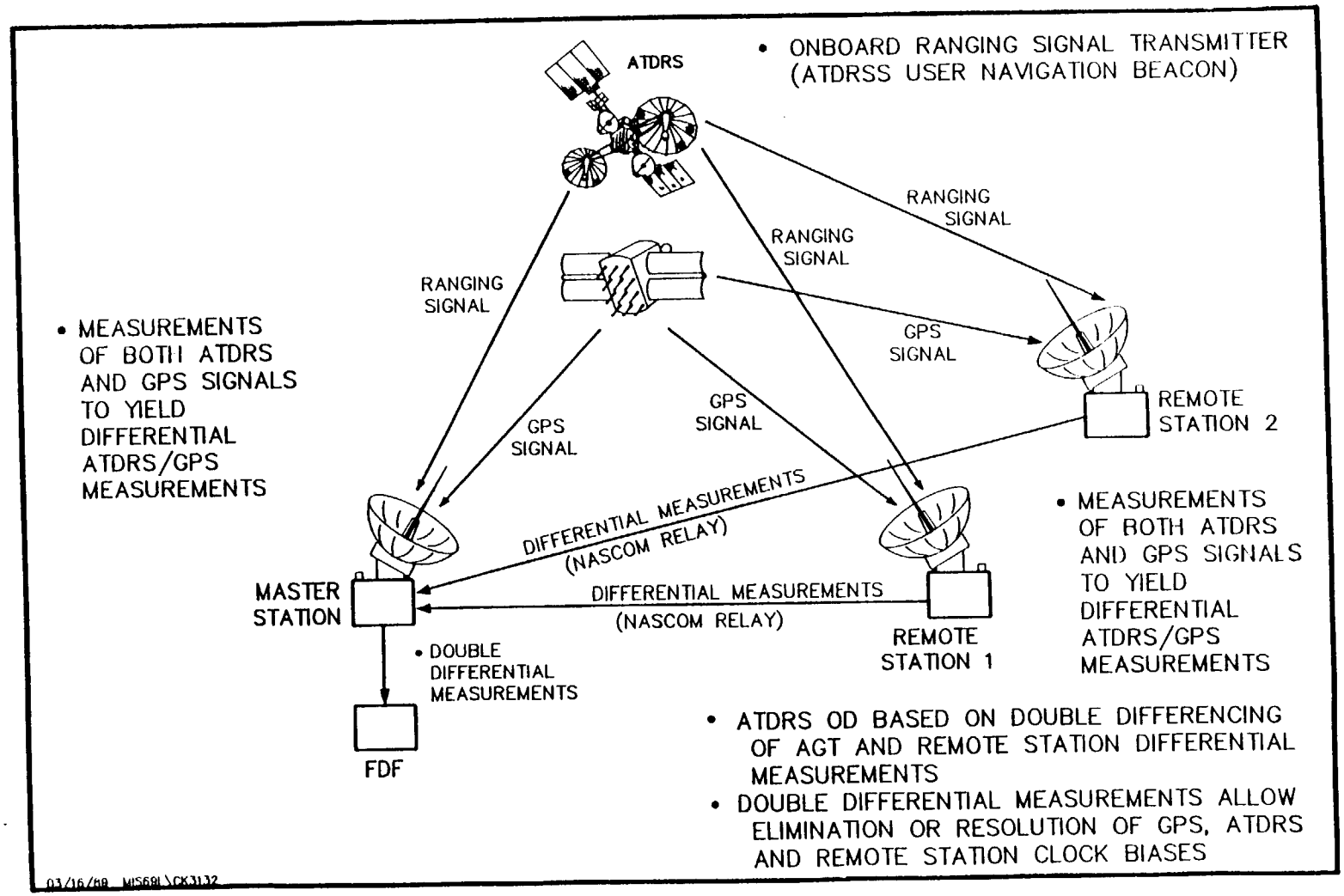

Figure 6-10. Passive Differential ATDRS/GPS Tracking System

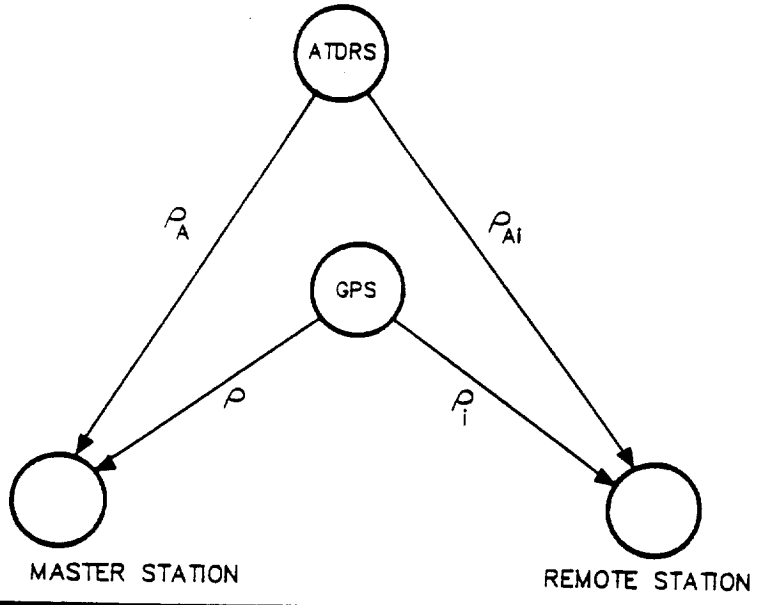

PASSIVE DIFFERENTIAL RANGE OBSERVATION

$$\Delta R_i = (\rho_A - \rho) - (\rho_{Ai} - \rho_i) + \text{OBSERVATION ERRORS}$$

$i = 1, 2, \bullet\bullet\bullet N$ (N = NUMBER OF REMOTE STATIONS)

SOURCES OF OBSERVATION ERROR	METHOD OF MITIGATION
GPS EPHEMERIS ERROR	GPS CONTROL SEGMENT PROVIDES UPDATES OF EACH SATELLITE EPHEMERIS EVERY 8 HOURS IN THE NAVIGATION MESSAGE
IONOSPHERIC DELAY	GPS MEASUREMENTS CORRECTED THROUGH GPS SIGNAL STRUCTURE, ATDRS MEASUREMENTS REQUIRE INDEPENDENT CORRECTION CAPABILITY (I.E., SIGNAL STRUCTURE OR USE OF HIGH TRANSMIT FREQUENCY)
TROPOSPHERIC DELAY	METEOROLOGICAL MEASUREMENTS AND DELAY MODELING AND/OR WATER VAPOR RADIOMETER MEASUREMENTS
STATION POSITION UNCERTAINTY	ACCURATE SURVEYS
CHANNEL NOISE	ATDRSS GROUND STATION GPS RECEIVER DESIGN; ATDRS RANGING SIGNAL AND RECEIVER CHARACTERISTICS

3/16/89 MIS89L\CK5v32

Figure 6-11. Passive Differential ATDRS/GPS Tracking System Measurement Model

- Receives remote station telemetry and forms the double differential measurement
- Relays the double differential measurements to the FDF for ATDRS OD processing

6.3.1.2 ATDRS Ranging Signal

The ATDRS ranging signal required by the Passive Differential ATDRS/GPS Tracking System must allow pseudorange and pseudorange-rate measurements to be taken at the system's ground stations. An ATDRSS user navigation beacon is ideally suited for this purpose because, as a consequence of its support of ATDRSS users, it provides maximum Earth coverage and is available continuously with no impact on ATDRSS user services. The characteristics of such an ATDRSS navigation beacon depend on the requirements of the ATDRSS user community and the ATDRSS design. Three obvious alternatives are possible: an S-band beacon (Reference 6-7); an S-band PRTS beacon, as discussed in Section 4 of this report; or a Ku-band beacon, as discussed in Section 3. Although the GPS signals intrinsically allow correction of the range bias due to ionospheric delay uncertainties, correction of this uncertainty for the measurements of the ATDRS ranging signal is a major distinction among the three likely options.

Use of an S-band ATDRS navigation beacon will support autonomous user navigation with a minimal increase in current TDRSS user capabilities: the addition of a navigation processing module and the current second-generation TDRSS user transponder, equipped with a Doppler extractor unit and external Ultra-Stable Oscillator as frequency reference. In the Passive Differential ATDRS/GPS Tracking System, however, pseudorange measurements of an S-band ATDRS navigation beacon will suffer range biases due to uncertainties in the signal's ionospheric delay, as seen from the system's ground stations.

The range bias involved in ground station measurement of an S-band navigation beacon might be reduced by estimating the ionospheric path delay through modeling. Data for ionospheric modeling can be augmented by the collection of GPS L-band ionospheric correction data to aid in real-time estimates of the S-band ionospheric delay. Estimates of the ionospheric delay at L-band can be obtained as part of the normal GPS measurement process. Because there are four or more GPS satellites are simultaneously visible from any station location at any time, estimates can be made for a variety of pointing angles, both near and far from the

station-to-ATDRS line-of-sight. Averaged over time, the GPS satellites are distributed uniformly over that section of the GPS orbital sphere in which the constellation is constrained. As a result, the GPS satellites are widely distributed over any ground station's view of the sky, making it possible to map the L-band ionospheric delay. The L-band ionospheric delay estimates can then be extrapolated to provide the S-band ionospheric delay for the station-to-ATDRS line-of-sight, thereby significantly reducing the range bias of the S-band beacon pseudorange measurements.

Use of an S-band PRTS navigation beacon, as discussed in Section 4, will support ATDRSS users in the same manner as an S-band beacon or, if users are equipped with PRTS receivers, will allow greater levels of pseudorange precision to be achieved. Use of PRTS receivers at the ground stations of the Passive Differential ATDRS/GPS Tracking System will allow the beacon signal path delay due to the ionosphere to be resolved, exploiting the properties of the PRTS signal structure. In this manner, ionospheric range biases in the ATDRS ranging signal measurements may be estimated and effectively eliminated.

Use of a Ku-band ATDRS navigation beacon makes negligible the ionospheric delay as a result of its higher frequency, mitigating the impact of ionospheric range biases. A Ku-band user navigation beacon, however, implies development of a standard Ku-band user transceiver at a time when NASA is being encouraged to reduce its employment of Ku-band frequencies.

6.3.1.3 Passive Differential ATDRS/GPS Tracking System Ground Station Architecture

Figure 6-12 shows the ground station architecture for the Passive Differential ATDRS/GPS Tracking System. Each ground station comprises a station executive, ATDRSS ranging receiver, ATDRSS ground station GPS receiver, station clock, atmospheric monitoring equipment, and Nascom interface. The ground stations are fully automated and require personnel only to perform routine scheduled maintenance or to make repairs when autonomous performance monitoring reports a degradation in system health.

6.3.1.3.1 Station Executive

As in the AKuRS and PRTS ground stations, the station executive is a microcomputer programmed to control autonomously the operations of the various subsystems that

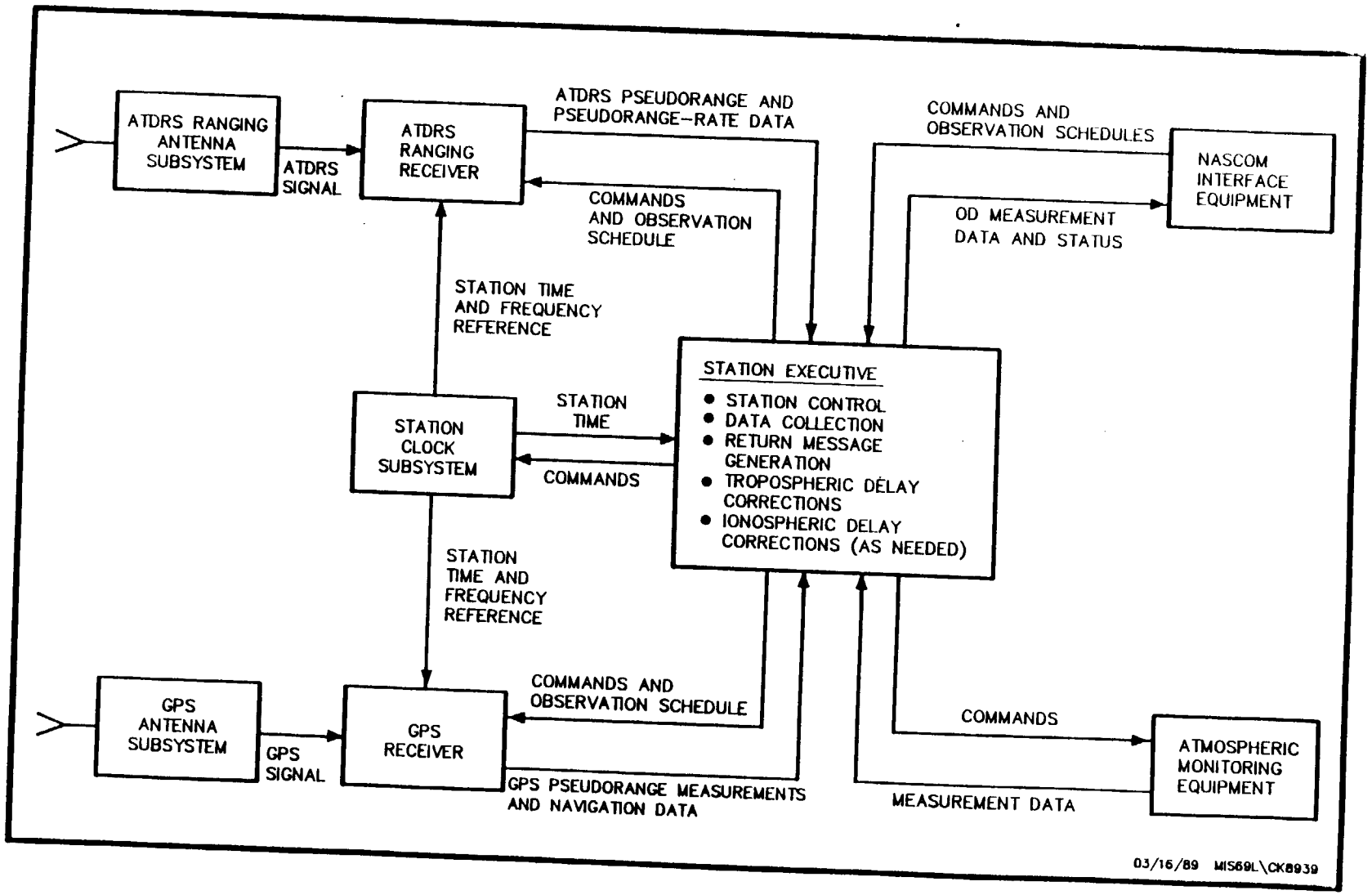

Figure 6-12. Passive Differential ATDRS/GPS Tracking System: Ground Station Architecture

constitute the ground station and to support the relay of command and telemetry data. The station executive responds to hardware and software interrupts generated throughout the system, functioning as the system's real-time controller, issuing commands to the equipment to perform their initialization functions at system startup and to invoke periodic equipment status reports.

In the remote stations, the station executive receives and processes observation schedules and control commands from the master station and collects and transmits ground station measurement and status data back to the master station. The executive provides the relayed observation schedules to the ATDRSS ranging and ground station GPS receivers and collects measurement data and navigational message information from them. The executive performs tropospheric delay corrections for both the ATDRSS ranging and ground station GPS receivers, using the atmospheric monitoring equipment's meteorological measurements. If the ATDRSS ranging receiver requires ionospheric delay corrections, the executive performs the necessary correction processing prior to relaying the measurement data to the master station.

In the master station, the station executive performs the same functions as the remote station. In addition, however, the station executive for the master station monitors the health and status of the remote stations, commands and controls operation of the remote stations, forms the double differential measurements, and maintains the interface with the FDF.

6.3.1.3.2 ATDRSS Ground Station GPS Receiver and Antenna Subsystems

The ATDRSS ground station GPS receiver and antenna subsystems used by the Passive Differential ATDRS/GPS Tracking System are similar to the typical GPS receiver discussed in Section 6.1.5. Unlike a typical GPS receiver, however, the navigation processor subsystem in the ATDRSS ground station GPS receiver does not develop an instantaneous position, velocity, and/or time solution. Instead, pseudorange and pseudorange-rate measurement data to selected GPS satellites, corrected for ionospheric delay by the receiver's navigation processor, are output to the station executive for correction of tropospheric effects. Then they are relayed to the FDF for use in the ATDRS OD process. Because the passive differential system eliminates GPS receiver clock biases through the double differencing of GPS and ATDRS ranging measurements, stability of the GPS

receiver's frequency reference (the station clock) need be no better than that of a typical GPS receiver. It is possible that commercial GPS receivers might be modified to provide the necessary functions and interfaces required for use in the Passive Differential ATDRS/GPS Tracking System ground stations.

6.3.1.3.3 ATDRSS Ranging Signal Receiver and Antenna Subsystems

The ground station's ATDRSS ranging signal receiver must be capable of making pseudorange and pseudorange-rate measurements of the ATDRS ranging signal. Three distinct options are likely for the ranging signal: an S-band navigation beacon, an S-band PRTS navigation beacon, or a Ku-band navigation beacon. The ground station receiver must operate using whichever ATDRS ranging signal is employed, in each case extracting pseudorange and pseudorange-rate from the beacon. Since the ATDRSS satellites are essentially fixed in position, no antenna pointing system is necessary if the beamwidth of the antenna is large enough to accommodate motion of the ATDRSS satellite after the antenna is initially installed. As detailed in Sections 3 and 4, a representative antenna size to receive an S-band navigation beacon is 1 meter, whereas the aperture for a Ku-band beacon is on the order of 10 cm.

In the case of an S-band navigation beacon, range biases due to uncertainties in the ionospheric delay cannot be resolved through measurement of the beacon signal. As discussed in Section 6.3.1.2, however, S-band ionospheric delays along the ground station-to-ATDRS signal path may be estimated using the L-band ionospheric delays measured by the ground station GPS receiver. The station executive, in that case, would collect the GPS data, extrapolate to S-band and the proper signal path, and correct the ATDRSS ranging signal receiver's pseudorange estimates.

In the case of an S-band PRTS navigation beacon, the ATDRSS ranging receiver may use the PRTS signal structure and associated signal processing to measure the ionospheric delay directly along the ATDRS ranging signal path. In the case of a Ku-band navigation beacon, the path delay due to the ionosphere is negligible and no special processing is necessary.

6.3.1.3.4 Station Clock Subsystem

The station clock subsystem provides a frequency standard for use as a reference for digital circuit elements in the ground station equipment. Station system time is provided

by the clock and used in the determination of pseudorange and pseudorange-rate for both the ATDRS and GPS measurements. Because the measurements will be double differenced, the station time bias will be eliminated from the measurement type. As a result, a thermally regulated high-quality crystal oscillator is sufficient for use as the station frequency standard.

6.3.1.3.5 Atmospheric Monitoring Equipment

The atmospheric monitoring equipment provides meteorological data to the station executive to allow estimation of the signal path delays due to the troposphere. Estimates of the tropospheric delay are accomplished by the use of mathematical models with surface meteorological measurements as inputs to the models. Raw atmospheric data may be relayed from the remote stations to the master station for offsite processing, or corrections to the pseudorange and pseudorange-rate measurements may be developed locally.

6.3.1.3.6 Nascom Interface Equipment

Nascom interface equipment is used to link the remote ground stations of the Passive Differential ATDRS/GPS Tracking System with the master station and the master station with the FDF. The master station oversees remote ground station operations, issuing commands and satellite observation schedules and receiving status reports to and from the remote stations through Nascom facilities. Remote station observations are relayed to the master station through Nascom; the measurements are validated and, if appropriate, corrected for atmospheric effects; and the double differential measurements are formed and relayed to the FDF, also via Nascom. In all cases, the data rates Nascom supportes are quite low: data rates of 4800 bps or even as low as 100 bps could be used, indicating the suitability of voice-quality or other limited bandwidth Nascom channels.

6.3.1.4 Passive Differential ATDRS/GPS Tracking System Network Options

The location of the Passive Differential ATDRS/GPS Tracking System's ground stations are dependent on

- Common visibility of the GPS satellites and ATDRS from different station sites
- Geographical, political, and climatic constraints

- ATDRS OD performance as a function of the geometry of the network with respect to the observed satellites

Figure 4-8 shows the geographical boundaries of the 10-degree elevation masks for ranging signal footprints from ATDRS-E, ATDRS-C, and ATDRS-W, assuming use of a navigation beacon as the ATDRS ranging signal. Ground station locations for a particular ATDRSS satellite must be located within the appropriate footprint. The length of the tracking network baselines are thus constrained by the boundaries of the ATDRS ranging signal footprints and then further limited by any geopolitical and climatic constraints.

The system's ATDRS OD accuracy is influenced by the length of the baseline between each pair of ground stations used to construct the system's double differential measurement. The effectiveness of the measurement in determining the ATDRS orbit increases as the angular separation between ATDRS and the GPS satellite, as viewed from the ground station, increases. This increase in accuracy results from the corresponding reduction in the geometrical dilution of precision. Both stations must observe the same GPS satellite, but the number of GPS satellites visible to both stations decreases as the length of the baseline between stations increases. On one hand, large baselines reduce the number of GPS satellites in common view of both stations, thereby reducing the number of observations with different GPS satellites at a given time and restricting the number and diversity of possible measurements. On the other hand, large station baselines provide the greatest degree of angular diversity to the measurements, reducing the geometrical dilution of precision and improving the accuracy of ATDRS OD.

The relative angular separation between ATDRS and the GPS satellite under observation is functionally determined for a given station site. Because the position of ATDRS is virtually fixed and the position of the visible GPS satellites is specified by the initial conditions of the constellation, GPS satellites may be selected for observation based on the magnitude of the angular displacement between ATDRS and the GPS satellite and common visibility with the two ground stations forming the double differential measurement.

As in Sections 3 and 4, network station sites have been chosen to provide short (CONUS-based), intermediate, and long baselines between the master and remote stations. The

selection of a remote station site is influenced by the desire to obtain the maximum separation between stations in both latitude and longitude. Greater site dispersion reduces the geometric dilution of precision and fosters OD processing accuracy. As has been discussed, the master station is collocated with the AGT at White Sands, NM, and is thus visible to all ATDRSS satellites. Using the station sites listed in Table 4-3, the same tracking networks for ATDRS-W and ATDRS-E as in the PRTS, MPRTS, and AKuRS tracking systems have been chosen for initial examination in this study of the Passive Differential ATDRS/GPS Tracking System.

6.3.2 PASSIVE DIFFERENTIAL ATDRS/GPS TRACKING SYSTEM ASSESSMENT

The following sections assess the impact on ATDRSS development and operations; cost and staffing requirements; reliability, maintainability, and availability; the technological risks associated with the implementation of the Passive Differential ATDRS/GPS Tracking System; and the system's ATDRSS OD performance.

6.3.2.1 Cost and Staffing Requirements

The ground station architecture of the Passive Differential ATDRS/GPS Tracking System is directly comparable to that of PRTS; the major differences between the two tracking systems are the station clock, the transmitter, and the GPS receiver subsystems. The clock subsystems in the PRTS ground stations use a cesium frequency standard, whereas the passive differential system ground station clocks use a thermally controlled crystal oscillator. The PRTS transmitter subsystems are required for network clock synchronization and are not present in the passive differential ground station. Furthermore, the PRTS ground station does not require a GPS receiver subsystem.

Noting the differences and similarities between the PRTS and Passive Differential ATDRS/GPS Tracking System ground station architectures, it is possible to establish a cost for the Passive Differential ATDRS/GPS Tracking System by adjusting the PRTS baseline life-cycle cost, as detailed in Appendix D. The replacement of the PRTS ground station cesium frequency standard with a crystal oscillator in the passive differential ground station reduces the system costs. Costs are further reduced by the absence of an ATDRS transmitter subsystem in the Passive Differential ATDRS/GPS

Tracking System. The only added in cost to the PRTS baseline is the GPS receiver and antenna subsystem. Taking all of these adjustments into account provides a baseline life-cycle cost estimate of $23.3 million for the Passive Differential ATDRS/GPS Tracking System. This estimate includes $6.1 million for operations and maintenance over a 10-year period.

As described in Section 6.3.1, one of three types of ATDRS navigation beacons--the S-band, the Ku-band, or the PRTS S-band beacon--may be used as the ATDRS ranging signal. The architecture of the master and remote stations would have to be somewhat different to accommodate any particular one of these signal types; use of the PRTS beacon would probably have marginally higher costs than the others because of the additional development required. For all three options, however, the receiver subsystem technologies are similar. The cost estimates presented here assume use of the PRTS beacon ATDRS ranging signal.

These cost estimates assume that complete system specifications (as opposed to the conceptual design presented here) have been developed and would be available at the start of the design and development cycle. It is estimated that an additional $2.5 million study phase would be required to produce such system specifications, supporting further analysis and the development of an engineering model for field testing. Results from the field tests would be used to complete the specifications for implementing the operational Passive Differential ATDRS/GPS Tracking System.

Staffing requirements for the passive differential tracking system are restricted to operations, maintenance, and repair of the ground facilities. It has been estimated in Section 4.2.2 that a seven-member staff would be required to perform these functions for PRTS over 10-year period. Based on the similarities between PRTS and the passive differential tracking system, it is assumed that the same size staff would be required for both systems. Staffing costs for the 10-year period are included in the $6.1 million operations estimate previously cited.

6.3.2.2 Reliability/Maintainability/Availability

Reliability, maintainability, and availability of the Passive Differential ATDRS/GPS Tracking System are beyond the scope of this report but should be considered as part of future efforts.

6.3.2.3 Technological Risks

The technology to be used in the Passive Differential ATDRS/GPS Tracking System requires a GPS receiver and antenna in addition to hardware and software similar to that described in the PRTS remote station subsystem discussed in Section 4. The technology for the GPS receiver has been operational for nearly a decade and presents no implementation risks for the Passive Differential ATDRS/GPS Tracking System. The hardware and software required for making the ATDRS pseudorange and pseudorange-rate measurements depend on which ranging signal option is chosen, but the technological risks are minimal. The technological risks associated with use of the PRTS beacon are the greatest of the three options and are discussed in Section 4.2.4. In general, the Passive Differential ATDRS/GPS Tracking System involves no new technology and could be implemented with currently available, off-the-shelf components.

6.3.2.4 External Dependencies

As in any GPS-based tracking system, performance is dependent on GPS. If any elements of GPS fail, performance of the ATDRS/GPS tracking systems will be affected. Deliberate degradation of GPS capabilities through selective availability will also affect ATDRS/GPS tracking system performance, unless the ATDRSS GPS receivers have been authorized and designed to operate during selective availability periods.

The Passive Differential ATDRS/GPS Tracking System relies on Nascom facilities to relay commands and measurements between the remote and master stations and between the master station and the FDF. The use of dedicated lines is assumed to ensure 24-hour communications support; redundancy may also be desired.

6.3.2.5 ATDRSS Impacts

The Passive Differential ATDRS/GPS Tracking System depends upon the existence of an ATDRS-emitted navigation beacon for its operation. Any one-way navigation beacon supporting user spacecraft will support the passive differential system with no additional ATDRSS impacts. As discussed, three beacon options are likely for use with the passive differential system: an S-band single channel beacon, an S-band multichannel PRTS beacon, or a Ku-band single channel beacon.

In general, the implementation of a navigation beacon affects ATDRSS in the following ways:

- Bandwidth and frequency allocations for the beacon and its uplink to the ATDRSS satellites
- Transmit EIRP, as supported by an ATDRS beacon antenna and high-power amplifier
- Delay calibration as needed to reduce epoch uncertainties
- Ground segment support to provide beacon generation and uplink to the ATDRSS satellite

These issues have been discussed at length in Sections 3 and 4 of this report for the AKuRS and PRTS navigation beacons. The reliance of the Passive Differential ATDRS/GPS Tracking System on an ATDRS navigation beacon in no way affects the beacon itself and results in no other ATDRSS impacts.

6.3.2.6 OD Performance

The OD performance of the Passive Differential ATDRS/GPS Tracking System has not been assessed using ORAN due to incompleteness of the existing software and the current inability to modify ORAN with the NASA computer facilities. This situation is regrettable, since the Passive Differential ATDRS/GPS Tracking System promises the potential of OD performance superior to that of the Direct ATDRS/GPS Tracking System. Despite the absence of ORAN results, an ORAN error budget has been developed here in the event that future work will attempt to assess the performance of this system.

The error budget used with ORAN in modeling the Passive Differential ATDRS/GPS Tracking System is provided in Table 6-4. Since the passive differential tracking system is modeled as shown in Figure 6-11, measurement errors are given in Table 6-4 for both the ATDRS-to-ground station and the GPS satellite-to-ground station signal paths. Measurement errors common to both the ATDRS and GPS measurements are also presented.

As discussed in Section 6.3.1.3.3, the ATDRS ranging signal may be implemented as one of the following: a generic S-band navigation beacon, a PRTS S-band beacon, or a Ku-band

beacon. Table 6-4 consequently indicates three cases for the range and range-rate noise values corresponding to each case. Since the ground station ATDRS and GPS measurements are double differenced to form the passive differential measurement type, the pseudorange-rate and clock measurement biases associated with each signal type will be effectively eliminated.

The ionospheric refraction error associated with the ATDRS measurements depends on the type of beacon being observed. A generic S-band beacon suffers 100 percent of the uncertainty due to the ionospheric delay, while the PRTS signal structure allows estimation and the effective elimination of the ionospheric delay uncertainty. No such capability is provided by the Ku-band beacon, but the high frequency results in a relatively insignificant ionospheric delay.

The ATDRS PRTS S-band, S-band, and Ku-band pseudorange and pseudorange-rate measurement noise values given in Table 6-4 are derived from the PRTS, MPRTS, and AKuRS values, where those values are discussed at length in Appendix C. The PRTS S-band noise measurement values are taken from the one-way PRTS ORAN noise values listed in Table 4-4 without modification; to apply the MPRTS and AKuRS values, however, those two-way range and range-rate values must be multiplied by two to model the ground station's one-way measurements and adhere to the conventions adopted in this study.

Modeling of the ground station GPS measurements is exactly the same as for the Direct ATDRS/GPS Tracking System. The pseudorange and pseudorange-rate measurement noise values for the GPS satellite-to-ground P-code signals are thus the same, although the double-differencing implicit in the passive differential measurement process ultimately eliminates the GPS measurement biases. The uncertainty in knowledge of the GPS satellite positions is handled as in the Direct ATDRS/GPS Tracking System; i.e., through use of an imaginary GPS satellite tracking network whose measurements are weighted to be separate from those of the ATDRS tracking network. Finally, because the GPS signal structure allows estimation of the ionospheric delay, the ionospheric refraction error for the ground station GPS measurements has been set equal to zero.

The remaining contributors to the Passive Differential ATDRS/GPS Tracking System ORAN error budget are those common to both the ATDRS and GPS measurements, which have been assigned the standard values used throughout this study. The ground station network can then be chosen as desired, only constrained by the requirement for joint visibility to the ATDRS and GPS satellites.

Table 6-4. Passive Differential ATDRS/GPS Tracking System ORAN Error Modeling (3-σ Values)

STATION LOCATION	ATDRS/GPS ANNULAR VISIBILITY REGION	PROBABILITY (%)
GUAM	ATDRS-E	43
WAKE ISLAND	ATDRS-E	41
AMERICAN SAMOA	ATDRS-E	37
HAWAII	ATDRS-E	7
PUERTO RICO	ATDRS-W	2
MERRITT ISLAND, FL	ATDRS-W	<1

MIS69L

6.4 DIRECT DIFFERENTIAL ATDRS/GPS TRACKING SYSTEM

The Direct Differential ATDRS/GPS Tracking System relies on GPS measurements made both by the ATDRSS satellites and by a network of ground stations. Simultaneous pseudorange and pseudorange-rate measurements to two GPS satellites by ATDRS and the ground stations are differenced, relayed to a central processing facility, and then double differenced to form the measurement used in ATDRS OD processing. The Direct Differential ATDRS/GPS Tracking System thus combines aspects of the direct system in that the ATDRSS satellites directly measure their range to the GPS satellites, and the passive differential system, because the GPS measurements are double differenced for ATDRS tracking and ground stations are required. As has been noted for the passive differential tracking system, differential measurements allow the elimination of the effect of clock biases. Geographical visibility restrictions and inherent limitations in the measurement process, however, significantly reduce the suitability of this tracking system approach.

6.4.1 DIRECT DIFFERENTIAL ATDRS/GPS TRACKING SYSTEM DEFINITION

This section provides an overview of the Direct Differential ATDRS/GPS Tracking System architecture, operations concept, and tracking network options.

6.4.1.1 Architecture and Operations Concept

The Direct Differential ATDRS/GPS Tracking System is an extension of the Direct ATDRS/GPS Tracking System discussed in Section 6.2 to yield differential measurements and thereby remove clock biases. In the Direct Differential ATDRS/GPS Tracking System, illustrated in Figure 6-13, two GPS satellites are simultaneously observed by the ATDRS using an onboard GPS receiver to provide pseudorange and pseudorange-rate measurements. The ATDRS GPS measurements are relayed to the AGT and then to the FDF. Simultaneously, a ground station equipped with a GPS receiver observes the same two GPS satellites, and the ground station measurements are relayed to the FDF. Double differencing of the two ATDRS and GPS measurements is performed at the FDF to construct the direct differential measurement type for use in ATDRS dynamic OD processing, as shown in Figure 6-14.

The ATDRSS onboard GPS receiver used here is the same as that described for the Direct ATDRS/GPS Tracking System. Similarly, the ground stations and the ATDRSS ground station GPS receiver are identical to those described for the Passive Differential ATDRS/GPS Tracking System.

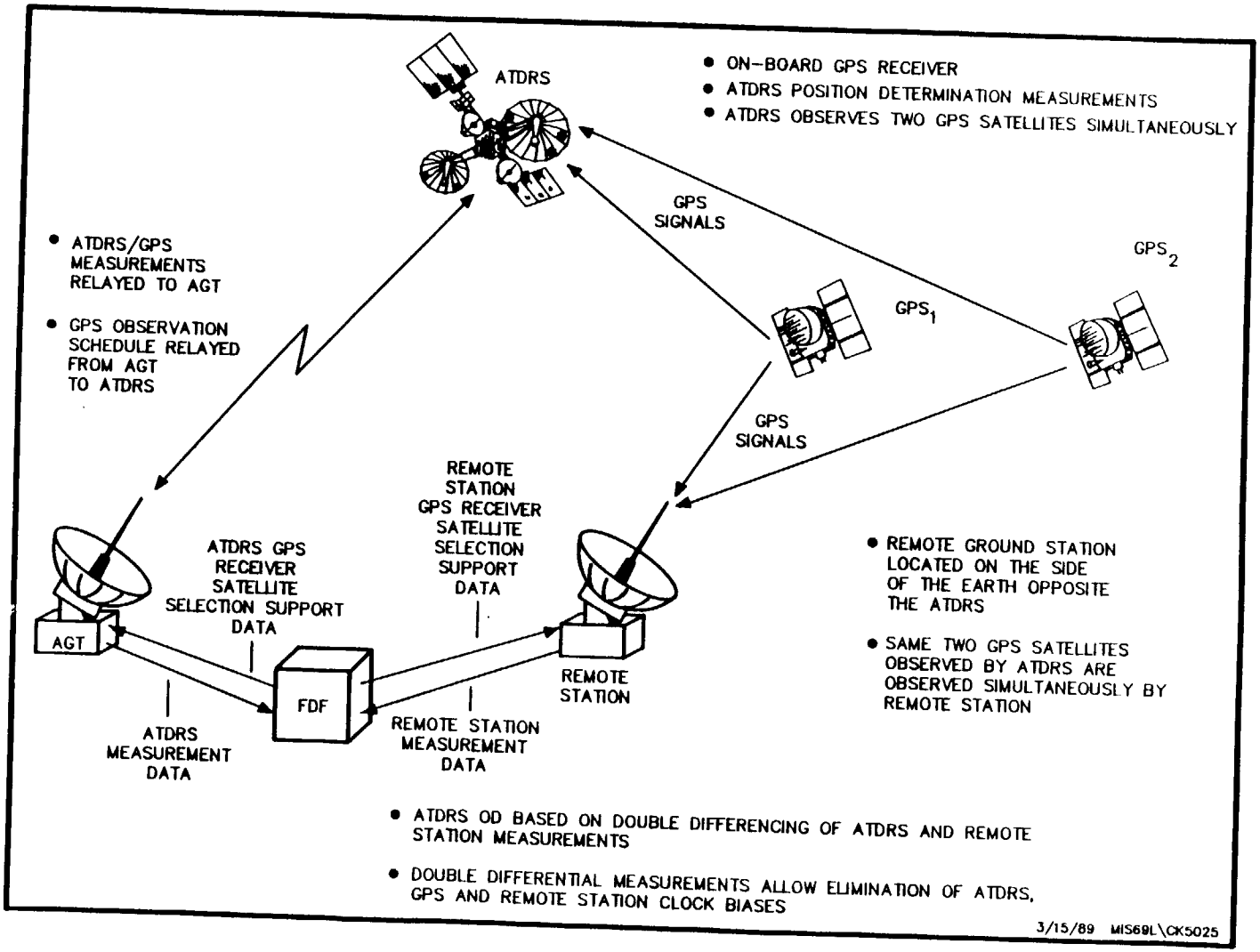

Figure 6-13. Direct Differential ATDRS/GPS Tracking System

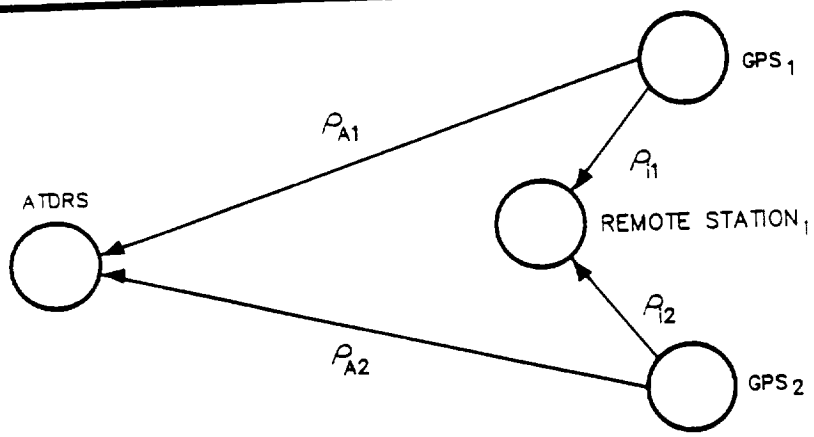

DIRECT DIFFERENTIAL RANGE OBSERVATION

$$\Delta R_i = (\rho_{A1} - \rho_{i1}) - (\rho_{A2} - \rho_{i2}) + \text{OBSERVATION ERRORS}$$

$i = 1, 2, .. N$ (NUMBER OF REMOTE STATIONS)

SOURCES OF OBSERVATION ERROR	METHOD OF MITIGATION
GPS EPHEMERIS ERROR	GPS CONTROL SEGMENT PROVIDES UPDATES OF EACH SATELLITE EPHEMERIS EVERY 8 HOURS IN THE NAVIGATION MESSAGE
IONOSPHERIC DELAY	GPS MEASUREMENTS CORRECTED THROUGH GPS SIGNAL STRUCTURE; ATDRS MEASUREMENTS INCUR MINIMAL ERROR DUE TO LIMITED IONOSPHERIC SIGNAL PATH AND ARE CORRECTED VIA GPS SIGNAL STRUCTURE
TROPOSPHERIC DELAY	GPS MEASUREMENTS CORRECTED VIA METEOROLOGICAL MEASUREMENTS AND DELAY MODELING AND/OR WATER VAPOR RADIOMETER MEASUREMENTS; MEASUREMENTS INCUR MINIMAL ERROR DUE TO LIMITED TROPOSPHERIC SIGNAL PATH
STATION POSITION UNCERTAINTY	ACCURATE SURVEYS
CHANNEL NOISE	ATDRS ONBOARD AND REMOTE STATION GPS RECEIVER DESIGN

3/16/89 MIS69L\CK5034

Figure 6-14. Direct Differential ATDRS/GPS Tracking System Measurement Model

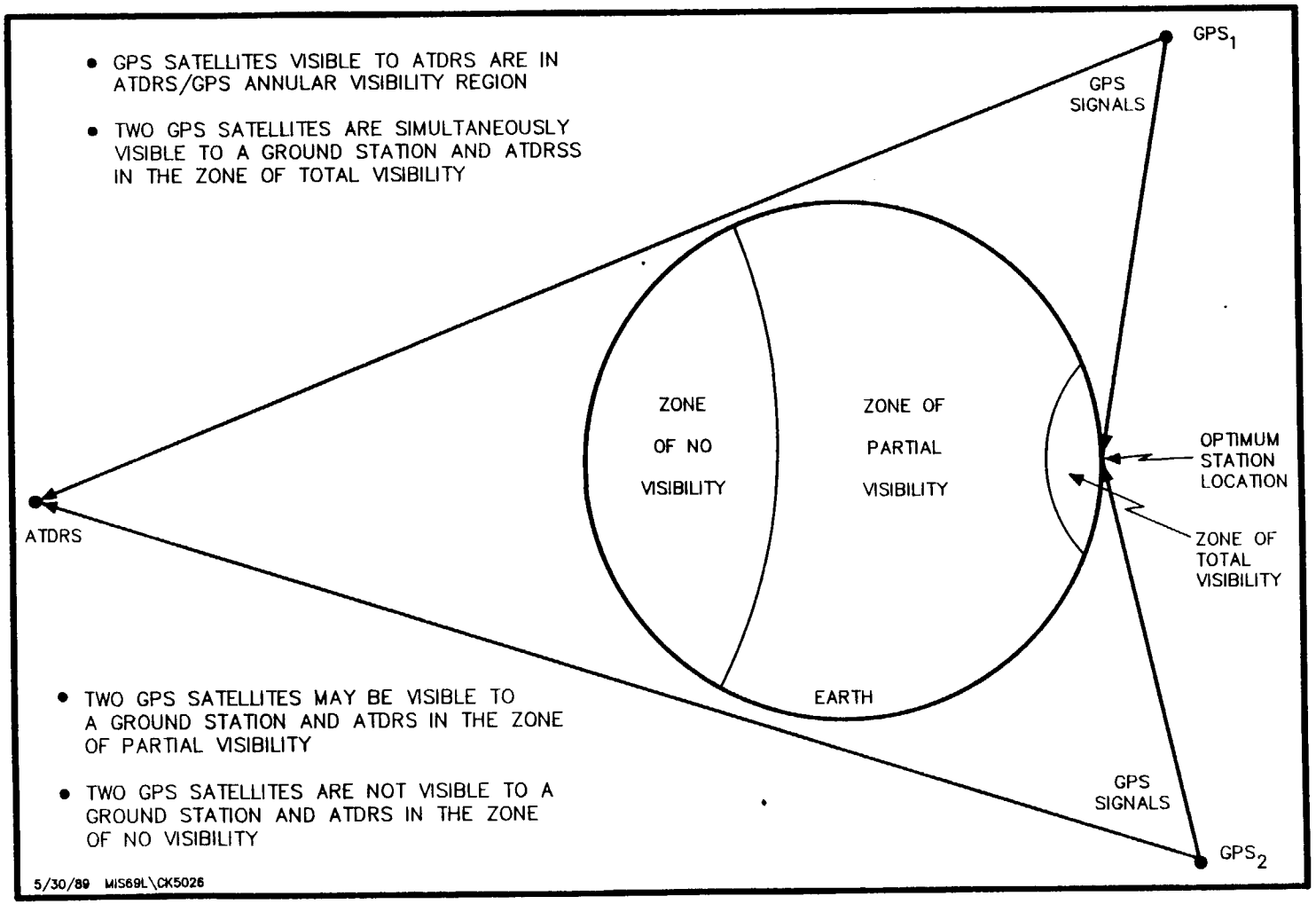

Figure 6-15. Ground Station Zones of ATDRS/GPS Annular Region Visibility

6.4.1.2 Joint ATDRS/Ground Station GPS Visibility Constraints

In order to provide the required simultaneous GPS observation capabilities, the ground stations must be located so that all or part of the ATDRS/GPS annular visibility region for that particular ATDRS is also visible to the ground stations. As Figure 6-15 shows, the optimum position for a ground station is directly opposite that of the ATDRS subsatellite points, that is, shifted 180 degrees from 171 and 41 degrees west longitude. At these points on the Earth's surface, the respective ATDRS/GPS annular visibility regions are directly overhead, concentric about the local zenith. The optimum direct differential ground station sites for the ATDRS-E and ATDRS-W ground stations are on the equator at 139 and 9 degrees east longitude, respectively.

Moving away from the optimum station location along any great circle causes the centroid of the ATDRS/GPS annular visibility region to undergo an angular displacement from the local zenith. A movement of 27.5 degrees along a great circle causes a point on the outer edge of the annular region to come in contact with the 10-degree local horizon elevation mask. Great circle angular displacements greater than 27.5 degrees cause the annular region to be partially or totally eclipsed by the local horizon elevation mask. Loss of visibility is partial until the angular displacement on the great circle is 105.6 degrees or more, when the annular visibility region is totally eclipsed by the local horizon.

Because the complete ATDRS/GPS annular visibility region is visible to ground stations within a 27.5-degree angular displacement along a great circle from the optimum position, a zone of total visibility in the shape of a spherical cap is generated by the set of all station location points satisfying this condition. Simultaneous visibility of GPS satellite pairs by a ground station and a particular ATDRS is ensured, provided the station is located in the zone of total visibility corresponding to that ATDRS. This zone of total visibility extends radially on the Earth's surface from the optimum direct differential ground station site for a distance of 3058 km in all directions.

Outside the zone of total visibility, a ground station can view only a portion of the ATDRS/GPS annular visibility region. As a consequence, the probability that at least two GPS satellites are visible to the ground station and ATDRS

decreases as the station site moves farther away from the zone of total visibility. Ultimately, station sites near the ATDRS subsatellite point are unable to see the ATDRS/GPS visibility region and, thus, may not be used in the Direct Differential ATDRS/GPS Tracking System. Figure 6-15 shows three distinct Direct Differential ATDRS/GPS Tracking System visibility zones: a zone of total visibility, a zone of partial visibility, and a zone of no visibility. The maps of Figures 6-16 and 6-17 show these visibility zones for ATDRS-E and ATDRS-W, respectively.

Figures 6-16 and 6-17 reveal that a limited range of station locations within CONUS provide the visibility required for the Direct Differential ATDRS/GPS Tracking System. Station locations are further limited if they are to support both ATDRS-E and ATDRS-W. Moreover, station locations within CONUS are in the ATDRS-E and ATDRS-W partial visibility zones bordering the zones of no visibility. Thus implies that most of the ATDRS-E and ATDRS-W GPS annular visibility regions are well below the local horizon for CONUS-based ground stations. Because only a small section of the ATDRS/GPS annular region is visible from CONUS-based ground stations, the probability of a CONUS-based ground station and a particular ATDRS simultaneously viewing two GPS satellites is negligible. Therefore, CONUS-based ground stations for the Direct Differential ATDRS/GPS Tracking System are not considered feasible.

As just noted, the best locations for the Direct Differential ATDRS/GPS Tracking System ground stations are within the zones of total visibility for ATDRS-E and ATDRS-W. If ground station sites are further limited to American territories, the visibility maps of Figures 6-16 and 6-17 may be used to select possible station sites. For example, GWM is within the total visibility zone for ATDRS-E and Wake Island, AMS, and Midway Island are located in the ATDRS-E zone of partial visibility. No American territories, however, lie within the zone of total visibility for ATDRS-W. Station locations in Puerto Rico are within the ATDRS-W zone of partial visibility, but because of the distance from the zone of total visibility, there are few observation opportunities.

The conditions for making direct differential measurements require that an ATDRS and a ground station make simultaneous observations of the same two GPS satellites. At least two satellites must be in the portion of the ATDRS/GPS annular visibility region that is visible to the ground station before they can be simultaneously observed by both the ATDRS

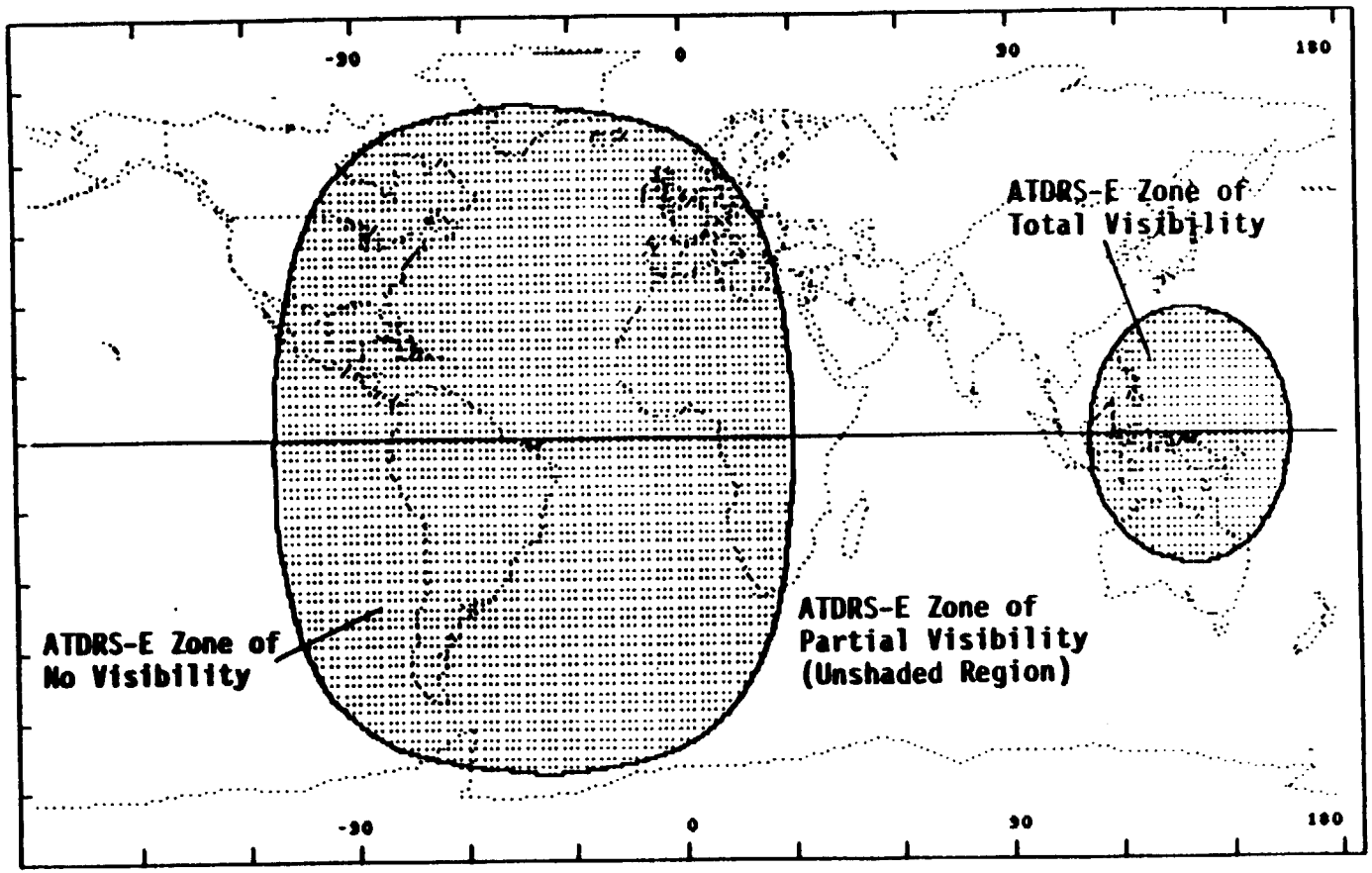

Figure 6-16. ATDRS-E Direct Differential ATDRS/GPS Tracking System Visibility Zones

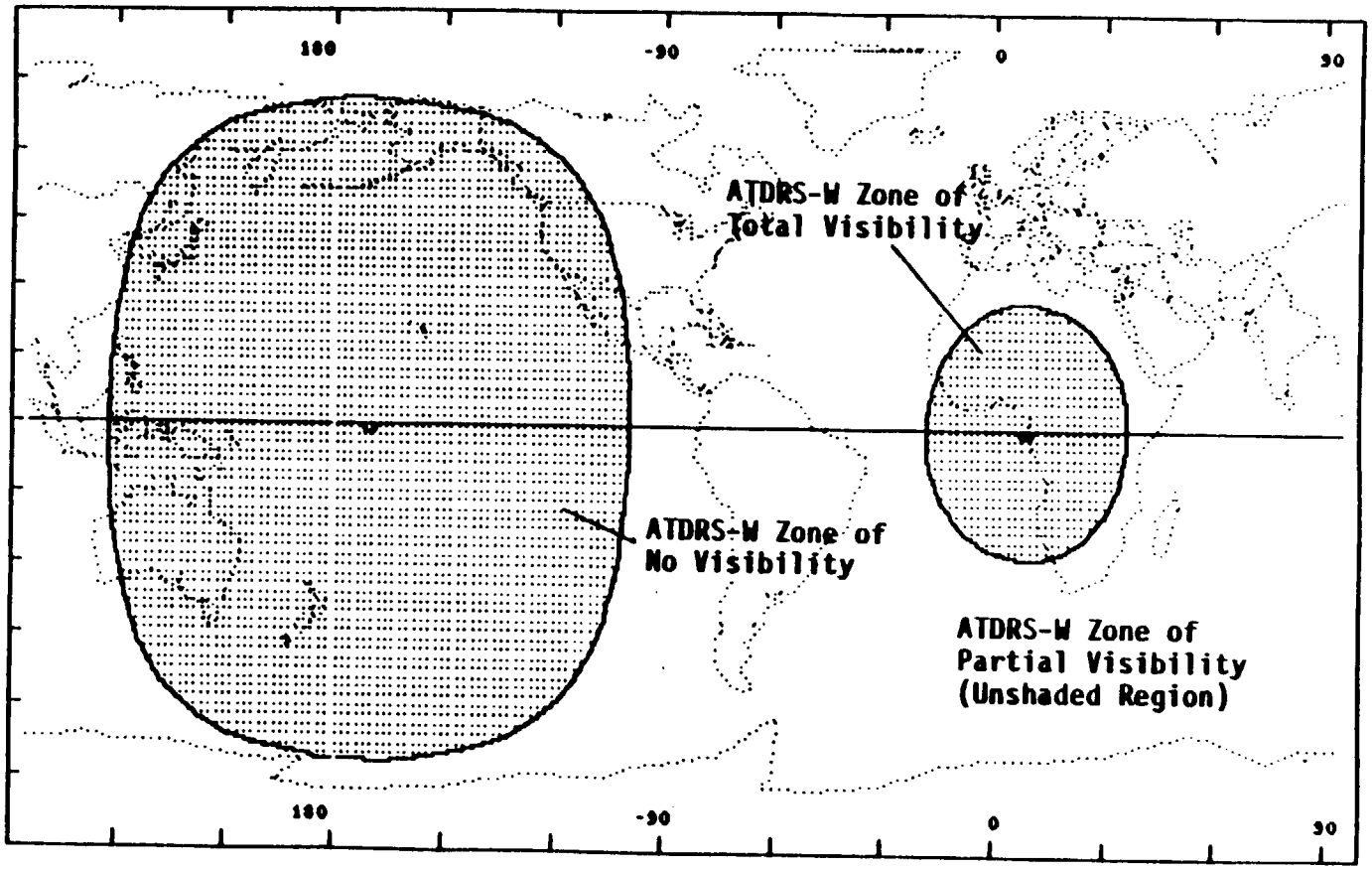

Figure 6-17. ATDRS-W Direct Differential ATDRS/GPS Tracking System Visibility Zones

and the ground station. Table 6-5 shows the probability of this simultaneity event occurring for potential CONUS and American territory ground station sites for the ATDRS-E and ATDRS-W ATDRS/GPS annular visibility regions. GWM lies within the zone of total visibility for the ATDRS-E/GPS annular visibility region and for 43 percent of the time is capable of observing two or more GPS satellites simultaneously with ATDRS-W's observation of those satellites. The remaining station locations associated with ATDRS-E, however, are outside the zone of total visibility and are only capable of observing two GPS satellites simultaneously with the ATDRS-E for 41 percent of the time or less. Puerto Rico is in the zone of partial visibility for ATDRS-W and represents the closest US territory to the zone of total visibility. This location, however, is capable of observing two or more GPS satellites simultaneously with the ATDRS-W for only 2 percent of the time. A CONUS-based site such as MIL is the next nearest to the zone of total visibility, but this location (and any other CONUS-based site) can observe two GPS satellites simultaneously with the ATDRS-W for less than 1 percent of the time.

6.4.2 DIRECT DIFFERENTIAL ATDRS/GPS TRACKING SYSTEM ASSESSMENT

The Direct Differential ATDRS/GPS Tracking System has inherent weaknesses due to the limited availability of observations when the ground stations are constrained to US soil or its territories. Suitable station location sites for the ATDRS-W tracking system are especially lacking. The following sections discuss the tracking network limitations and the impact of reduced visibility in general on OD performance for this tracking system.

6.4.2.1 Tracking Network Limitations

The CONUS and territorial station location constraints discussed in Section 6.4.1.2.3 form the most significant limitations for direct differential tracking of ATDRS. No CONUS-based ground stations meet the optimum visibility requirements for an ATDRS-E or ATDRS-W Direct Differential ATDRS/GPS Tracking System. Alternatively, ground stations might be located on American territory outside CONUS. Station locations for ATDRS-E are ideally located in the western Pacific, possibly using stations located in GWM, AMS, or the Micronesian Islands to provide optimum to near-optimum visibility. Ideal ground station locations on American territory for ATDRS-W, however, do not exist.

Table 6-5. Probability of a Ground Station Observing at Least Two GPS Satellites Simultaneously in an ATDRS/GPS Annular Visibility Region

STATION LOCATION	ATDRS/GPS ANNULAR VISIBILITY REGION	PROBABILITY (%)
GUAM	ATDRS-E	43
WAKE ISLAND	ATDRS-E	41
AMERICAN SAMOA	ATDRS-E	37
HAWAII	ATDRS-E	7
PUERTO RICO	ATDRS-W	2
MERRITT ISLAND, FL	ATDRS-W	<1

MIS69L

Although limited partial joint ATDRS/GPS visibility is possible from Puerto Rico and the eastern portion of the United States, the frequency of dual GPS sightings from stations within these regions is small enough to make use of these ground stations impractical.

6.4.2.2 Direct Differential ATDRS OD Performance

The previous discussion on the geometrical constraints of the station location points out the limited visibility opportunities for this particular type of ATDRS/GPS tracking system. At best, GPS satellite pairs are observable in the total visibility region only 43 percent of the time. The smaller the GPS satellite observation time by the space and ground elements of the direct differential tracking system, the greater the overall error in the results of the OD process. Independent research (Reference 6-8) has shown that direct differential GPS tracking systems are best suited for satellites with altitudes between 6,000 and 10,000 km. Above 10,000 km, the visibility limitations are severe enough to drive the errors in the OD process to relatively high levels compared to passive differential GPS tracking systems discussed in Section 6.3. At geosynchronous altitude, the direct differential OD errors can reach an order of magnitude more than those obtained by passive differential GPS tracking systems due to the visibility constraints placed on the observation process.

6.4.2.3 Conclusion

The tracking network limitations due to visibility and the corresponding impact on ATDRS OD as discussed here are seen as significant cause to rule out further consideration of the Direct Differential ATDRS/GPS Tracking System.

SECTION 7 - SYSTEM COMPARISONS

This section is intended to be a summary of the evaluations of ATDRS tracking alternatives that were presented in more detail in the previous sections. We divide the tracking systems into two general types: ranging and interferometric. Slant range and often range-rate between a ground tracking station and the ATDRS are the observables used by the ranging systems. Interferometry systems use a range difference from two ground stations as its observable. Key elements of these systems are reviewed in the following, including staffing, impacts on other elements of the ATDRS (present or planned) and its operations, and technological risks. The ATDRS tracking systems considered are:

- Ranging systems
  - Two-way systems
    - -- Bilateration Ranging Transponder System (BRTS)
    - -- ATDRS Ku-Band Ranging System (AKuRS)
    - -- Modified Precise Ranging and Timing System (MPRTS)
  - One-way system
    - -- Precise Ranging and Timing System (PRTS)
  - Global Positioning System (GPS) based
    - -- Direct ATDRS/GPS Tracking System (GPS-D)
    - -- Passive Differential ATDRS/GPS Tracking System (GPS-PD)
    - -- Direct Differential ATDRS/GPS Tracking System (GPS-DD)
- Interferometric systems
  - Quasar calibrated
    - -- Quasar-calibrated connected element interferometry (CEI-Q)

-- Quasar-calibrated very long baseline interferometry (VLBI-Q)

- Multiple ATDRS calibrated

  -- Two-satellite VLBI (VLBI-2S)
  -- Three-satellite VLBI (VLBI-3S)
  -- Ku-band beacon VLBI (VLBI-Ku)

- GPS calibrated

  -- GPS Time Transfer Calibrated VLBI (VLBI-GT)

  -- Coded GPS Calibrated VLBI (VLBI-GC)

  -- Hybrid GPS Calibrated VLBI (VLBI-GH)

7.1 KEY SYSTEM ELEMENTS

The key elements for the ranging systems are as follows:

- BRTS

  - One central site and one remote site for each ATDRS

  - Currently the operational system used for tracking TDRS with remote stations at AUS and ACN

  - Scheduled S-band two-way range and range-rate

  - Remote sites use transponders with crystal oscillators

- AKuRS

  Same as BRTS, except:

  - Unscheduled Ku-band beacon and dedicated return channel are used

  - Ku-band rather than S-band is used, thus minimizing ionosphere effects

  - For each ATDRS there are one central and two remote stations

- There are three network options: CONUS, intermediate baseline (i.e., one offshore site), and long baseline (i.e., global)

- PRTS
  - S-band navigation beacon for user and ATDRS navigation with PRTS signal structure
  - One-way pseudorange and pseudorange-rate measurements using 1-meter antennas
  - PRTS signal structure processing at remote sites corrects for ionospheric effects
  - For each ATDRS there are one central and two remote stations, each using cesium beam clocks
  - Three network options: CONUS, intermediate baseline (i.e., one offshore site), and long baseline (i.e., global).
  - Low data rate return communications via ATDRSS scheduled or dedicated channel for network synchronization

- MPRTS
  - Same as PRTS, except:
    -- Two-way rather than one-way measurements are used with no remote timekeeping

- GPS-D
  - Onboard GPS receiver observes coded GPS ranging signal to obtain pseudorange and pseudorange-rate
  - Limited visibility of GPS satellites (when within GPS transmitter footprint and not blocked by the Earth)
  - Has advantages of long baselines and little or no atmospheric errors

- GPS-PD

  - Simultaneous pseudorange and pseudorange-rate measurements of the ATDRS and all visible GPS satellites are taken at Master Station and two Remote Stations

  - Pseudorange to ATDRS is measured using navigation beacon signal (PRTS, S-band, or Ku-band signal)

  - Pseudoranges to the ATDRS and to a single GPS satellite are differenced at each station to remove station clock errors

  - The Master Station range difference is again differenced with each Remote Station range difference to provide input for OD solution at the FDF

- GPS-DD

  - Simultaneous pseudorange and pseudorange-rate measurements of two GPS satellites are taken by GPS receivers at the Master Station, two Remote Stations, and the ATDRS

  - GPS pseudorange and pseudorange-rate differences are computed at each receiver and transmitted to the FDF for orbit determination

  - Differencing technique eliminates clock bias errors

The key elements for the interferometric systems are as follows:

- CEI-Q

  - Separate CONUS networks comprising three stations for each ATDRS

  - Ku-band SGL is passively observed but not interpreted using 2-meter antennas

  - Quasar signals are observed for cesium clock calibration using 12-meter antennas at each station

- Cross-correlation processing onsite allows low data rate transfer requirements to AGT

- VLBI-Q

  - Three CONUS-based stations tracking each of ATDRS-E and ATDRS-W within each SGL footprint with two stations in common

  - Ku-band SGL is passively observed but not decoded using 2-meter antennas

  - Quasar signals are observed for hydrogen maser clock and atmosphere calibration using 12-meter antennas at each station

  - High data rate transfer to support centralized cross-correlation processing

- VLBI-2S

  Same as VLBI-Q except

  - Observation of some other Ku-band transmitting satellite (e.g., ATDRS-C) rather than quasar for calibration of station clocks

  - Moderate data rate transfer to support centralized cross-correlation processing

- VLBI-3S

  Same as VLBI-2S except

  - All three satellite orbits are determined in a single solution

- VLBI-Ku

  Same as VLBI-2S except

  - A hypothetical Ku-band beacon of sufficient bandwidth is observed by a set of three stations that have baselines longer than for VLBI-2S

- VLBI-GT

  Same as VLBI-2S except

  - Time synchronization among the stations is achieved by time transfer from the GPS satellite constellation
  - Second satellite is not observed

- VLBI-GH

  - VLBI observation of ATDRS-E and ATDRS-W is the same as for VLBI-2S
  - Interferometric phase tracking of full 24 satellite GPS constellation provides data for calibration of clocks and atmosphere
  - Initial phase ambiguity is set by group delay measurement

- VLBI-GC

  - VLBI observation of ATDRS-E and ATDRS-W is the same as for VLBI-2S
  - GPS 24 satellite constellation is tracked using range differences, provides data for calibration of clocks and atmosphere measured from decoding of GPS broadcast ranging signals

7.2 OVERVIEW OF ERROR ANALYSIS TECHNIQUE

The orbit analysis (ORAN) computer program was used to evaluate the orbit determination and trajectory recovery performance of the proposed ATDRS tracking systems discussed in this study. Figure 7-1 illustrates this process. The tracking configuration, spacecraft epoch, orbit state, error sources, and solution type are prepared in ORAN input format. Each scenario uses a unique ORAN computer run that simulates the tracking system measurements and computes the errors in orbit state and other relevant parameters that would result if the ATDRS were actually tracked and its orbit determined. The results (in abbreviated form) are presented later in this chapter and in more complete detail in Appendix A.

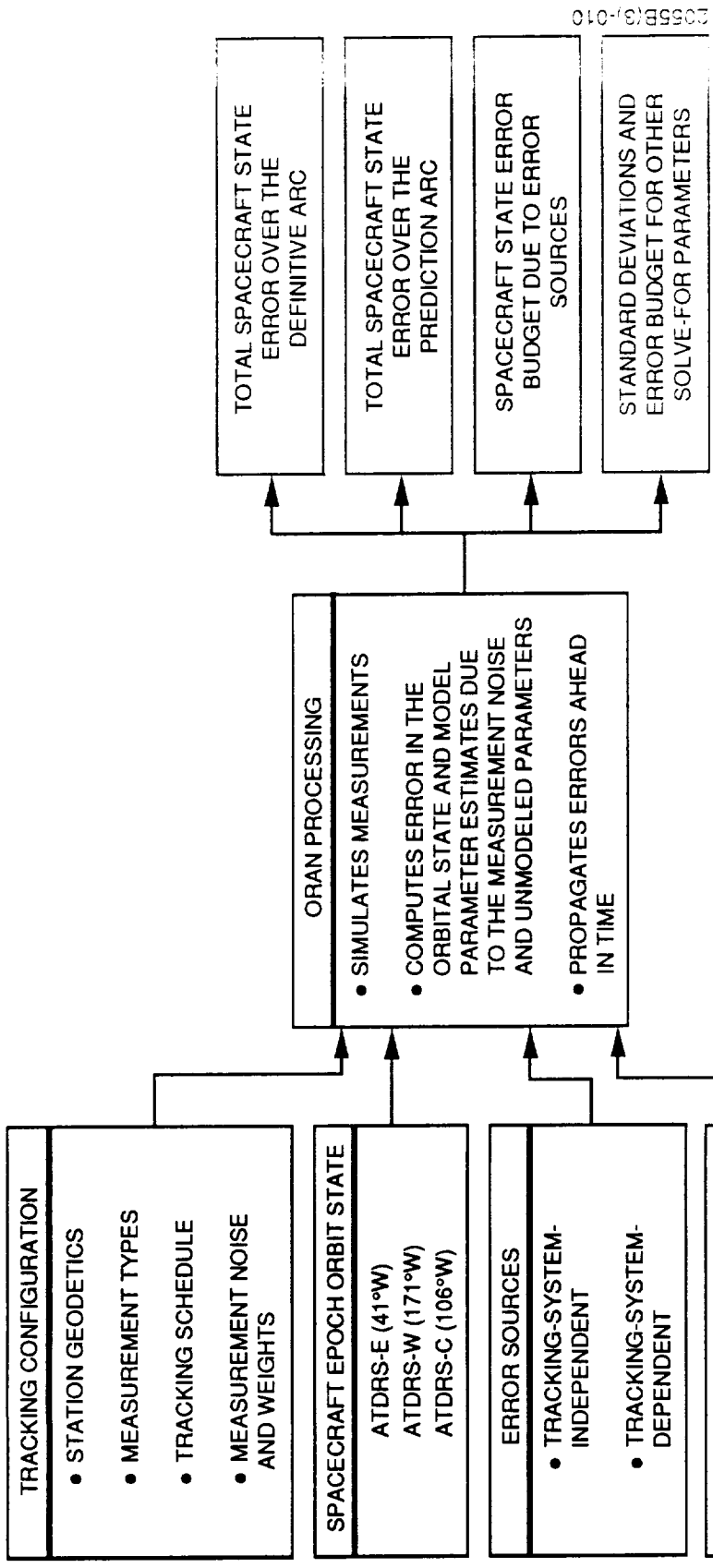

Figure 7-1. OD Performance for the Proposed ATDRSS Ranging Systems

The actual values used for the errors in the ORAN simulations are displayed in Tables 7-1 through 7-3. Errors that were common throughout the study for all tracking systems are shown in Table 7-1. Those errors that were specific to individual tracking systems are found in Table 7-2, except for clock errors, which are displayed in Table 7-3.

7.3 ATDRS TRACKING SCENARIOS

The positions of orbiting satellites are inferred from measurements such as range, range-rate, or angles. In the ideal world of perfectly accurate measurements, a very few measurements would be sufficient to determine an orbit. However, even relatively small measurement errors can make it necessary to use favorable observing geometry and/or measurement arcs of sufficient duration (which allows constraint by the laws of orbital mechanics).

Previous experience indicates that tracking data beyond 24 hours for a geosynchronous satellite such as ATDRS yields diminishing returns in terms of OD accuracy. Operationally, OD for the present generation of TDRS satellites is performed using 30-hour arcs every 24 hours. The day-to-day overlap allows for isolation of bad data and inaccurate OD results and avoids discontinuities in computed orbits. Therefore, for the normal case of the ATDRS unaffected by maneuvers, 30-hour OD periods were chosen for this study.

Eventually, geosynchronous satellites drift from their assigned positions. When this occurs for the ATDRS, small onboard thrusters will be used to nudge it back toward its assigned location. During and immediately after such maneuvers, the uncertainty in the satellite position grows due to inevitable thrust modeling errors. Because user satellites may depend on continuous tracking by ATDRS, a new OD solution needs to be made as quickly as possible after the maneuver. Henceforth, OD after such a maneuver will be termed trajectory recovery, or TR, which by convention can use tracking data of durations of up to 2 hours. Performance for a TR scenario is another criterion for judging the various tracking systems.

Accurate ATDRS ephemeris prediction information will, in some cases, need to be provided to user satellites for real-time onboard data processing. Orbit-prediction simulations were performed for up to 72 hours after OD or TR definitive periods. The performance of the tracking alternatives for orbit prediction is also considered as a standard of comparison in this study.

Table 7-1. Force Model and Measurement-Independent Errors

MODEL PARAMETER	UNCERTAINTY (3 σ)
GM	6×10^{-8} (FRACTIONAL ERROR)
GEOPOTENTIAL COEFFICIENTS	135 PERCENT OF (GEM-10 – GEM-7)
C_R	2 PERCENT
POLAR MOTION X	0.015 ARCSECOND
POLAR MOTION Y	0.015 ARCSECOND
A1 – UT1	0.09 ARCSECOND

2055B(3)-011

Table 7-2. Tracking System Dependent Errors (1 of 2)

SYSTEM	MEASUREMENT NOISE*		INSTRUMENT BIASES		STATION POSITION ERRORS		TROPOSPHERE/IONOSPHERE ERRORS	
	RANGE (RANGE DIFFERENCE) ERROR (3σ) (meters)	RANGE-RATE ERROR (3σ) (mm/second)	RANGE (RANGE DIFFERENCE) ERROR (3σ) (meters)	RANGE-RATE ERROR (3σ) (mm/second)	NETWORK ERROR (3σ) (meters)	BASELINE ERROR (3σ) (mm/second)	TROPOSPHERE ERROR (3σ) (percent)	IONOSPHERE ERROR (3σ) (percent)
BRTS	10	0.13	12.0 (MASTER STATION) 6.0 (REMOTE STATION)	NONE	0.75 E, N, V	N/A	4.5	100
PRTS	1.5 (FORWARD) 7.5 (RETURN)	1.31 (FORWARD) (NOT MODELLED)	3.0 (FORWARD) 6.0 (RETURN)	NONE	0.75 E, N, V	N/A	4.5	0
AKuRS	4.0	0.15	12.0 (MASTER STATION) 6.0 (REMOTE STATION)	NONE	0.75 E, N, V	N/A	4.5	100 (14 GHz)
MPRTS	2.2	0.75	12.0 (MASTER STATION) 6.0 (REMOTE STATION)	NONE	0.75 E, N, V	N/A	4.5	0
VLBI-Q	0.073	–	NONE	–	0.75 ECF x, y, z	0.06 (E, N) 0.24 (V)	2	12
CEI-Q	0.014 - 0.020	–	NONE	–	0.75 ECF x, y, z	0.06 (E, N, V)	0.003 - 0.036	0.006 - 0.0012
VLBI-2S (VLBI-3S)	0.05 - 0.07	–	NONE	–	0.75 ECF x, y, z	0.08-0.18 (E, N) 0.23-0.56 (V)	4.5	100
ATDRS GT RANGING	1.0	–	3.0	–	0.75 E, N, V	N/A	6	100

2055B(3)-012

* INCLUDES THERMAL NOISE AND TROPOSPHERIC AND IONOSPHERIC TURBULENCE

NOTES: E, N, V = EAST, NORTH, VERTICAL TOPOCENTRIC COORDINATES
ECF = EARTH-CENTERED, FIXED COORDINATES

Table 7-2. Tracking System Dependent Errors (2 of 2)

SYSTEM	MEASUREMENT NOISE*		INSTRUMENT BIASES		STATION POSITION ERRORS		TROPOSPHERE/IONOSPHERE ERRORS	
	RANGE (RANGE DIFFERENCE) ERROR (3σ) (meters)	RANGE-RATE ERROR (3σ) (mm/second)	RANGE (RANGE DIFFERENCE) ERROR (3σ) (meters)	RANGE-RATE ERROR (3σ) (mm/second)	NETWORK ERROR (3σ) (meters)	BASELINE ERROR (3σ) (mm/second)	TROPOSPHERE ERROR (3σ) (percent)	IONOSPHERE ERROR (3σ) (percent)
GPS-D	9.0	10.5	13.4	1.5	0.75 E, N, V	N/A	0	0
GPS-PD ATDRS S-BAND PRTS Ku-BAND GPS	 4.4 1.5 8.8 9.0	 0.75 1.31 0.30 10.5	 9.0 9.0 9.0 13.4	 0 0 0 1.5	 0.75 E, N, V 0.75 E, N, V 0.75 E, N, V 0.75 E, N, V	 N/A N/A N/A N/A	 4.5 4.5 4.5 0	 0 0 0 0
VLBI-Ku	0.1	–	NONE	–	0.75 ECF x, y, z	0.06 (E, N) 0.24 (V)	4.5	100
VLBI-GC ATDRS GPS	0.05 - 0.07 0.05	– –	NONE 0.15	– –	0.75 ECF x, y, z	0.08-0.18 (E, N) 0.23-0.56 (V)	4.5	100
VLBI-GH ATDRS GPS	0.05 - 0.07 0.09	– –	NONE 0.09	– –	0.75 ECF x, y, z	0.08-0.18 (E, N) 0.23-0.56 (V)	4.5	100
VLBI-GT (ATDRS)	0.05 - 0.07	–	NONE	–	0.75 ECF x, y, z	0.08-0.18 (E, N) 0.23-0.56 (V)	4.5	100

* INCLUDES THERMAL NOISE AND TROPOSPHERIC AND IONOSPHERIC TURBULENCE

NOTES: E, N, V = EAST, NORTH, VERTICAL TOPOCENTRIC COORDINATES
ECF = EARTH-CENTERED, FIXED COORDINATES

2055B/3-013

Table 7-3. Clock Errors Model

$$\Delta t = a_0 + a_1 t + a_2 t^2$$

WHERE Δt = CLOCK ERROR
t = CLOCK TIME
a_0 , a_1 , a_2 = CLOCK COEFFICIENTS (SEE TABLE BELOW)

SYSTEM	CLOCK COEFFICIENTS		
	a_0	a_1	a_2
BRTS[b]	0	0	0
PRTS[a]	ESTIMATED	0	0
AKuRS[b]	0	0	0
MPRTS[b]	0	0	0
VLBI-Q	45 mm (150 ps)	0	0
CEI-Q	0.3 mm (1 ps)	0	0
VLBI-2S	ESTIMATED	ESTIMATED	ESTIMATED
VLBI-3S	ESTIMATED	ESTIMATED	ESTIMATED
VLBI-Ku	ESTIMATED	ESTIMATED	ESTIMATED
VLBI-GC	ESTIMATED	ESTIMATED	ESTIMATED
VLBI-GH	ESTIMATED	ESTIMATED	ESTIMATED
VLBI-GT	89 cm (3ns)	0	0
–			
GPS-D	ESTIMATED/10 m	0	0
GPS-PD	0	0	0
GPS-DD			

2055B(3)-014

[a] PRTS FREQUENCY SYNCHRONIZATION ELIMINATES THE a_1 , a_2 CLOCK ERRORS.

[b] NO CLOCK SYNCHRONIZATION ERROR WITH TWO-WAY MEASUREMENTS.

7.4 SYSTEM PERFORMANCE

One goal of ATDRSS is to track other satellites and to provide the means for user satellites to establish their own position. The determination of the position of other satellites depends on accurate knowledge of ATDRS orbits, the primary figure of merit for this study. The goal is to provide 3-σ ATDRS position errors of less than 75 m under several different tracking scenarios. Statistically, this means that the ATDRS position will be known to within 75 m more than 99 percent of the time.

7.4.1 DEFINITIVE PERIOD PERFORMANCE

This section summarizes the results of the OD error-analysis simulations over the tracking arc. Detailed results are presented in Appendix A. Tracking accuracy is evaluated using two definitive periods, 30 hours (OD) and 2 hours (TR), relative to the study goal of 75-m accuracy (3 σ).

Results for definitive period for both OD and TR tracking scenarios for ATDRS-E are presented in the following sections. The corresponding results for ATDRS-W are similar and may be found in Appendix A. Figures 7-2 and 7-3 show the level in bar-chart form of orbit accuracy for each tracking system. The length of each bar represents the total 3-σ OD error including both noise and systematic effects. Also displayed is largest error source and its level. The corresponding accuracies computed for the BRTS system on the present TDRS-E are also included.

Two of the GPS-based ranging systems were not included in the results. GPS-PD was not included because of ORAN's inability to model the system adequately without major program code revision. The GPS-DD system was not included because it was determined before ORAN simulations were run that the limited visibility of GPS satellite pairs resulted in this system being inadequate for satellite tracking. The VLBI-3S system results were included rather than those for VLBI-2S, because the former performed better and they differed only in solution method.

7.4.1.1 Orbit Determination Scenario

OD definitive period tracking results for the various tracking systems on ATDRS-E are displayed in Figure 7-2. The corresponding results in most cases for ATDRS-W are similar to these. The length of each bar represents the total 3-σ OD error, including both noise and unmodeled effects. Also displayed is the largest error source for

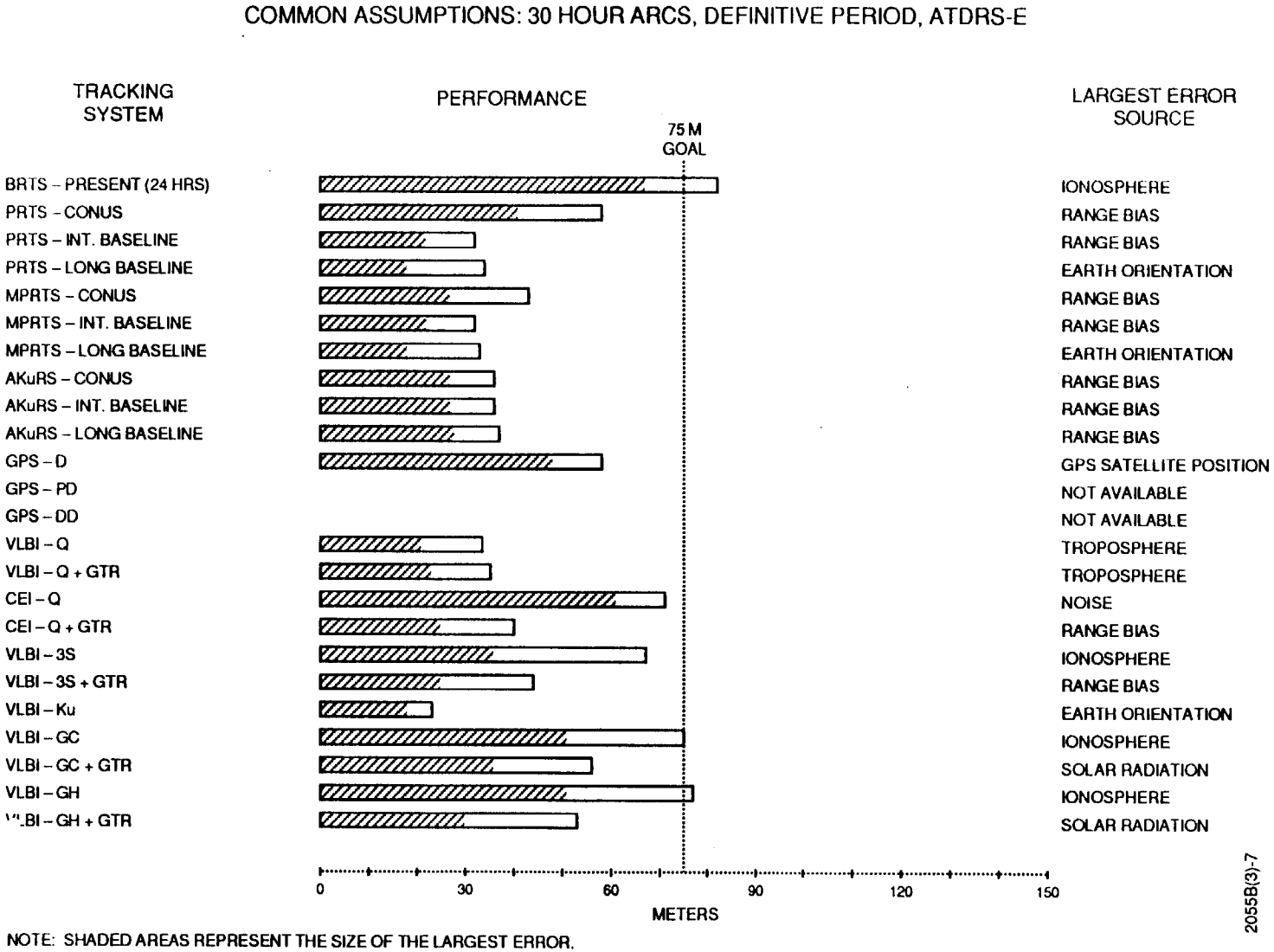

Figure 7-2. OD Performance for the ATDRSS Tracking Systems

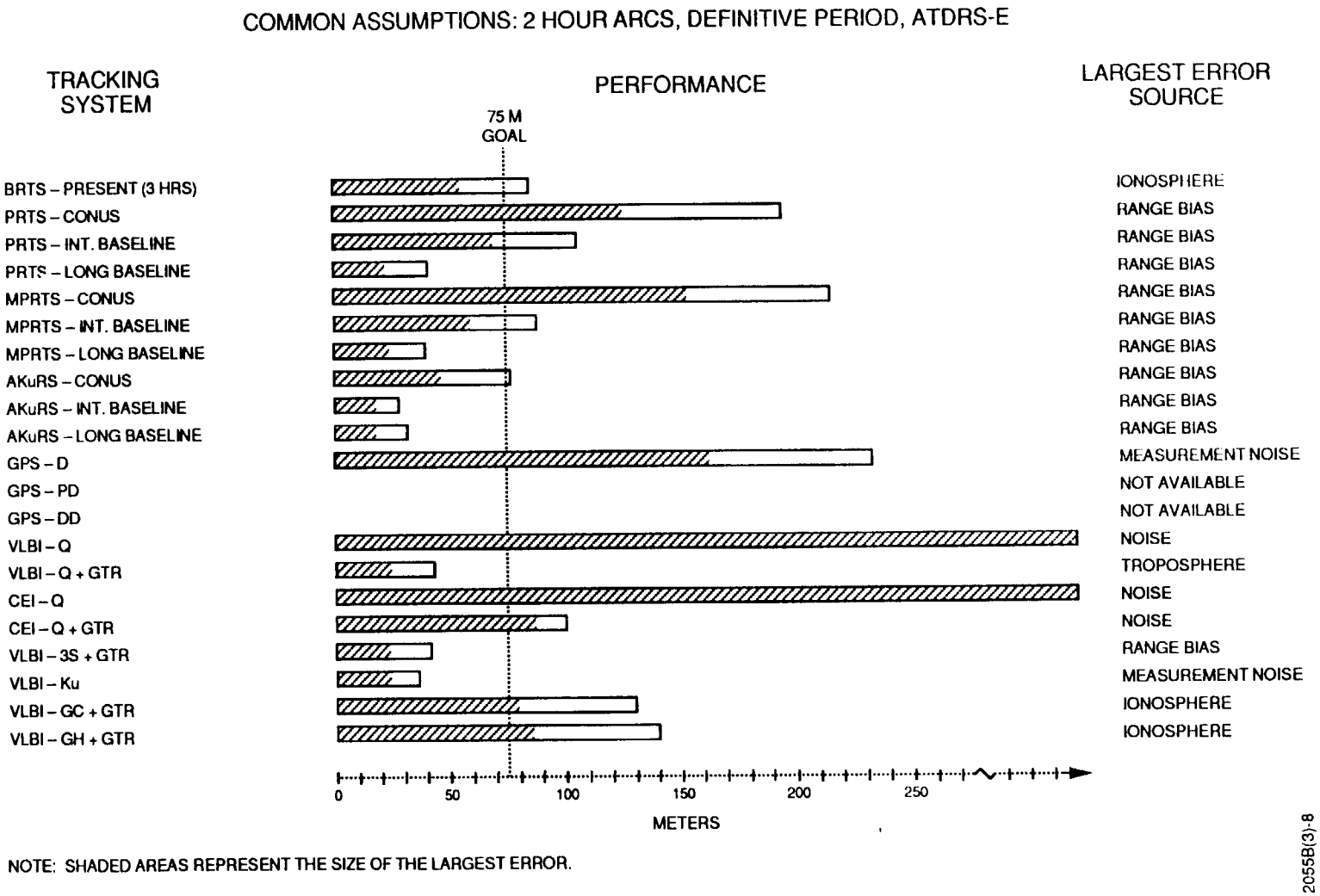

Figure 7-3. TR Performance for the ATDRSS Tracking Systems

each case and its value as the hatched area within the bar. In addition to the proposed tracking systems investigated in this report, information on the performance of the currently operational BRTS is included.

The results show that nearly all of the tracking systems studied meet the 75-meter performance goal in the definitive period in the OD scenario. Exceptions to this include the present BRTS system and the following interferometric systems without benefit of GTR to White Sands: VLBI-GT, VLBI-GC, VLBI-GH, CEI-Q. (Although the performance of the latter two of these systems was barely adequate for ATDRS-E, it was not for ATDRS-W.) Using an optimistic model for GTR to White Sands, the latter three systems meet the tracking goal. The performance of VLBI-GT was so inadequate that ORAN studies of it were not continued to deal with other scenarios.

Notably, without exception, all of the basing options of PRTS, MPRTS, and AKuRS track the ATDRS to less than 45 meters, 3 σ. The best performance was given by VLBI-Ku, undoubtedly due to the fact that it has longer baseline lengths than VLBI-3S.

7.4.1.2 Trajectory Recovery Scenario

Our TR simulations show that the present BRTS system cannot meet the study goal, although its level of performance degradation from the OD scenario relative to the other systems in this study is quite good.

Among the ranging systems (PRTS, MPRTS, and AKuRS), only those that are based outside CONUS meet the tracking goal, although AKuRS nearly does so. For both intermediate and long baseline lengths, these systems easily meet the goal with the exception of intermediate baseline MPRTS.

Among the interferometry systems, VLBI-Q and VLBI-3S can meet the study goal for definitive period TR if and only if GTR to White Sands is used. The VLBI-Ku system can meet the goal without GTR. No other interferometric system can track to 75 meters, 3 σ.

7.5 PREDICTIVE PERIOD PERFORMANCE

The durations of accurate orbit prediction after the definitive period are listed in Table 7-4. Predictions were calculated up to 72 hours in the simulations; when accurate predictions extended beyond this time, the duration is indicated by ">72".

Table 7-4. Duration of ATDRS-E Accurate Orbit Prediction

TRACKING SYSTEM	TIME* (HOURS)	
	AFTER ORBIT DETERMINATION (30 HOURS OF TRACKING)	AFTER TRAJECTORY RECOVERY (2 HOURS OF TRACKING)
BRTS	0	0
PRTS (CONUS BASELINE)	> 72	0
PRTS (INTERMEDIATE BASELINE)	52	0
PRTS (LONG BASELINE)	45	31
MPRTS (CONUS BASELINE)	> 72	0
MPRTS (INTERMEDIATE BASELINE)	53	0
MPRTS (LONG BASELINE)	46	34
AKuRS (CONUS BASELINE)	> 72	4
AKuRS (INTERMEDIATE BASELINE)	> 72	17
AKuRS (LONG BASELINE)	> 72	67
GPS-D	23	0
GPS-PD	N.A.	
GPS-DD	N.A.	
VLBI-Q	> 72	0
VLBI-Q + GTR	> 72	8
CEI-Q	2	0
CEI-Q + GTR	> 72	0
VLBI-3S	54	0
VLBI-3S + GTR	> 72	8
VLBI-Ku	> 72	4
VLBI-GH + GTR	43	0
VLBI-GC + GTR	22	0

*THE TIMES LISTED INDICATE THE AMOUNT OF TIME FOR WHICH A TRACKING ACCURACY OF ≤ 75 METERS IS MAINTAINED.

2055B(3)-016

The BRTS system again cannot meet the study goal for the predictive period for either the OD or TR scenarios. This result is expected since BRTS does not meet the same goal in the definitive period.

Among the ranging system alternatives, the AKuRS system provided the best performance. For the long baseline case it met the study goal of 3-day predicts after OD and 1-day predicts after TR. For the CONUS and intermediate baseline cases, prediction after OD exceeded 3 days but predictions after TR fell short of the 1-day goal. PRTS and MPRTS had very similar results. The long baseline cases satisfied the study goal for TR but not OD. The CONUS and intermediate baseline cases met the 3-day goal for OD but not the 1-day goal for TR. The GPS-D system does not meet the study goal for OD or TR.

The VLBI-Q tracking system met the study goal for prediction after OD without the benefit of GTR but not after TR. If GTR is used, the goal is also met by VLBI-3S and CEI-Q after OD. In no scenario using interferometry is the 1-day goal for predictions after TR met. None of the GPS calibrated interferometry systems (i.e., VLBI-GC, VLBI-GH, or VLBI-GT) met the study goals for OD or TR.

7.6 ATDRSS IMPACTS OF THE PROPOSED TRACKING SYSTEMS

This section discusses the impact of each tracking system on the ATDRSS ground segment, space segment, and operations. What follows is summarized in Table 7-5.

7.6.1 GROUND SEGMENT

PRTS and MPRTS affect the ATDRSS ground segment in several ways. First, the PRTS signals must be put on the ATDRS beacon uplink. Second, the PRTS signal structure must be processed to yield the range and range-rate observables received at the remote stations from the navigation beacon. For the PRTS system only, processing of the PRTS one-way range return signal must be supported at the AGT. This is not required for MPRTS because it uses a two-way range, as does BRTS.

The AKuRS tracking approach requires that the reception and coherent turnaround of the Ku-band beacon signal be supported by the ground network. In addition, extraction of remote tropospheric conditions will be required at the AGT.

Table 7-5. Impacts on ATDRSS

SYSTEM	GROUND SEGMENT	SPACE SEGMENT	SCHEDULING	DATA STALENESS
PRTS AND MPRTS	GENERATION AND UPLINK OF ATDRS BEACON SIGNALS CALIBRATION OF SIGNAL DELAYS	PRTS SIGNAL STRUCTURE SUPPORTED ON S-BAND NAVIGATION BEACON FREQUENCY REALLOCATION TO SUPPORT DEDICATED CHANNELS CALIBRATION OF ONBOARD SIGNAL DELAYS DEDICATED RETURN CHANNEL	OPTIONAL USE OF THE NONDEDICATED RETURN CHANNEL WOULD REQUIRE SCHEDULING	NONE
AKuRS	SUPPORT FOR GENERATION AND RECEPTION OF Ku-BAND BEACON CALIBRATION OF SIGNAL DELAYS	Ku-BAND NAVIGATION BEACON CALIBRATION OF ONBOARD SIGNAL DELAYS DEDICATED Ku-BAND RETURN CHANNEL	NONE	NONE
VLBI-Q, CEI-Q, VLBI-2S VLBI-3S VLBI-GC VLBI-GH VLBI-GT	SUPPLEMENTARY AGT RADIAL RANGING	GT TT&C RANGING MAY BE INADEQUATE, THUS REQUIRING A NEW AND MORE ACCURATE SYSTEM	AGT RANGING REQUIRES SCHEDULING AT A FREQUENCY DEPENDING ON THE TYPE OF SYSTEM USED	VLBI-Q = 10 MINUTES CEI-Q = 3.5 MINUTES VLBI-3S = 7 MINUTES VLBI-GC = 7 MINUTES VLBI-GH = 7 MINUTES VLBI-GT = 7 MINUTES
VLBI-Ku	NONE (EXCEPT IF BEACON IS TO BE USED FOR UNRELATED NAVIGATION PURPOSES)	Ku-BAND NAVIGATION BEACON OF SUFFICIENT BANDWIDTH	NONE	7 MINUTES
GPS-D	NONE	GPS RECEIVER ADDED TO ATDRS	NONE	NONE
GPS-PD	SUPPORT FOR GENERATION AND RECEPTION OF BEACON CALIBRATION OF SIGNAL DELAYS	ONE-WAY NAVIGATION BEACON SUPPORT FREQUENCY REALLOCATION (IF PRTS-LIKE) CALIBRATION OF SIGNAL DELAYS DEDICATED RETURN CHANNEL	NONE	NONE
GPS-DD	NONE	GPS RECEIVER ADDED TO ATDRS	NONE	NONE

2055B(3)-015

There are no ground segment impacts of the GPS-D or the GPS-DD tracking systems. The GPS-PD system can have impacts on the ATDRSS ground segment depending on which type of one-way navigation beacon is used. In the case of use of the current ATDRSS navigation S-band beacon, there is no further impact. If the PRTS style signal structure is used on the beacon, the PRTS ground segment impacts apply here. If a Ku-band navigation beacon is used to support VLBI-Ku, the impacts given above apply.

Interferometric tracking will require GTR data from the White Sands GT at a rate required by the particular interferometric tracking system used. If the present TDRS GTR system proves to be not sufficiently accurate, an improved ranging system will have to be implemented.

7.6.2 SPACE SEGMENT

For AKuRS, a Ku-band navigation beacon is required. For PRTS and MPRTS, the S-band navigation beacon that supports the PRTS signal structure is required. The onboard signal delays would be calibrated dynamically on the satellite or before flight, on the ground. In the present design, the return channels are dedicated. For PRTS and MPRTS, a nondedicated return channel might be used to reduce costs. New frequency allocation or reorganization of existing bands may be required to support the dedicated channels without interfering with other planned ATDRSS services.

For the GPS-D and GPS-DD systems, a GPS receiver similar to those used on the ground would have to be added to the ATDRS design. As for the ground segment, the impacts of the GPS-PD system depend on the type of navigation beacon that is chosen. If the baseline S-band beacon is used, there is no impact. If the PRTS style signal structure is used on the S-band beacon, the PRTS space segment impacts apply. If the Ku-band beacon is used, the AKuRS impacts apply.

In concept, interferometry systems are nonintrusive on the space segment. However, orbit-analysis studies have shown that supplementary GTR is at least occasionally required for each interferometric tracking alternative. As described for the ground segment, if the existing TDRS GTR proves inadequate, some other system will be required.

7.6.3 OPERATIONS

Because dedicated forward beacon and return channels are used, there are no particular scheduling requirements for any of the ranging systems. However, if the option of a

nondedicated return channel is chosen for PRTS, MPRTS, or GPS-PD, scheduling of this return will be required. The return link is used for calibration of the remote clocks. The scheduling requirement is not rigorous because the performance of the remote clocks degrades gracefully. Furthermore, because observables are available almost immediately, data staleness for PRTS and MPRTS is not important.

In the case of VLBI-Q and VLBI-3S, the GTR would require scheduling, and this ranging would need only be scheduled immediately after a maneuver. For the other interferometric systems, CEI-Q, VLBI-GC, and VLBI-GH, GTR is needed more or less continuously.

Data staleness can be significant for the interferometric systems. In the case of VLBI-Q, the time delay observable is provided to FDF in 15 minutes, whereas for CEI-Q and VLBI-2S, this time is 6 minutes.

7.7 TRACKING SYSTEM COSTS

The costs of operation of the various tracking alternatives are displayed in Figure 7-4. The total costs shown are subdivided into the initial outlay and the sum of yearly operation and maintenance costs over the 10-year life cycle of the program. Except for MPRTS, PRTS, and AKuRS, the incremental costs to the ATDRSS Ground Terminal or the Flight Dynamics Facility were not included in these estimates. Further, costs of the ranging and interferometric systems were estimated independently, possibly resulting in inconsistencies embedded in the estimates.

The following particular qualifications should be recognized. The PRTS option for water vapor radiometers ($1M), which could enhance tracking performance, was not included in the figures used for the summary bar chart. For the interferometric systems, costs imposed by the use of GTR are also not included.

The least expensive systems studied are the GPS-based ranging systems with the GPS-D system estimated to cost only $8M. The sole cost for this system stem from the addition of a GPS receiver to the ATDRS spacecraft. Among the remaining systems, the least expensive are the multiple satellite interferometric and MPRTS systems, each having about the same total cost of around $35 to $45M.

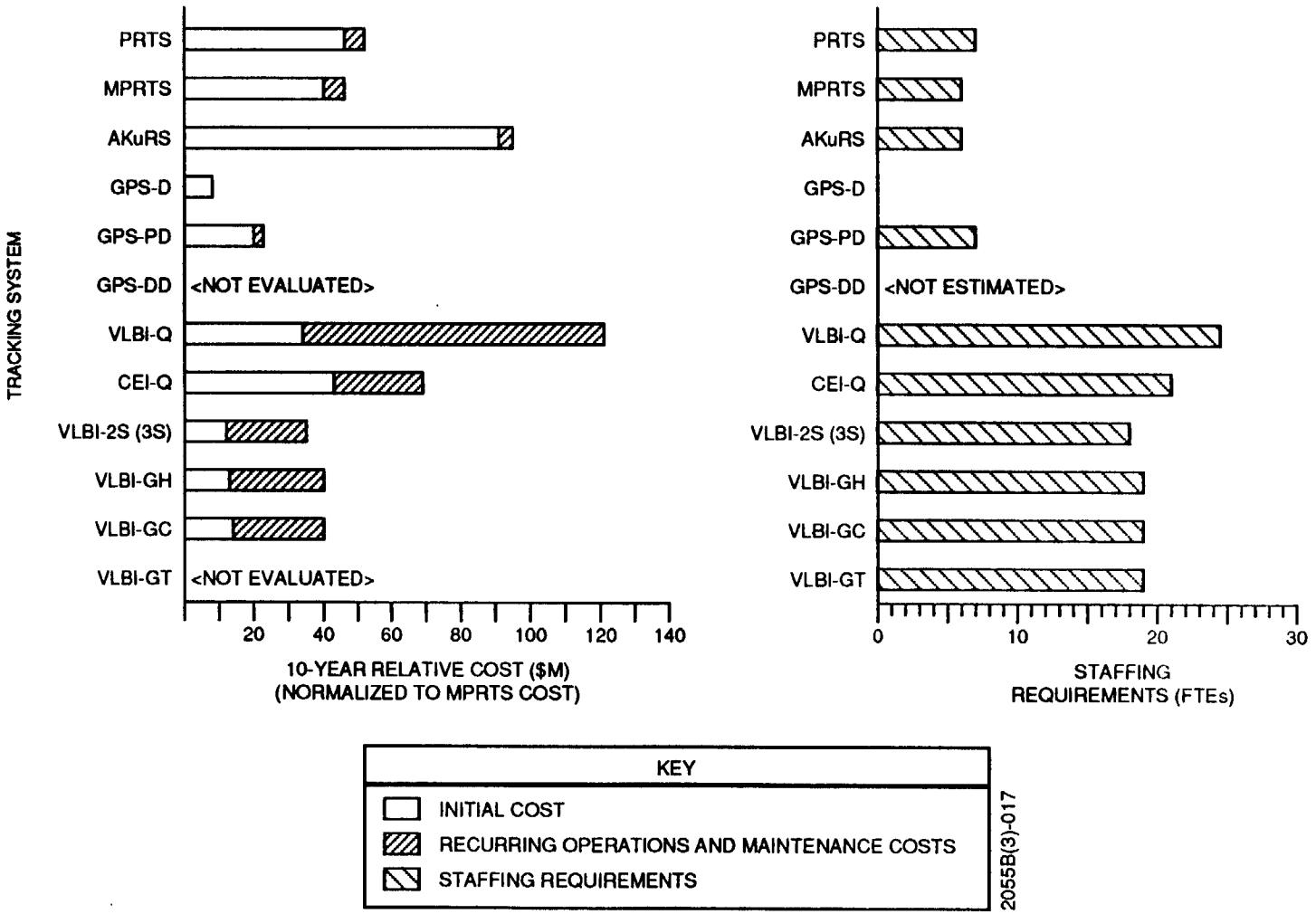

Figure 7-4. Tracking System Cost Comparisons

The quasar-calibrated interferometry systems have large initial costs due to the required 12-meter quasar observing antennas. In general, interferometry systems require a relatively higher level of staffing, resulting in larger yearly continuing costs. The AKuRS system's large initial costs result from full incorporation of the Ku-band beacon on each ATDRS spacecraft not presently in the ATDRS baseline design.

7.8 STAFFING

Total staffing requirements are also displayed in Figure 7-4. Managerial and nontechnical support personnel are not included in these estimates, nor are additional staffing for the AGT or FDF. Interferometric tracking systems considered in this report require three more people for continuing operations and maintenance than the ranging systems.

7.9 TECHNOLOGICAL RISKS

All of the analyses given here use state-of-the-art relative-position determinations for the ground stations in each tracking system. These station-position coordinates are determined either by VLBI-Q techniques outside the scope of ATDRS tracking or through the use of GPS terminals.

Technological risks include use of unproven or innovative hardware or software technology or solution algorithms. For the PRTS technology, the precise tracking technique and implementation have been validated; the processing algorithms to remove the ionospheric effects need further development and verification.

If a different set of station positions is chosen for any of the range/range-rate systems, new orbit analyses will need to be performed to ensure similar tracking accuracy results. This stems from the apparent sensitivity of these systems to station position.

For VLBI and CEI, the basic principles of physics and engineering have already been applied in related fields. Despite the fact that this particular implementation is in some sense unique, the risk seems low because the requirements call only for different combinations of well-established subsystems.

The estimate for tropospheric modeling errors that was used in the error analysis was 3 percent. On extremely overcast or rainy days, this estimate may be exceeded, resulting in less accurate OD performance. In the particular case of

VLBI-3S, adequate performance is achieved only when the troposphere height is solved for as a part of the OD algorithm. This technique needs further study to evaluate its validity and risk properly.

7.10 EXTERNAL SYSTEM DEPENDENCIES

PRTS and MPRTS have only one external dependency. A relatively low-bandwidth Nascom ground link will have to be used as a secondary command link for system reconfiguration. For PRTS, this link will also be used for transfer of timing information and the return of measurements if the dedicated return link is lost.

The VLBI-Q system depends for its success on a data link that can send up to 32 Mbits/sec of data from each of at least three stations to the central processing facility. The duty cycle on this link is 17 percent during normal operations and 50 percent during TR. The data transport requirements for VLBI-3S and the other multiple satellite interferometric systems are for smaller (approximately 30 Mbits per measurement). This amount of data can be cached and sent when convenient at the cost of data staleness. The CEI-Q system is not constrained by data transport requirements.

Ranging from each ATDRS to the AGT is required at some level for all interferometric tracking approaches. The impact of this requirement has not been fully addressed in this report. An a priori ephemeris is required for the CEI-Q system to resolve phase ambiguities encountered while processing the first data from a new orbit.

7.11 TRACKING SYSTEM COMPARISONS: OVERALL SUMMARY

Table 7-6 displays all the principal factors upon which the various tracking alternatives are to be evaluated. The tracking systems are listed in the first column and each tracking system's performance for each criterion is listed in the remaining columns. The criteria include both definitive and predictive OD and TR performance, 10-year cost, and network basing.

The short answer that summarizes the performance of the tracking alternatives examined is that none meets all of the goals set for this study. However, many of these nearly do so.

The AKuRS satisfies every goal except that to do so requires non-CONUS basing. Further, because the Ku-band beacon must be added to the ATDRS design, it is one of the most

Table 7-6. ATDRSS Tracking System Overall Performance

TRACKING SYSTEM	OD PERFORMANCE: 75-METER (3σ) ACCURACY MET		TR PERFORMANCE: 75-METER (3σ) ACCURACY MET		CONUS NETWORK	TOTAL 10-YEAR COST (RELATIVE TO MPRTS)
	DEFINITIVE (30 HOURS)	PREDICTIVE (3 DAYS)	DEFINITIVE (2 HOURS)	PREDICTIVE (1 DAY)		
BRTS	NEARLY[a]	NO	NEARLY[a]	NO	NO	–
AKuRS (CONUS)	YES	YES	NEARLY[a]	NO	YES	2.2
AKuRS (NON-CONUS)	YES	YES	YES	YES	NO	2.2
PRTS (CONUS)	YES	NEARLY[a, b]	NO	NO	YES	1.2
PRTS (NON-CONUS)	YES	NO	YES	YES	NO	1.2
MPRTS (CONUS)	YES	NEARLY[a, b]	NO	NO	YES	1.0
MPRTS (NON-CONUS)	YES	NO	YES	YES	NO	1.0
VLBI-Q	YES	YES	YES	NEARLY[c]	YES	2.8
CEI-Q*	YES	YES	NEARLY[a]	NO	YES	1.6
VLBI-3S*	YES	YES	YES	NEARLY[c]	YES	.80
GPS-D	YES	NO	NO	NO	YES	.18
GPS-PD	–	–	–	–	YES	.52
GPS-DD	–	–	–	–	YES	–
VLBI-Ku	YES	YES	YES	NO	YES	NA
VLBI-GT	NO	–	–	–	YES	.80
VLBI-GC	YES	NEARLY[a]	NEARLY[a]	NO	YES	.92
VLBI-GH	YES	NEARLY[a]	NEARLY[a]	NO	YES	.92

2055B(3)-018

[a] 100-METER (3σ) ACCURACY MET

[b] 75-METER (3σ) ACCURACY OBTAINED FOR A 2-DAY PREDICTION PERIOD

[c] 75-METER (3σ) ACCURACY OBTAINED FOR A 6-HOUR PREDICTION PERIOD

*PERFORMANCE LISTED IS CONTINGENT ON OPTIMISTIC GT RANGING WITH 1-METER NOISE AND 3-METER BIAS

expensive tracking systems studied. The non-CONUS-based PRTS and MPRTS systems can satisfy every study goal if and only if one uses more than one network basing to satisfy the different tracking criteria. Of these two systems, MPRTS seems to be the preferred choice, since it costs 20 percent less. The GPS-D and GPS-DD systems did not perform well in locating the ATDRS. The GPS-PD system could not be simulated due to a lack of time and resources.

Among the interferometric systems, none can meet the goal of 1-day accurate predicts after 2 hours of tracking (TR scenario) even with supplementary ranging (GTR) to the AGT. Of these alternatives, the best performing were the VLBI-Q, VLBI-3S, and VLBI-Ku systems. The least expensive of these is the VLBI-3S system, as VLBI-Q requires large quasar observing antennas and VLBI-Ku requires addition of a Ku-band beacon to the ATDRS.

7.12 CONCLUSION AND RECOMMENDATIONS

In the previous section, it was established that none of the tracking systems studied meets all the goals of the project. This result suggest the following approaches to the ATDRS tracking problem:

- Relax the goals to allow some of these tracking systems to qualify
- Reevaluate and revise error models and/or simulation methods to possibly yield favorable results
- Consider new tracking systems that may provide the required performance

These options are discussed below.

The most obvious goal that could be relaxed is the CONUS basing requirement. In that case, the AKuRS would then meet the requirements, as its tracking performance is acceptable. However, its high cost is a drawback. The MPRTS system with non-CONUS basing comes close to satisfying the remaining study goals. Perhaps a different choice of station positions or additional stations would be sufficient for it to reach an acceptable level of tracking performance.

Another study goal that might be relaxed is the requirement that accurate 1-day predicts are necessary in the trajectory recovery scenario (i.e., 2 hours of tracking). If the predict time period could be relaxed to 6 hours, the VLBI-3S

would meet the study goals. This would also be true of VLBI-Q, but its high cost does not favor it.

Improved simulations may improve the performance of the multiple satellite systems because measurements from three nonindependent baselines could be used in orbit solutions. A new orbit analysis tool would allow the evaluation of the GPS-PD, a system whose performance could not be evaluated using ORAN in its present form.

There are tracking systems that were not considered in this study. Obviously, the GPS-PD system must be included in this classification. The VLBI-Ku system shows great promise; perhaps with some kind of supplementary ranging it could meet ATDRSS requirements. The least expensive new system possibility is the use of GTR to White Sands to supplement the BRTS ranging, although this alternative still does not meet the goal of a CONUS-based system. This alternative is now being investigated [Reference 7-1].

7.13 REFERENCE

7.1 CSC, Error Analysis for the ATDRSS Using K-Band TT&C Data With Remote BRTS Transponders (TDRS Report No. 1),

APPENDIX A - THE ORAN SIMULATIONS

A.1 INTRODUCTION

Two measures of system performance have been defined for this study: (1) the maximum error in orbital position of ATDRS over a data arc, and (2) the maximum error in predicted orbital position of ATDRS over a given period after the end of the data arc.

Considerations of orbital operations require that two cases of data arcs be examined: (1) the normal operational situation, in which a 30-hour data arc is used and predictions are made from this data, and (2) the postmaneuver TR situation, in which the orbit of ATDRS must be recovered to a satisfactory level of accuracy as quickly as possible. To make comparison of the tracking performance among the various systems expedient, a TR arc of 2 hours was made the basis for comparison.

In the studies described in this appendix, data arcs have been varied for up to 30 hours for all systems, and the maximum orbital-position error has been tabulated. Plots of orbital position versus time have been made for selected cases to examine the prediction capabilities of the systems.

The same satellite orbits and parameters have been used for all cases and are described in Table A.1-1. The force model errors common to all systems are tabulated in Table A.1-2.

A.2 ERROR SOURCES FOR SIMULATIONS

A.2.1 FORCE MODEL ERRORS

A.2.1.1 GM Error

The GM error used in the ORAN simulations has a value of 2×10^{-8} (1 σ) or 6×10^{-8} (3 σ). The latest results (Reference A-1) for the determination of GM from the LAGEOS satellite studies give the value

$$GM = 398600.440 \pm 0.005 \ km^3/s^2$$

The uncertainty in this result represents a fractional error of 1.25×10^{-8}; therefore, the value chosen for the ORAN simulations is reasonable and slightly conservative.

Table A.1-1. ATDRS Satellite Parameters

Epoch time 1980 March 01 0h 0m 0.0s	
Keplerian elements	
Semimajor axis	42166663.000 m
Eccentricity	0.0000245
Inclination	0.5°
Right ascension of the ascending node	
ATDRS-E	319.00°
ATDRS-W	189.00°
ATDRS-C	254.00°
Argument of perigee	0.0°
Mean anomaly	158.9252°
ATDRS area/mass ratio	0.0227 (m^2/kg)
ATDRS coefficient of reflectivity	1.4

Table A.1-2. Measurement Independent Errors

Model parameter	Uncertainty (3 σ)
GM	6×10^{-8} (fractional error)
Geopotential coefficients	135% of (GEM-10 - GEM-7)
C_R (solar radiation)	2%
Polar motion X	0.015 arcsec
Polar motion Y	0.015 arcsec
A1 - UT1	0.09 arcsec

A.2.1.2 Gravity-Model Errors

The gravity model difference error source in ORAN allows the user to estimate the effect of the overall uncertainty in the Earth's gravitational field on the position and velocity of the satellite being studied. ORAN uses the coefficient differences of two different (independent, it is hoped) gravity models to estimate the uncertainties in the coefficients. Because two perfect, independent gravity models would have the same coefficients, the size of the coefficient differences is some measure of the error in the coefficients of these gravity models.

The models chosen for this ORAN simulation are Goddard Earth Model (GEM)-7 and GEM-10. These models are not independent--they share the same data and were computed by the same group--however, GEM-10 contains significantly more data than GEM-7. Therefore, their differences will provide a measure of the error in contemporary gravity models. For a 3-σ error, 135 percent of the difference between GEM-7 and GEM-10 was used.

There are no planned U.S. gravity missions at present; therefore, unless a European gravity mission is launched in the near future, these geopotential coefficient error estimates will be valid until at least 1995.

The gravity-model error source is relatively unimportant for geostationary satellites because the perturbing effects of the high degree and order coefficients decrease rapidly with altitude.

A.2.1.3 Pole and A1 - UT1 Errors

The errors in the X and Y coordinates of the pole express the error in the tracking-station locations due to errors in the transformation for the polar motion of the Earth. This transformation is necessary to compensate for the deviation of the motion of the Earth's crust (and the stations situated on it) from the average rotational motion of the Earth. The A1 - UT1 error expresses the error in converting the UT1 time system, which expresses the relation between the average Earth-fixed coordinate system and the inertial coordinate system, to the A1 atomic time system, which is used for satellite orbit integration.

The following errors have been used in the ORAN simulations:

Pole X	15 milliarcsec
Pole Y	15 milliarcsec
A1 - UT1	90 milliarcsec (= 6 millisec)

Errors in both UT1 and polar motion are according to the USNO-estimated accuracy of their 10-day predicts, as listed in the International Earth Rotation Service bulletin. UT1 predicts are much less accurate than predicts for polar motion because of the high degree of coupling to atmospheric angular momentum, which fluctuates on short time scales.

A USNO study (Reference A-2) indicates that the errors in 30-day predictions for the pole and A1 - UT1 would not exceed the 3-σ errors used in the ORAN studies.

A.2.1.4 Solar Radiation Coefficient Error

The ORAN simulations used a 3-σ value of 2 percent for the solar radiation error. This value is currently used as a 3-σ error for TDRS by the Flight Dynamics Branch at GSFC because observed variations in the C_R of TDRS are on the 0.5 percent level.

A.2.2 MEASUREMENT ERRORS

Tables A.2-1 through A.2-13 list the measurement errors for the systems considered in this report. Tables A.2-14 through A.2-18 contain the station positions used for the different tracking systems.

A.2.2.1 Station-Position Errors

The report mentioned earlier (Reference A-1) also gives estimates of the height of laser tracking stations used to track the LAGEOS satellite. The report quotes monthly mean height precision as 2 cm and the yearly mean height precision as 4 cm. Inspection of the graphs of monthly height estimates versus time shows a large scatter in these estimates, on the order of 10 to 20 cm. It may be concluded that a realistic station-position error for these laser stations is at least 10 cm in each coordinate, possibly more. These results apply to the ATDRS stations only if there is a laser station at the ATDRS site or if the ATDRS site position could be determined relative to a laser site within a few cm.

Because of the differences in the tracking systems under consideration here, the station-position errors are treated differently for the VLBI and PRTS systems. The VLBI system is particularly suited for determining baselines between the tracking stations of the system. Such baselines can be determined to within 2 to 5 cm. Similarly high precision of such baseline determinations is not achievable for the determination of the position of the stations relative to the center of mass of the Earth. The accuracy of the

Table A.2-1. VLBI-Q Measurement Errors

Station positions

Station c1 x	0.06 m
Station c1 y	0.06 m
Station c1 z	0.24 m
Station c2 x	0.06 m
Station c2 y	0.06 m
Station c2 z	0.24 m
Station ce x	0.06 m
Station ce y	0.06 m
Station ce z	0.24 m
Station cw x	0.06 m
Station cw y	0.06 m
Station cw z	0.24 m

Network location error

X	0.75 m
Y	0.75 m
Z	0.75 m

Troposphere error 2% for all stations

Ionosphere error 12% for all stations

Clock error
a0 0.045 m = 150
a1 and a2 = 0

Measurement noise

Quasar observation	(0.056 m)
ATDRS observation	(<0.008 m)
Troposphere	(0.045 m)
Ionosphere	(0.008 m)
Noise total	0.073 m

Table A.2-2. White Sands Range Measurement Errors

Station positions	
Station WHSK x	0.75 m
Station WHSK y	0.75 m
Station WHSK z	0.75 m
Troposphere error	6%
Ionosphere error	100%
Range bias error	3.0 m
Measurement noise	1.0 m

Table A.2-3. CEI-Q (Alabama) Measurement Errors

Station positions

Station site 1 x	0.006 m
Station site 1 y	0.006 m
Station site 1 z	0.006 m
Station site 2 x	0.006 m
Station site 2 y	0.006 m
Station site 2 z	0.006 m
Station site 3 x	0.006 m
Station site 3 y	0.006 m
Station site 3 z	0.006 m

Network location error

X	0.75 m
Y	0.75 m
Z	0.75 m

Troposphere error

Baseline 1-2	0.015%
Baseline 1-3	0.006%
Baseline 2-3	0.015%

Ionosphere error

Baseline 1-2	0.0012%
Baseline 1-3	0.0006%
Baseline 2-3	0.0012%

Clock error

a0 0.0003 m = 1 ps
a1 and a2 = 0

Measurement noise

Instrumental	0.001 m
Tropospheric	
Average day	0.014 m
(Poor day)	(0.050 m)

Table A.2-4. CEI-Q (California) Measurement Errors

Station positions

Station site 1 x	0.006 m
Station site 1 y	0.006 m
Station site 1 z	0.006 m
Station site 2 x	0.006 m
Station site 2 y	0.006 m
Station site 2 z	0.006 m
Station site 3 x	0.006 m
Station site 3 y	0.006 m
Station site 3 z	0.006 m

Network location error

X	0.75 m
Y	0.75 m
Z	0.75 m

Troposphere error

Baseline 1-2	0.036%
Baseline 1-3	0.030%
Baseline 2-3	0.003%

Ionosphere error

Baseline 1-2	0.0012%
Baseline 1-3	0.0006%
Baseline 2-3	0.0012%

Clock error

a0 0.0003 m = 1 ps
a1 and a2 = 0

Measurement noise

Instrumental	0.001 m
Tropospheric	
Average day	0.020 m
(Poor day)	(0.077 m)

Table A.2-5. VLBI-2S, VLBI-3S Measurement Errors

Relative station positions

Station c1-c2 x	0.076 m
Station c1-c2 y	0.076 m
Station c1-c2 z	0.228 m
Station c1-ce x	0.154 m
Station c1-ce y	0.154 m
Station c1-ce z	0.462 m
Station c2-ce x	0.186 m
Station c2-ce y	0.186 m
Station c2-ce z	0.558 m
Station c1-cw x	0.168 m
Station c1-cw y	0.168 m
Station c1-cw z	0.504 m
Station c2-cw x	0.156 m
Station c2-cw y	0.156 m
Station c2-cw z	0.468 m

Network location error

X	0.75 m
Y	0.75 m
Z	0.75 m

Troposphere error 4.5% for all stations

Ionosphere error 100% for all stations

Clock errors are always solved for (a_0, a_1, and a_2)

Noise Instrumental 0.001 m

Noise Tropospheric

Average day	East	West
Baseline c1-c2	.072 m	
Baseline c1-ce	.057 m	
Baseline c2-ce	.063 m	.073 m
Baseline c1-cw		.073 m
Baseline c2-cw		.073 m

Table A.2-6. VLBI-Ku Measurement Errors (3 σ)

Relative station positions

Station WST-FTD x	.06 m
Station WST-FTD y	.06 m
Station WST-FTD z	.24 m
Station WST-RCH x	.06 m
Station WST-RCH y	.06 m
Station WST-RCH z	.24 m
Station FTD-RCH x	.06 m
Station FTD-RCH y	.06 m
Station FTD-RCH z	.24 m

Network location error

X	0.75 m
Y	0.75 m
Z	0.75 m

Troposphere error 4.5% for all stations

Ionosphere error 100% for all stations

Clock errors are always solved for (a_0, a_1, and a_2)

Noise Instrumental 0.01 m

Noise Tropospheric 0.099 m

Table A.2-7. VLBI-GH Measurement Errors (1 of 2)

Relative station positions

Station c1-c2 x	0.076 m
Station c1-c2 y	0.076 m
Station c1-c2 z	0.228 m
Station c1-ce x	0.154 m
Station c1-ce y	0.154 m
Station c1-ce z	0.462 m
Station c2-ce x	0.186 m
Station c2-ce y	0.186 m
Station c2-ce z	0.558 m
Station c1-cw x	0.168 m
Station c1-cw y	0.168 m
Station c1-cw z	0.504 m
Station c2-cw x	0.156 m
Station c2-cw y	0.156 m
Station c2-cw z	0.468 m

Network location error

X	0.75 m
Y	0.75 m
Z	0.75 m

Clock errors are always solved for on each independent base line

ATDRS:

Systematic Errors (3σ)

Troposphere (when not solved for)	4.5% for all stations
Ionosphere	100.% for all stations

Noise Errors (3σ)

Instrumental	.01 m
Troposphere	

Average day	East	West
Baseline c1-c2	.072 m	.076 m
Baseline c1-ce	.054 m	

Table A.2-7. VLBI-GH Measurement Errors (2 of 2)

Average day	East	West
Baseline c2-ce	.058 m	
Baseline c1-cw		.059 m
Baseline c2-cw		.060 m

GPS:

Systematic Errors (3σ)	
Troposphere (when not solved for)	4.5% for all stations
Instrumental (range difference) offset	.015 m for all satellites
Noise Errors (3σ)	
Instrumental	.02 m
Tropospheric	.048 m

Table A.2-8. VLBI-GC Measurement Errors (1 of 2)

Relative station positions

Station c1-c2 x	0.076 m
Station c1-c2 y	0.076 m
Station c1-c2 z	0.228 m
Station c1-ce x	0.154 m
Station c1-ce y	0.154 m
Station c1-ce z	0.462 m
Station c2-ce x	0.186 m
Station c2-ce y	0.186 m
Station c2-ce z	0.558 m
Station c1-cw x	0.168 m
Station c1-cw y	0.168 m
Station c1-cw z	0.504 m
Station c2-cw x	0.156 m
Station c2-cw y	0.156 m
Station c2-cw z	0.468 m

Network location error

X	0.75 m
Y	0.75 m
Z	0.75 m

Clock errors are always solved for on each independent base line

ATDRS:

Systematic Errors (3σ)

Troposphere (when not solved for)	4.5% for all stations
Ionosphere	100.% for all stations

Noise Errors (3σ)

Instrumental	.01 m
Troposphere	

Average day	East	West
Baseline c1-c2	.072 m	.076 m
Baseline c1-ce	.054 m	

Table A.2-8. VLBI-GC Measurement Errors (2 of 2)

Average day	East	West
Baseline c2-ce	.058 m	
Baseline c1-cw		.059 m
Baseline c2-cw		.060 m

GPS:

Systematic Errors (3σ)	
Troposphere (when not solved for)	4.5% for all stations
Instrumental offset	.09 m for all satellites
Noise Errors (3σ)	
Instrumental	.074 m
Tropospheric	.048 m

Table A.2-9. VLBI-GT Measurement Errors

Relative station positions

Station c1-c2 x	0.076 m
Station c1-c2 y	0.076 m
Station c1-c2 z	0.228 m
Station c1-ce x	0.154 m
Station c1-ce y	0.154 m
Station c1-ce z	0.462 m
Station c2-ce x	0.186 m
Station c2-ce y	0.186 m
Station c2-ce z	0.558 m
Station c1-cw x	0.168 m
Station c1-cw y	0.168 m
Station c1-cw z	0.504 m
Station c2-cw x	0.156 m
Station c2-cw y	0.156 m
Station c2-cw z	0.468 m

Network location error

X	0.75 m
Y	0.75 m
Z	0.75 m

Troposphere error 4.5% for all stations

Ionosphere error 100% for all stations

Clock errors (3σ)

a_o 3ns

Noise Instrumental 0.001 m

Noise Tropospheric

Average day	East	West
Baseline c1-c2	.072 m	.076 m
Baseline c1-ce	.054 m	
Baseline c2-ce	.058 m	
Baseline c1-cw		.059 m
Baseline c2-cw		.060 m

Table A.2-10. Measurement Errors for Baseline PRTS (3 σ)

Station positions for all stations

Local	X	0.75 m
Local	Y	0.75 m
Local	Z	0.75 m

Troposphere error 4.5%

Ionosphere error none

Clock error

a0 solved for
a1 and a2 = 0

a0 0.25 m
for measurements not in clock solution

Range biases

1-way forward measurements

Master station 6 m (uplink)
Remote station 3 m (downlink)

1-way return measurements

Master station 6 m (downlink)
Remote station 3 m (uplink)

Measurement noise

1-way forward range	1.5 m
1-way return range	7.5 m
1-way forward range rate	1.31 mm/s

Table A.2-11. Measurement Errors for MPRTS (3 σ)

Station positions for all stations

Local	X	0.75 m
Local	Y	0.75 m
Local	Z	0.75 m

Troposphere error 4.5%

Ionosphere error

none
frequency 2200 MHz

Clock error none

Range biases

Uplink (ATDRSS GT - ATDRS):	6.0 m
Forward (ATDRS - REMOTE STATION):	3.0 m
Return (REMOTE STATION - ATDRS):	3.0 m
Downlink (ATDRS - ATDRSS GT):	6.0 m

Measurement noise

2-way range:	2.2 m
2-way range-rate:	0.75 mm/s

Table A.2-12. Measurement Errors for AKuRS (3 σ)

Station positions for all stations

Local	X	0.75 m
Local	Y	0.75 m
Local	Z	0.75 m

Troposphere error 4.5%

Ionosphere error

100%
frequency 14000 MHz

Clock error none

Range biases

Uplink (ATDRSS GT - ATDRS):	6.0 m
Forward (ATDRS - REMOTE STATION):	3.0 m
Return (REMOTE STATION - ATDRS):	3.0 m
Downlink (ATDRS - ATDRSS GT):	6.0 m

Measurement noise

2-way range:	4.0 m
2-way range-rate:	0.15 mm/s

Table A.2-13. Measurement Errors for Direct ATDRS/GPS Tracking System (3 σ)

GPS satellite ephemeris error
- uncertainty in position: 6.0 m
- uncertainty in velocity: 6.0 mm/s

Troposhere error 0.0

Ionosphere error 0.0

ATDRS/GPS clock bias

- solved-for over 30-hour tracking arc
- 10.0 m over 2-hour tracking arc

ATDRS/GPS pseudorange measurements (per measurement)

- noise: 9.0 m
- bias: 13.4 m

ATDRS/GPS pseudorange-rate measurements (per measurement)

- noise: 10.5 mm/s
- bias: 1.5 mm/s

Table A.2-14. Stations for VLBI-Q

Station name	Latitude (deg min sec)	Longitude (deg min sec)	Height (m)
	TDRS-E Stations		
C1	31 00 00.	255 00 00.	1500.
C2	36 00 00.	254 00 00.	2500.
CE	31 00 00.	265 00 00.	100.
	TDRS-W Stations		
C1	31 00 00.	255 00 00.	1500.
C2	36 00 00.	254 00 00.	2500.
CW	33 00 00.	244 00 00.	0.0

Table A.2-15. Stations for CEI-Q

Station name	Latitude (deg min sec)	Longitude (deg min sec)	Height (m)
	TDRS-E (Alabama)		
SITE1	32 00 00.0	273 57 18.3000	150.0
SITE2	32 00 00.0000	274 02 41.7000	150.0
SITE3	32 04 40.0700	274 00 00.0000	150.0
	TDRS-W (California)		
SITE1	33 00 00.0	243 57 18.3040	00.00
SITE2	33 00 00.0	244 02 41.6960	00.00
SITE3	33 04 40.0667	244 00 00.0000	00.00

Table A.2-16. Stations for Multiple Satellite, VLBI Configurations

Station name	Latitude (deg min sec)	Longitude (deg min sec)	Height (m)
C1	31 00 00.	255 00 00.	1500.
C2	36 00 00.	254 00 00.	2500.
CE	31 00 00.	265 30 00.	100.
CW	33 00 00.	244 00 00.	0.0
WHSK	32 30 03.857	253 23 29.16	1441.37
WST	42 37 00.	288 31 00.	110.
FTD	30 06 00.	256 03 00.	1603.
RCH	25 36 00.	279 37 00.	26.

Table A.2-17. Stations for PRTS, MPRTS, and AKuRS (ATDRS-E)

Station name	Latitude (deg min sec)	Longitude (deg min sec)	Height (m)
Short-Baseline Stations			
WHSK	32 30 03.857	253 23 29.16	1441.37
GSFC	39 00 09.697	283 09 43.654	-9.904
MIL	28 30 21.986	279 18 25.388	-58.6510
WHS	32 30 03.857	253 23 29.66	1441.37
Intermediate-Baseline Stations			
WHSK	32 30 03.857	253 23 29.16	1441.37
GSFC	39 00 09.697	283 09 43.654	-9.904
ACN	-7-57-17.370	345 40 22.570	528.000
WHS	32 30 03.857	253 23 29.66	1441.37
Long-Baseline Stations			
WHSK	32 30 03.857	253 23 29.16	1441.37
REY	64 09 00.000	338 21 00.000	0.000
ACN	-7-57-17.370	345 40 22.570	528.000
WHS	32 30 03.857	53 23 29.66	1441.37

Table A.2-18. Stations for PRTS, MPRTS, and AKuRS (ATDRS-W)

Station name	Latitude (deg min sec)	Longitude (deg min sec)	Height (m)
	Short-Baseline Stations		
WHSK	32 30 03.857	253 23 29.16	1441.37
VAN	34 33 56.280	239 29 54.521	583.421
WAS	46 10 12.000	240 48 36.000	152.5000
WHS	32 30 03.857	253 23 29.66	1441.37
	Intermediate-Baseline Stations		
WHSK	32 30 03.857	253 23 29.16	1441.37
HAW	22 07 34.460	200 20 05.430	1139.000
WAS	46 10 12.000	240 48 36.000	152.5000
WHS	32 30 03.857	253 23 29.66	1441.37
	Long-Baseline Stations		
WHSK	32 30 03.857	253 23 29.16	1441.37
GWM	13 18 38.250	144 44 12.530	116.00
AMS	-1-42-25.00	189 16 35.000	3.00
WHS	32 30 03.857	253 23 29.66	1441.37

station positions relative to the center of mass of the Earth is the relevant quantity for OD. To estimate the station-position errors for ORAN correctly, two sets of station-position errors have been used. The first set, called the center of mass error, represents the error in determining the position of one of the stations (the master station) with respect to the center of mass of the Earth; it is applied only to the master station. The second set of station-position errors, the relative error, represents the error in determining the position of the other stations with respect to the master station. This set uses errors related to the baseline determinations made possible by the VLBI system. Only the relative station-position errors are used for the remote stations.

The center of mass errors were chosen to be 75 cm (3 σ) because, as discussed earlier, the best center of mass position determinations have an error of about 10 to 20 cm. The 3-σ relative errors were chosen to be 6 cm for most VLBI configurations. The relative errors are in a local coordinate system and are designated x, y, and z for east, north, and vertical directions, respectively. For VLBI-Q, a local height error (z-error) of 24 cm was used because the baseline determinations do not resolve the height differences of the stations well. For the CEI system, the relative errors are all 6 cm because local surveying can be used to determine the station relative positions more accurately.

For VLBI-Q, the relative station locations can be made by quasar observations by the network itself. Error estimates are based on currently achieved accuracies using this technique (Reference A-3). It is assumed that ties between quasar antennas and ATDRS antennas are done by conventional surveying techniques.

For CEI-Q arrays, again the quasar antennas can be surveyed by quasar observations. This is a standard technique at the VLA, for example. Baseline solutions are assumed to be accurate to $\lambda/30$, a figure that needs verification. A conventional survey tie between each quasar antenna and the associated ATDRS antenna is assumed accurate to 2 mm (1 σ) and can be verified by observing strong natural radio sources.

Multiple satellite systems (e.g. VLBI-2S) would be calibrated by accurate GPS surveying. Accuracy is assumed to be three parts in 10^8 (1 σ) in length and cross, three times worse in vertical. Current practitioners (e.g., Reference A-4) claim accuracies of 3×10^{-8} for all three components on a 2000 km baseline.

PRTS has no special advantage for determining baselines between stations; therefore, the only position errors used were 75-cm center of mass errors, applied independently to each station. These errors are in a local coordinate system and are designated x, y, and z for east, north, and vertical directions, respectively.

A.2.2.2 ORAN Clock Error Modeling

The studies done for the ATDRS tracking systems during the past year used a clock model of the following form:

$$t_C = t + a_0 + a_1 * t + a_2 * t^2$$

where t_C = clock time
t = true time
a_0, a_1, a_2 are clock coefficients

ORAN can treat all three clock coefficients as solved-for or unmodelled errors. Various combinations of solved-for and unmodelled clock parameters were used in different VLBI simulations.

In both VLBI systems calibrated by quasar observations, clock errors are nearly completely eliminated by simultaneous observation and subtraction of the delay toward ATDRS and the delay toward the quasar. For the VLBI-Q, a small residual offset is present because of uncalibrated instrumental hardware delays that differ between the quasar receiver and the ATDRS receiver. For the quasar-calibrated CEI, any such offset is assumed to be 100 percent calibrated by observations.

In VLBI-2S, a clock model is fitted to the observations, along with the satellite orbits. The clock model is quadratic with 3 parameters: offset, rate, and rate drift. Quadratic models are found to fit real masers to an accuracy of, typically, 85 ps over the course of a day (Reference A-5); therefore, it is appropriate to add 85 ps of noise due to maser fluctuations in quadrature with other noise sources.

For PRTS, it is claimed that the PRTS signal allows the clocks to be locked in frequency to the master station clock so that no drifts of the clocks will occur. Therefore, the parameters a_1 and a_2 have been set to zero for all the PRTS ORAN simulations.

Because PRTS uses two one-way range measurements (forward and return) to solve for the remote station clock biases,

ORAN has been modified to use such measurements. The return measurement has been implemented in ORAN to have a sign on the clock bias partial opposite to the sign of the clock bias partial on the forward measurement, following the description of the forward and return PRTS measurements provided by STI.

A.2.2.3 Tropospheric Errors

ORAN expresses errors in measurement corrections for systematic tropospheric refraction as a percentage of the calculated correction. The calculated correction depends on default values of atmospheric pressure, temperature, and humidity at the tracking location and on the elevation of the satellite as seen by the tracking site. For VLBI systems, fluctuations in the tropospheric refraction also produce an increase in the noise on the measurement, as discussed in the next paragraphs. For the PRTS simulations, ORAN has used a 3-σ error of 4.5 percent for all measurements.

The VLBI measurements have various troposphere error values, which depend on the type of VLBI tracking system and on the VLBI baseline length and orientation, because some degree of self-calibration is possible on the VLBI systems. In addition, for the short-baseline CEI systems, troposphere errors from two stations will be correlated because the signals travel along almost the same path. This situation leads to reductions in the troposphere error parameters, as discussed in the following paragraph. The troposphere error values for the various VLBI systems appear in Tables A.2-1 to A.2-5.

The tropospheric path delay is to be estimated from local meteorological data (pressure, temperature, and relative humidity). The dominant error in this determination comes in estimation of the effective thickness, i.e., the path delay at zenith. Zenith delay errors are budgeted as 1.5 percent (1-σ) of the total. This is based on a recent dissertation by Ifadis (Reference A-6) in which predictions of atmospheric models were compared to actual radiosonde profiles. Typical rms errors were found to be about 3 cm in zenith delay due to modeling errors. This corresponds to 1.4 percent of the total. The numbers may overestimate actual errors because, for sites in Albuquerque and El Paso, the errors are lower than average (2 cm, 2.6 cm). However, these estimates include only modeling error and neglect effects of measurement error in local meteorological measurements.

A.2.2.3.1 CEI-Q

Delay errors used in ORAN are derived from the assumed 1.5 percent error in zenith delay. The elevation of ATDRS is found for each antenna in the array. The atmosphere height is assumed uniform over the (10-km) array but with misestimated thickness. The delay error on each baseline is the added path difference through the added sheet of delay, due to the zenith angle (ZA) difference at the two sites. To obtain a fractional error, this delay error is normalized by the total delay at elevation and assigned to one of the antennas on the baseline. In addition, subtraction with respect to quasar observations is assumed to provide a reduction by at least a factor of three. This is because a nearby quasar will suffer a similar degree of unmodelled delay. The factor of three corresponds to the median reduction expected for the less favorable case: an array in California observing ATDRS at longitude 171 degrees (elevation angle 20.6 degrees). In fact, this error may be reduced further by observing each calibrator when it is at the same elevation angle as the ATDRS.

A.2.2.3.2 VLBI-Q

For quasar-calculated VLBI measurements, the same calculation is performed but the zenith delay errors are assumed to be uncorrelated at the two sites. (If the errors are correlated, the delay difference error is somewhat reduced.) The median reduction expected is 0.07/cos (ZA) for the expected median calibrator elevation difference of 4 degrees.

A.2.2.3.3 VLBI-2S

For VLBI-2S observations, in general the satellites are at quite different elevations; therefore, no such partial cancellation is assumed to take place.

A.2.2.3.4 Comments

Neglected in these calculations is any consideration of error in scaling from zenith to elevation of observation. These errors are expected to be about one order of magnitude smaller than zenith delay estimates themselves. If, however, improved zenith delay estimates can somehow be obtained, (e.g., treating as considered parameters or using water vapor radiometers), it would become necessary to consider the scaling law or mapping function error, as it is called.

Water vapor radiometry is not considered because it is not yet reliable, and there is some question whether it can be used in rainy weather.

A.2.2.3.5 Tropospheric Fluctuations

Noise in VLBI systems due to tropospheric fluctuations is calculated based on the model described in Reference A-7. The model assumes a Kolmogorov spectrum of three dimensional fluctuations, characterized by a single parameter r0 describing the minimum turbulent scale (Fried's length). For observations calibrated by subtraction, Ray et al. (Reference A-7) found

$$\sigma(\tau) = 1.4 \text{ ps}/\sqrt{\cos(ZA)} * (r/r0)^{5/6}$$

where τ = measured delay difference
ZA = Zenith angle of satellite
r = L2 km*sin (10 deg)/cos(ZA)
r0 = turbulent scale length
= 200 m (median) or 35 m (1 percent likelihood)
L2 = 5.6 km = scale height of troposphere

A slightly different formula applies when the two objects are far apart on the sky. In such a case

$$\sigma(\tau) = 1.4 \text{ ps} * \sqrt{(L2/r0*\cos ZA)} * (r/r0)^{1/3}$$

For quasar-calibrated systems, the calibrator source is assumed to be 10 degrees away. Estimates predict that there will be a quasar at least this close about 80 percent of the time.

For the VLBI-2S observations, the noise is modeled as that from calculating the difference between two objects differing in azimuth by 90 degrees and at the elevation of the lower satellite. For GPS observations, the noise is modeled as though one satellite is at zenith and the other is at 20 degrees of elevation (the elevation cutoff).

A.2.2.4 Ionosphere Errors

Because it is claimed that PRTS can eliminate all ionospheric effects on the measurements, no ionosphere errors have been used in the ORAN simulations of PRTS. The measurement noise levels, however, are conservatively modelled to effectively include the random error in the estimation of the ionospheric delay.

The VLBI measurements have various ionospheric error values, which depend on the type of VLBI tracking system and on the VLBI baseline length and orientation, because some degree of self-calibration is possible on the VLBI systems.

Furthermore, for the short baseline CEI systems, ionosphere errors from two stations will be correlated because the signals travel along almost the same path, thereby reducing ionosphere error parameters. As for the troposphere, fluctuations in the ionosphere increase the measurement noise.

The ionosphere error values for the various VLBI systems appear in Tables A.2-1 to A.2-7. The F10.7 solar flux value, which indicates the level of solar activity, and thereby affects the ionospheric error, has been set to 250, which is appropriate for the high levels of solar activity expected for the mid-1990s.

The ionospheric delays are not explicitly calibrated in the VLBI systems proposed here because the effects at Ku-band are expected to be rather small; however, they are included in the ORAN simulations.

For the VLBI-Q tracking systems, systematic ionosphere error is modeled as due to the elevation difference at the two stations. The delay is modeled according to a rather simple azimuthally symmetric model given by Reference A-8. A factor of three is assumed for reduction from differencing with respect to quasar observations. This gives the proportion of the total ionospheric delay as calculated in ORAN that is assumed as systematic error. The same calculation is performed for CEI-Q system as for the VLBI system.

For VLBI-2S, the ionospheric delay is 100 percent uncalibrated.

Noise in VLBI systems due to ionospheric fluctuations is derived by a model similar to the tropospheric error model. Parameters come from Reference A-9. For CEI, the error is calculated to contribute 9 ps of noise at Ku-band. Variation with elevation is neglected because the effective angle of traversal through the ionosphere never falls below about 23 degrees. For VLBI systems, this error source is neglected, being far below measurement system noise.

A.2.2.5 Measurement Noise

The measurement noise values for PRTS, MPRTS, and AKuRS are listed in Tables A.2-10 through A.2-12. See Sections 3 and 4 and Appendix C of this report for a discussion of the calculation of these noise values.

The VLBI measurement precision calculation is presented in Section 5.1.8. The result shows that the contribution of measurement noise observing ATDRS is 2 ps for group delay, 0.87 ps for phase delay. In the quasar-calibrated systems, the noise on the quasar measurements is larger: 62 ps and 0.8 ps.

An additional system noise-like effect occurs in the VLBI systems from the phase-calibration system. This comes from the limited precision of measurement of that signal and from environmental sensitivities. In current Crustal Dynamics Project (CDP) systems, the latter are thought to contribute about 15 ps of error and the former less than 5 ps. Using the current CDP system, the error due to SNR would be greatly increased under some circumstances; however, it is expected that some optimization of signal levels would reduce effects to nearby the current values.

For the phase delay systems, an additional noise contribution occurs due to errors in synchronizing local oscillators at the antennas to the array master clock. This is estimated at the VLA to add noise of about 3 ps. For phase delay systems, this noise source and measurement noise are both dwarfed by noise due to atmospheric fluctuations.

A.3 VLBI QUASAR SIMULATION RESULTS

The VLBI quasar system consists of two VLBI networks, one for ATDRS-E (stations c1, c2, ce) and one for ATDRS-W (stations c1, c2, cw). Table A.3-1 (Figure A.3-1) shows the OD results for ATDRS-E using only VLBI measurements. The error results are acceptable until the data arc becomes shorter than 6 hours. For these short arcs, measurement noise dominates the orbit solution, and the total orbital-position error exceeds the required 75 m. The errors for ATDRS-W (shown in Table A.3-2 and Figure A.3-2) show a similar pattern.

The addition of range measurements (range sigma = 1 m) from WHS greatly improves the 1- and 2-hour short arc solutions and moderately improves the 12- and 6-hour arc solutions so that all arcs meet the 75-m requirement. (See Table A.3-3

Table A.3-1. ATDRS-E Orbit Errors Using VLBI-Q Without Range Data

Arc Length (hours)	Data Characteristics	Maximum Position Error in Definitive Period (m)	
30	No range	33	c1 trop (21) A1 - Ut1 (18)
24	No range	33	c1 trop (21) a1-ut1 (18)
18	No range	41	c1 trop (24) c2 trop (22)
12	No range	48	c2 trop (32) c1 trop (24)
6	No range	62	noise (40) c2 trop (31)
2	No range	647	noise (643) c2 trop (55)
1	No range	3432	noise (3231) c2 trop (67)

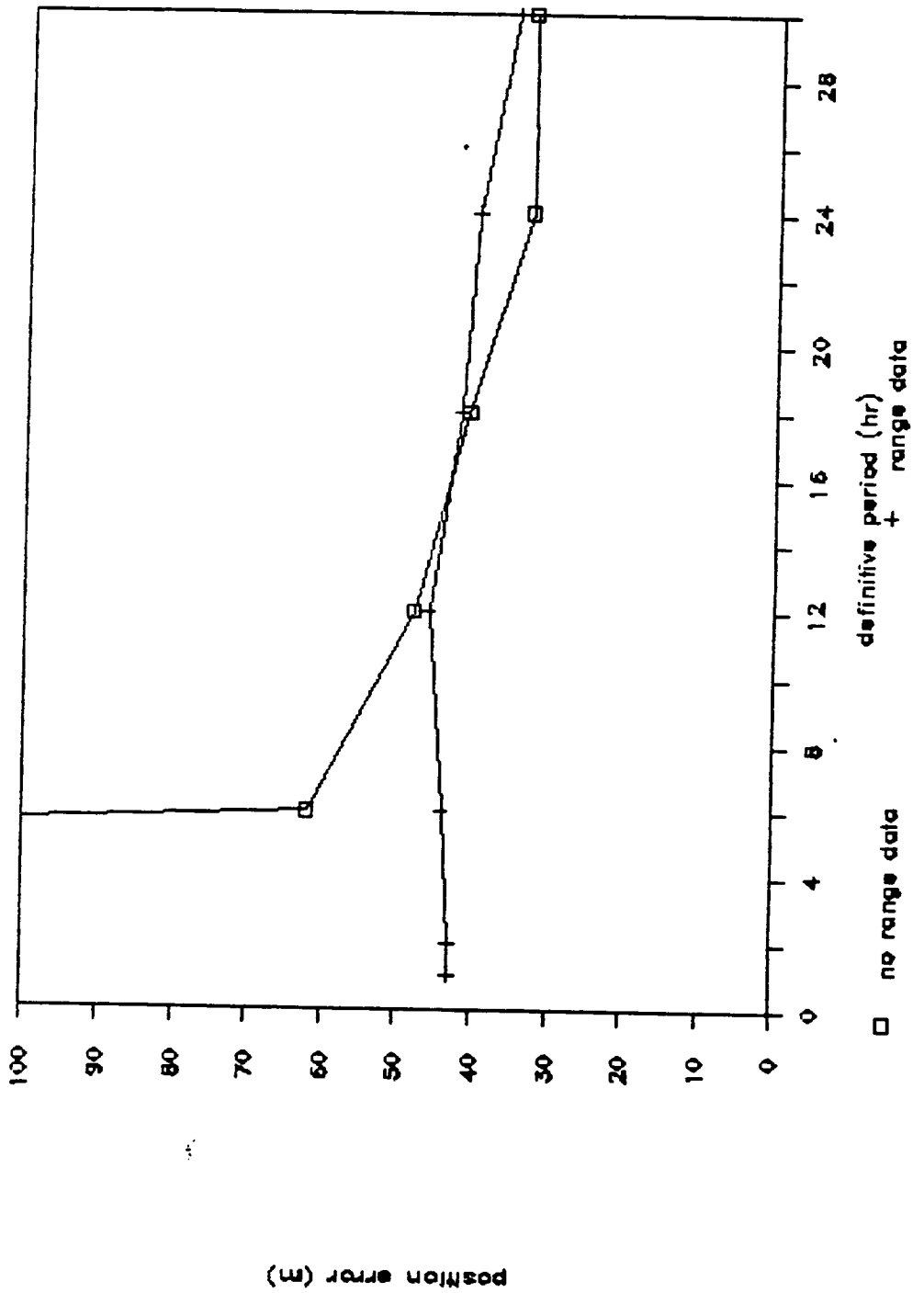

Figure A.3-1. Maximum Definitive Position Error for VLBI-Q--ATDRS-E

Table A.3-2. ATDRS-W Orbit Errors Using VLBI-Q Without Range Data

Arc Length (hours)	Data Characteristics	Maximum Position Error in Definitive Period (m)	
30	No range	34	c1 trop (21) A1 - Ut1 (18)
24	No range	43	c2 trop (25) c1 trop (24)
18	No range	43	c2 trop (25) c1 trop (24)
12	No range	64	c2 trop (48) cw trop (24)
6	No range	70	noise (50) c2 trop (41)
2	No range	909	noise (907) c2 trop (54)
1	No range	4154	noise (4153) c2 trop (76)

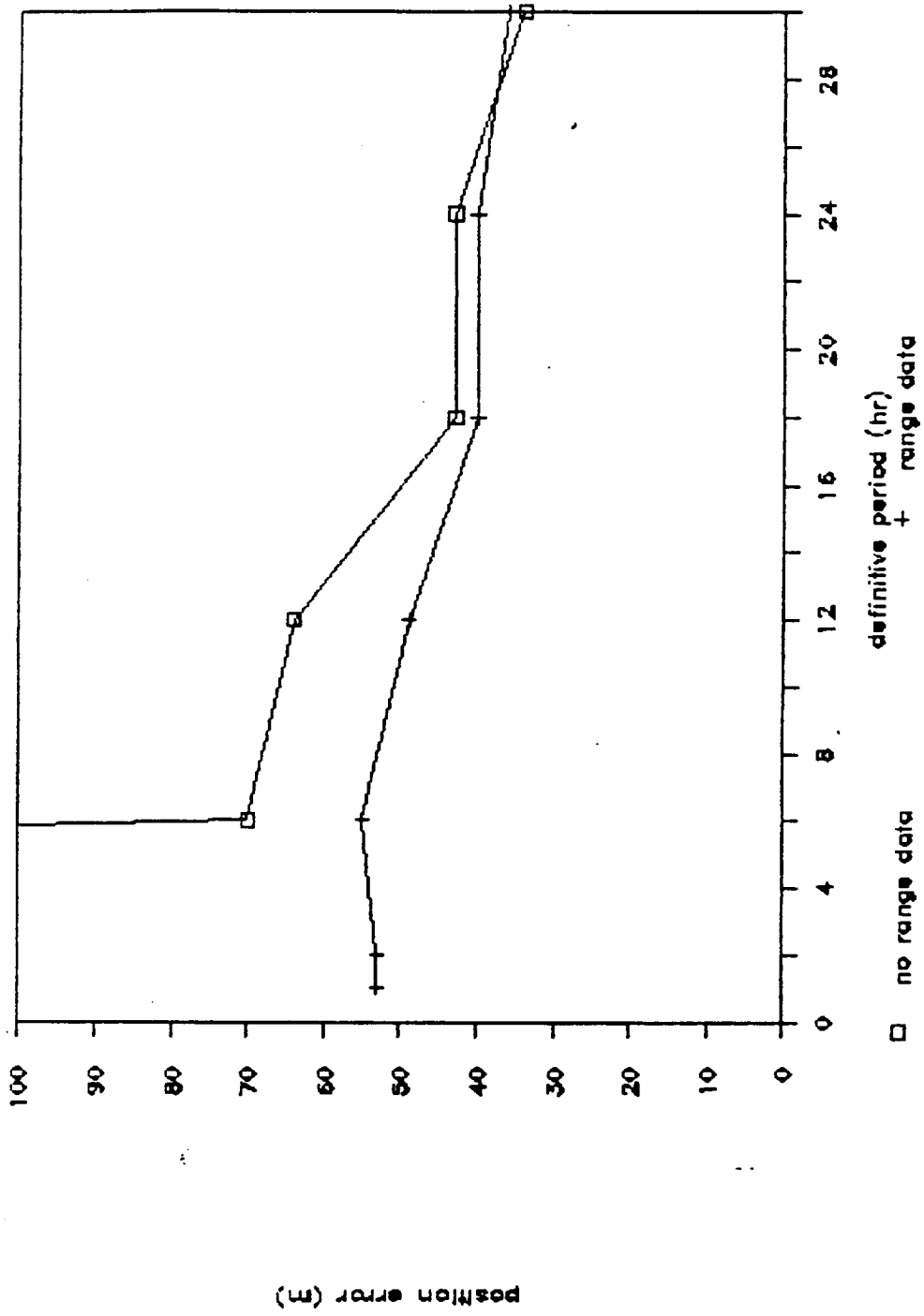

Figure A.3-2. Maximum Definitive Position Error for VLBI-Q--ATDRS-W

Table A.3-3. ATDRS-E Orbit Errors Using VLBI-Q With Range Data

Arc Length (hours)	Data Characteristics	Maximum Position Error in Definitive Period (m)
30	Range; sigma = 1.0 m	35 c1 trop (23) A1 - Ut1 (18)
30	Range; solve for range bias noise sigma = wt. sigma = 1 m	32 c1 trop (21) A1 - ut1 (18)
30	Range; solve for range bias noise sigma = 1 m; wt. sigma = 3 m	33 c1 trop (21) A1 - Ut1 (18)
24	Range; sigma = 1.0 m	40 c1 trop (27) A1 - Ut1 (18)
18	Range; sigma = 1.0 m	42 c1 trop (27) A1 - Ut1 (18)
12	Range; sigma = 1.0 m 1 meas/ 30 min	46 c2 trop (29) c1 trop (22)
12	Range; sigma = 1.0 m 1 meas/ 10 min	46 c2 trop (30) c1 trop (22)
6	Range; sigma = 1.0 m	44 c2 trop (27) c1 trop (20)
2	Range; sigma = 1.0 m	43 c2 trop (24) c1 trop (20)
1	Range; sigma = 1.0 m	43 c2 trop (24) c1 trop (20)

and Figure A.3-1.) The large improvement in the short arcs is the result of the improved knowledge of the satellite range and, thus, the satellite orbit's semimajor axis. The longer arcs provide enough geometrical information to fix this orbital parameter and are not greatly improved by the addition of range data.

Although the results in Table A.3-3 were obtained with range measurements precise within 1 m, the studies of the effect of varying the range sigma demonstrate that, even if the range sigma is increased to 100 m, the range measurements will provide enough strength in the short-arc orbital solution to bring the maximum position error below the required 75 m.

Results for ATDRS-W using range measurements are shown in Table A.3-4 and Figure A.3-2. These results are similar to the corresponding results for ATDRS-E. Although no studies of the effects of varying the range sigma were made for ATDRS-W, it is likely that results comparable to those of the ATDRS-E study would be obtained.

Tables A.3-5 and A.3-6 present a summary of the VLBI-Q prediction results for ATDRS-E and ATDRS-W, respectively. These tables show that, whereas many simulations can achieve orbit accuracies of less than 75 m in the definitive period, only the longest arcs (30 and 24 hours) can achieve this goal over three days of prediction.

A.3.1 RANGE SIGMA SIMULATION RESULTS

To examine the effect of range noise on the tracking system performance, several simulations have been made using the VLBI quasar tracking system supplemented by range measurements from WHS. The noise on the range measurements has been varied widely to show the contribution of these measurements to ATDRS OD.

Tables A.3-7 and A.3-8 show the effects of varying the range sigma in data arcs of 2 hours and 1 hour, respectively. These results are also plotted in Figure A.3-3. It is clear that, for these arc lengths, using range data of any precision provides a better orbital solution than solutions in which no range data is used. Furthermore, at least with respect to the orbital error during the data arc, lowering the range sigma below 30 m does not significantly improve the solution. The effect of the range sigma becomes more pronounced if the orbit error in the predicted position long after the data span is considered, as shown in Table A.3-9.

Table A.3-4. ATDRS-W Orbit Errors Using VLBI-Q With Range Data

Arc Length (hours)	Data Characteristics	Maximum Position Error in Definitive Period (m)		
30	Range; sigma = 1.0 m	36	c1 trop A1 - Ut1	(23) (18)
24	Range; sigma = 1.0 m	40	c1 trop A1 - Ut1	(27) (18)
18	Range; sigma = 1.0 m	40	c1 trop A1 - Ut1	(26) (18)
12	Range; sigma = 1.0 m 1 meas/ 10 min	49	c2 trop cw trop	(34) (20)
6	Range; sigma = 1.0 m	55	c2 trop cw trop	(40) (23)
2	Range; sigma = 1.0 m	53	c2 trop cw trop	(37) (21)
1	Range; sigma = 1.0 m	53	c2 trop cw trop	(36) (20)

Table A.3-5. VLBI-Q Orbit-Prediction Errors Using ATDRS-E

Arc Length (hours)	Data Characteristics	Maximum Position Error (m) Def. Period	1 Day	2 Day	3 Day
30	Range data	35	54	77	101
30	Solve range bias noise = wt. = 1 m	32	37	49	66
30	Solve range bias noise = 1 m; wt. = 3 m	33	37	49	64
24	Range data	40	69	100	133
18	Range data	42	75	113	152
12	Range data	46	74	116	158
6	Range data	44	84	136	190
6	Solve range bias	45	80	141	207
2	Range data	43	217	419	623
2	Solve range bias	45	332	658	986
1	Range data	43	737	1454	2171
30	No range data	33	38	50	66
24	No Range data	33	37	52	71
18	No range data	41	65	111	160
12	No range data	48	208	401	596
6	No range data	62	952	1899	2847
2	No range data	608	21341	42816	64298
1	No range data	3432	122143	244833	367551

Table A.3-6. VLBI-Q Orbit-Prediction Errors Using ATDRS-W

Arc Length (hours)	Data Characteristics	Maximum Position Error (m) Def. Period	1 Day	2 Day	3 Day
30	Solve range	33	39	55	75
30	Range	36	43	66	94
24	Range	40	45	76	112
18	Range	40	47	84	127
12	Range	49	55	89	134
6	Range	55	64	112	169
6	Solve range	55	101	165	234
2	Range	53	213	424	638
1	Range	53	764	1508	2252
30	No range	34	38	48	64
24	No range	54	77	106	139
18	No range	43	64	93	126
12	No range	64	147	274	404
6	No range	70	1050	2092	3134
2	No range	909	30590	61771	92614
1	No range	4154	15503	300446	450416

Table A.3-7. Range-Sigma Effects on ATDRS-E Orbit Errors Using VLBI-Q (2-Hour Arcs)

Arc Length (hours)	Data Characteristics	Maximum Position Error in Definitive Period (m)		
		Bias: 3	30*	
2	No range	647		noise (643) c2 trop (55)
2	Range Sigma = 100.0 m	58	65	noise (41) c2 trop (23) rbias (3)
2	Range Sigma = 30.0 m	45	54	c2 trop (24) c1 trop (19) rbias (3)
2	Range Sigma = 10.0 m	43	52	c2 trop (24) c1 trop (19) rbias (3)
2	Range Sigma = 3.0 m	42	52	c2 trop (24) c2 trop (19) rbias (3)
2	Range Sigma = 1.0 m	43	52	c2 trop (24) c1 trop (20) rbias (3)
2	Range Sigma = 0.3 m	43	52	c2 trop (24) c1 trop (20) rbias (3)
2	Range Sigma = 0.1 m	43	52	c2 trop (24) c2 trop (20) rbias (3)

*The 30 m error computed from error $(30)^2$ = error$(3)^2$ - $3^2 + 30^2$

Table A.3-8. Range Sigma Effects on ATDRS-E Orbit Errors Using VLBI-Q (1-Hour Arc)

Arc Length (hours)	Data Characteristics	Maximum Position Error in Definitive Period (m)		
1	No range	3432	noise	(3231)
			c2 trop	(67)
			rbias	(3)
1	Range sigma = 100.0 m	74	noise	(62)
			c2 trop	(24)
			rbias	(3)
1	Range sigma = 30.0 m	47	c2 trop	(24)
			noise	(23)
			rbias	(3)
1	Range sigma = 10.0 m	43	c2 trop	(24)
			c1 trop	(19)
			rbias	(3)
1	Range sigma = 3.0 m	43	c2 trop	(24)
			c1 trop	(20)
			rbias	(3)
1	Range sigma = 1.0 m	43	c2 trop	(24)
			c1 trop	(20)
			rbias	(3)
1	Range Sigma = 0.3 m	43	c2 trop	(24)
			c1 trop	(19)
			rbias	(3)
1	Range sigma = 0.1 m	43	c2 trop	(24)
			c1 trop	(19)
			rbias	(3)

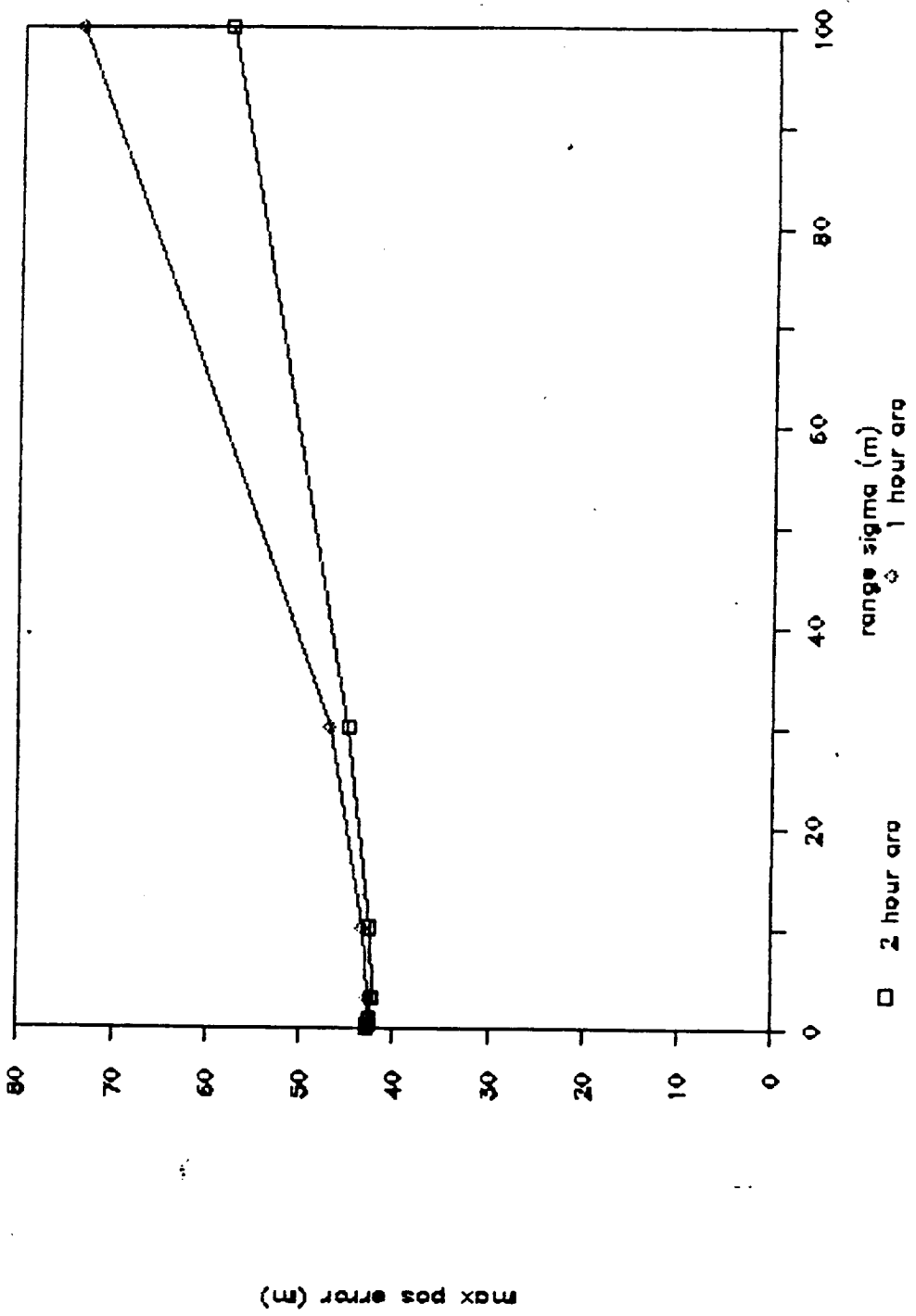

Figure A.3-3. Maximum Definitive Position Error With Range Sigma for ATDRS-E

Table A.3-9. Range Sigma Effects on VLBI-Q Orbit Prediction Errors Using ATDRS-E

Arc Length (hours)	Data Characteristics	Def. Period	Maximum Position Error (m) 1 Day	2 Day	3 Day
2	Range sigma = 0.1 m	43	81	132	186
2	Range sigma = 0.3 m	43	103	182	265
2	Range sigma = 1.0 m	43	217	419	623
2	Range sigma = 3.0 m	42	370	725	1080
2	Range sigma = 10.0 m	43	435	854	1273
2	Range sigma = 30.0 m	45	539	1059	1581
2	Range sigma = 100.0 m	58	1124	2237	3351

Table A.3-7 also shows the effect of increasing the range bias from the nominal value of 3 m to 30 m. The position errors for a range bias of 30 m were computed from the numbers shown in Table A.3-7 and from the formula displayed at the bottom of the table. It is clear that a large increase in range bias will not have much effect on the definitive-period position error. Table A.3-9 shows that the range sigma value will affect the 1-, 2- and 3-day predictions of the ATDRS orbital position considerably and that no case achieves the desired 75 m position error after only 1 day of prediction.

A.4 CEI SIMULATION RESULTS

The advantage of short-baseline CEI over long-baseline VLBI networks is that the stations in a CEI are directly connected by cables and can synchronize their clocks easily; the disadvantage is that its short baselines do not provide good geometry for measurements to be used in OD Tables A.4-1 through A.4-3 show OD results for CEI (Alabama) for ATDRS-E. Tables A.4-4 through A.4-6 show OD results for CEI (California) for ATDRS-W.

This disadvantage shows up very clearly in a comparison of ATDRS OD results done with the CEI and with the quasar-calibrated VLBI systems. Table A.4-1 (and Figure A.4-1) shows that the CEI, without range data, can provide an orbit solution with maximum position error less than 75 m only with a 30-hour arc, whereas the VLBI quasar (without range data) was able to exceed this criterion for all arcs longer than the 1- and 2-hour arcs. Table A.4-4 (Figure A.4-2) shows that, without range data, the CEI system in California cannot meet the 75-m requirement for any of the arcs, including the 30-hour arc.

When range data from WHS is added to the solution, Tables A.4-2 and A.4-5 (see Figures A.4-1 and A.4-2) show that the requirement of 75-m maximum orbital-position error during the data arc can be met by the CEI system but only for data arcs longer than 12 hours. It should also be noted that the range measurements have noise values of 1 m. If the future ranging system has a larger noise than this, these CEI plus range solutions will be degraded even further. Table A.4-7 (Figure A.4-3) shows the effect on a 30-hour ATDRS-E arc of varying the range noise values from 1 to 30 m. The effect of increasing the range noise shows up most clearly in the predicted error values. If the range noise increases beyond 10 m, then even the 1-day predictions from a 30-hour arc would not satisfy the 75 m position-error criterion.

The OD error results shown in Tables A.4-1 to A.4-5 (Figures A.4-1 and A.4-2) indicate that the CEI system would be unable to provide any TR solutions for ATDRS using short 1- or 2-hour data arcs.

Table A.4-1. ATDRS-E Orbit Errors Using CEI (Alabama) Without Range Data

Arc Length (hours)	Data Characteristics	Maximum Position Error in Definitive Period (m)	
30	No range	71	noise (61) site1 X (19)
24	No range	86	noise (79) A1 - Ut1 (18)
18	No range	119	noise (111) site3 X (22)
12	No range	91	noise (186) site3 X (30)
6	No range	468	noise (465) site2 X (28)
2	No range	8132	noise (8132) site3 X (41)
1	No range	45772	noise (45772) site3 X (52)

Table A.4-2. ATDRS-E Orbit Errors Using CEI (Alabama) With Range Data

Arc Length (hours)	Data Characteristics	Maximum Position Error in Definitive Period (m)	
30	Range data	40	rbias ws (25) noise (21)
30	Solve range	44	a1 - Utl (18) site1 X (16)
24	Range data	57	solrad (42) rbias ws (22)
18	Range data	69	solrad (53) A1 - Utl (18)
12	Range data	68	site2 X (23) A1 - Utl (18)
6	Range data	77	site2 X (30) site3 X (24)
6	Solve range	92	site2 X (26) A1 - Utl (18)
2	Range data	100	site2 X (28) site3 X (24)
1	Range data	122	site2 X (25) site3 X (23)

Table A.4-3. ATDRS-E Orbit Prediction Errors Using CEI (Alabama)

Arc Length (hours)	Data Characteristics	Maximum Position Error (m) Def. Period	1 Day	2 Day	3 Day
30	Range data	40	45	57	73
30	Solve range	44	47	57	73
24	Range data	57	82	110	140
18	Range data	69	102	139	189
12	Range data	68	115	168	222
6	Range data	77	135	202	272
6	Solve range	92	403	756	1110
2	Range data	100	310	512	732
1	Range data	122	1171	2198	3256
30	No range data	71	105	149	196
24	No range data	86	163	257	355
18	No range data	119	366	662	961
12	No range data	191	1411	2752	4096
6	No range data	468	9541	19047	28556
2	No range data	8132	2.8 E5	5.6 E5	8.4 E5
1	No range data	45772	1.7 E6	3.3 E6	5.0 E6

Table A.4-4. ATDRS-W Orbit Errors Using CEI (California) Without Range Data

Arc Length (hours)	Data Characteristics	Maximum Position Error in Definitive Period (m)	
30	No range	87	noise (78) site3 X (23)
24	No range	103	noise (97) site3 X (22)
18	No range	143	noise (133) site2 X (34)
12	No range	220	noise (213) site2 X (54)
6	No range	519	noise (514) site2 X (47)
2	No range	9741	noise (9740) site2 X (50)
1	No range	58025	noise (58024) site1 X (66)

Table A.4-5. ATDRS-W Orbit Errors Using CEI (California) With Range Data

Arc Length (hours)	Data Characteristics	Maximum Position Error in Definitive Period (m)	
30	Range data	59	solrad (43) rbias ws (25)
30	Solve range	52	solrad (22) site3 X (22)
24	Range data	40	rbias ws (22) A1 - Utl (18)
18	Range data	60	solrad (39) A1 - Utl (18)
12	Range data	62	site2 X (28) solrad (22)
6	Range data	102	site2 X (50) site1 X (36)
6	Solve range	118	site2 X (42) site1 X (31)
2	Range data	131	site2 X (47) site1 X (37)
1	Range data	159	site2 X (46) site1 X (36)

Table A.4-6. ATDRS-E Orbit Prediction Errors Using CEI (California)

Arc Length (hours)	Data Characteristics	Maximum Position Error (m) Def. Period	1 Day	2 Day	3 Day
30	Solve range	52	63	87	116
30	Range data	59	45	66	94
30	No range data	87	123	170	223

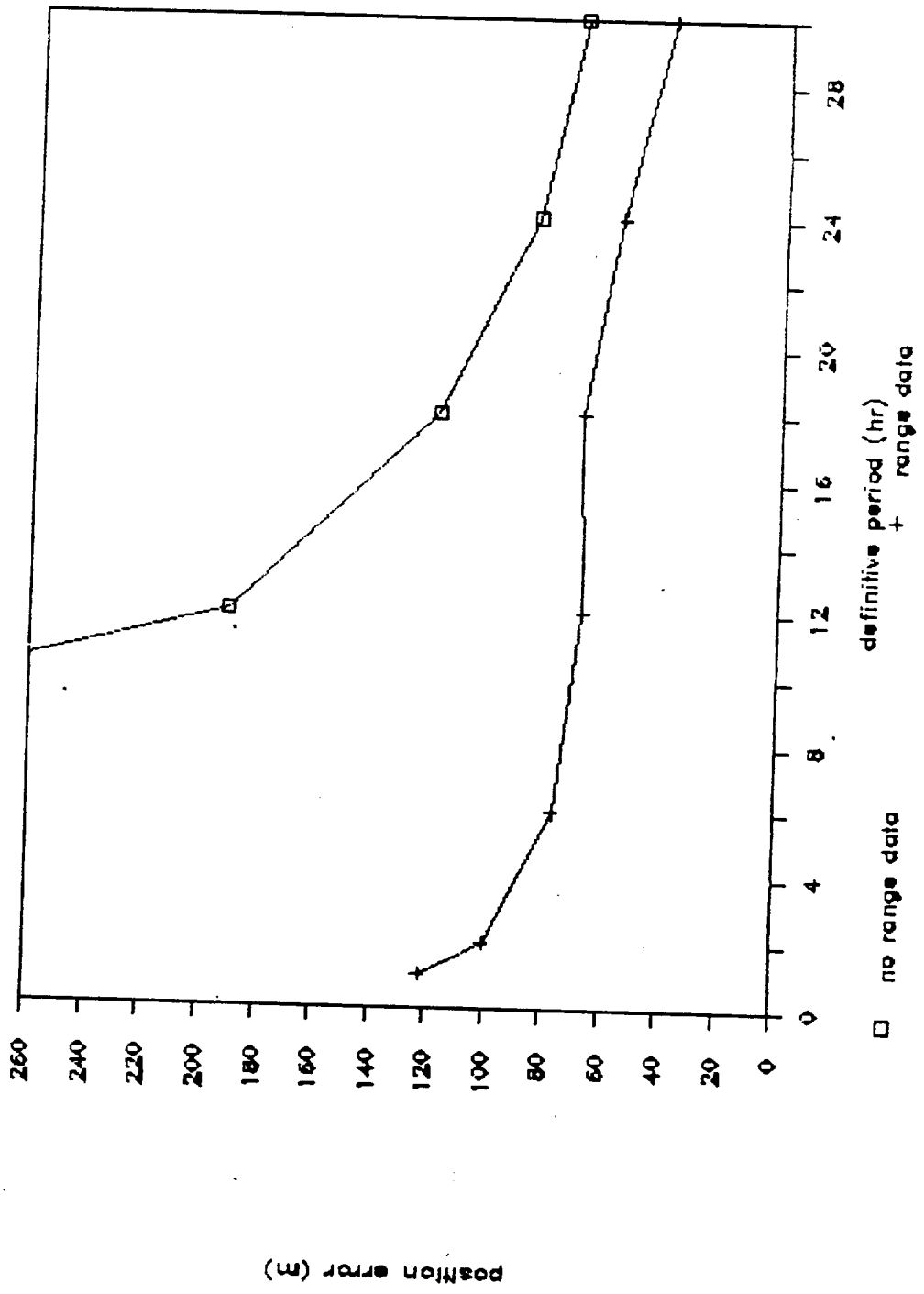

Figure A.4-1. Maximum Definitive Position Error for CEI ATDRS-E (Alabama)

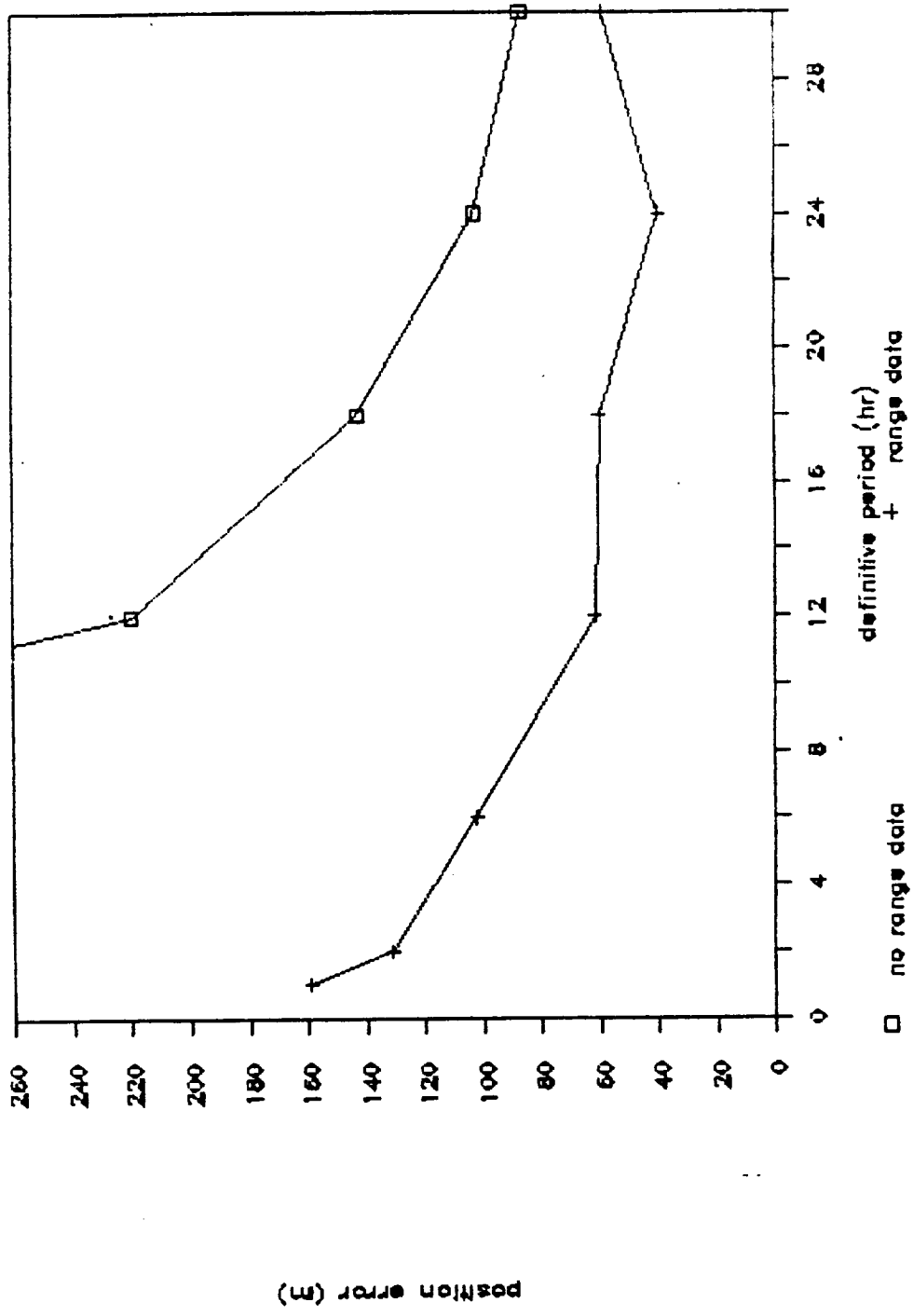

Figure A.4-2. Maximum Definitive Position Error for CEI ATDRS-W (California)

Table A.4-7. ATDRS-E Range Noise Study Using CEI (Alabama)

Arc Length (hours)	Data Characteristics	Maximum Position Error (m) Def. Period	1 Day	2 Day	3 Day
30	Solve range	44	47	57	73
30	Range sigma = 1 m	40	45	56	72
30	Range sigma = 3 m	38	43	57	74
30	Range sigma = 10 m	48	72	99	128
30	Range sigma = 30 m	57	87	122	158

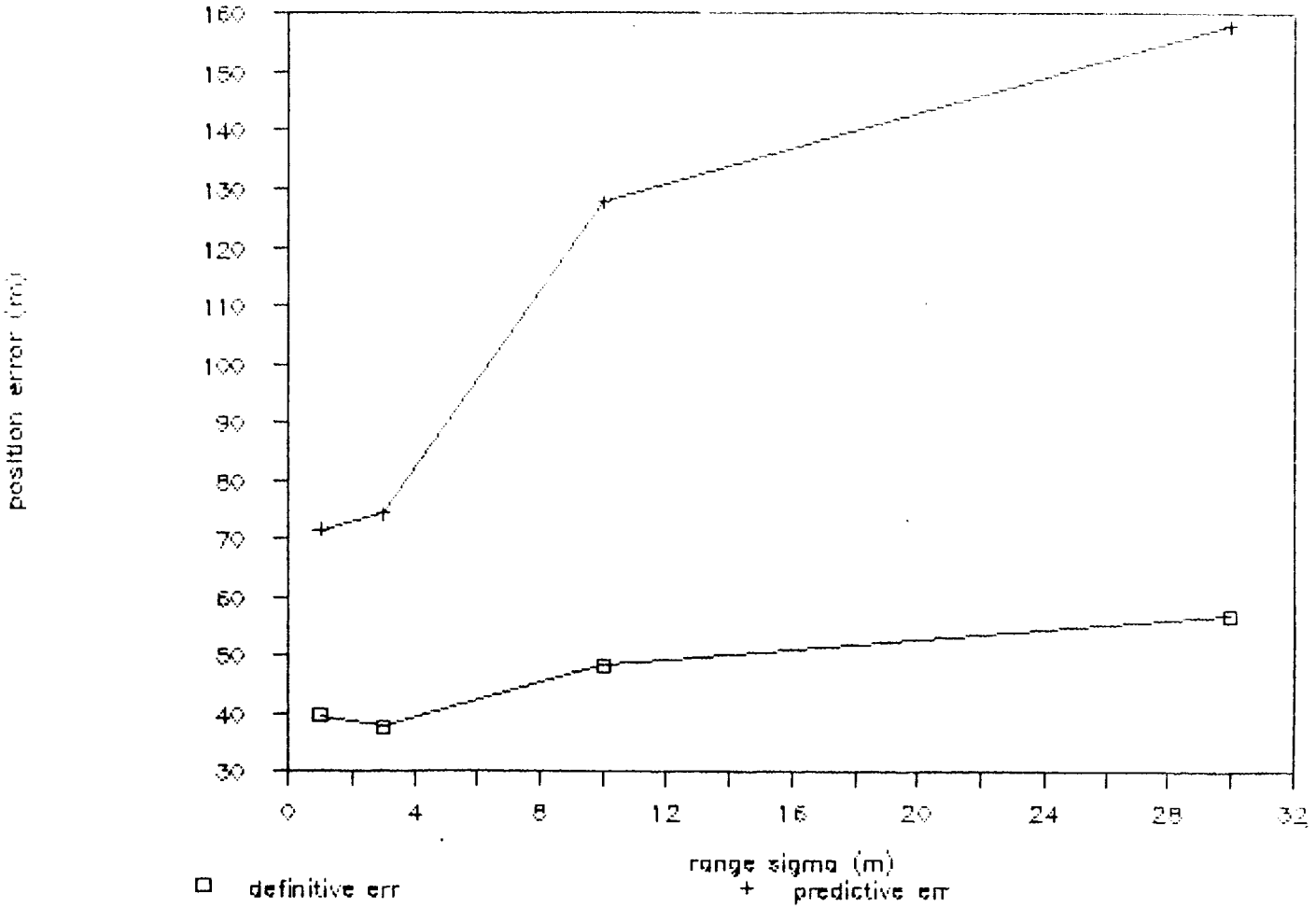

Figure A.4-3. Maximum Position Error for CEI (Alabama) (Fixed Range Bias)

A.5 VLBI-2S SIMULATION RESULTS

The VLBI-2S is another form of VLBI tracking system, which approaches the problem of remote-station clock synchronization from a third direction. The quasar-calibrated VLBI system solves for the remote clocks by observing quasars located near the ATDRSS satellites and using the known quasar positions to remove the clock differences from the solution. The CEI system connects all stations with cables so the clocks can be synchronized directly. The VLBI-2S system uses a second geostationary satellite, placed for these simulations midway in longitude between ATDRS-E and ATDRS-W. The system solves for the coordinates of both satellites and the remote clock biases simultaneously; the additional measurements on the second satellite provide the extra information needed to solve for the clock parameters.

The VLBI-2S results presented in the following were performed in two phases, Phase I and Phase II. Tables A.5-1 through A.5-14 display results found in Phase I of the study while the results in A.5-15 and A.5.16 were found in Phase II. The Phase II results for VLBI-2S should be considered definitive. The assumptions used in the two phases differed in two respects. First, an improved estimate of noise in the VLBI measurements was used in the Phase II results. Second, only measurements from independent baselines contributed to the second phase orbit determination results. The bases for this latter approach are presented at the start of Section 5. To speed up the analysis part of this project, the results of the Phase I were instrumental for determining which simulations were necessary for the Phase II study. We present the Phase I VLBI-2S OD and TR results because a more complete parameter study was done for Phase I than for Phase II.

A.5.1 PHASE I VLBI-2S TRACKING RESULTS

Tables A.5-1 through A.5-8 show various VLBI OD results for ATDRS-E. Table A.5-9 shows ATDRS-E OD results using a two-arc OD solution. Table A.5-10 shows ATDRS-E OD results using differential VLBI (DVLBI). Tables A-5.11 through A.5-14 show OD results for ATDRS-W.

If only VLBI measurements are used, the solution for all these parameters is not strong enough to determine the ATDRS orbit to the desired precision of 75-m maximum position error over the data arc. Tables A.5-1 through A.5-3 (Figure A.5-1) show the results for various data arcs when

Table A.5-1. ATDRS-E Orbit Errors Using a Dual-Satellite System (Varying Arc Lengths)

Arc Length (hours)	Data Characteristics	Maximum Position Error in Definitive Period (m)	
30	Range; solve clock a0	77	c2 trop (51) c1 trop (44)
24	Range; solve clock a0	104	c2 trop (70) c1 trop (60)
18	Range; solve clock a0	115	c2 trop (80) c1 trop (68)
12	Range; solve clock a0	96	c2 trop (67) c1 trop (58)
6	Range; solve clock a0	88	c2 trop (47) c1 trop (42)
2	Range; solve clock a0	146	noise (90) c1 ion (64)
1	Range; solve clock a0	330	noise (311) ce ion (60)

Table A.5-2. ATDRS-E Orbit Errors Using a Dual-Satellite System (30-Hour Arc Lengths)

Arc Length (hours)	Data Characteristics	Maximum Position Error in Definitive Period (m)	
30	Range; solve clock a0	77	c2 trop (51) c1 trop (44)
30	Range; solve clock a0, a1	89	c2 trop (62) c1 trop (53)
30	Range; solve all clocks	89	c2 trop (62) c1 trop (53)
30	Range; solve all clocks and solve solrad	90	c2 trop (63) c1 trop (54)
30	Range; solve clock a0 and solve troposphere	49	clk3 a1 (28) rbias (25)
30	Range; solve troposphere	84	clk3 a0 (53) clk2 a0 (45)

Table A.5-3. ATDRS-E Orbit Errors Using a Dual-Satellite System Without Range Data (Varying Arc Lengths)

Arc Length (hours)	Data Characteristics	Maximum Position Error in Definitive Period (m)	
30	No range; solve clock a0	106	c2 trop (70) c1 trop (60)
24	No range; solve clock a0	106	c2 trop (70) c1 trop (60)
18	No range; solve clock a0	108	c2 trop (71) c1 trop (60)
12	No range; solve clock a0	111	c2 trop (76) c1 trop (68)
6	No range; solve clock a0	135	c2 trop (77) c1 trop (66)
2	No range; solve clock a0	1055	noise (1049) c2 trop (75)
1	No range; solve clock a0	8968	noise (8967) c1 ion (88)

Table A.5-4. ATDRS-E Orbit Errors Using a Dual-Satellite System Without Range Data (30-Hour Arc Lengths)

Arc Length (hours)	Data Characteristics	Maximum Position Error in Definitive Period (m)	
30	No range; solve clock a0	106	c2 trop (70) c1 trop (60)
30	No range; solve clock a0, a1	104	c2 trop (70) c1 trop (60)
30	No range; solve all clocks	104	c2 trop (70) c1 trop (59)
30	No range; solve all clocks and solve solrad	104	c2 trop (70) c1 trop (59)
30	No range; solve clock a0 and troposphere	3797	clk2 a1 (2901) c1 ion (1510)
30	No range; solve all clocks and troposphere	2377	c1 ion (1740) noise (1162)

Table A.5-5. ATDRS-E Orbit Errors Using a Dual-Satellite System With Different Clock Models

Arc Length (hours)	Data Characteristics	Maximum Position Error in Definitive Period (m)	
6	Range; solve clock a0	88	c2 trop (47) c1 trop (42)
6	Range; apply clock a0 clk2a0 = 0.42, clk3a0 = 0.33	120	clk2 a0 (62) c2 trop (60)
2	Range; solve clock a0	146	noise (90) c1 ion (64)
2	Range; apply clock a0 clk2a0 = 0.42, clk3a0 = 0.33	115	clk2 a0 (58) c2 trop (54)
1	Range; solve clock a0	330	noise (311) ce ion (60)
1	Range; apply clock a0 clk2a0 = 0.42, clk3a0 = 0.33	115	clk2 a0 (58) c2 trop (54)

Table A.5-6. VLBI-2S Orbit-Prediction Errors for ATRS-E (30-Hour Arc Lengths)

Arc Length (hours)	Data Characteristics	Maximum Position Error (m) Def. Period	1 Day	2 Day	3 Day
30	Range data; solve clocks A0,A1	89	139	190	242
30	Range data; solve all clocks	89	138	189	241
30	Range data; solve troposphere	84	109	137	168
30	Range data; solve A0; solve troposphere	49	64	82	104
30	Range data; solve all clocks; solve solrad	90	140	191	243
30	No range data; solve all clocks; solve solrad	104	111	131	161
30	No range data; solve A0; solve troposphere	8099	8099	8121	8133
30	No range data	251	269	294	324
30	No range data; solve all clocks; solve troposphere	5178	5177	5176	5176
30	No range data; solve all clocks	104	104	106	114
30	No range data; solve clocks A0, A1	104	104	107	114

Table A.5-7. VLBI-2S Orbit-Prediction Errors for ATDRS-E (Varying Arc Lengths)

Arc Length (hours)	Data Characteristics	Maximum Position Error (m) Def. Period	1 Day	2 Day	3 Day
30	range data; solve clock A0	77	117	159	202
24	range data; solve clock A0	104	170	237	305
18	range data; solve clock A0	115	202	292	383
12	Range data; solve clock A0	96	185	277	369
6	Range data; solve clock A0	88	168	256	346
6	Range data	120	225	347	471
	TR Arcs				
2	Range data; solve A0 nominal clock A0 sigma	146	394	686	983
2	Range data; predicted clock A0 sigma(1)	116	397	736	1074
1	Range data; solve A0 nominal clock A0 sigma	330	69941	2933	4270
1	Range data; predicted clock A0 sigma(1)	115	836	1617	2400

NOTE: Clock sigmas of 0.42 and 0.33 meters were used. These sigmas were computed using a 30-hour data arc.

Table A.5-8. VLBI-2S Orbit-Prediction Errors for ATDRS-E Without Range Data

Arc Length (hours)	Data Characteristics	Maximum Position Error (m) Def. Period	1 Day	2 Day	3 Day
30	No range data; solve clock A0	106	125	157	194
24	No range data; solve clock A0	106	123	153	190
18	No range data; solve clock A0	108	134	175	223
12	No range data; solve clock A0	111	175	303	443
6	No range data; solve clock A0	135	1079	2136	3196
	TR Arcs				
2	No range data; solve A0; nominal clock A0 sigma	1055	29346	58443	87550
1	No range data; solve A0; nominal clock A0 sigma	8968	282835	562720	842675

Table A.5-9. VLBI-2S Orbit Errors Using Two Arc Solutions (30 Hours + 2 Hours)

Data Characteristics	Maximum Position Error (m) Def. Period	+6hr.	1 Day	2 Day	3 Day
ATDRS-E					
Range data; all global parameters; solve all clocks and troposphere using data from 1st arc only	34	71	206	401	596
Range data; all global parameters; solve all clocks and troposphere using data from both arcs	45	68	198	383	570
Range data; all global parameters; solve all clocks and troposphere and r bias using data from both arcs	880	888	941	1031	1144
ATDRS-W					
Range data; all global parameters; solve all clocks and troposphere using data from both arcs	56	75	193	375	561

Table A.5-10. ATDRS-E Orbit Errors Using the VLBI-2S System DVLBI Measurements

Arc Length (hours)	Data Characteristics	Maximum Position Error in Definitive Period (m)	
30	Range; solve satellite position	135	clk3 a0 (98) clk3 a1 (57)
30	Range; solve satellite position; solve clock A0	75	c2 trop (44) c1 trop (38)
30	Range; solve satellite position; solve troposphere	57	clk3 a0 (26) rbias ws (25)
30	Range; solve clock A0 solve troposphere	57	clk3 a1 (33) rbias ws (26)
2	Range; solve clock A0	171	noise (115) c1 ion (63)
2	Range; solve troposphere	775	noise (766) c1-ce z (51)
2	Range data	185	clk3 a0 (118) clk2 a0 (112)

Table A.5-11. ATDRS-W Orbit Errors Using the VLBI-2S System Without Range Data

Arc Length (hours)	Data Characteristics	Maximum Position Error in Definitive Period (m)	
30	No range; solve clock a0	104	c2 trop (65) c1 trop (64)
2	No range; solve clock a0	1086	noise (1081) c2 trop (69)
1	No range; solve clock a0	8864	noise (8864) c2 trop (69)

Table A.5-12. ATDRS-W Orbit Errors Using the VLBI-2S System With Range Data

Arc Length (hours)	Data Characteristics	Maximum Position Error in Definitive Period (m)	
30	Range; solve clock a0	84	c2 trop (53) c1 trop (52) c1 ion (20)
24	Range; solve clock a0	114	c2 trop (75) c1 trop (73) c2 ion (25)
18	Range; solve clock a0	124	c2 trop (83) c1 trop (80) c1 ion (26)
12	Range; solve clock a0	104	c2 trop (68) c1 trop (65) c1 ion (27)
6	Range; solve clock a0	101	c2 trop (47) cw ion (44) c1 ion (38)
2	Range; solve clock a0	150	noise (97) cw ion (65) c2 ion (48)
1	Range; solve clock a0	326	noise (310) cw ion (55) c2 ion (44)

Table A.5-13. ATDRS-W Orbit Errors Using the VLBI-2S System With Different Clock Models

Arc Length (hours)	Data Characteristics	Maximum Position Error in Definitive Period (m)	
6	Range; solve clock a0	101	c2 trop (47) cw ion (44)
6	Range; apply clock a0 clk2a0 = 0.44, clk3a0 = 0.41	160	clk2 a0 (94) c2 trop (89)
2	Range; solve clock a0	150	noise (97) cw ion (65)
2	Range; apply clock a0 clk2a0 = 0.44, clk3a0 = 0.41	158	clk2 a0 (90) c2 trop (83)
1	Range; solve clock a0	326	noise (310) cw ion (55)
1	Range; apply clock a0 clk2a0 = 0.44, clk3a0 = 0.41	155	clk2 a0 (87) c2 trop (81)

Table A.5-14. ATDRS-W Orbit-Prediction Errors Using the VLBI-2S System

Arc Length (hours)	Data Characteristics	Maximum Position Error (m) Def. Period	1 Day	2 Day	3 Day
30	Range data	84	84	84	130
30	No range data	104	115	135	162
24	Range; solve clock A0	114	114	119	193
18	Range; solve clock A0	124	124	146	242
12	Range; solve clock A0	104	104	144	241
6	Range data; predicted clock A0 sigma(1)	160	160	238	375
6	Range; solve clock A0	101	101	146	244
	TR Arcs				
2	Range data, solve A0; nominal clock A0 sigma	150	244	514	799
2	Range data; predicted clock A0 sigma(1)	158	297	616	947
2	Range data	150	244	514	799
2	No range data; nominal clock A0 sigma	1086	28410	57057	85714
1	Range data; solve A0 nominal clock A0 sigma	326	1119	2395	3698
1	Range data; predicted clock A0 sigma(1)	155	850	1712	2578
1	Range data	326	1119	2395	3698
1	No range; nominal clock A0 sigma	8864	275806	554114	832483

NOTE: Clock sigmas of 0.42 and 0.33 meters were used. These sigmas were computed using a 30-hour data arc.

Table A.5-15. **VLBI-2S ATDRS-E ORAN Simulation Result Summaries**

Arc Length	Data Characteristics	Definitive Accuracy (m)	Predictive Accuracy (m)
30	ATDRS-E+C; GTR Apply Troposphere Height Offset Largest Def. Errors: C2 Trop(41), C1 Trop(37)	67	100, 136, 181
30	ATDRS-E+C; GTR Solve Troposphere Height Offset Largest Def. Errors: Solrad C(48); Rbias(25)	62	64, 70, 80
30	ATDRS-E+C; GTR Apply Troposphere Height Offset Largest Def. Errors: C1 Trop(51), C2 Trop(45)	67	100, 136, 181
2	ATDRS-E+C; GTR Apply Troposphere Height Offset Largest Def. Errors: C2 Trop(43), C1 Trop(40)	77	99, 225
2	ATDRS-E+C; GTR Solve Troposphere Height Offset Largest Def. Errors: Rbias(25), A1-UT1(18)	47	51, 202

Table A.5-16. VLBI-2S ATDRS-W ORAN Simulation Result Summaries

Arc Length	Data Characteristics	Definitive Accuracy (m)	Predictive Accuracy (m)
30	ATDRS-W+C; GTR Apply Troposphere Height Offset	72	50, 79, 116
	Largest Def. Errors: C2 Trop(41), C1 Trop(37)		
30	ATDRS-W+C; GTR Solve Troposphere Height Offset	121	118, 122,131
	Largest Def. Errors: CW Ion(71), Solrad C(66)		
30	ATDRS-W+C; no GTR Apply Troposphere Height Offset	102	102, 106, 112
	Largest Def. Errors: C2 Trop(56), C1 Trop(51)		
30	ATDRS-W+C; no GTR Solve Troposphere Height Offset	6482	6484, 6491, 6493
	Largest Def. Errors: C1 Ion(5073), Solrad C(3208)		
2	ATDRS-W+C; GTR Solve Troposphere Height Offset	127	87, 251
	CW Ion(58), Solrad C(42)		
2	ATDRS-W+C; GTR Apply Troposphere Height Offset	99	75, 236
	C1 Trop(46), C2 Trop(54)		

NOTE: Prediction accuracies listed for 30 hr arcs are for 1, 2 and 3 days, respectively.

Prediction accuracies for 2 hr arcs are for 6 hours and 1 day, respectively.

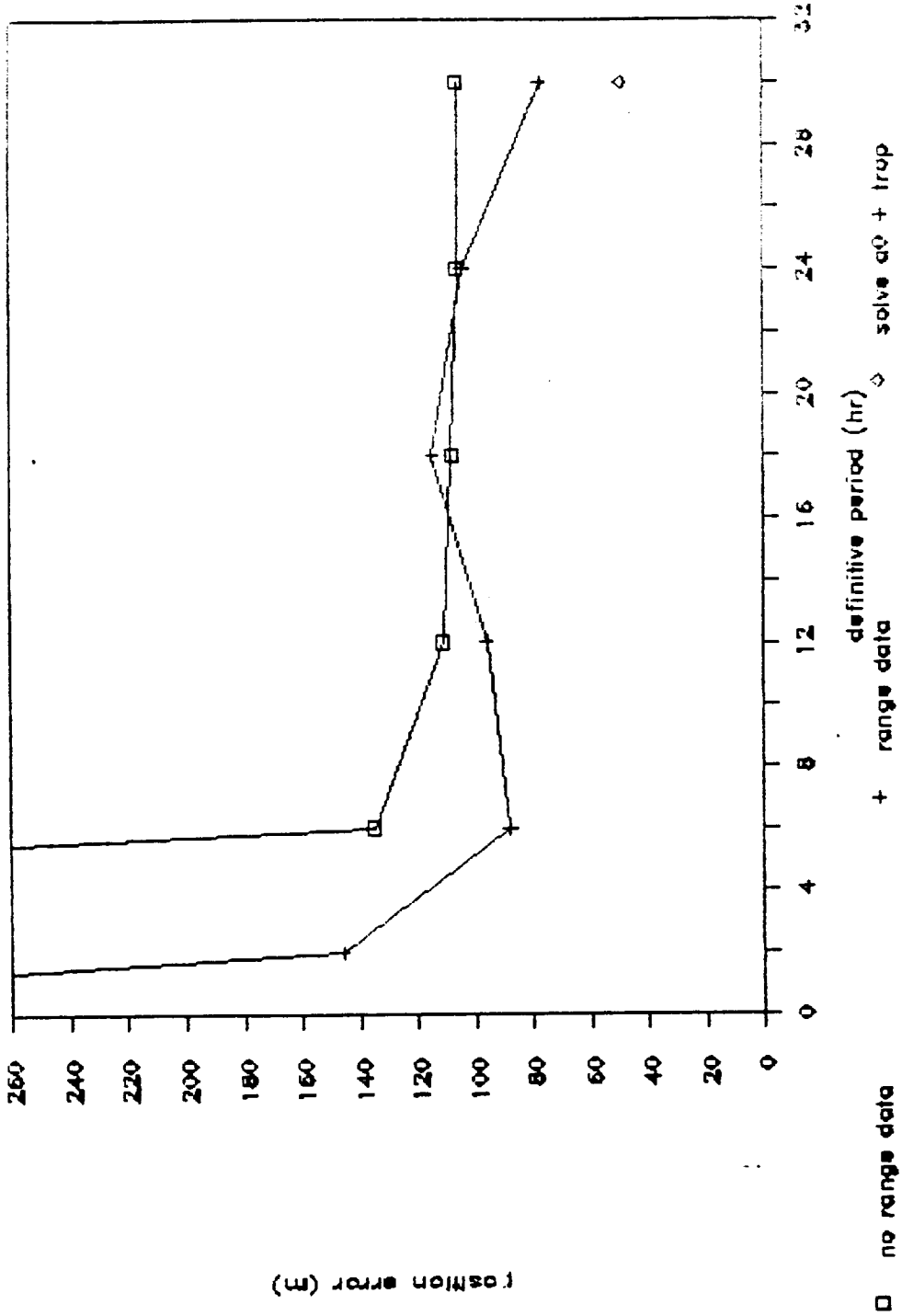

Figure A.5-1. Maximum Definitive Period Position Error for ATDRS-E Dual Satellite With and Without Range Data

ATDRS-E is tracked with only VLBI measurements and only the remote clock biases are calculated. None of the data arcs satisfies the orbital-position requirement. Table A.5-11 shows results for ATDRS-W with only VLBI measurements. Here the OD for ATDRS-W is acceptable for the 30-hour arc. The source of this improvement relative to ATDRS-E is the higher elevation of ATDRS-W as seen by the western tracking network, with the consequent reduction in the tropospheric errors that are the major error sources in this system.

Table A.5-6 shows various simulations for a 30-hour arc of VLBI measurements tracking ATDRS-E. This table shows that solving for additional clock parameters (linear and quadratic drifts with time) and for the solar radiation parameter improves the orbital solution only slightly; the dominant errors are still the troposphere errors. Attempts to solve for the troposphere parameters in addition to the clock parameters result in extremely poor solutions. Because the satellite is almost stationary with respect to the tracking station, there is little variation in its elevation; therefore, the troposphere errors are almost constant range biases. The clock-bias parameter also behaves as a range bias, so a simultaneous calculation for troposphere and clock bias cannot separate these parameters and results in a very poor solution.

When range measurements from WHS are added to the solution, the results are much better. Table A.5-1 and Figure A.5-1 show the results for various data arc for ATDRS-E tracked with VLBI and range measurements and solving for the clock bias. The 30-hour arc produces a maximum 77 m error, almost satisfying the OD criterion. Table A.5-2 shows what happens when other parameters are calculated (as in Table A.5-4 for the no range case) in the presence of range data. The best results are obtained when the remote clock bias and the troposphere parameters are solved for (see Figure A.5-1). The range data from White Sands allows the separation between the constant clock bias and the almost constant troposphere effects, giving a solution with only 49 m maximum position error.

Tables A.5-12 and A.5-13 and Figure A.5-2 show the results for ATDRS-W tracked with VLBI measurements and range from WHS using various data arcs. These results are much better than the ATDRS-E results, with all arcs from 6 hours to 30 hours giving maximum orbital position errors below 45 m. The superiority of these results is a consequence of the higher elevation of ATDRS-W at the tracking stations, which greatly reduces the tropospheric errors, the major source of error for this system.

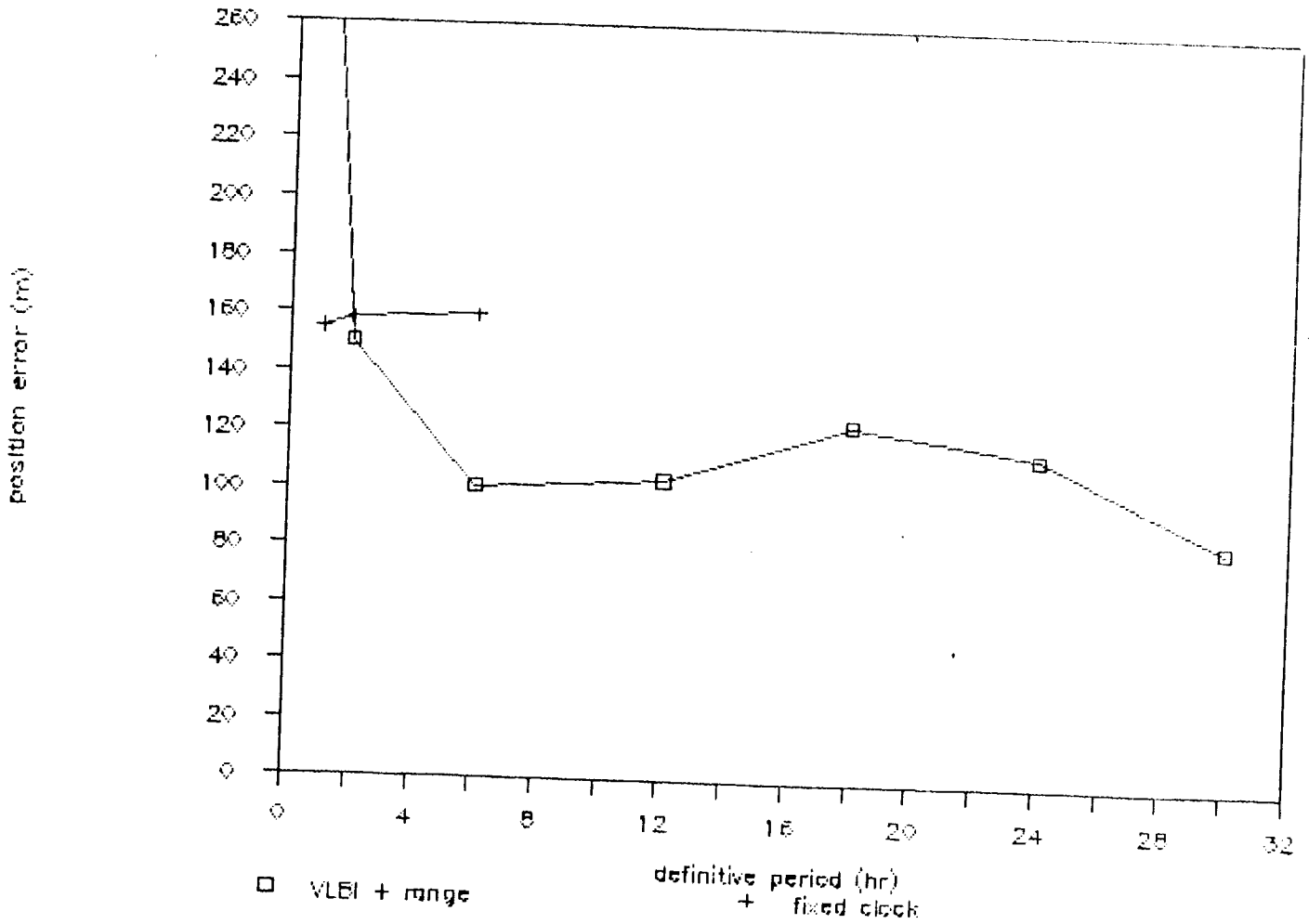

Figure A.5-2. Maximum Definitive Position Error for ATDRS-W Dual Satellite

Table A.5-5 compares the results for ATDRS-E from some short data arcs (1, 2, and 6 hours) with solved-for clock biases and results for arcs where the clocks are not solved for but values for clock-bias uncertainties determined on a 30-hour arc are applied as unmodelled parameters. These results are also plotted in Figure A.5-3. The rationale for this approach is that, at the time of a satellite maneuver, the satellite has been tracked for 30 hours, and the clocks have been solved to a certain level of accuracy. If the assumption is made that the clock synchronization will not change appreciably in the next few hours, the clock parameters determined during the previous 30 hours can be used, with no clock solution performed in the TR orbital solution. Applying unmodelled clock biases reduces the total position error for the noise-dominated 1- and 2-hour arcs but makes the 6-hour arc worse; in none of these cases is the total orbital error small enough to be acceptable. This same approach for the ATDRS-W satellite is shown in Table A.5-14 (and in Figure A.5-4) and is again a failure.

Another variation on the VLBI-2S system has been tried. This technique takes one VLBI measurement of the second satellite and combines it with a DVLBI measurement involving ATDRS and the second satellite. The DVLBI measurement is the difference between the time delay of signals from ATDRS as seen by two tracking stations and the time delay of signals from the second satellite as seen by the same two tracking stations. Subtracting these time delays may cancel some of the effects due to atmospheric refraction. Table A.5-10 shows the results obtained with the DVLBI measurements. The results obtained by solving for the troposphere parameters, either with or without the clock-bias parameter, provide good determination of the ATDRS-E orbit, with a maximum orbital error of 57 m. Two-hour arcs are still not acceptable in terms of orbit error. Figure A.5-4 compares the results obtained using the VLBI data with range, solving for clock bias, and the DVLBI measurements, solving for clock bias only and solving for clock bias and troposphere.

Another approach to the problem of TR using the VLBI-2S system assumes that TR will take place shortly after some event that requires a new orbit to be determined for the satellite (such as an orbital maneuver) and that this event will be preceded by a 30-hour tracking period. If this scenario is valid, a two-arc OD can be performed solving for ATDRS and the overhead satellite orbits before the event, using the 30-hour arc, and using a 2-hour arc after the event. The clock parameters and the troposphere parameters

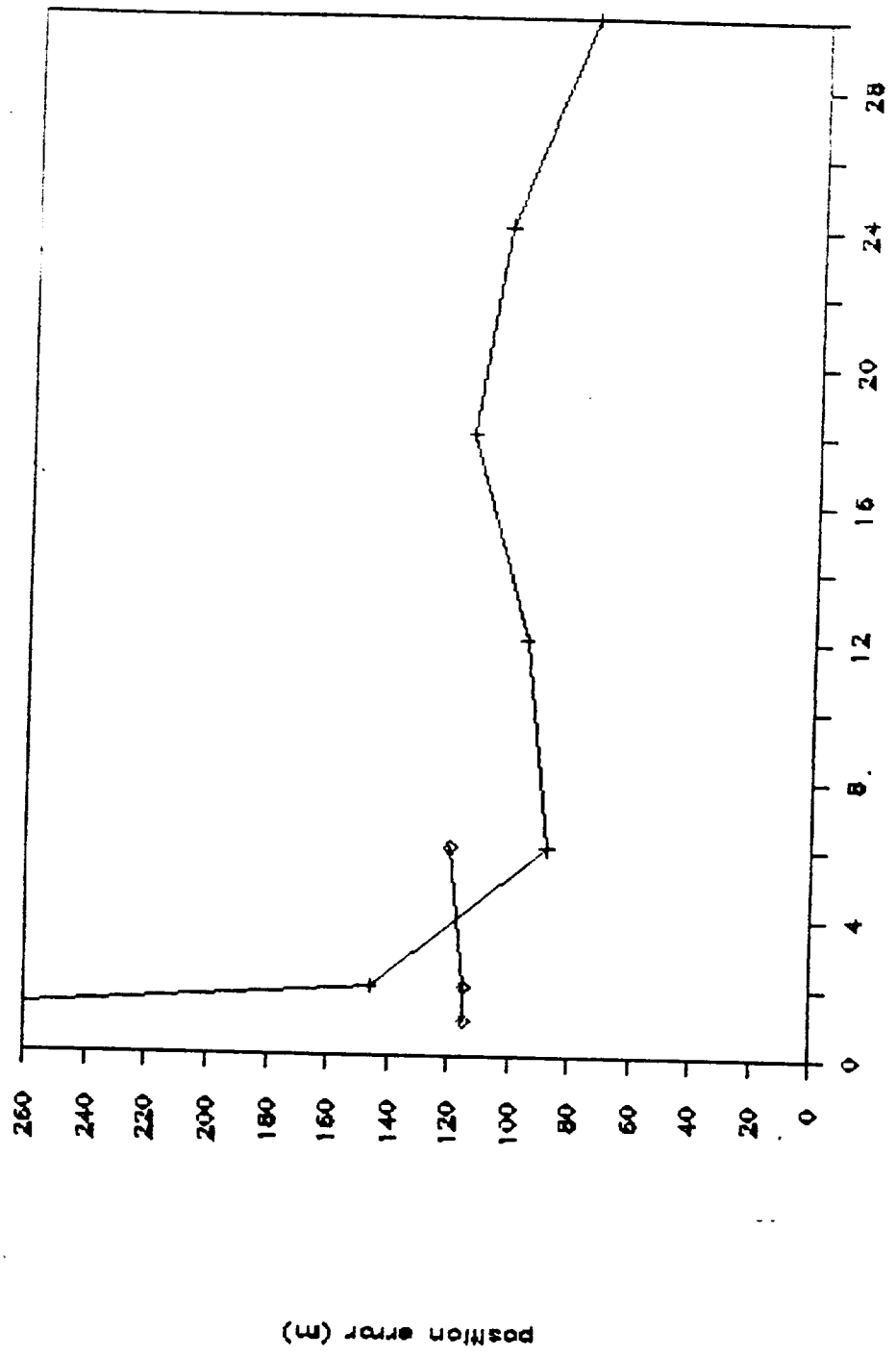

Figure A.5-3. Maximum Definitive Position Error for ATDRS-E Dual Satellite With and Without Clock Solutions

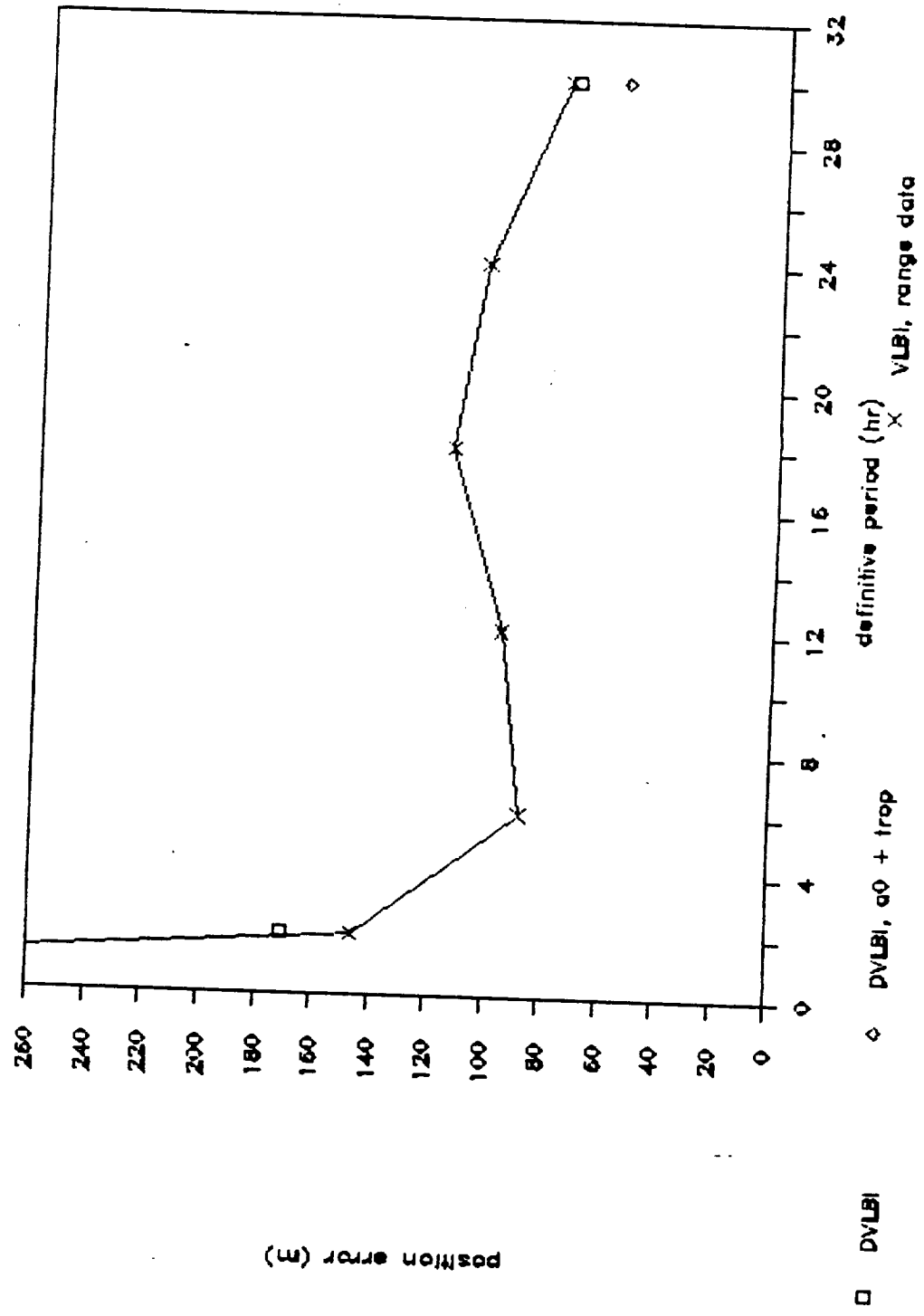

Figure A.5-4. Maximum Definitive-Period Position Error for ATDRS-E Dual Satellite--Comparison of DVLBI and VLBI-2S

may be calculated using data taken from either the first arc only or from both arcs. This approach allows determination of the clock parameters from the long arc before the event and does not require the assumption that the clock parameters will remain constant into the future during the TR arc (as is done in simulations shown in Table A.5-5); these parameters can be determined using data from this period.

The results obtained using this approach are shown in Table A.5-9. The difference in the first two runs is that the first run solves for the clock and troposphere parameters using only data in the first arc, whereas the second run uses data from both arcs. Using data from both arcs gives a slightly worse definitive-position error, but all errors after that are slightly smaller than those obtained using only one arc. The overall difference in the results for these cases is not significant, and both runs give acceptably small errors for the definitive period and for 8 hours thereafter. Because the major source of error in the second run was the range bias error, an attempt was made to solve for the range bias-in the third case. This obviously does not work because all of the solved-for parameters--clock bias, troposphere, and range bias--are similar to range biases and are highly correlated with the range bias. Solving for all these correlated parameters simultaneously is not possible, and it increases the noise tremendously. The fourth run shows the results for ATDRS-W using both arcs for the solution of the clock and troposphere parameters.

In summary, the VLBI-2S system is very complex, and several approaches to using it remain to be studied. The most promising technique for the long arc, nominal OD uses range data from WHS and requires that the clock parameters and (especially) the troposphere parameters be calculated. The results from this VLBI-2S Phase I study show that this provides acceptable OD for both ATDRS-E and ATDRS-W. The technique of solving for the clock and troposphere parameters with a 30-hour arc followed by a 2-hour arc provides acceptable levels of satellite-position error in short-arc TR.

A.5.2 SECOND PHASE VLBI-2S TRACKING STUDIES

During the second phase of this study, the VLBI-2S (two satellite) system was studied in greater detail. In particular, the measurement noise values used in the simulations and other aspects of the ORAN simulation method were reviewed and modified.

ORAN results presented in this section are based on the noise values presented in Table A.5-17.

Table A.5-17. VLBI-2S Phase II Noise Values

Baseline	Satellite	Noise value
C1-C2	E	.074
C1-CE	E	.056
C2-CE	E	.060
C1-C2	C	.023
C1-CW	C	.022
C1-CE	C	.022
C2-CE	C	.023
C2-CW	C	.023
C1-C2	W	.078
C1-CW	W	.061
C2-CW	W	.062

A.5.2.1 VLBI-2S ORAN Clock Modelling

In the VLBI-2S tracking system, each station has an its own clock which is not calibrated in advance to support the VLBI orbit determination solution. For VLBI, the individual station times need only be determined relative to each other rather than to some absolute time standard. The clock biases and rates must therefore be solved for as a part of the orbit determination process. The assumed quadratic model for the clock offsets implies:

$$t_n' = A_o + A_1 t\ A_2 t^2$$

$$T_n' = t_n' - t = A_0 + (A_1 - 1)t + A_2 t^2$$

where t_n' is the relative time for each station n and t is the absolute time. The Tn' represent the station clock errors. A_o, A_1, A_2 are the parameters to be determined.

Since only relative time is required we choose $t_1' = t \Rightarrow T_1' = 0$. Thus, quadratic clock offsets can be modeled for three stations can be modeled by just two sets of three parameters.

A.5.2.2 Number of Baselines Used in ORAN Simulations

VLBI measures the range difference from the satellite to stations located at both ends of a given baseline. Suppose that we are using a three station (S1, S2, S3) interferometric network as shown in the figure below. The station clock errors propagate into the VLBI measurements as follows. On the baseline between S1 and S2, the S1 and S2 clock errors would be applied except that we have chosen the former to be zero. Similarly, only S3 clock errors are applied to the S1-S3 baseline. For the third (S2-S3) baseline both S2 and S3 clock errors need be applied which result in interferometric measurement clock errors that are proportional to the difference of the clock errors of each of the stations.

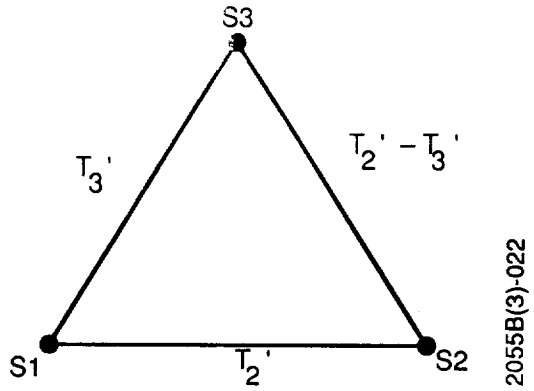

Figure A.5-5 Generic Three Station VLBI Network and Delays

In modeling interferometric measurements, we assign a noise value to each measurement. Noise derives from non-modeled random varying effects. These effects may be classified as either baseline dependent or station dependent. Types of station dependent noise include propagation delays in the troposphere and ionosphere as well as timing errors. The baseline dependent errors arise from limited SNR in detecting both the satellite signals and the phase calibration signals.

For data with low thermal noise, the baseline dependent errors are negligible. In that case the delays around a closed loop add to zero, i.e.

$$D_{12} + D_{23} + D_{31} = (r_1 - r_2) + (r_2 - r_3) + (r_3 - r_1)$$

where D_{mn} are the delay differences found on each baseline and r_k are the site delays. It follows that the delay

measurements from any one station to all others suffice to predict the measurements of the remaining baselines. This means that the input measurements are correlated. This is true even in the case that the station dependent noise is quite large.

For the conceptual two satellite system, a typical noise budget is:

receiver noise	2ps	baseline
phase cal noise	10ps	baseline
ionosphere noise	15ps	station
troposphere noise	60ps	station

In this case, the station noise dominates by factor of five or six over the baseline noise. ORAN modeling using only two of three baselines should thus be a good approximation of the actual system, giving, in this case, only a modest underestimate of performance. Addition of the third baseline should give an overestimate of performance due to the neglect of large correlations among the input measurements.

For variants of the two satellite system where the thermal noise (i.e. baseline dependent) dominates such as interferometric GPS observations, all baselines should be included as the input observations are largely uncorrelated.

In the case of the three satellite variation of VLBI-2S, four ground stations (C1, C2, CE, CW) are used to observe three satellites (ATDRS-E, ATDRS-W, and ATDRS-C). All stations observe ATDRS-C and the measurements are dominated by station noise. In this case only three baselines should be used (the ones connected to C1).

A.5.2.3 Phase II ATDRS VLBI-2S ORAN Results

The results for the second phase of VLBI-2S simulations for both ATDRS-E and ATDRS-W satellites are listed below. As before, OD solutions consisted of 30 hours of VLBI tracking on both the ATDRS-E(W) and ATDRS-C satellites. Post-maneuver ATDRS TR solutions consisted of 30 hours of tracking of both satellites followed by 2 hours of tracking of ATDRS-E(W). This method provided more data for the determination of clock parameters required for accurate TR solutions. The parameters that varied in this study were the use of ranging (GTR) and whether the troposphere height was solved for.

While encouraging in terms of raw OD numbers, the VLBI-2S solutions are also seen to exhibit tenuous stability. For example, solving for troposphere height without GTR results in orbit errors in excess of 5km for ATDRS-W. Due to unknown aspects of the solution, solving for the troposhere height (with GTR) improves the solution for ATDRS-E and degrades it for ATDRS-W. The latter solution exhibited large correlations (>.9999) in the solution of some parameters and also the ATDRS-C orbit determination was severely degraded.

In some cases for ATDRS-W the tracking results, i.e. the maximum error during that period, for the first predictive period is sometimes better than the definitive period. This situation arises when the dominant errors for a given simulation are periodic and do not have maxima during the first predictive period.

A.6 VLBI-3S SATELLITE SYSTEM RESULTS

A variant of the VLBI-2S system is what may be termed the three satellite system VLBI-3S. Operationally, data is taken in the same way and by the same equipment as for conventional VLBI-2S. The difference between these approaches lies entirely in the method of tracking data analysis. In the three satellite variation, the data from both ATDRS-E and ATDRS-W are integrated with the data from a third satellite, ATDRS-C. The rationale behind this approach stems from the fact that in conventional VLBI-2S method of solution, the orbit elements of ATDRS-C and the relative clock offset for the two central stations are determined twice, once in the solution for ATDRS-E and again for the solution of ATDRS-W. Uniting these separate solutions into a single solution determination should yield better determinations overall.

Examination of the OD and TR results for this alternative shows marked improvement over that for conventional VLBI-2S orbit solutions (see Table A.6-1). OD solutions do not require GTR from White Sands except to meet accuracy goals for the longest prediction periods. GTR is required to ensure accurate TR solutions as these TR solutions will require determination of troposphere height.

A.7 Ku-BAND BEACON INTERFEROMETRY RESULTS (VLBI-Ku)

A short study was undertaken to assess the orbit accuracies that would be obtained if a Ku-band beacon were available of sufficient band with for ATDRS tracking. The principal advantage of such a VLBI-Ku system over the considered VLBI-2S system is that ground station positions are no

Table A.6-1 VLBI-3S ORAN Simulation Summary

Arc Length	Data Characteristics	Definitive Accuracy (m)	Predictive Accuracy (m)
30	VLBI-3S ATDRS-E+W+C; no GTR Apply Troposphere Height Offset		
	ATDRS-E	67	68 72 82
	ATDRS-W	70	69 75 85
	Largest Definitive Errors:		
	ATDRS-E - Iono(36), Trop (35) ATDRS-W - Iono(38), Trop (37)		
2	VLBI-3S ATDRS-E+W+C; GTR Solve Troposphere Height		
	ATDRS-E	41	73 217
	ATDRS-W	68	85 217
	Largest Definitive Errors:		
	ATDRS-E - Rbias(25), Al-UT1(18) ATDRS-W - Solrad(26), Rbias(37)		

NOTE: Prediction accuracies listed for 30 hr arcs are for 1, 2 and 3 days, respectively.

Prediction accuracies for 2 hr arcs are for 6 hours and 1 day, respectively.

longer restricted to the SGL footprint. By using longer baseline lengths, more accurate tracking should result, even in the presence of greater signal noise.

The considered system uses the so called IRIS network: Westford, MA; Richmond FL; and Fort Davis, TX. A system noise somewhat larger than that for VLBI-2S was chosen somewhat arbitrarily. Otherwise, the system resembles that of VLBI-2S. Only tracking of the ATDRS-E was considered.

As shown in Table A.7-1, the OD results for ATDRS-E were outstanding both for the predictive and definitive periods demonstrating the power of the VLBI technique when baselines of sufficient length are used. The results for TR were not satisfactory as the 75 meter study accuracy goal was maintained only for 4 hours in the predictive period.

Table A.7-1 VLBI-Ku ATDRS-E Run Result Summaries

Arc Length	Data Characteristics	Definitive Accuracy (m)	Predictive Accuracy (m)
30	ATDRS-E+C; no GTR Apply Troposphere Height Offset Largest Def. Errors: A1-UT1(18), FTD Ion(8)	23	29, 43, 59
2	ATDRS-E+C; no GTR Apply Troposphere Height Offset Largest Def. Errors: Noise(24); A1-UT1(18)	36	122, 877

NOTE: Prediction accuracies listed for 30 hr arcs are for 1, 2 and 3 days, respectively.

Prediction accuracies for 2 hr arcs are for 6 hours and 1 day, respectively.

A.8 VLBI AIDED BY HYBRID INTERFEROMETRIC TRACKING OF GPS

The VLBI-GH (hybrid VLBI) system calibrates the conceptual network clocks through tracking of the planned constellation (including spares) of 24 GPS satellites. It differs from

the VLBI-GC in the method of GPS satellite tracking. The carrier phase of the L1 and L2 downlinks is used for generation of the phase observable. Group delay is used at start of each pass of each GPS satellite to establish the starting phase bias. Because two frequencies are used, it is assumed that the ionosphere delay errors are completely calibrated and thus are not applied in the ORAN error analysis.

The VLBI data type is used for the GPS measurements in the ORAN simulations. Both a range difference noise (5 cm) and range difference bias (15 cm) were assumed for the interference measurement. As is the case for VLBI-GC, the ATDRS-E and ATDRS-W satellites are tracked in the same manner as for the VLBI-2S system.

The VLBI-GH OD scenario consists of 48 hours of GPS tracking with the last 30 of which either the ATDRS-E or ATDRS-W is tracked. The VLBI-GH TR scenario is the same except the ATDRS is tracked only for the last 2 hours of GPS tracking.

Generally, the results displayed in Tables A.8-1 and A.8-2 show that the GPS satellites provide adequate calibration for the station clocks required for accurate ATDRS tracking. Orbit determinations of of the GPS satellites themselves are always less than 40 m, 3 sigma. Correlations between solved for clocks and troposphere height are always less than .99.

OD definitive period results for the ATDRS showed that ATDRS-E, the 75 m tracking goal is nearly met without GTR ranging for both ATDRS-E and ATDRS-W. This result was obtained by the solution of troposhere height for each ground station. With the addition of GTR, the tracking goal for definitive period is met for VLBI-GH.

OD predictive period results showed that the definitive period tracking accuarcies were generally well maintained into the predictive period when GTR was not used. Although GTR improves definitive period performance, predictions based on orbit determinations using range data degraded more quickly than those that did not. It is likely that more studies of this technique would reveal optimal use of ranging data in such orbital solutions.

TR results do not meet the tracking goals for either the definitive or predictive period. The dominant errors were systematic in nature due to unmodelled ionosphere path delays.

Table A.8-1 VLBI-GH ATDRS-E Run Result Summaries

Arc Length	Data Characteristics	Definitive Accuracy (m)	Predictive Accuracy (m)
30	ATDRS-E+C; No GTR Apply Troposphere Height Offset Largest Def. Errors: C1 Ion(56), C2 Ion(36)	02	91, 93, 96
30	ATDRS-E+C; No GTR Solve Troposphere Height Offset Largest Def. Errors: C1 Ion(51), CE Ion(37)	77	78, 80, 82
30	ATDRS-E+C; GTR Solve Troposphere Height Offset Largest Def. Errors:	Results Pending	
30	ATDRS-E+C; GTR Apply Troposphere Height Offset Largest Def. Errors: C1 Ion(38), C2 Ion(30)	66	91, 123, 158
2	ATDRS-E+C; GTR Solve Troposphere Height Offset Largest Def. Errors C2 Ion(46), C1 Ion(40)	89	123, 378

Table A.8-2 VLBI-GH ATDRS-W Run Result Summaries

Arc Length	Data Characteristics	Definitive Accuracy (m)	Predictive Accuracy (m)
30	ATDRS-W+C; No GTR Apply Troposphere Height Offset Largest Def. Errors: C2 Ion(62), C2 RDiffBias (26)	90	93, 98, 105
30	ATDRS-W+C; No GTR Solve Troposphere Height Offset Largest Def. Errors: CW Ion(46), C2 Ion(43)	82	81, 81, 83
30	ATDRS-W+C; GTR Solve Troposphere Height Offset Largest Def. Errors: C1 Ion(30), A1-UT1(18)	46	49, 62, 82
30	ATDRS-W+C; GTR Solve Troposphere Height Offset Largest Def. Errors:	Results Pending	

NOTE: Prediction accuracies listed for 30 hr arcs are for 1, 2 and 3 days, respectively.

Prediction accuracies for 2 hr arcs are for 6 hours and 1 day, respectively.

A.9 VLBI AIDED BY CODED GPS TRACKING RESULTS

The VLBI-GC system calibrates the conceptual network station clocks by observation of the pseudorandom coded signal from the constellation of 24 GPS satellites. To account for the unknown clock bias between the satellite and ground station clocks, a range difference data type (i.e. VLBI) is used in the ORAN simulations. Both a range difference noise and bias were assumed for the pseudorange. The very same ORAN setups are used as for VLBI-GH except that the noise and bias values for the GPS measurements are different. The ATDRS satellites are tracked in the same manner as for the VLBI-2S system except that the second satellite (ATDRS-C) is not tracked.

The VLBI-GC OD scenario consists of 48 hours of GPS tracking with the last 30 of which either the ATDRS-E or ATDRS-W is tracked. The VLBI-GC TR scenario is the same except the ATDRS is tracked only for the last 2 hours of GPS tracking.

The results shown in Table A.9-1 are very similar to that found for VLBI-GH. This is not surprising given that the only difference in the corresponding simulations is the noise and bias error levels. The ATDRS orbits are determined to the desired 75 m accuracy only using GTR to White Sands.

A.10 ATDRS TRACKING USING CLOCKS CALIBRATED BY GPS TIME TRANSFER

The VLBI-GT system tracks the ATDRSS satellites in a way similar to that of the VLBI-2S system except that only the subject satellite is tracked. The station clocks are calibrated through direct time transfer from GPS satellites.

Only one simulation run was made using this system because the results, as shown in Table A.10-1, fell far short of the goals of this study.

Table A.9-1. VLBI-GC ATDRS-E Run Result Summaries (1 of 2)

Arc Length	Data Characteristics	Definitive Accuracy (m)	Predictive Accuracy (m)
30	ATDRS-E+C; No GTR Apply Troposphere Height Offset Largest Def. Errors: C1 Ion(58), C2 Ion(38)	91	93, 95, 98
30	ATDRS-E+C; No GTR Solve Troposphere Height Offset Largest Def. Errors: C1 Ion(51), CE Ion(37)	75	76, 78, 80
30	ATDRS-E+C; GTR Solve Troposphere Height Offset Largest Def. Errors: C1 Ion(34), C2 Ion(28)	61	83, 113, 144
2	ATDRS-E+C; GTR Solve Troposphere Height Offset Largest Def. Errors: C2 Ion(45), C1 Ion(40)	80	112, 358
30	ATDRS-W+C; No GTR Apply Troposphere Height Offset Largest Def. Errors: C1 Ion(51), C2 Ion(45)	91	93, 98, 105
30	ATDRS-W+C; No GTR Solve Troposphere Height Offset Largest Definitive Errors: CW Ion(45), C2 Ion(42)	80	79, 79, 80

Table A.9-1. VLBI-GC ATDRS-E Run Result Summaries (2 of 2)

Arc Length	Data Characteristics	Definitive Accuracy (m)	Predictive Accuracy (m)
30	ATDRS-W+C; GTR Apply Troposphere Height Offset Largest Def. Errors: C1 Ion(28), C2 Ion(22)	51	49, 62, 83
2	ATDRS-W+C; GTR Solve Troposphere Height Offset Largest Def. Errors:		

NOTE: Prediction accuracies listed for 30 hr arcs are for 1, 2, and 3 days, respectively.

Prediction accuracies for 2 hr arcs are for 6 hours and 1 day, respectively.

Table A.10-1. VLBI-GT ATDRS-E ORAN Simulation Results

Arc Length	Data Characteristics	Definitive Accuracy (m)	Predictive Accuracy (m)
30	ATDRS-E+C; No GTR Apply Troposphere Height Offset Largest Def. Errors: Clock3(158), C1 Trop(48)	185	218, 271, 335

A.11 BASELINE PRTS SIMULATION RESULTS

Baseline PRTS uses one-way ranging from a master tracking station located at WHS to various remote tracking stations. The special signal structure of PRTS is supposed to permit the synchronization of the remote station clocks to the master station and is claimed to have other desirable features, such as the elimination of ionospheric effects on the measurements.

PRTS uses two kinds of one-way ranges: a range measurement from a master station to ATDRS to a remote station (forward measurements) and a range measurement from the remote station to ATDRS to the master station (return measurements). When both of these measurements are combined, the remote-station clocks may be synchronized with the master-station clock. These two measurements have been simulated in ORAN and are used to solve for the remote-station clocks in the simulations. The treatment in ORAN of this feature and of others unique to PRTS is described in Section A-2.2.2.

Operation of PRTS is envisioned to depend mainly on frequent forward measurements for OD and to use infrequently scheduled pairs of forward and return measurements for the determination of the remote-station clock biases (linear and quadratic terms in the time variation of the clocks are assumed to be zero). For all the simulations here, forward measurements were scheduled for a 5-minute period at the start of every hour, taken at a rate of one measurement every 30 seconds. The pairs of forward and return measurements used for the clock solution were similarly scheduled, except that they were made only every 12 hours instead of every hour. Because the method of solving for the clock in PRTS tends to decouple the orbit and the clock determinations, the forward measurements not used in the clock solution had unmodelled clock errors assigned to them. The magnitude of these errors was 0.25, approximately the uncertainty in the clock solution for a 30-hour arc.

In all cases in this simulation, there are three remote stations and the master station at WHS. Because one of the remote stations in each case is located at WHS, it is assumed that this station's clock is perfectly synchronized to the master station; therefore, no clock bias was calculated for it.

In addition to the remote station clock biases, PRTS has signal delay uncertainties in the ATDRS transponder and in

the master and remote station electronics. These delays were modeled as range biases in this simulation, with a 6-m (20 ns time delay) bias always applied to the master-station-to-ATDRS link and a 3-m (10 ns time delay) bias always applied to each remote-station-to-ATDRS link. These biases are the most significant error parameters in the simulation.

PRTS OD performance results are summarized in Tables A.11-1 through A.11-4, where Tables A.11-3 and A.11-4 consider PRTS system performance when the number of stations is reduced from three to two by eliminating one of the remote stations. The ORAN error budget is summarized in Tables A.2-10 and 4-4.

All the tables indicate the maximum definitive period 3-sigma error over either a 30-hour or 2-hour tracking arc. For the 30-hour tracking arcs, the remote station clock biases are solved-for; for the 2-hour arcs, an unmodelled clock bias of 0.25 m is applied. This bias is comparable to the clock solution obtained over a 30-hour arc; use of an applied clock bias for the 2-hour arc thereby models estimation of the clock biases over a 30-hour arc immediately prior to the maneuver.

For all the PRTS networks, the maximum definitive period error over a 30-hour tracking arc is better than (less than) this study's 75 m (3-sigma) goal. Trajectory recovery performance over a 2-hour tracking arc, however, only meets this goal for the 3-station login baseline PRTS networks. The dominant error source is in almost all cases the range biases to the PRTS tracking stations, implying that further system resolution of electronic and propagation delays would improve PRTS OD performance. Previous runs with different PRTS ORAN error budgets than that presented in Section 4 also reveal that performance is generally somewhat sensitive to the level of range-rate noise, although, as seen here, noise is not a dominant error contributor.

Predictive period performance is represented by the maximum 3-sigma position error for predictive periods after the end of the definitive tracking period. For 2-hour trajectory recovery tracking arcs, the most important predictive periods are 6, 12, and 24 hours after the end of the definitive arc as further data is collected to allow batch processing of a definitive 30-hour arc. As shown in the tables, only the 3-station long baseline PRTS networks are able to maintain predictive period performance less than the 75 m over 24 hours.

Table A.11-1 PRTS OD Performance for ATDRS-E (3 σ)

BASELINE PRTS

	SHORT BASELINE (GSFC, MIL, WHS)		INTERMEDIATE BASELINE (ACN, GSFC, WHS)		LONG BASELINE (REY, ACN, WHS)	
MAXIMUM DEFINITIVE PERIOD ERROR (m)	30 HRS	2 HRS	30 HRS	2 HRS	30 HRS	2 HRS
TOTAL:	58.18	271.44	31.62	106.42	33.57	40.71
DOMINANT ERROR SOURCES:	36.04 (GSFC RANGE) 28.36 (WHSK RANGE)	194.06 (MIL RANGE) 125.82 (WHS RANGE)	21.71 (WHSK RANGE) 18.40 (A1–UT1)	70.41 (GSFC RANGE) 66.87 (WHS RANGE)	18.40 (A1–UT1) 17.85 (WHS RANGE)	23.12 (REY RANGE) 18.99 (WHS RANGE)
MAXIMUM PREDICTIVE PERIOD ERROR (m)						
6 HR. TOTAL:	–	279.15	–	91.41	–	39.85
12 HR. TOTAL:	–	338.03	–	121.21	–	54.05
1 DAY TOTAL:	59.83	375.69	47.26	140.38	54.01	70.74
2 DAY TOTAL:	65.46	509.68	68.37	189.85	78.87	118.27
3 DAY TOTAL:	74.12	655.43	91.08	245.66	105.08	169.14
DURATION OF ACCURATE ORBIT PREDICTION* (MINUTES)	6120+	0	4920	0	4500	1980

*INDICATED VALUE IS THE TIME FOR WHICH A TRACKING ACCURACY (3σ) ≤ 75 m IS MAINTAINED

07/28/89 MIS83P\AK7395

Table A.11-2 PRTS OD Performance for ATDRS-W (3 σ)

BASELINE PRTS

	SHORT BASELINE (VAN, WAS, WHS)		INTERMEDIATE BASELINE (HAW, WAS, WHS)		LONG BASELINE (AMS, GWM, WHS)	
MAXIMUM DEFINITIVE PERIOD ERROR (m)	30 HRS	2 HRS	30 HRS	2 HRS	30 HRS	2 HRS
TOTAL:	65.00	625.36	53.10	119.49	33.99	44.58
DOMINANT ERROR SOURCES:	40.28 (SOLRAD) 28.95 (WAS RANGE)	463.32 (VAN RANGE) 312.44 (WHS RANGE)	35.28 (SOLRAD) 18.53 (WHSK RANGE)	80.13 (WAS RANGE) 65.51 (WHS RANGE)	18.40 (A1–UT1) 16.54 (GWM RANGE)	28.14 (AMS RANGE) 19.70 (GWM RANGE)
MAXIMUM PREDICTIVE PERIOD ERROR (m)						
6 HR. TOTAL:	–	436.71	–	117.72	–	43.64
12 HR. TOTAL:	–	529.59	–	117.72	–	53.03
1 DAY TOTAL:	54.49	529.59	47.93	117.72	52.81	66.61
2 DAY TOTAL:	69.96	712.38	66.21	154.83	78.19	113.03
3 DAY TOTAL:	93.39	1143.93	91.45	213.02	105.19	164.63
DURATION OF ACCURATE ORBIT PREDICTION* (MINUTES)	5520	0	5520	0	4500	2100

*INDICATED VALUE IS THE TIME FOR WHICH A TRACKING ACCURACY (3σ) ≤ 75 m IS MAINTAINED

07/28/89 MIS83P\AK7396

Table A.11-3 Two-Station PRTS OD Performance for ATDRS-E (3 σ)

BASELINE PRTS

	(REY, WHS)		(ACN, WHS)	
MAXIMUM DEFINITIVE PERIOD ERROR (m)	30 HRS	2 HRS	30 HRS	2 HRS
TOTAL:	38.04	240.59	34.87	174.48
DOMINANT ERROR SOURCES:	21.91 (REY RANGE) 20.97 (WHS RANGE)	237.97 (NOISE) 19.85 (WHS RANGE)	20.47 (ACN RANGE) 18.40 (A1–UT1)	172.06 (NOISE) 18.40 (A1–UT1)
MAXIMUM PREDICTIVE PERIOD ERROR (m)				
6 HR. TOTAL:	–	249.97	–	143.20
12 HR. TOTAL:	–	280.99	–	188.91
1 DAY TOTAL:	54.21	292.47	55.12	208.96
2 DAY TOTAL:	74.82	366.47	79.82	260.44
3 DAY TOTAL:	97.13	451.88	105.93	320.86
DURATION OF ACCURATE ORBIT PREDICTION* (MINUTES)	4740	0	4500	0

*INDICATED VALUE IS THE TIME FOR WHICH A TRACKING ACCURACY (3σ) ≤ 75 m IS MAINTAINED

07/28/89 MIS83P\AK7299

Table A.11-4 Two-Station PRTS OD Performance for ATDRS-W (3 σ)

BASELINE PRTS

	(HAW, WHS)		(GWM, WHS)	
MAXIMUM DEFINITIVE PERIOD ERROR (m)	30 HRS	2 HRS	30 HRS	2 HRS
TOTAL:	65.28	655.91	38.48	275.53
DOMINANT ERROR SOURCES:	40.45 (SOLRAD) 28.00 (HAW RANGE)	653.40 (NOISE) 35.10 (HAW RANGE)	20.02 (GWM RANGE) 19.85 (WHSK RANGE)	273.88 (NOISE) 18.40 (A1--UT1)
MAXIMUM PREDICTIVE PERIOD ERROR (m)				
6 HR. TOTAL:	–	668.93	–	282.26
12 HR. TOTAL:	–	668.93	–	282.26
1 DAY TOTAL:	64.86	668.93	56.11	282.26
2 DAY TOTAL:	78.23	668.93	82.43	294.18
3 DAY TOTAL:	98.36	722.96	110.31	323.37
DURATION OF ACCURATE ORBIT PREDICTION* (MINUTES)	4440	0	4260	0

*INDICATED VALUE IS THE TIME FOR WHICH A TRACKING ACCURACY (3σ) ≤ 75 m IS MAINTAINED

07/28/89 MIS83P\AK7300

For 30-hour tracking arcs, predictive periods of 1, 2, and 3 days after the end of the definitive arc are important in the event of system failure or disruption. In general, all the PRTS networks are able to support predictive performance less than 75 m for the first 24 hours; predictive periods greater than 1 day, however, show deterioration of the orbit uncertainty to greater than 75 m after 30 hours or more past the end of the definitive period.

A.12 MPRTS SIMULATION RESULTS

As discussed in Section 4, MPRTS represents use of the PRTS signal structure to solve ionospheric delay uncertainties in an S-band 2-way ranging system. Tables A.2-11 and 4-5 detail the ORAN error budget for MPRTS, while Tables A.12-1 through A.12-4 summarize the MPRTS ORAN results.

All MPRTS networks show OD performance over a 30-hour tracking arc which is better than (less than) the goal of 75 m (3-sigma). Only the longest baseline two- and three-station MPRTS networks, however, show definitive period OD performance less than 75 m over the 2-hour trajectory recovery tracking arcs. Range biases are consistently among the dominant definitive period error contributors.

Predictive performance after 30-hour tracking arcs generally meets the goal of 75 m up to 2 days after the end of the definitive period. The shorter baseline networks, however, surprisingly show marginally better predictive performance than do the longer baseline networks. This behavior is not thought to be significant and most likely reflects artifacts of the ORAN modelling, including the choice of initial tracking epoch.

A.13 AKuRS SIMULATION RESULTS

AKuRS, as discussed in Section 3, is effectively a Ku-band version of the TDRSS BRTS, relying upon 2-way range and range-rate measurements between White Sands and one or more remote stations. Because of its use of 2-way measurements, no clock biases exist between White Sands and the remote stations. ORAN modelling parameters for AKuRS are summarized in Tables A.2-12 and 3-6, while Tables A.13-1 through A.13-4 show the obtained OD results.

As shown, all three- and two-station AKuRS networks provide definitive period OD accuracies better than (less than) the goal of 75 m (3-sigma) for 30-hour tracking arcs. Trajectory recovery tracking arcs of 2 hours also provide better than 75 m performance except in the case of the short baseline CONUS-based networks. AKuRS trajectory recovery performance is superior to that of PRTS or MPRTS and, at times, shows better performance that those of comparable AKuRS 30-hour arcs. On the basis of

Table A.12-1 MPRTS OD Performance for ATDRS-E (3 σ)

MPRTS

	SHORT BASELINE (GSFC, MIL, WHS)		INTERMEDIATE BASELINE (ACN, GSFC, WHS)		LONG BASELINE (REY, ACN, WHS)	
MAXIMUM DEFINITIVE PERIOD ERROR (m)	30 HRS	2 HRS	30 HRS	2 HRS	30 HRS	2 HRS
TOTAL:	43.42	215.31	31.82	87.65	32.62	40.45
DOMINANT ERROR SOURCES:	26.69 (WHS RANGE) 18.40 (A1–UT1)	153.02 (MIL RANGE) 103.04 (WHSK RANGE)	21.53 (WHS RANGE) 18.40 (A1–UT1)	59.62 (GSFC RANGE) 54.50 (WHSK RANGE)	18.40 (A1–UT1) 17.71 (WHSK RANGE)	23.74 (REY RANGE) 19.08 (WHSK RANGE)
MAXIMUM PREDICTIVE PERIOD ERROR (m)						
6 HR. TOTAL:	–	212.11	–	74.06	–	37.25
12 HR. TOTAL:	–	265.70	–	97.84	–	48.70
1 DAY TOTAL:	45.29	303.75	45.67	112.90	52.57	65.01
2 DAY TOTAL:	52.12	414.49	66.57	150.02	77.17	104.22
3 DAY TOTAL:	62.12	533.84	89.10	192.81	103.21	146.50
DURATION OF ACCURATE ORBIT PREDICTION* (MINUTES)	6120+	0	4980	0	4560	2160

*INDICATED VALUE IS THE TIME FOR WHICH A TRACKING ACCURACY (3σ) ≤ 75 m IS MAINTAINED

07/28/89 MIS83P\AK7400

Table A.12-2 MPRTS OD Performance for ATDRS-W (3 σ)

MPRTS

	SHORT BASELINE (VAN, WAS, WHS)		INTERMEDIATE BASELINE (HAW, WAS, WHS)		LONG BASELINE (AMS, GWM, WHS)	
MAXIMUM DEFINITIVE PERIOD ERROR (m)	30 HRS	2 HRS	30 HRS	2 HRS	30 HRS	2 HRS
TOTAL:	57.06	392.77	50.90	109.16	33.24	43.86
DOMINANT ERROR SOURCES:	42.55 (SOLRAD) 25.96 (WHS RANGE)	291.91 (VAN RANGE) 206.37 (WHSK RANGE)	37.11 (SOLRAD) 19.02 (WHS RANGE)	72.75 (WAS RANGE) 63.95 (WHSK RANGE)	18.40 (A1-UT1) 16.69 (GWM RANGE)	27.21 (AMS RANGE) 21.11 (GWM RANGE)
MAXIMUM PREDICTIVE PERIOD ERROR (m)						
6 HR. TOTAL:	–	274.04	–	100.11	–	39.78
12 HR. TOTAL:	–	332.88	–	100.11	–	46.77
1 DAY TOTAL:	45.05	332.88	43.89	101.69	53.11	60.44
2 DAY TOTAL:	62.98	440.63	63.95	133.77	78.67	97.44
3 DAY TOTAL:	87.69	711.53	89.92	186.12	106.02	139.69
DURATION OF ACCURATE ORBIT PREDICTION* (MINUTES)	5580	0	5520	0	4440	2520

*INDICATED VALUE IS THE TIME FOR WHICH A TRACKING ACCURACY (3σ) ≤ 75 m IS MAINTAINED

07/28/89 MIS83P\AK7397

Table A.12-3 Two-Station MPRTS OD Performance for ATDRS-E (3 σ)

MPRTS

	(REY, WHS)		(ACN, WHS)	
MAXIMUM DEFINITIVE PERIOD ERROR (m)	30 HRS	2 HRS	30 HRS	2 HRS
TOTAL:	35.70	43.64	33.28	34.45
DOMINANT ERROR SOURCES:	20.31 (WHSK RANGE) 19.81 (REY RANGE)	25.43 (NOISE) 20.51 (WHSK RANGE)	19.77 (ACN RANGE) 18.40 (A1–UT1)	18.40 (A1–UT1) 16.93 (NOISE)
MAXIMUM PREDICTIVE PERIOD ERROR (m)				
6 HR. TOTAL:	–	49.11	–	36.77
12 HR. TOTAL:	–	61.46	–	43.58
1 DAY TOTAL:	51.32	75.30	53.34	61.31
2 DAY TOTAL:	71.68	118.01	77.90	99.51
3 DAY TOTAL:	93.82	163.36	103.87	140.12
DURATION OF ACCURATE ORBIT PREDICTION* (MINUTES)	4920	1560	4500	2460

*INDICATED VALUE IS THE TIME FOR WHICH A TRACKING ACCURACY (3σ) ≤ 75 m IS MAINTAINED

07/28/89 MIS83P\AK7166

Table A.12-4 Two-Station MPRTS OD Performance for ATDRS-W (3 σ)

MPRTS

	(HAW, WHS)		(GWM, WHS)	
MAXIMUM DEFINITIVE PERIOD ERROR (m)	30 HRS	2 HRS	30 HRS	2 HRS
TOTAL:	54.90	88.17	33.41	39.78
DOMINANT ERROR SOURCES:	37.92 (SOLRAD) 20.39 (WHSK RANGE)	69.72 (NOISE) 34.68 (HAW RANGE)	20.23 (WHS RANGE) 18.40 (A1–UT1)	29.24 (NOISE) 18.40 (A1–UT1)
MAXIMUM PREDICTIVE PERIOD ERROR (m)				
6 HR. TOTAL:	–	87.96	–	39.87
12 HR. TOTAL:	–	87.96	–	43.46
1 DAY TOTAL:	53.77	87.96	54.53	53.52
2 DAY TOTAL:	70.12	115.28	80.60	87.35
3 DAY TOTAL:	94.72	166.93	108.54	126.85
DURATION OF ACCURATE ORBIT PREDICTION* (MINUTES)	5400	0	4320	2580

*INDICATED VALUE IS THE TIME FOR WHICH A TRACKING ACCURACY (3σ) ≤ 75 m IS MAINTAINED

07/28/89 MIS83P\AK7240

Table A.13-1 AKuRS OD Performance for ATDRS-E (3 σ)

AKuRS

MAXIMUM DEFINITIVE PERIOD ERROR (m)	SHORT BASELINE (GSFC, MIL, WHS)		INTERMEDIATE BASELINE (ACN, GSFC, WHS)		LONG BASELINE (REY, ACN, WHS)	
	30 HRS	2 HRS	30 HRS	2 HRS	30 HRS	2 HRS
TOTAL:	35.96	76.76	35.69	28.29	37.41	30.81
DOMINANT ERROR SOURCES:	27.16 (WHS RANGE) 18.39 (A1−UT1)	46.70 (GSFC RANGE) 40.92 (WHSK RANGE)	26.81 (WHS RANGE) 18.40 (A1−UT1)	18.40 (A1−UT1) 13.28 (ACN RANGE)	28.01 (WHS RANGE) 18.40 (A1−UT1)	18.40 (A1−UT1) 15.40 (WHS RANGE)
MAXIMUM PREDICTIVE PERIOD ERROR (m)						
6 HR. TOTAL:	–	78.44	–	29.91	–	30.12
12 HR TOTAL:	–	106.65	–	33.77	–	30.57
1 DAY TOTAL:	38.11	129.85	32.94	49.25	31.49	41.14
2 DAY TOTAL:	44.78	192.18	39.72	82.18	37.74	66.46
3 DAY TOTAL:	54.10	256.97	50.63	117.46	49.15	95.49
DURATION OF ACCURATE ORBIT PREDICTION* (MINUTES)	6120+	480	6120+	2820	6120+	4140

*INDICATED VALUE IS THE TIME FOR WHICH A TRACKING ACCURACY (3σ) ≤ 75 m IS MAINTAINED

07/28/89 MIS83P\AK7398

Table A.13-2 AKuRS OD Performance for ATDRS-W (3 σ)

AKuRS

	SHORT BASELINE (VAN, WAS, WHS)		INTERMEDIATE BASELINE (HAW, WAS, WHS)		LONG BASELINE (AMS, GWM, WHS)	
MAXIMUM DEFINITIVE PERIOD ERROR (m)	30 HRS	2 HRS	30 HRS	2 HRS	30 HRS	2 HRS
TOTAL:	48.26	110.99	51.32	50.16	36.60	31.27
DOMINANT ERROR SOURCES:	32.68 (SOLRAD) 26.51 (WHS RANGE)	64.93 (WHSK RANGE) 61.17 (WAS RANGE)	36.27 (SOLRAD) 27.37 (WHS RANGE)	30.67 (WHSK RANGE) 20.35 (HAW RANGE)	26.57 (WHS RANGE) 18.40 (A1–UT1)	18.40 (A1–UT1) 16.60 (WHS RANGE)
MAXIMUM PREDICTIVE PERIOD ERROR (m)						
6 HR. TOTAL:	–	99.84	–	46.73	–	30.19
12 HR. TOTAL:	–	99.84	–	46.73	–	35.81
1 DAY TOTAL:	39.85	99.84	41.56	51.15	44.97	46.79
2 DAY TOTAL:	56.45	152.06	59.27	83.87	56.52	73.19
3 DAY TOTAL:	78.25	265.46	82.49	125.84	71.53	102.70
DURATION OF ACCURATE ORBIT PREDICTION* (MINUTES)	5640	0	5580	2700	6120+	3900

*INDICATED VALUE IS THE TIME FOR WHICH A TRACKING ACCURACY (3σ) ≤ 75 m IS MAINTAINED

07/28/89 MIS83P\AK7399

Table A.13-3 Two-Station AKuRS OD Performance for ATDRS-E (3 σ)

AKuRS

	(REY, WHS)		(ACN, WHS)	
MAXIMUM DEFINITIVE PERIOD ERROR (m)	30 HRS	2 HRS	30 HRS	2 HRS
TOTAL:	37.58	36.13	35.70	30.42
DOMINANT ERROR SOURCES:	27.96 (WHS RANGE) 18.40 (A1−UT1)	20.50 (WHSK RANGE) 20.25 (REY RANGE)	25.50 (WHS RANGE) 18.40 (A1−UT1)	18.40 (A1−UT1) 16.30 (ACN RANGE)
MAXIMUM PREDICTIVE PERIOD ERROR (m)				
6 HR. TOTAL:	–	45.77	–	35.34
12 HR. TOTAL:	–	54.96	–	39.74
1 DAY TOTAL:	35.71	69.79	32.35	58.41
2 DAY TOTAL:	41.31	112.99	39.92	96.83
3 DAY TOTAL:	50.55	158.13	51.87	137.22
DURATION OF ACCURATE ORBIT PREDICTION* (MINUTES)	6120+	1800	6120+	2520

*INDICATED VALUE IS THE TIME FOR WHICH A TRACKING ACCURACY (3σ) ≤ 75 m IS MAINTAINED

07/28/89 MIS83P\AK7241

Table A.13-4 Two-Station AKuRS OD Performance for ATDRS-W (3 σ)

AKuRS

	(HAW, WHS)		(GWM, WHS)	
MAXIMUM DEFINITIVE PERIOD ERROR (m)	30 HRS	2 HRS	30 HRS	2 HRS
TOTAL:	51.17	62.87	34.50	31.80
DOMINANT ERROR SOURCES:	34.75 (SOLRAD) 26.69 (WHS RANGE)	39.70 (HAW RANGE) 36.92 (WHSK RANGE)	23.25 (WHS RANGE) 18.40 (A1–UT1)	18.40 (A1–UT1) 15.44 (GWM RANGE)
MAXIMUM PREDICTIVE PERIOD ERROR (m)				
6 HR. TOTAL:	–	55.28	–	35.08
12 HR. TOTAL:	–	55.28	–	35.63
1 DAY TOTAL:	42.94	55.28	42.44	47.94
2 DAY TOTAL:	59.45	94.29	52.99	83.16
3 DAY TOTAL:	81.39	150.87	66.54	123.38
DURATION OF ACCURATE ORBIT PREDICTION* (MINUTES)	5580	2460	6120+	2580

*INDICATED VALUE IS THE TIME FOR WHICH A TRACKING ACCURACY (3σ) ≤ 75 m IS MAINTAINED

07/28/89 MIS83P\AK7242

the ORAN runs, it appears that this phenomena is due to the low pseudorange-rate noise associated with AKuRS measurements, allowing relative better orbit accuracies to be obtained over short arcs. In general, range biases are the dominant AKuRS error sources, again emphasizing the importance of reducing system propagation uncertainties through calibration.

Predictive performance for AKuRS generally meets the goal of 75 m, except for trajectory recovery predictive performance for the short baseline CONUS networks. Comparison between AKuRS OD performances for ATDRS-E and ATDRS-W shows that the geometry of the AKuRS networks may have a significant effect on the results, where this effect is especially visible over the predictive periods. Further consideration of the AKuRS remote station sites would thus be necessary in any future study.

The differences between MPRTS and AKuRS as systems are relatively minor---both are 2-way systems that reduce the error due to the ionosphere to effectively zero. Due to the systems' different link budgets and operating radio frequencies, however, the pseudorange and pseudorange-rate noise levels of the two systems are different, as discussed in Appendix C. The superior AKuRS modelled range-rate noise level accounts for the marginally superior OD performance of AKuRS relative to MPRTS for the short arcs and short baselines, while the superior MPRTS range noise level results in relatively better performance for the long arcs.

A.14 DIRECT ATDRS/GPS TRACKING SYSTEM SIMULATION RESULTS

The Direct ATDRS/GPS Tracking System relies upon ranging measurements made by the ATDRS to each of the GPS satellites visible to the ATDRS at a given instant. To make these measurements, the ATDRS satellite must be within the beamwidth of the GPS satellites, limiting the visible GPS satellites to those traversing an annular region of the GPS orbital sphere diametrically opposite the orbital location of the ATDRS. GPS visibility to the ATDRSS satellites has been discussed at length in Section 6. The Direct ATDRS/GPS Tracking System provides the advantages of measurements which are virtually unperturbed by the Earth's atmosphere, an extended geometry provided by a relatively large baseline defined by the mean diameter of the ATDRS/GPS annular visibility region, and a large number of GPS satellites appearing within the annular region to provide near-continuous observations over the duration of a 30-hour tracking arc.

In order to restrict ORAN's ATDRS observations of the GPS satellites to only those which are within the ATDRS/GPS annular

visibility region, a scheduling program independent of ORAN was developed to determine the visibility of the GPS satellites. This off-line visibility program provides a visibility schedule for input to ORAN with time resolved to the nearest minute. For purposes of ORAN modelling of the Direct ATDRS/GPS Tracking System, the 30-hour ATDRS-E and ATDRS-W visibility profile of Figures A.14-1 and A.14-2 have been randomly selected and used in this study for the simulation of both the 30-hour and 2-hour tracking arcs.

The selection of a two-hour trajectory recovery tracking arc must take into consideration the variation of the number of GPS satellites visible from an ATDRS, where this number may range from 0 to 4 at any instant, as shown in Figure 6-9. In worst case scenarios, time intervals on the order of one hour may occur when no GPS satellites are visible to the ATDRS. Operationally, ATDRS maneuvers would be scheduled so that the trajectory recovery period would avoid such periods of limited GPS visibility. Two hour blocks of multiple GPS satellite visibility are relatively common, so it is reasonable to assume that ATDRS orbital maneuvers could be scheduled to avoid full loss of ATDRS/GPS visibility. For the 2-hour tracking arcs, the first two hours of the visibility profiles of Figures A.14-1 and A.14-2 have been used as a convenience in setting up the runs; although not optimum, the first two hours of this profile provide many more measurements than have been modelled for the other ATDRS ranging systems.

Use of ORAN to model the OD performance of the Direct ATDRS/GPS Tracking System has required some level of experimentation to determine the most meaningful modelling approach. Tables A.14-1 and A.14-2 summarize the various ORAN runs that were conducted, although a different ORAN error budget than that shown in Tables A.2-13 and 6-2 was used for those results. Drawing conclusions from Tables A.14-1 and A.14-2, results for the Direct ATDRS/GPS Tracking System using the error budget of Tables A.2-13 and 6-2 were then obtained, where these results are summarized in Table A.14-3.

Table A.14-1 documents different approaches to modelling the clock biases existing between the ATDRS GPS receiver and the GPS satellites for a 30-hour tracking arc. Runs 1 and 2 reveal that, as expected, artificially separating the pseudorange bias due to ATDRS/GPS oscillator drift from those due to uncertainties in the GPS ephemeris, the GPS satellite perturbations, and the GPS and ATDRS equipment group delays makes no difference: if applied as two distinct (pseudorange and clock) biases to each GPS measurement or as one summed bias, the ATDRS OD accuracy is virtually the same. The addition of

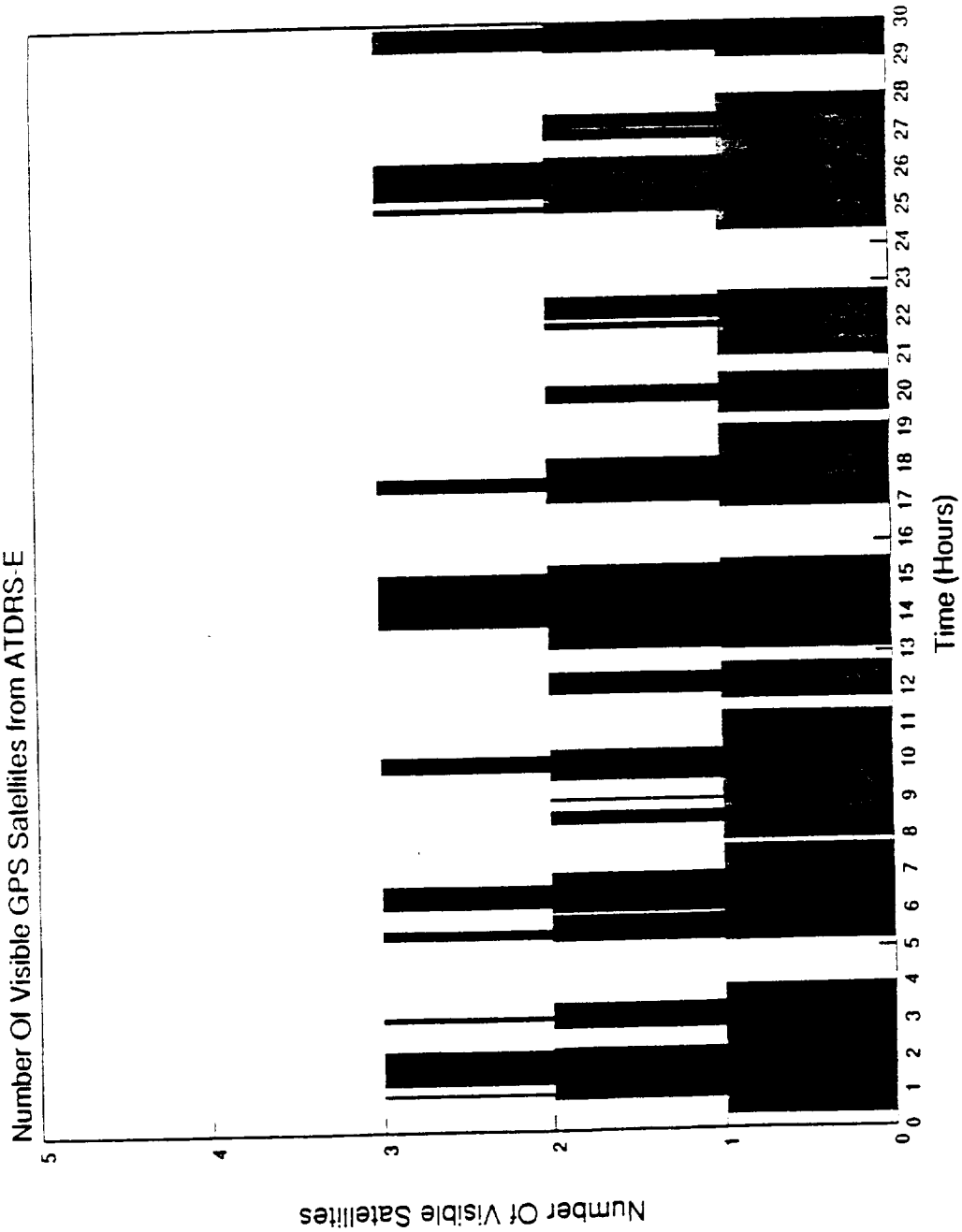

Figure A.14-1. ATDRS-E 30-Hour Visibility Profile

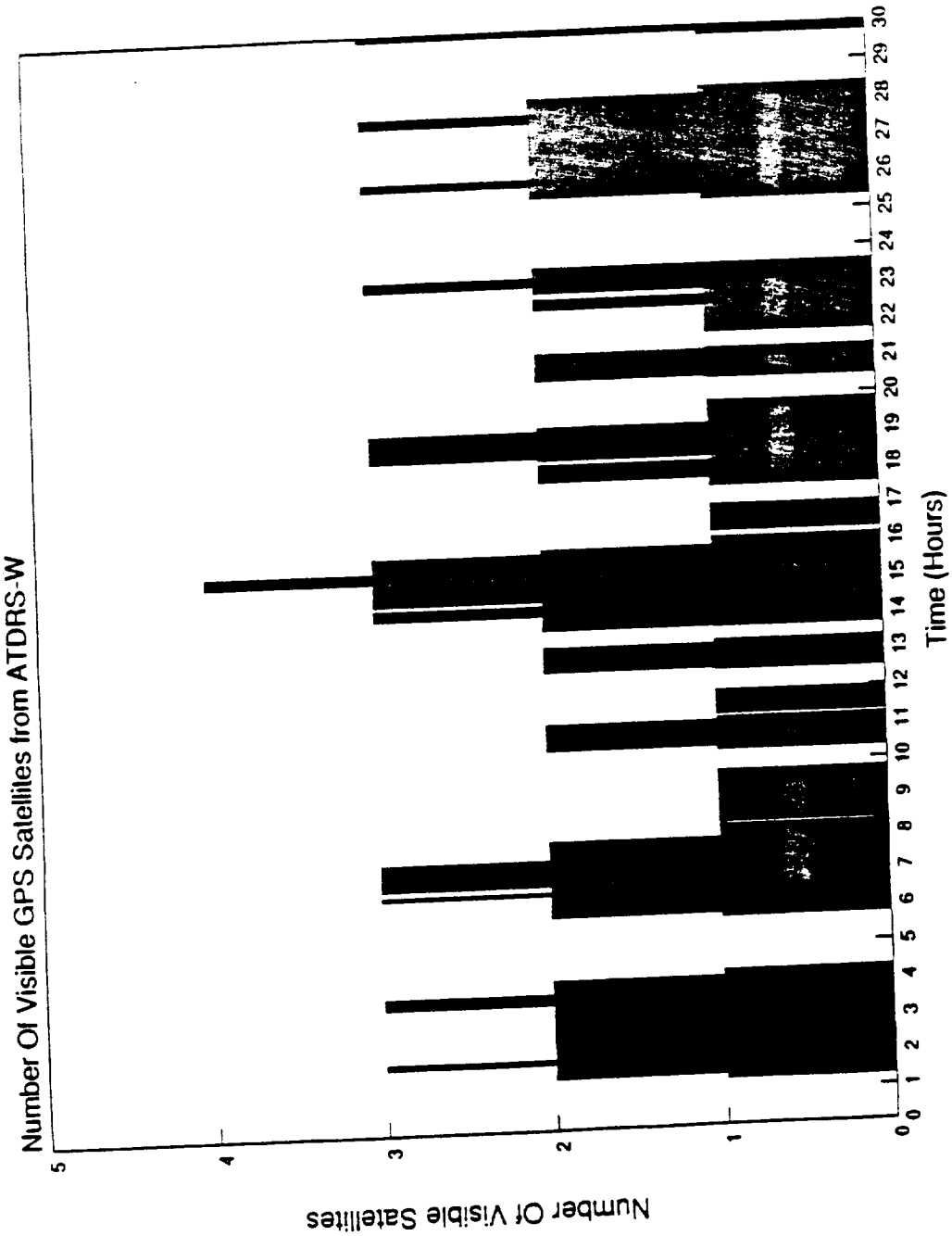

Figure A.14-2. ATDRS-W 30-Hour Visibility Profile

Table A.14-1. Direct GPS Tracking System OD Performance Trial Results* (ATDRS-E; 30-Hour Tracking Arc)

RUN #	RUN TYPE	MAXIMUM TOTAL ERROR (METERS)	DOMINANT ERROR CONTRIBUTORS
1	• apply single ATDRS/GPS clock bias of 0.0 meters • apply range biases of 19.2 meters for each GPS satellite	55.4	GPS8 range bias (38.4 m) GM (23.8 m)
2	• apply clock biases of 14.0 meters for each GPS satellite • apply range biases of 13.4 meters	55.7	Clock8 (28.0 m) GPS8 range bias (26.8 m)
3	• same as run 2 • apply drift term of 10^{-13}	55.7	Clock8 bias (28.0 m) GPS8 range bias (26.8 m)
4	• solve for single ATDRS/GPS clock bias • apply range biases of 19.2 meters	59.5	GM (40.1 m) GPS8 range bias (17.0 m)
5	• solve for ATDRS/GPS clock biases for all visible GPS satellites • apply range biases of 19.2 meters	1201.2	GM (1185.7 m)
6	• same as run 2 • reduce range noise to 4.0 meters	55.7	Clock8 bias (28.0 m) GPS8 range bias (26.8 m)
7	• apply single ATDRS/GPS clock bias of 14.0 meters • apply range biases of 13.4 meters	80.6	Clock bias (68.7 m) GPS8 range bias (26.8 m) GM (23.8 m)

MIS55Q

* ORAN error budget for these runs is slightly different than those used for the results of Table A.14-3.

Table A.14-2. Direct GPS Tracking System OD Performance Trial Results* (ATDRS-E; 2-Hour Tracking Arc)

RUN #	RUN TYPE	MAXIMUM TOTAL ERROR (METERS)	DOMINANT ERROR CONTRIBUTORS
1A	• apply clock biases of 14.0 meters for each GPS satellite • apply range biases of 13.4 meters for each GPS satellite	302.2	Clock17 (135.4 m) Clock24 (174.3 m)
2A	• same as run 1A • reduce range noise to 4.0 meters	301.4	Clock17 (135.4 m) Clock24 (134.3 m)
3A	• apply single ATDRS/GPS clock bias of 14.0 meters • apply range biases of 13.4 meters	210.4	GPS17 range bias (129.6 m) GPS24 range bias (128.5 m)
4A	• solve for single ATDRS/GPS clock bias • apply range biases of 13.4 meters	5390.9	GM (3234.4 m) Range noise (2851.5 m)

MIS65Q

* ORAN error budget for these runs is slightly different than those used for the results of Table A.14-3.

Table A.14-3. Direct ATDRS/GPS Tracking System OD Performance for ATDRS-W and ATDRS-E (3 σ)

DIRECT ATDRS/GPS TRACKING SYSTEM

	(ATDRS-W)		(ATDRS-E)	
MAXIMUM DEFINITIVE PERIOD ERROR (m)	30 HRS	2 HRS	30 HRS	2 HRS
TOTAL:	65.5	232.7	58.1	208.3
DOMINANT ERROR SOURCES:	45.1 (GRAVCO) 21.0 (TGPS9 RANGE)	162.5 (NOISE) 129.1 (TGPS22 RANGE)	48.1 (GRAVCO) 11.8 (TGPS8 RANGE)	128.4 (TGPS17 RANGE) 127.5 (TGPS8 RANGE)
MAXIMUM PREDICTIVE PERIOD ERROR (m)				
6 HR. TOTAL:	–	753.0	–	692.3
12 HR. TOTAL:	–	2969.5	–	1492.1
1 DAY TOTAL:	110.3	5237.2	80.0	2556.0
2 DAY TOTAL:	162.4	10295.8	130.6	4991.5
3 DAY TOTAL:	215.9	15356.7	182.7	7440.9
DURATION OF ACCURATE ORBIT PREDICTION* (MINUTES)	2160	0	3180	0

*INDICATED VALUE IS THE TIME FOR WHICH A TRACKING ACCURACY (3σ) ≤ 75 m IS MAINTAINED

07/31/89 MIS83P\AJ7500

clock drift to each GPS satellite (run 3) has no effect, as does reduction of the range noise to more optimistically model GPS receiver performance (run 6). Performance is also closely equivalent if a single clock bias, representing the bias between the ATDRS clock and GPS system time, is solved-for, with a pseudorange bias applied to each GPS measurement (run 4). This approach is consistent with that used to model PRTS performance, where PRTS, like the Direct ATDRS/GPS Tracking System, is a 1-way ranging system. If a single clock bias is applied, however, then definitive period OD performance deteriorates to worse than (greater than) the 75 m (3-sigma) goal (run 7). If one further attempts to solve for 24 clock biases, representing the biases between the ATDRS clock and each GPS satellite's uncorrected clock, then performance is significantly degraded (run 5).

On the basis of the results of Table A.14-1, modelling of the Direct ATDRS/GPS Tracking System was then conducted for a 2-hour trajectory recover tracking arc, as shown in Table A.14-2. Unless one attempts to solve for a single ATDRS/GPS clock bias, which produces exceptionally poor orbit accuracy, the different modelling approaches generally yield the same results in excess of the goal of 75 m (3-sigma). The approach most consistent with both run 4 of Table A.14-1 and the modelling approach used for PRTS is that of run 3A, where a single ATDRS/GPS clock bias is applied as a consider parameter.

The final results for the Direct ATDRS/GPS Tracking System then used the ORAN error budget of Table 6-2 and the techniques of run 4 and run 3A. For 30-hour tracking arcs, a single ATDRS/GPS clock bias is solved-for and additional range biases representing the uncertainties in the signal path delays are applied to each of the GPS measurements. For 2-hour tracking arcs, however, a single ATDRS/GPS clock bias and range biases for each of the GPS measurements are applied. The results are summarized in Table A.14-3.

As can be seen, the gravitation coefficient GM is the dominant error source for the 30-hour tracking arcs. It is believed that this result is an artifact of the ORAN estimation process--the solutions for the GPS satellite orbits, the ATDRS orbit, and the ATDRS/GPS clock bias interact in such a way as to place the dominant error contribution with the gravitation coefficient. Since the GPS satellite orbits are solved-for, the contribution of the uncertainty of their orbits to the ATDRS orbit solution cannot be determined. The 6 m GPS satellite position uncertainty is dominated by the error in the gravitation

coefficient, suggesting that it is this contribution which propagates through to dominate the solution for the ATDRS orbit. To prove this conjecture, however, would require that two gravitation coefficients be identified separately for the GPS and ATDRS satellites; unfortunately, ORAN does not allow GM, as a dynamic parameter, to be treated in this way. Performance over the 30-hour arc for ATDRS-W and ATDRS-E are better than (less than) the goal of 75 m (3-sigma); the difference in performance between ATDRS-W and ATDRS-E are better than (less than) the goal of 75 m (3-sigma); the difference in performance between ATDRS-W and ATDRS-E is due to the differences in relative ATDRS/GPS visibility over the 30-hour arcs. For the 2-hour tracking arcs, the Direct ATDRS/GPS Tracking System is considerably worse than (greater than) the goal of 75 m.

A.15 KU-BAND GROUND SPACEFLIGHT TRACKING AND DATA NETWORK (GSTDN) STUDIES

Another system for tracking ATDRS, which is a future version of the GSTDN system, which uses Ku-band frequencies to eliminate the effects of the ionosphere. One preliminary study of this system has been made using the ATDRS-E satellite and three stations from GSTDN: WHS, MIL, and Bermuda. The measurement parameters for the run were the current GSTDN parameters (shown in Table A.15-1).

The definitive-period position error for a 30-hour arc was obtained from the run. The major sources of error were the station range biases and the ionosphere error, for the S-band case. Because it is possible that the future GSTDN system will have smaller range biases than the 15-m biases of the current GSTDN system, the value of the definitive position error has been calculated for several range biases and for S-band and Ku-band transmission frequencies. These position errors are shown in Table A.15-1.

The results shown in Table A.15-1 are much worse than those achieved by other systems with short baselines. The poor position determination achieved here may be due to an inappropriate choice of tracking stations. MIL and Bermuda are not widely separated in distance, and the three stations are nearly collinear so that the triangle they form is long and flat, with very short north-south projections of the station baselines. Such a station configuration would be expected to produce large cross-track errors in ATDRS, and this was observed in the ORAN simulation.

Future studies of GSTDN will examine a wider set of station locations and will consider ATDRS-E and ATDRS-W, as well as arc lengths other than 30 hours.

Table A.15-1. Preliminary GSTDN Error Analysis Results

Run Description: 30-hour arc
WHS, MIL, Bermuda
range + range-rate
S-band

range: noise 2m; weight 15 m;
bias 15 m

range rate: noise 0.2m/sec;
weight 2 m/sec

ionosphere: 100% sflux 250

Maximum Total Position Error in Definitive Period

	Range-Bias Value			
	15 m	10 m	5 m	0 m
S-band	458	374	312	289
K-band	357	239	123	31

Error with no biases, no ionosphere = 31 m

APPENDIX B - INTERFEROMETRIC SYSTEMS SPECIFICATIONS AND COSTS

This appendix gives specifications, cost estimates, and staffing estimates for the interferometric systems evaluated in Section 5.

B.1 SYSTEM SPECIFICATIONS

Specifications are provided for three systems described in the text. Cost estimates assume that a third ATDRS satellite is to be tracked, located over WHS. The OD and TR results in Section 5, however, refer only to satellites in the east and west orbital slots.

B.1.1 SYSTEM SPECIFICATION--VLBI-Q

The VLBI array will consist of five sites, shown in Figure 5-2 in Section 5. ATDRS observations are passive observations of the Ku-band SGL. These locations are chosen assuming ATDRS satellites with SGL beam characteristics similar to those of the current TDRS, located over longitudes 41°E and 171°E, and a GT located at WHS. Two of the sites are common sites and will observe both ATDRSs. The eastern site (East Texas) observes only ATDRS-E, and the western site (southern California) observes only ATDRS-W. The fifth site would be dedicated to providing east-west baselines for an overhead ATDRS. Its location has not been studied but would probably be about 200 km east of WSGT. Site surveys are assumed to tie the two antennas at each site (intersection of axes) to within 0.5 cm. One site must be tied to the VLBI reference frame to within 25 cm. Accurate ties between sites will be achieved through interferometric observations by the array itself.

The IF signals from each receiver (Ku or S for TDRS tracking; Ku and S for observing natural sources) are converted to video, sampled, and formatted at each receiving station. The data is then sent from each remote receiving station via satellite link to the central processing facility. This facility will control and monitor operations at all sites and may be colocated with one of the common observing sites.

Each site will be equipped with the following:

- One calibrator antenna and receiver
- One or two ATDRS-tracking antennas and receivers
- Hydrogen maser time/frequency standard

- Electronics rack to process signals from receivers
- Calibration apparatus
- Communications link to transmit data
- Station control computer

These components are discussed in the subsections that follow.

B.1.1.1 Calibrator Antenna

One calibrator antenna is located at each of the five stations. It will observe natural radio sources, down to a limiting flux density of -260 dBW/Hz/m^2. The antenna will be a 12-m diameter Cassegrain-focus parabolic reflector with subreflector. Aperture efficiency will be at least 50 percent, to provide overall gain of 61.9 dB at Ku-band. It will be fully steerable with a slewing rate of 1 degree per second or faster. Located at each site will be the antenna control unit, which will provide tracking accuracy such that the antenna can be pointed blind to within about 37 arcsec.

The receiver for the calibrator antenna is located at the focus of the 12-m antenna. Concentric beams should be formed, and it must provide for simultaneous reception of Ku-band and S-band. The spanned bandwidth must be at least 500 MHz at Ku-band and 100 MHz at S-band. The receiver will contain cryogenically cooled FET amplifiers, will have gain of at least 30 dB, and will have receiver temperatures of about 45°K at Ku-band and 15°K at S-band. Overall system temperatures will be not more than 100°K at Ku-band and 50°K at S-band. The receiver will contain noise-calibration and phase-calibration systems. Detailed specifications appear in Reference 5-2.

B.1.1.2 TDRS-Tracking Antenna

One 2-m diameter antenna, fully steerable, with slew rates of at least 1 degree per sec, controller, pointing accuracy of about 4 arcmin blind, and aperture efficiency of 0.5 (gain of 46.3 dB), will be at the east and west sites; there will be two at each common site.

The ATDRS antenna will observe the ATDRS SGL, centered at 13.9285 GHz. Capability for observing the SSA forward link (2070 MHz) will also be provided. The ATDRS receiver will be located at the focus of the 2-m ATDRS antenna. Design and function are similar to those of the natural calibrator receiver except that (1) the receiver is uncooled, (2) total system temperatures of 200°K at Ku-band and 100°K at

S-band are adequate, and (3) total bandwidths of 260 MHz at Ku-band and 50 MHz at S-band are adequate.

B.1.1.3 Time/Frequency Standard

The hydrogen maser frequency standard shall be monitored remotely and by reference to an on-site GPS receiver.

B.1.1.4 Electronics Rack

The electronics rack contains modules that select, sample, and format the desired signals. It should have the following capabilities:

- IF Distributor--This will distribute signals from receiver IFs to video converters in any combination under computer control.
- IF-to-video converters (28 total)--These convert IF signals from the antenna to baseband and filter to the desired channel bandwidth. Frequency and bandwidth are selected under computer control. Frequency range must be at least 500 MHz and bandwidth selectable up to at least 2 MHz.
- Formatter--Functions include clipping/sampling, time-tagging, synch block generation, parity generation, and mode switching.
- Data buffer--This buffer should be capable of storing formatter output for a 1-second observation, a total of 14 times 4 megabits (Mb). This allows later transmission of ATDRS observation.

B.1.1.5 Calibration Apparatus

This shall include phase and cable calibration systems (the new Haystack system is adequate); a meteorological sensor to measure local barometric pressure, temperature, and relative humidity; and possibly a water vapor radiometer (budgeted).

B.1.1.6 Communications Links

A postformatter will merge data streams from the formatter into a single bit stream. A satellite communications link will transmit data in real time to the correlator facility. The minimum transponder requirement will be for 7 megabytes (MB) per second of instantaneous capacity if the data transfer from the remote stations is multiplexed. The total transponder volume will be 16828 MB per hour, assuming two

observations per hour of each TDRS and of each calibrator by each network (with the observational data being sampled at the Nyquist rate). A small additional capacity will be used to transfer monitor and control information.

Satellite data transfer capability will be required for only three of the remote stations if the central processing facility is colocated at one of the common sites.

B.1.1.7 Station Control Computer

This will control antenna pointing, data acquisition modules, monitor/control data, and communications with the array control center.

The central processing facility will perform array control functions. The data received from the four observing stations is cross-correlated to extract differential delay observables. Together with pertinent external information, the interferometric delays are used to produce an updated ephemeris, to be supplied to the stations and to the correlator. Functions include the following:

- SGL--The SGL will handle up to 7 MB/sec from each of three remote sites.
- Demultiplexer/Decoder
- Short-Term Archive--This enables recorrelation of ATDRS observations when a priori delay estimates are too inaccurate for proper results, as is expected in TR situations.
- Delay Compensation--Based on the latest projection of the satellite position for the observation epoch, an appropriate amount of a priori delay must be introduced in order to reduce the correlator search window. One delay line is required for each data channel to be processed. Data buffering will be required if data from the remote stations is transmitted sequentially over the satellite link. The total delay must be enough to allow for total difference in signal travel times, both to the different stations (about 3 milliseconds) and over the satellite link (unknown).
- Correlator--This device will compare the bit streams from each pair of stations (a total of three baselines for each of the two networks) and accumulate the number of matching bits in near real

time. Each baseline requires 14 correlator modules, each correlating data from one 2 MHz (4 Mbps) channel. This data is dumped onto disk.

- Fringe Search--A single-purpose computer can be dedicated to performing the Fourier transform necessary to calculate the delay observables.

- Monitor Data--Instrumental performance and meteorological information must be supplied to the orbital-analysis algorithm in order to calibrate for known systematic effects.

- UT1/PM--A file of extrapolated Earth orientation information (from the USNO, for example) must be maintained for input to the orbital-analysis routine.

- Orbital Analysis--A computer facility is needed that is adequate to provide ATDRS position predicts sufficiently accurate (about 1 km) for correlation.

- Archive--A system for automatic data archiving should be implemented at several points in the processing chain. Use of both disk and tape media is to be expected, with automatic recycling of space under the control of a system-wide computer monitor.

- Updated Ephemeris--The output from the OD processor will be used to extrapolate the ATDRS orbit forward in time for internal use in such tasks as antenna pointing and data correlation.

B.1.2 SYSTEM SPECIFICATIONS--CEI-Q

System specifications for CEI-Q systems are presented in Reference 5-1. The system specified here differs in that capability of measuring group delay is assumed. Although group-delay measurements are individually more complicated than phase-delay measurements, they solve the problem of phase-delay ambiguity resolution. Changes to the system design referenced are (1) the increase in receiver and fiberoptic link bandwidth to 1 GHz, (2) design and construction of a correlator to find group delay and phase delay, and (3) elimination of the two interior stations in each array.

B.1.2.1 Network Locations and Array Configuration

B.1.2.1.1 Candidate Array Locations

Three geographical regions within CONUS have been considered as candidates for array locations. Each array is to consist of three individual stations phase connected internally to form an independent tracking instrument. The three locations considered here are dedicated to tracking the ATDRSS satellites in orbital slots at longitudes of 41°E, 171°E, and 105°E. Array locations are shown in Figure 5-5 in Section 5 and are located as follows:

- E--Located in southeastern Alabama near the town of Orion (about 32° north latitude, 86° west longitude)
- W--Located in southern California near the Imperial Valley (about 33° north latitude, 116° west longitude)
- T--Located near WSGT in southern New Mexico (about 32.5° north latitude, 106.4° west longitude)

These specific east and west locations have been chosen to afford complete and explicit tracking scenarios representative of this particular observing strategy, i.e., optimization of the satellite viewing angle by using separate arrays for ATDRS-E and ATDRS-W. The E array will view ATDRS-E at about 28.5 degrees elevation; the W array will view ATDRS-W at about 20.6 degrees elevation; the T array near White Sands will view ATDRS-E at about 11.4 degrees elevation and ATDRS-W at about 12.8 degrees elevation. For a connected element interferometer, performance of which is expected to be limited by atmospheric disturbances in the line of sight, these differences in elevation angle are likely to be significant.

It should be recognized that the specific array locations used here are intended only as representative examples. Actual site locations will require detailed studies of local conditions.

Reference 5-1 describes considerations in selecting array locations.

B.1.2.1.2 Array Configuration

Each of the three candidate arrays consists of three stations arranged in the same basic scheme (refer to

Figure 5-5), a triangular array 10 km on a side. Each remote station will be connected via optical fibers for data transfer to the central processing facility, for frequency standard and timing distribution from the central facility, and for bidirectional monitor and control communication. The frequency standard for the array will be maintained in the central facility, and, from that point, the operations of the remote stations will be totally automated through monitor and control functions. The operation of the central facility itself should be as automated as practical. Minimal personnel requirements will be set by the need for routine maintenance functions associated with the cryogenic systems for the natural calibrator receivers, antenna and other hardware upkeep, and magnetic-tape archiving. Monitoring of the quality of OD and modifications to the programmed functions can be performed as required from remote array control facilities.

B.1.2.1.3 Station Plan

Each of the three stations forming a tracking array will consist of an antenna for tracking ATDRS and a larger antenna for observing natural radio sources. In addition, an adjacent facility will receive and implement remote instructions for driving the antennas and will relay observational data, together with monitor and control information, to the central facility. All functions at each remote station will be fully automated subject to routine maintenance operations.

B.1.2.2 Antenna Control

A dual-antenna configuration is planned for each of the three stations that make up a single CEI array. This will allow simultaneous observations of ATDRS and natural radio sources. Components are as follows:

- Antenna for observing natural radio sources--One 12-m Cassegrain-focus parabolic reflector with subreflector at each of three stations for each array, equipped to be fully steerable with a slewing rate of 1 degree per second or better

- ATDRS-tracking antenna--One 2-m dish at each of three stations for each array, with very limited steering capability as required to accommodate stationkeeping activity and normal drifting

- Antenna control unit--One at each of three stations for each array, equipped to provide tracking

accuracy such that each antenna can be pointed blind to within about 37 arcsec and 111 arcsec for the antennas just described

- Central antenna monitor and positioning computer--One facility for each array

B.1.2.3 Receiver

B.1.2.3.1 Natural Calibrators

This subsystem is located at the focal point of the 12-m antenna. It provides for the low-noise amplification and conversion to IF of signals from distant, naturally occurring sources of of radio emission, usually quasars. These sources have typical flux densities of approximately 1 Jansky or 10**-26 watt/((m**2) * Hz). Detailed specifications and suggested design for the receiver subsystem appear in Reference 5-2. Those specifications are summarized here, and modifications from the former design for group delay measurement are noted.

The receiver is located at the focal point of the 12-m antenna. The feed horn must provide for simultaneous reception of Ku-band (primary frequency) and S-band (backup frequency). Concentric beams should be formed. The Ku-band bandwidth should be about 1000 GHz and the S-band about 200 MHz, approximately double those specified in Reference 5-5.

The feeds will be circularly polarized. The receiver will have cryogenically cooled FET amplifiers, with receiver temperature about 45°K at Ku-band and about 15°K at S-band. Total system temperature will be less than 100°K at Ku-band and 50°K at S-band. The receiver will have a phase-calibration subsystem (the new Haystack unit is adequate) and a noise-calibration generator.

B.1.2.3.2 ATDRS Receiver

This subsystem is located at the focal point of the 2-m ATDRS-tracking antenna. It provides for the low-noise amplification and conversion to IF frequency of signals received from the geostationary ATDRS. The primary observing frequency will be that of the SGL (Ku-band centered at 13.9285 GHz). This emission source produces a flux density of 9 degrees east- 21 degrees west/((m**2)-Hz) at the WSGT. As a backup, the capability to observe the ATDRS SSA forward-link service (S-band at 2070 MHz) should also be provided.

The block diagram for the ATDRS-tracking receiver is essentially the same as for the natural calibrator dual-band subsystem; however, cryogenic cooling for the LNA is not required and the bandwidths required may be as much as four times smaller.

B.1.2.4 Signal Processing and Transmission

The IF signals from each receiver (Ku/S for ATDRS tracking and Ku/S for observing natural sources) are converted to video, sampled, and formatted at each receiving station. The data is then sent via optical fiber to a central processing facility. Alternatively, the signals may be sent as analog signals over the optical fiber, then sampled and formatted at the central processing facility. To observe a 1 GHz bandwidth, the signal may be divided into several smaller bandwidth increments of perhaps 50 or 100 MHz. This is feasible because the phase-calibration system encodes accurate timing data into each subband.

The subsystems required for timing and signal transmission are:

- Optical fiber modem/coupler
- Optical fiber link--A length of 10 km is sufficient to connect each remote station with the central processing facility, with repeaters as necessary.
- Master 5 MHz frequency standard--It generates a 5 MHz signal used for timing and synchronization; it is not necessary to use a hydrogen maser for this purpose.
- Phase calibration--The change in phase of each remote station must be monitored and used to correct the overall phase stability of the array.
- IF-to-video converters
- Formatter--Functions include clipping/sampling, time-tagging, sync block generation, parity generation, and mode switching.

B.1.2.5 Data Receipt, Correlation, Analysis, and Archiving

The data received at the central processing facility from the three observing stations is cross correlated to extract differential phase-delay observables. Together with pertinent external information, the interferometric delays

are used to produce an updated ephemeris. Functional components of the correlation facility are:

- Demultiplexer/decoder
- Delay compensation--Based on the latest projection of the satellite position for the observation epoch, an appropriate amount of a priori delay must be introduced in order to reduce the correlator search window. One delay line is required for each data channel to be processed.
- Correlator--This device will compare the bit streams from each channel from each pair of stations (a total of three baselines) and accumulate the number of matching bits in real time.
- Fringe search--A single-purpose computer can be dedicated to performing the Fourier transform necessary to calculate the delay observables.
- Delay observable--This will consist of phase- and group-delay observables and associated correlation amplitude, which will be archived and passed to the OD system.
- Monitor data--Instrumental performance and meteorological information must be supplied to the orbital analysis algorithm in order to calibrate for known systematic effects.
- UT1/PM--A file of extrapolated Earth orientation information (from the USNO, for example) must be maintained for input to the orbital-analysis routine.
- Orbital analysis--A computer facility must be provided that is adequate to handle OD with sufficient precision to produce results accurate at the 50-m level. This processing need not be performed at the array central facility. If expedient, the observational and ancillary data can be relayed to a convenient site for orbital reduction.
- Archive--A system for automatic data archiving should be implemented at several points in the processing chain. Use of both disk and tape media is expected, with automatic recycling of space implemented under the control of a system-wide computer monitor.

- Updated ephemeris--The output from the OD processor will be used to extrapolate the ATDRS orbit forward in time for internal use in such tasks as antenna pointing and data correlation.

B.1.3 SYSTEM SPECIFICATION--VLBI-2S

The dual-satellite system as specified here is a subset of the quasar-calibrated system specified earlier, with those parts of the system devoted solely to quasar observations omitted. Clock calibration is performed by observing more than one satellite and by fitting a clock model. Site locations and OD and TR results are predicated on the assumption of a satellite at the position of an ATDRS-like satellite located in the overhead slot but with a downlink main beam footprint encompassing all sites.

The VLBI array will consist of four sites, shown in Figure 5-2 in the main text.

These locations are chosen assuming ATDRS satellites with SGL beam characteristics similar to those of the current TDRS, located over longitudes 41°E and 171°E, and with the GT located at White Sands, NM. A third satellite is assumed located at the longitude of White Sands, with signal characteristics similar to ATDRS and with downlink coverage extending from East Texas to Southern California.

Two of the sites are common sites and will observe all three ATDRSs. The eastern site (East Texas) observes ATDRS-E and ATDRS-C, and the western site (Southern California) observes ATDRS-W and ATDRS-C. The TR and OD results in the text assume arrays of three stations observing two satellites. No simulations have been performed including all observations of all three satellites.

The IF signals from each receiver (Ku- or S-band) are converted to video, sampled, and formatted at each receiving station. The data is then sent from each remote receiving station via satellite link to the central processing facility, which will control and monitor operations at all sites. The facility may be colocated with one of the common observing sites.

Each site will be equipped with the following:

- One calibrator antenna and receiver
- One or two ATDRS-tracking antennas and receivers
- Hydrogen maser time/frequency standard
- Electronics rack to process signals from receivers

- Calibration apparatus
- Communications link to transmit data
- Station control computer

These should have the attributes described in the sections that follow.

B.1.3.1 TDRS-Tracking Antenna

Each site will have one 2-m diameter antenna, fully steerable, with slew rates of at least 1 degree per second, controller, pointing accuracy of about 4 arcmin blind, and aperture efficiency of 0.5 (gain of 46.3 dB).

The ATDRS antenna will observe the ATDRS SGL, centered at 13.9285 GHz. Capability of observing the SSA forward link (2070 MHz) will also be provided. The ATDRS receiver will be located at the focus of the 2-m ATDRS antenna. Design and function are similar to those of the natural calibrator receiver; however, the receiver is uncooled, total system temperatures of 200°K at Ku-band and 100°K at S-band are adequate, and total bandwidths of 260 MHz at Ku-band and 50 MHz at S-band are adequate.

B.1.3.2 Time/Frequency Standard

The hydrogen maser frequency standard shall be monitored remotely and by reference to an on-site GPS receiver.

B.1.3.3 Electronics Rack

The electronics rack contains modules that select, sample, and format the desired signals. It should have the following capabilities:

- IF distributor--This will distribute signals from receiver IFs to videoconverters in any combination, under computer control.

- IF-to-video converters (28 total)--These convert IF signals from the antenna to baseband and filter to the desired channel bandwidth. Frequency and bandwidth are selected under computer control. Frequency range must be at least 500 MHz and bandwidth selectable up to at least 2 MHz.

- Formatter--Functions include clipping/sampling, time-tagging, synch block generation, parity generation, and mode switching.

- Data buffer--This should be capable of storing formatter output for a 1-second observation, a total of 14 times 4 Mb. This allows later transmission of ATDRS observation.

B.1.3.4 Calibration Apparatus

This shall include phase and cable calibration systems (the new Haystack system is adequate); a meteorological sensor to measure local barometric pressure, temperature, and relative humidity; and possibly a water vapor radiometer (budgeted).

B.1.3.5 Communications Links

Data from the formatter will be written into cache memory. One 1-second observation will require 500 kilobytes (kB) per channel, or 4 Mb total. The data will be read back and transmitted over a satellite link. The minimum transponder volume will be 12 kB per second. Total transponder volume will be 64 MB per hour in normal OD operation. A small additional capacity will be used to transfer monitor and control information. Spooling takes 5 minutes. This contribution to observation staleness can be reduced by higher peak transponder volume.

Satellite data transfer capability will be required for only three of the remote stations if the central processing facility is colocated at one of the common sites.

B.1.3.6 Station Control Computer

This will control antenna pointing, data acquisition modules, monitor/control data, and communications with the array control center. The central processing facility will perform array control functions. The data received from the four observing stations is cross-correlated to extract differential delay observables. Together with pertinent external information, the interferometric delays are used to produce an updated ephemeris, to be supplied to the stations and to the correlator. Functions include the following:

- SGL--The SGL will handle up to 12 kB per second from each of three remote sites.
- Demultiplexer/decoder
- Short-term archive--This enables recorrelation of ATDRS observations when a priori delay estimates are too inaccurate for proper results, as is expected in TR situations.

- Delay compensation--Based on the latest projection of the satellite position for the observation epoch, an appropriate amount of a priori delay must be introduced in order to reduce the correlator search window. One delay line is required for each data channel to be processed. Data buffering will be required if data from the remote stations is transmitted sequentially over the satellite link. The total delay must be enough to allow for total difference in signal travel times, both to the different stations (about 3 milliseconds) and over the satellite link (unknown). However, if the data is accumulated for later correlation, minimal buffering may be needed.

- Correlator--This device will compare the bit streams from each pair of stations (a total of three baselines for each network) and accumulate the number of matching bits in near real time. Each baseline requires 14 correlator modules, each correlating data from one 2 MHz (4 Mbps) channel. This data is dumped onto disk.

- Fringe search--A single-purpose computer can be dedicated to performing the Fourier transform necessary to calculate the delay observables. The system must be able to perform an automated search for the single band delay.

- Monitor data--Instrumental performance and meteorological information must be supplied to the orbital-analysis algorithm in order to calibrate for known systematic effects.

- UT1/PM--A file of extrapolated Earth orientation information (from the USNO, for example) must be maintained for input to the orbital-analysis routine.

- Orbital analysis--A computer facility must be provided that is adequate to provide ATDRS position predicts of sufficient accuracy (about 1 km) for correlation.

- Archive--A system for automatic data archiving should be implemented at several points in the processing chain. Use of both disk and tape media is to be expected, with automatic recycling of space implemented under the control of a system-wide computer monitor.

- Updated ephemeris--The output from the OD processor will be used to extrapolate the TDRS orbit forward in time for internal use in such tasks as antenna pointing and data correlation.

B.1.4 SYSTEM SPECIFICATION - VLGI-GH

The GPS-calibrated system specified here is similar in concept to VLBI-2S except that GPS satellites are used instead of a second TDRS-like satellite. Three options are considered. In each, clock calibration is performed by observations of GPS satellites. Option 1 simply uses the GPS satellite as a means of time transfer. Option 2 employs omnidirectional receivers that can decode the GPS navigation message and uses the precise delay measurements to fit a clock model, a tropospheric zenith delay parameter, and the GPS orbits themselves. Option 3 employs a small, steerable antenna for group delay measurements plus an omnidirectional antenna for phase-tracking measurements of the GPS satellites. The clock model, troposphere zenith delay, and GPS orbits are then fitted without recourse to knowledge of codes. Option 3 is the one of greatest interest.

In each system, the GPS satellites allow clock synchronization. Except for the apparatus involved with observing and analyzing GPS observations, these systems are identical to the systems called VLBI-2S. Each consist of the same components as VLBI-2S plus additional elements required to observe and analyze the GPS signals. System differences are due to the different frequency, signal structure, and nongeosynchronous orbits of the GPS satellites. A description follows of the Option 3 system, which is the most complex and costly.

B.1.4.1 Array Geometry

Array geometry is chosen so that stations lie within the main lobe footprints of the Ku-band SGL to White Sands. Geometry is identical to that in VLBI-2S, shown as in Figure 5-2.

The IF signals from each steerable antenna (ATDRS, GPS) are converted to video, sampled, and formatted at each receiving station. The data are cached for transmission through satellite link or leased telephone line to the central processing facility. This central facility will control and monitor operations at all four sites. The facility may be colocated with one of the common observing sites.

Each site will be equipped with the following:

- GPS calibrator antenna (steerable) and receiver
- Omnidirectional GPS phase-tracking receiver
- ATDRS-tracking antenna and receiver
- H-maser time/frequency standard
- Electronics rack to process signals from receivers
- Calibration apparatus
- Communications link to transmit data
- Station control computer

These should have the following attributes:

- GPS group delay antenna. This is a 2-m diameter antenna, fully steerable, with slew rates of at least 1 deg/sec, controller, pointing accuracy of about 30 arcmin blind, and aperture efficiency of 0.5. This GPS antenna will observe the NAVSTAR satellites once per pass at both the L1 and L2 frequencies, centered at 1225 MHz and 1664 MHz. The signals received by this antenna will not be decoded. At each frequency, the receiver bandwidth must be at least 20 MHz and the system temperature not more than 250 K.

- GPS phase-tracking antenna. This omnidirectional antenna shall be able to track the carrier phase of both L1 and L2 signals for up to 8 satellites simultaneously. The antenna shall be designed to mitigate multipath effects for satellite elevations 20 degrees or more above the horizon. The phase-tracking antenna shall read the coarse acquisition (C/A code) navigation message to provide a priori delays for the correlator.

- TDRS-tracking antenna. This is a 2-m diameter antenna, fully steerable, with slew rates of at least 1 deg/sec, controller, pointing accuracy of about 4 arcmin blind, and aperture efficiency of 0.5 (gain of 46.3 dBi). There is one at each site. The ATDRS antenna will observe the ATDRS SGL centered at 13.9285 GHz. Capability of observing the SSA forward link (2070 MHz) will also be provided. The ATDRS receiver will be located at the focus of the 2-m ATDRS antenna. Design and function are identical to those described for VLBI-2S: (1) the receiver is uncooled; (2) total system temperatures of 200 K at Ku-band and 100 K at S-band are adequate; and (3) total bandwidths of 260 MHz at Ku-band and 50 MHz at S-band are adequate.

- Time/frequency standard. The hydrogen maser frequency standard shall be monitored remotely and by reference to an onsite GPS receiver.

- The electronics rank. This contains modules that select, sample, and format the desired signals. It should have the following capabilities:

  - IF distributor, to distribute signals from receiver IFs, to videoconverters in any combination, under computer control.

  - IF-to-video converters (24 total), which convert IF signals from the antenna to baseband and filter to the desired channel bandwidth. Frequency and bandwidth are selected under computer control. Frequency range must be at least 500 MHz and bandwidth selectable up to at least 4 MHz.

  - Formatter, functions of which include clipping/sampling, time-tagging, synch block generation, parity generation, and mode switching.

  - Cache memory capable of storing formatter output for a 1-sec observation. For the ATDRS, this is 8 channels times 4 Mbits, or 4 MBytes. For a GPS, this is 2 time 40 Mbits, or 10 MBytes. This allows later transmission of ATDRS and GPS group delay data.

- Calibration apparatus. Items included here are phase and cable calibration systems (the new Haystack system is adequate); a meteorological sensor to measure local barometric pressure, temperature, and relative humidity; and possibly a water vapor radiometer (budgeted). The cable calibration systems shall be implemented to both the ATDRS and the GPS receiver systems.

- Communications links. Data from the formatter will be written into cache memory. One 1-sec ATDRS observation will require 500 kBytes per channel or 4 MBytes total. During TR, the frequency of such observations is six per hour, or 24 MBytes/hr. During normal OD, the ATDRS observations require 8 MBytes/hr. Group delay observations of the GPS require 10 MBytes and are needed once per satellite pass, or a one every 30 minutes for a 24-satellite constellation, for an average data rate of 20 MBytes/hr. Maximum transponder volume thus averages 44 MBytes/hr (98 Kbits/sec) at each remote station, plus an additional 4 MBytes/hr for each additional ATDRS the site observes. A small additional capacity will be used to transfer monitor and control information. Spooling the ATDRS observation

takes 320 sec. This contribution to observation staleness can be reduced by higher peak transponder volume.

- Station control computer. This will control antenna pointing data acquisition modules, monitor/control data, and communications with array control center.

The central processing facility will perform array control functions. The data received from the observing stations will be cross-correlated to extract differential delay observables. Together with pertinent external information, the interferometric delays will be used to produce an updated ephemeris, to be supplied to the stations and to the correlator. Functions include the following:

- Satellite-to-ground data link. Up to 12 KBytes/sec from each of four remote sites.

- Demultiplexer/decoder.

- Short-term archive. This enables recorrelating ATDRS observations when a priori delay estimates are too inaccurate for proper results, as may occur in TR situations.

- Delay compensation. Based on the latest projection of the satellite position for the observation epoch, an appropriate amount of a priori delay must be introduced in order to reduce the correlator search window. As correlation is not to be done in real time, this delay compensation may be performed in software.

- Correlator. Device will compare the bit streams from each pair of stations (a total of three baselines for each of the networks) and accumulate the number of matching bits. Each baseline requires 8 correlator modules for ATDRS observations and 10 correlator modules (if using Mk III modules) for GPS observations. Resultant data are dumped onto disk.

- Fringe search. A single-purpose computer can be dedicated to performing the Fourier transform necessary to calculate the delay observables. The system must be able to perform an automated search for the single-band delay.

- Monitor data. Instrumental performance and meteorological information, must be supplied to the orbital analysis algorithm to calibrate for known systematic effects.

- UTI/PM. A file of extrapolated Earth orientation information (from the USNO, for example) must be maintained for input to the orbital analysis routine. Alternatively, Earth orientation may be estimated from the GPS observations.

- Orbital analysis. The computer facility must be adequate to provide ATDRS position predicts of sufficient accuracy (about 1 km) for correlation. Capability must be present to analyze the GPS data and derive precise GPS orbits. The GEODYNE program, adapted to utilize interferometric group delay in addition to phase tracking, should be sufficient.

- Archive. A system for automatic data archiving should be implemented at several points in the processing chain. Use of both disk and tape media is to be expected, with automatic recycling of space implemented under the control of a system-wide computer monitor.

- Updated ephemeris. The output from the orbit determination processor will be used to extrapolate the TDRS orbit forward in time for internal use in such tasks as antenna pointing and data correlation. Antenna pointing and a priori delays for the GPS may be obtained to adequate precision from the broadcast ephemerides.

B.2 STAFFING REQUIREMENTS

Staffing levels are estimated for support of interferometric tracking systems, based on the following assumptions:

- ATDRS satellites are in three orbital slots.
- VLBI systems each consist of five separate sites.
- The CEI system consists of three separate arrays with three stations each.
- Each system has a continuous array monitor primarily for fast problem recognition, although 24-hour coverage may not be absolutely necessary.

Staffing levels are specified in terms of number of full-time equivalent employees (FTEs). Managerial and other support is not considered; only technical-support staffing is estimated.

B.2.1 STAFFING: VLBI-Q

A VLBI system calibrated by natural radio sources requires technical support staffing as follows:

- One and one-half FTE site technicians per site (7.5 total) will perform regular and unscheduled inspection, maintenance, and some repairs for antennas, electronics modules, computers, data link, and other site maintenance functions.
- Five FTE array operators will provide full-time monitoring of proper array, communications, and correlator performance.
- Array and correlator technical support requires 12 FTEs:
  - Electronics
    - Systems engineer
    - Programmer
    - RF engineer
    - Digital engineer and technician
  - Correlator
    - Systems engineer
    - Systems programmer
  - Antenna
    - Mechanic
    - Technician
  - Source selection
    - Scientist
  - Maser support
    - Engineer
    - Technician

B.2.2 STAFFING: VLBI-2S SYSTEM

A VLBI-2S system requires technical support staffing as follows:

- One FTE site technician is needed per site (5 total) to perform regular and unscheduled

inspection, maintenance, and repairs for antennas, electronics modules, computers, and data link and to perform other site-maintenance functions. The reduced staff requirement as compared to the quasar-calibrated system is due to elimination of the 12-m antenna with the cooled receiver and to the somewhat simpler electronics package.

- Five FTE array operators will provide full-time monitoring of proper array and correlator performance.

- Array and correlator technical support requires eight FTEs:

  - Electronics

    - o Systems engineer
    - o Programmer
    - o RF engineer

  - Correlator

    - o Systems engineer
    - o Systems programmer

  - Antenna

    - o Mechanic

  - Maser support

    - o Engineer
    - o Technician

B.2.3 STAFFING: CEI-Q (GROUP DELAY) SYSTEM

A CEI system calibrated by natural radio sources requires technical support staffing as follows:

- Two FTE site technicians are required per site (6 total) to perform regular and unscheduled inspection, maintenance, and some repairs for antennas, electronics modules, computers, and data link and to perform other site maintenance functions. The increased staff compared to the VLBI-Q system is needed because there are three 12-m antennas at each site.

- Five FTE array operators will provide full-time monitoring of proper array, communications, and correlator performance.

- Array and correlator technical support requires ten FTEs:

  - Electronics

    - Systems engineer
    - Programmer
    - RF engineer
    - Digital engineer

  - Correlator

    - Technician
    - Systems engineer
    - Systems programmer

  - Antennas

    - Mechanic
    - Technician

  - Source selection

    - Scientist

B.2.4 STAFFING: VLBI-GH

A VLBI-GH system requires technical support staffing as follows:

- One FTE site technician is required per site (5 total) to perform regular and unscheduled inspection, maintenance, and repairs for antennas, electronics modules, computers, data link, and other site maintenance functions. The GPS group delay antenna is similar in complexity to the ATDRS antenna. The GPS phase-tracking antenna should require very little attention.

- Five FTE array operators will provide full-time monitoring of proper array and correlator performance.

- Array and correlator technical support requires 9 FTEs:
  - Electronics
    - o Systems engineer
    - o Programmer
    - o RF engineer
  - Correlator
    - o Systems engineer
    - o Systems programmer
  - Antenna
    - o Mechanic
  - Maser support
    - o Engineer
    - o Technician
  - GPS OD
    - o Scientist/engineer

Use of GPS solely for time synchronization (System I) requires a total of one more FTE than VLBI-2S. The RF, antenna, and receiver systems are similar in complexity and design to the systems observing the ATDRS. The new, different tasks are keeping track of the GPS satellites, performing the group delay observations, integrating the phase-tracking data, and supporting the GPS OD program.

B.3 COST ESTIMATES

Tables B-1 through B-5 present cost estimates for interferometric tracking systems. The starting point for these estimates is References 5-2 and 5-5.

Areas modified from that report are (1) consideration of the VLBI-2S configuration; (2) reestimation of manpower requirements for operations; (3) revision of CEI system specifications for measurement of group delay, including changes to receiver, fiber-optic link, and correlator; and (4) approximately 20 percent inflation allowance to translate 1985 costs to 1988 dollars.

Table B-1. Cost Estimates (in Thousands)

Design and Specification	VLBI-Q	CEI-Q	VLBI-2S	VLBI-GH
Antenna/positioner (ATDRS)	$ 10	$ 10	$ 10	$ 10
Antenna/positioner (Calib)	100	100	--	10
Receiver (ATDRS)	35	40	35	35
Receiver (Calib)	45	55	--	35
Receiver (GPS phase)	--	--	--	10
Data formatter	50	100	50	50
Communications	100	200	50	50
Station control	65	200	50	50
Time/frequency	5	5	5	5
Calibration (WVR)	25	25	25	25
Physical plant	75	100	50	50
Correlator	150	600	125	125
OD (GPS)	--	--	--	20
Detailed specifications	320	400	240	260
Total	$980	$1835	$620	$715

Table B-2. Implementation Costs (in Thousands)

Item	VLBI-Q		CEI-Q		VLBI-2S		VLBI-GH	
Antenna/positioner (ATDRS)	$ 125	7	$ 125	9	$ 125	5	$ 125	5
Antenna/positioner (Calib)	2500	5	2500	9	--		125	5
Receiver (ATDRS)	90	7	90	9	90	5	90	5
Receiver (Calib)	110	10	130	18	--		90	5
Il Receiver (GPS phase)	--		--		--		100	5
Data formatter	350	10	450	9	350	5	350	5
Communications	1000	4	450	3	200	4	200	4
Station control	25	5	100	3	20	5	20	5
Time/frequency	500	5	100	3	500	5	500	5
Calibration (WVR)	250	5	250	3	250	5	250	5
Physical plant	900	5	1500	3	600	5	700	5
Total	$33230		$37825		$10475		$12600	

NOTE: Entries reflect cost per item, number of items in complete system.

Table B-3. Total Additional Costs for Central Processing Facility (Colocated With One Site) (in Thousands)

Item	VLBI-Q	CEI-Q	VLBI-2S	VLBI-GH
Physical plant	$1500	$ 750	$1000	$1250
Correlation	750	900 3	500	600
I1 OD (GPS)	--	--	--	120
Total	$2250	$3450	$1500	$1970

Table B-4. Total Costs for Implementation of the Full Network (With Antenna, Correlator) (in Thousands)

Item	VLBI-Q	CEI-Q	VLBI-2S	VLBI-GH
Antenna/positioner (ATDRS)	$ 875	$ 1125	$ 625	$ 625
Antenna/positioner (Calib)	12500	22500	--	625
Receiver (ATDRS)	630	810	450	450
Receiver (Calib)	1100	2340	--	450
Il Receiver (GPS phase)	--	--	--	500
Data formatter	3500	4050	1750	1750
Communications	4000	1350	800	800
Station control	125	100	100	100
Time/frequency	2500	300	2500	2500
Calibration (WVR)	1250	750	1250	1250
Physical plant	6000	4800	3000	3500
Correlation	750	2700	500	600
Design and specification	980	1835	620	715
Total design and implementation	$34210	$42660	$11595	$13365

Table B-5. Sustaining Costs (Annual) (in Thousands)

Item	VLBI-O		CEI-O		VLBI-2S		VLBI-GH	
Antenna/positioner (ATDRS)	$ 12	5	$ 12	9	$ 12	5	$ 12	5
Antenna/positioner (Calib)	60	5	60	9	--		12	5
Receiver (ATDRS)	3	5	3	9	3	5	3	5
Receiver (Calib)	5	10	5	9	--		3	5
I1 Receiver (GPS Phase)	--		--		--		3	5
Data formatter	4	10	8	9	4	5	4	5
Communications	1500	4	15	3	120	4	150	4
Station control	4	5	10	3	3	5	3	5
Time/frequency	25	5	4	3	25	5	25	5
Calibration (WVR)	10	5	12	3	15	5	15	5
Physical plant	50	5	60	3	50	5	50	5
On-site operations personnel	105	5	140	3	70	5	70	5
Physical plant/ operations center	75	1	25	1	75	1	75	1
Correlator	20	1	20	3	10	1	15	1
I2 Orbit determination (GPS)	--		--		--		40	1
Central operations personnel	1190	1	1050	1	910	1	980	1
Total sustaining costs/year	8720		2650		2360		2685	
Total design and implementation	$33960		$42660		$11515		$13315	
Total sustaining cost (10 years)	$87200		$26500		$23600		$26850	
Total 10-year life-cycle cost	$121160		$68760		$35115		$40165	

NOTE: Entries reflect cost per item, number in complete system excluding utilities.

The costs shown here for VLBI-GH are for the hybrid (group delay and phase delay) system. The system calibrated by GPS pseudorange measurements would be less costly than the hybrid system. The savings would be the cost of the GPS group delay antennas and receivers, a small portion of the maintenance costs, and the reduction in communications costs from halving data transfer requirements. However, costs might be increased by security requirements for using classified access code receivers.

In these estimates, salaries have all been estimated at $70k/year gross cost. The estimates do not include management or other nontechnical personnel costs, electricity costs, or any costs associated with a ranging system to the AGT.

B.3.1 COMMENTS

The costs for 12-m class antennas are in rough concordance with estimated costs of $7M for 25-m VLBI antennas. Considerable savings may be possible for multiple antennas, as in a CEI system, but no such assumption has been made in the estimates here.

Receiver costs are based on the Bendix estimates referenced earlier. A differential is made for the natural calibrator receivers because they must be housed in a dewar. A further differential applies for the CEI natural calibration receivers because of the wide bandwidth design required.

The data formatter for the VLBI systems is assumed to be commercially available MK-III components. It is assumed that the quasar and the ATDRS observations are time-multiplexed. Simultaneous observation would double this cost. Recent information indicates that the estimate is considerably (30 to 40 percent) below the current market quote; however, that is a quote for a single system, and there is expected to be more than one vendor soon.

Communications costs for the VLBI-Q system encompass transmitting a peak data rate of 4 MB/sec for the quasar observations from each remote site. A cost of $125k/month has been quoted. The initial cost ($1M) for setting up the link is based on the Bendix estimate and is highly uncertain. Life-cycle costs for this link are such that construction of a dedicated fiber-optic link would probably be cost-competitive.

Communications costs for the VLBI-2S system are based on commercial rates for a 56-kilohertz wide satellite channel. A wider link, at greater cost, would reduce data transmission time and observation staleness. Ground-based links were not investigated.

Communications costs for the CEI systems assume fiber-optic links to three antennas. A phase-delay-only system would require much less bandwidth but a trench just as long plus interfaces at two additional antennas.

Correlation costs for the VLBI-Q system assume a system like the new MK-III VLBI correlator at the USNO, but with slightly reduced capabilities. The VLBI-2S correlator would be the same but with capabilities further reduced. In each case, some additional work is needed to design buffering for real-time correlation.

Correlator costs for the CEI-Q system assume group-delay processing of the entire 1-GHz bandwidth. This entails an entirely new correlator design, estimated at 6-8 staff years of development effort. The implementation cost may fall dramatically when the new correlator chips from Westerbrook Observatory become commercially available. A correlator to process phase-delay data only would also be very much less expensive.

Costs for station control, water vapor radiometers, physical plant, and hardware maintenance are scaled from BFEC estimates. Personnel costs are based on staffing requirements contained in Section B-2 of this appendix.

APPENDIX C - PRTS, MPRTS, AND AKuRS MEASUREMENT NOISE LEVELS

This appendix details the range and range-rate measurement noise levels used to model PRTS, MPRTS, and AKuRS. Both worst case values based on the TDRSS and ATDRSS specifications and system-based values reflecting the various system aspects are developed. Finally, a discussion of the values derived here and those derived operationally from the TDRSS BRTS is presented.

C.1 RANGE MEASUREMENT NOISE

Noise levels in the range measurements for MPRTS and AKuRS have been estimated on the basis of typical tracking performance for pseudonoise range codes. Due to the specific nature of PRTS signal processing, range measurement noise for PRTS has been assumed to be 1.5 meters (3 σ); this value stems from simulation of PRTS signal processing conducted as part of the PRTS Phase II SBIR investigation. For MPRTS and AKuRS, range measurement noise values may be estimated in two different ways, as discussed in the sections that follow. The first set of estimates derives from the TDRSS specifications and represents a worst case, conservative value; the second set of estimates represents an approximate calculation based on the systems' respective link budgets.

C.1.1 WORST CASE RANGE MEASUREMENT ERRORS

The specification for TDRSS services (Reference C-1) indicates that, for data rates greater than 1000 bps and thus for relatively strong return signals, the "maximum rms error contribution to range measurement from TDRS and ground terminal equipment" is 10 ns for user spacecraft meeting minimum EIRP requirements. In contrast, the more recent specifications for the STGT are concerned only with ground equipment performance and do not attempt to treat end-to-end range measurement performance (Reference C-2). No distinction is made in the specification between one-way and two-way range estimates, suggesting that the 10 ns total rms range error yields a one-way rms range error of 3.0 m and a two-way rms range error of 1.5 m. These values may be used to model conservatively the two-way range error noise associated with MPRTS and AKuRs, converted to a 3-σ value of 4.5 m.

C.1.2 SYSTEM-BASED RANGE MEASUREMENT ERRORS

Alternatively, MPRTS and AKuRS range measurement noise may be characterized more directly by considering the performance of the associated PN tracking loops. Tracking loop performance may be simplified as a function of input signal C/N_O, tracking loop bandwidth B_L, and aspects of the loop design. Neglecting the specifics of the various possible loop designs, it can be shown that the rms tracking error (as a fraction of a PN chip) due to thermal noise is approximately given by (Reference C-3)

$$\left(\frac{\sigma}{T_C}\right)^2 = \frac{B_L}{2\left(\frac{C}{N_O}\right)}$$

Clearly, the higher the value of the carrier power to noise spectral density ratio and/or the lower the tracking loop bandwidth, the lower the range measurement noise. However, the loop bandwidth B_L cannot be arbitrarily set as low as desired if the effects of phase noise, rate error, and signal dynamics are to be limited. For the PN chip rates and carrier frequencies of interest here, phase noise effects on PN tracking are not a major concern. The impacts due to rate error and signal dynamics may be reduced if the PN tracking loop design takes advantage of information derived from the receiver's carrier loop. Such an approach is taken in the TDRSS second generation user transponder, where B_L is reduced to 0.125 Hz. Other receiver designs may require higher loop bandwidths; for example, the Wide Dynamics Demodulator uses a 4 Hz loop bandwidth in its tracking mode.

The link budgets for MPRTS and AKuRS have been constructed to provide sufficient C/N_O to support the data rates involved and to reduce the carrier phase-tracking error, assuming a reasonable value for the carrier tracking loop bandwidth. For MPRTS, the received C/N_O obtained at the AGT from two-way turnaround of the PRTS signal reference channel depends on the characteristics of the dedicated S-band return channel, as discussed in Section 4.1.3. Assuming a single element of the SMA array is used to support the dedicated return channel, providing a G/T of -11 dB/K, and 1 W of transmit power is used by the MPRTS ground station, then Table 4-2 of the study indicates that the received C/N_O is 45.9 dB-Hz. In the case of AKuRS, the received C/N_O is given in Table 3-4 to be 40.6 dB-Hz.

Assuming then that the loop bandwidth is 4 Hz, and knowing that the chip rate for both MPRTS and AKuRS is approximately 3 Mcps, then the range measurement noise levels (1 σ) for MPRTS and AKuRS can be computed to be 0.72 and 1.32 m, respectively.

C.2 RANGE-RATE MEASUREMENT NOISE

Noise levels in the range-rate measurements for MPRTS and AKuRS have been estimated on the basis of typical carrier tracking performance. The conversion of phase-locked loop tracking noise to the corresponding range-rate measurement noise is discussed below. Two sets of range-rate measurement noise estimates are then calculated: worst case, conservative values derived from the TDRSS specifications and a second, system-based set derived from consideration of system thermal and oscillator phase noise contributions.

The process of Doppler extraction is effectively the estimation of the received carrier frequency obtained by counting positive-going zero-crossings, N(t), over an averaging time T_{AV}. The estimate, R, of the true one-way range-rate, R, is then

$$R = \lambda \left[\frac{N \quad t+T_{AV} - N(t)}{T_{AV}} \right] = R + \frac{\lambda}{2\pi} \left[\frac{\delta\phi \quad t+T_{AV} - \delta\phi(t)}{T_{AV}} \right]$$

where $\delta\phi(t)$ is the noise in the phase measurement and λ is the carrier wavelength.

Assuming that T_{AV} is long enough so that the phase samples are i.i.d., which is a valid assumption for T_{AV} greater than the inverse loop bandwidth of the tracking loop, the one-way rms range-rate error is

$$\sigma_R = \frac{\lambda}{2\pi T_{AV}} \sqrt{\sigma^2_{\varphi \; t+T_{AV}} + \sigma^2_{\varphi(t)}} = \frac{\lambda}{2\pi T_{AV}} \sqrt{2 \; \sigma_\varphi} \quad \text{(1-way)}$$

where $\sigma\varphi$ is the rms phase-tracking error in radians.

For two-way measurements, the measurement process described above results in an estimate of 2R. Obtaining R then

requires dividing by 2, so the two-way rms range-rate error is similarly reduced:

$$\sigma_{\dot{R}} = \frac{\lambda}{2\pi T_{AV}} \frac{\sqrt{2}}{2} \sigma_{\varphi} \quad \text{(2-way)}$$

C.2.1 WORST CASE RANGE-RATE MEASUREMENT ERRORS

The performance specification for the TDRSS services (Reference C-1) gives Doppler tracking performance in terms of "phase noise contributions to Doppler tracking resulting from TDRS and ground equipment" for TDRSS users meeting minimum EIRP levels for a particular range of data rates. Use of the term "phase noise" implies that the specified value includes all phase noise contributors, especially thermal noise and oscillator phase noise. Because Doppler tracking performance is specified in this way, it is assumed that the specified values reflect the Doppler measurement process and must be interpreted in terms of either one- or two-way range rate. For MA and SSA return service at less than 500 bps, as would be appropriate for PRTS and MPRTS, the specified maximum rms phase-tracking error is 0.4 radians (22.9 deg). For KSA return service at data rates greater than 1000 bps, as would apply to AKuRS, the maximum rms phase-tracking error is given as 0.2 radians (11.5 deg). These two values have been used to provide worst case range-rate error values for MPRTS and AKuRS.

At the S-band forward frequency of 2106.4 MHz, λ is 0.1424 m; at the S-band return frequency of 2287.5 MHz, λ is 0.1311 m. Assuming 10-sec averaging and σ_{φ} equal to 0.4 radians, the one-way range-rate measurement noise, appropriate for the one-way range-rate measurements of PRTS, is equal to 0.128 cm/sec (1 σ). For two-way range-rate measurements, as appropriate for MPRTS, the error in the estimated R is reduced by a factor of two and, neglecting the difference in forward and return frequencies, is equal to 0.059 cm/sec (1 σ), assuming a worst case tracking error of 0.4 radians. At the Ku-band return frequency of 13.775 GHz, λ is 0.0218 m. Assuming 10-sec averaging and σ_{φ} equal to 0.2 radians, the two-way range-rate measurement noise corresponding to AKuRS is equal to 0.0049 cm/sec (1 σ).

C.2.2 SYSTEM-BASED RANGE-RATE MEASUREMENT ERRORS

More representative system-based values may be computed on the basis of the anticipated carrier tracking loop

performance and the oscillator phase noise. As documented in Sections 3 and 4, the link budgets for MPRTS and AKuRS are tailored to provide sufficient C/N_O to allow an rms phase-tracking error of 5 deg (.087 radians).

Assuming 10-sec averaging and σ_φ equal to 5 deg, the PRTS range-rate measurement noise due to thermal noise is 0.028 cm/sec (1 σ). For the MPRTS two-way range-rate measurements, assuming a tracking error of 5 deg, the range-rate error is equal to 0.013 cm/sec (1 σ). For AKuRS, the two-way range-rate measurement noise due to thermal noise is equal to 0.0021 cm/sec (1 σ).

In addition to the contribution of thermal noise to range-rate measurements, oscillator phase noise, Doppler quantization noise, and sampling jitter also contribute to the measurement error. Of these error contributors, only oscillator phase noise typically compares in magnitude to the error due to thermal noise. The contribution of oscillator phase noise to one-way and two-way range-rate measurements has been documented in References C-4 and C-5.

In PRTS, the range-rate measurements are one-way forward measurements at S-band. It can be shown (Reference C-5) that the range-rate error due to oscillator phase noise can be modeled as

$$\sigma^2_{\dot{R}} = c^2\, \sigma_y^2(T_{AV})\Big|_{station} + c^2\, \sigma_y^2(T_{AV})\Big|_{AGT}$$

where $\sigma_y^2\, T_{AV}$ refers to the zero-dead-time two-sample variance of the fractional frequency fluctuations (i.e., the Allan variance for averaging time T_{AV}) of either the PRTS tracking station ("station") or the AGT ("AGT"). Assuming that the PRTS tracking stations possess frequency standards comparable to an oven-stabilized crystal oscillator, the square root of the Allan variance for an averaging time of 10 sec may be taken as 5×10^{-13}. Assuming that the AGT frequency standard is comparable to the TDRSS Common Time and Frequency Standard, the corresponding value for the square root of the Allan variance may be taken as 1×10^{-12} (Reference C-5). With these values, the one-way range-rate error contribution due to oscillator phase noise is 0.0335 cm/sec. The phase error contributions due to thermal noise and phase noise are independent; therefore, the total 1-σ effect is given by the square root of the sum of their

variances. For the system-based values due to thermal noise computed previously, the corresponding total 1-σ PRTS range-rate error is 0.044 cm/sec.

In the case of two-way range-rate measurements as used in MPRTS and AKuRS, the effect of oscillator phase noise depends, to first order, only on the oscillator that generates the original transmitted signal. Here, the AGT oscillator determines the phase noise contribution. The various frequency translations and path delays involved in two-way transmission through ATDRSS, however, affect the value of the AGT oscillator phase noise contribution. Assuming worst case that the ATDRSS frequency system design does not incorporate use of return pilots, the range-rate error due to oscillator phase noise may be modeled (Reference C-5) as

$$\sigma_R^2 = \left(\frac{c}{1+\varphi}\right)^2 \frac{2}{T_{AV}} \left[\left(\frac{f_{SGL}}{f_u}\right)^2 T_{SGL} + Q^2 T_u\right] \sigma_y^2 \; T_{AV} \Big|_{AGT}$$

where Q is the two-way turnaround ratio, T_{AV} is the Doppler averaging time, f_{SGL} is the ATDRS-to-AGT frequency, f_u is the ATDRS-to-tracking station frequency, T_{SGL} is the round-trip AGT-ATDRS path delay, and T_u is the round-trip ATDRS-to-tracking station path delay.

Although the ATDRSS frequency plan and other aspects of ATDRS are not yet fully defined, typical TDRSS values will be assumed for the purposes of this calculation. Accordingly, let Q equal 240/221 for MPRTS and 1600/1469 for AKuRS, T_{AV} equal 10 sec, f_{SGL} equal 13.6775 GHz, f_u equal 2106.4 MHz for MPRTS and 13.77522432 GHz for AKuRS, and T_{SGL} and T_u both equal 0.25 sec. Substituting these values, the range-rate error contributions due to phase noise for MPRTS and AKuRS are 0.0212 and 0.00473 cm/sec, respectively. For the system-based values due to thermal noise computed previously, the corresponding total 1-σ MPRTS range-rate error is 0.0249 cm/sec; for AKuRS, the total system-based 1-σ range-rate error is 0.0052 cm/sec (system-based). Although operation at the smaller wavelength in AKuRS effectively improves the range-rate error due to thermal noise, compared to MPRTS, phase noise proves to be the dominant error contributor for both AKuRS and MPRTS.

C.3 DISCUSSION OF MEASUREMENT NOISE VALUES

The various measurement noise values discussed are summarized in Table C-1 as 3-σ values. To gauge the validity of these values somewhat independently, comparison has been made with the values obtained operationally by GSFC Code 554 for TDRS position estimation using BRTS (Reference C-6).

The Code 554 BRTS values are directly comparable to those of MPRTS since both are two-way ranging systems operating at S-band. The Code 554 range error is given as 1.5 m (3 σ), compared to the MPRTS value of 2.2 m (3 σ). Because the MPRTS value is worse than (greater than) the Code 554 value, the MPRTS range performance is effectively being conservatively modeled. The BRTS range value most likely arises from variate difference analysis of the observed minus corrected (O-C) BRTS tracking data, suggesting that the range measurements have been effectively filtered and reduced in the process (Reference C-7). Code 554 has not confirmed this interpretation (Reference C-8), but, in any case, conservative modeling of MPRTS is not necessarily undesirable.

The Code 554 BRTS value for range-rate error is derived from an observed rms Doppler deviation of .01 Hz seen in operations from the two-way Doppler measurement. Later conversations with Code 554 revealed that the rms error might be more like .005 Hz (Reference C-8). Converting this raw Doppler measurement error to a 3-σ range-rate error yields 0.197 cm/sec, corresponding to estimation of 2R. Division by two to conform to the conventions of this appendix then yields 0.0984 cm/sec (3 σ), in comparison to 0.075 cm/sec (3 σ) obtained for the system-based value. The magnitude of the discrepancy between the two values is not large and is likely due to the link budget assumed for MPRTS as compared to that of BRTS. Unfortunately, the Code 554 documentation does not indicate the underlying BRTS measurements; therefore, direct comparison is not readily possible. In addition, the Code 554 range-rate noise value might include other error sources, error sources that may be otherwise modeled in the ORAN analysis.

Table C-1. PRTS, MPRTS, and AKuRS Range and Range-Rate Errors

SYSTEM	ERROR VALUES (3-SIGMA)	
	WORST-CASE	SYSTEM-BASED
PRTS		
- Range (m)	-	1.5
- Range-Rate (cm/sec)	0.38	0.131
MPRTS		
- Range (m)	4.5	2.2
- Range-Rate (cm/sec)	0.177	0.075
AKuRS		
- Range (m)	4.5	4.0
- Range-Rate (cm/sec)	0.015	0.015

MIS51P

C.4 REFERENCES

C-1. NASA/GSFC, S-805-1, Performance Specification for Services via the Tracking and Data Relay Satellite System, Revision B, April 1983

C-2. NASA/GSFC Mission Operations and Data Systems Directorate, Phase II Requirements Specification for the Second TDRSS Ground Terminal (STGT), November 1988

C-3. T. Benjamin, "STGT Range Measurement Accuracy," Stanford Telecom memorandum to Denver Herr (NASA/GSFC), 12 December 1988

C-4. R. C. Bruno and B. D. Elrod, "TDAS 1-Way Navigation Alternatives: Impact Assessments," Revision 1, STI/E-TR850104, Stanford Telecom report to NASA/GSFC, October 1986

C-5. A. Jacobsen and K. Cunningham, STI/TR870110, "Performance Assessment of the COBE Ultra-Stable Oscillator," Revision 1, Stanford Telecom report to NASA/GSFC, May 1987

C-6. J. Pitsenberger and J. Teles, "Nominal Error Sources for Orbit Determination Error Analysis," NASA/GSFC Code 554.0 internal memorandum, 22 March 1989

C-7. R. Bruno, Stanford Telecom, personal communications, 6 April 1989

C-8. J. Teles, NASA/GSFC Code 554.0, personal communications, 7 April 1989

APPENDIX D - PASSIVE DIFFERENTIAL ATDRS/GPS TRACKING SYSTEM LIFE-CYCLE COSTING

This appendix derives a life-cycle cost estimate for the Passive Differential ATDRS/GPS Tracking System described and assessed in Section 6.3.

D.1 INTRODUCTION

The Passive Differential ATDRS/GPS Tracking System station hardware and software requirements are similar to the PRTS and MPRTS station requirements presented in Section 4. Consequently, the similarities between this system and the baseline PRTS and MPRTS systems have been used to provide a basis for estimating the life-cycle costs for the Passive Differential ATDRS/GPS Tracking System. As discussed in Section 6.3, a generic S-band navigation beacon, a Ku-band navigation beacon, or the S-band PRTS navigation beacon may be employed as the ATDRS ranging signal for the Passive Differential ATDRS/GPS Tracking System. Costing of the system, however, has assumed use of the PRTS beacon as marginally the most expensive option. In terms of the ground station hardware and software, the choice of any one of these three beacons has negligible impact on the estimated costs of the ATDRS ranging signal receiver because all require the same functions. By noting the functional similarities and differences among PRTS, MPRTS, and the Passive Differential ATDRS/GPS Tracking System, adjustment to the PRTS life-cycle cost estimates can be used to derive the passive differential system cost estimates.

D.2 LIFE-CYCLE COSTING METHODOLOGY

Similarities among PRTS, MPRTS, and the Passive Differential ATDRS/GPS Tracking System can be used to derive a cost estimate of the passive differential system based on the results of previous PRTS and MPRTS life-cycle cost estimates (References D-1 and D-2). The differences among PRTS, MPRTS and the passive differential tracking system cost estimates are restricted to several hardware subsystems in the systems' respective master and remote stations. The PRTS ground stations most closely resemble the passive differential tracking systems ground stations in terms of hardware and software functions. Eliminating the costs of those PRTS station subsystems that are not used in the passive differential system, and adding any additional subsystem costs, provides a ready means of estimating life-cycle costs for the Passive Differential ATDRS/GPS Tracking system.

The PRTS, MPRTS, and Passive Differential ATDRS/GPS Tracking System ground station architectures are shown in Figures 4-6, 4-7, and 6-12, respectively. Differences between the PRTS and passive differential station subsystems are associated with the station clocks, the transmitter and antenna subsystems, and the GPS receiver and antenna subsystems. The PRTS station clock subsystem uses a cesium clock as its frequency standard, whereas the passive differential system, like MPRTS, uses a thermally controlled crystal oscillator. The cost of the cesium standard can therefore be removed from the PRTS station clock subsystem cost estimates, and the cost of the thermally controlled crystal oscillator used in MPRTS can be used as a replacement for the passive differential system's cost estimate.

Unlike PRTS, the passive differential system does not require network clock synchronization and therefore does not require an ATDRS transmitter. As a result, the cost of the PRTS transmitter subsystem can be eliminated from the PRTS baseline costs in forming the Passive Differential ATDRS/GPS Tracking System cost estimate. For the same reason, the cost of the diplexer in the PRTS antenna subsystem can be eliminated in estimating the cost of the passive differential ATDRS ranging signal antenna subsystem. On the other hand, neither PRTS nor MPRTS requires the GPS receiver and antenna subsystems used by the passive differential system; therefore, the cost of these subsystems must be independently determined and added to the cost of the Passive Differential ATDRS/GPS Tracking System.

D.3 PASSIVE DIFFERENTIAL LIFE-CYCLE COSTING

Figures D-1, D-2, and D-3 present the the Passive Differential ATDRS/GPS Passive Differential Tracking System life-cycle costing estimates. The overall system cost shown in Figure D-1 is divided into two parts: a ground segment and the associated operations and maintenance costs. Decomposition of these parts into recurring and nonrecurring costs is performed to identify contributions due to each component within the system specifications.

The costing is broken down into tree structures for organizational purposes. Blocks within the figures' illustrated tree structures contain cost estimates required to reach that level of development or to provide a degree of service. Where appropriate, the blocks contain two sets of numbers. Each number represents a cost in thousands of dollars for the item indicated by the block. The left-hand numbers represent the nonrecurring costs, and the right-hand

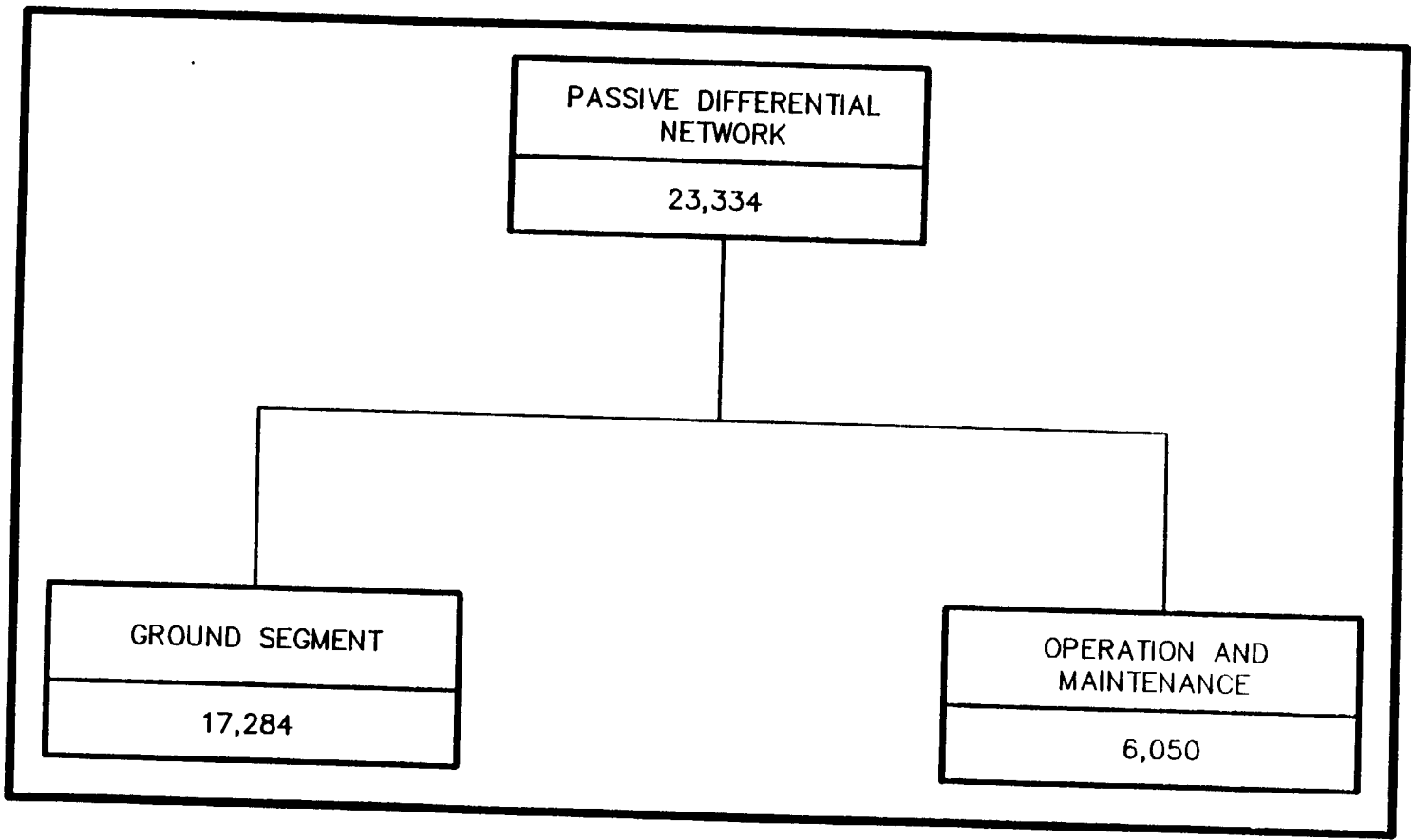

Figure D-1. Passive Differential ATDRS/GPS Tracking System Life-Cycle Costing (in Thousands, Based on 1988 Dollars)

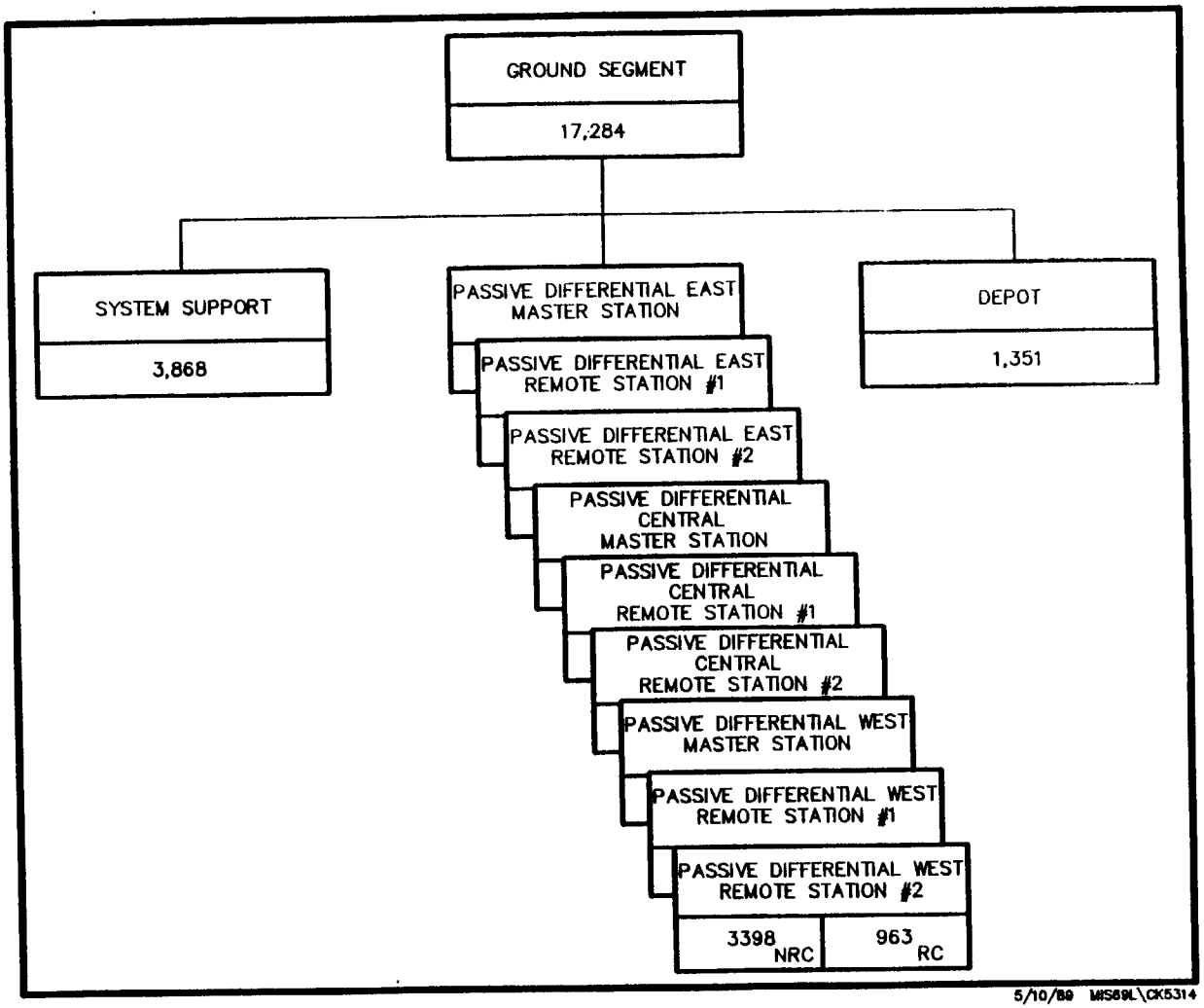

Figure D-2. Ground Segment Costing (in Thousands, Based on 1988 Dollars)

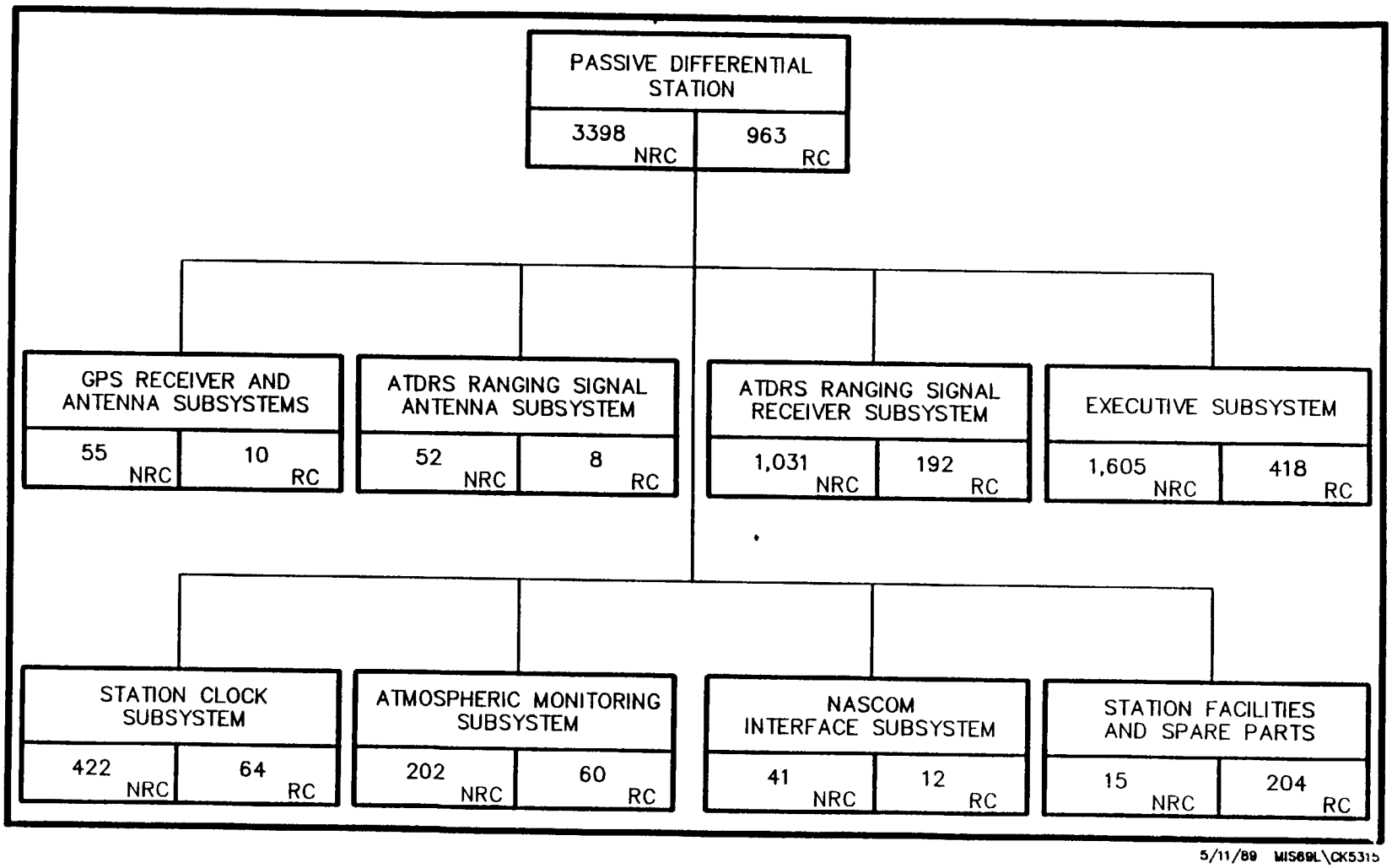

Figure D-3. Passive Differential ATDRS/GPS Tracking System Station Costing (in Thousands, Based on 1988 Dollars)

numbers are the recurring costs. Multiple blocks (N in number) are used in Figure D-2 to make up a node on that tree. The total cost of this node is found by adding the nonrecurring cost to N times the recurring cost.

The ground segment breakdown shown in Figure D-2 comprises design, development, procurement, and installation of all equipment, software, and facilities required to field the Passive Differential ATDRS/GPS Tracking System and interface fully with ATDRSS. The ground segment is broken down to the module level; functions are specifically defined, enabling a reasonable estimate of expense for these items to be made. The costs emphasize development in order to reduce risk associated with fielding a new system.

Operation and maintenance reflect the staffing and depot supplies required to sustain the Passive Differential ATDRS/GPS Tracking System over a 10-year period of operation. Staffing estimates are conservative and may be substantially reduced as computer automation and reliability technologies progress. The costs developed for the system reflect the worst case possibility of long-distance travel by the support crew, costs that could be cut by use of a CONUS-based system.

To perform the costing for the ground segment, the ground segment has been broken down into three categories: system support, a parts depot, and the nine ground stations as required for tracking of the three ATDRSS satellites. The ground stations were further divided into station subsystems, as shown in Figure D-3. Hardware and software modules for each of the subsystems were identified and pricing estimates applied for nonrecurring design and development and recurring procurement and installation of these items. After the costs for each module were determined, cost estimates for the subsystems and total ground stations were made. All the resources required to complete the system were converted to 1988 dollars for comparative purposes with the other cost estimates of this study. Two principal conversion factors were employed: the conversion of staff-years to dollars, assuming a factor of $100,000 per staff-year, and the conversion of lines of code to dollars, assuming a cost of $50 per line of source code. The remaining two categories, system support and depot stocking, have used separately developed costing rules based on the corresponding percentages of the ground station costs used in past ATDRSS life-cycle costing efforts. Those estimates themselves rely on the Air Force's unmanned spacecraft cost estimation model (Reference D-3).

Detailed breakdowns of the ground station subsystem costs shown in Figure D-3 are presented at the module level for PRTS and MPRTS in References D-1 and D-2, respectively. Costs shown in the subsystem blocks in Figure D-3 were derived using the life-cycle costing methodology of Section D.2. The costs of the ATDRSS ground station GPS receiver and antenna subsystems represent their combined procurement, installation, and testing costs.

D.4 REFERENCES

D-1. K. Cunningham, STI/TR880123, Precise Ranging and Timing System (PRTS): Life Cycle Costing, September 1988

D-2. K. Cunningham, STI/TR880124, Modified Precise Ranging and Timing System (MPRTS): Life-Cycle Costing, September 1988

D-3. Stanford Telecommunications, Inc., STI/TB880161, ATDRSS Life-Cycle Costs Architectural Summaries, Revision B, June 1988

APPENDIX E - MPRTS and AKuRS LIFE-CYCLE COST UPDATES

This appendix updates the life-cycle cost estimate for MPRTS and provides a rough order of magnitude life-cycle cost estimate for AKuRS. During the course of this study, life-cycle costs for PRTS and MPRTS were estimated independent of the costs of the ATDRSS navigation beacon and any associated ATDRSS expenses (References E-1 and E-2). Only the ground station development, deployment, and operations costs were estimated for those systems. Life-cycle costs for AKuRS were not explicitly estimated for this study, although they were indicated to be comparable to those of MPRTS.

With MPRTS and AKuRS identified as two prominent candidates for future consideration as the ATDRSS Position Location Service, the ATDRSS study group at Stanford Telecom was instructed to independently update the life-cycle cost estimates for those two systems. In general, the ATDRSS study group relied upon the MPRTS life-cycle cost estimates (Reference E-2) but additionally included the costs of modifying the ATDRSS ground and space segments to support the navigation beacon. Cost estimates were converted from 1988 dollars to 1987 dollars to maintain compatibility with other ATDRSS cost estimates. Life-cycle costs for AKuRS were later developed in a similar manner, using the MPRTS equipment cost estimates to substitute for explicit AKuRS estimates. The following sections outline the ATDRSS study group's findings for MPRTS and AKuRS life-cycle costs.

E.1 MPRTS LIFE-CYCLE COSTS

The costs of the MPRTS ground stations and their operational requirements have been estimated in detail (Reference E-2), but, as noted above, impacts to ATDRSS were not explicitly costed nor were the estimates made consistent with other ATDRSS cost estimates. As assumed through this study, three MPRTS master stations and six MPRTS remote stations are assumed to be in CONUS, with one master and two remote stations supporting each of the three on-orbit ATDRSS satellites. Each ATDRSS space-to-ground link terminal (ASGLT) is interconnected to one of three selectable MPRTS master stations. The MPRTS cost estimates are summarized in Figure E-1, showing the results for two distinct options: with or without the provision of a dedicated return channel to support the return path of the MPRTS two-way measurement.

	FY 87 ($M)					
	SPACE SEGMENT	GROUND SEGMENT	15 YEAR OPS	UST	TOTAL	% Δ TO REF. ARCH.
REFERENCE ARCHITECTURE Z-BAND = Ka	2,600.6	440.7	584.6	--	3,625.9	--
MPRTS* ENHANCEMENT	**Δ TO REF. ARCH.**					
ALTERNATIVE 1: WITHOUT DEDICATED RETURN CHANNEL	10.9**	14.7	5.3	--	30.9	+0.9
ALTERNATIVE 2: WITH DEDICATED RETURN CHANNEL	15.6**	24.8	5.3	--	45.7	+ 1.3%

20QM3/AJ/021/6-19-89

* MPRTS = MODIFIED PRECISE RANGING AND TRACKING SYSTEM
** ASSUMING S-BAND BEACON IS IN BASELINE

Figure E-1. ATDRS MPRTS Enhancement LCC Impact Summary

If no dedicated return path is provided, the MPRTS return signal would be supported by existing ATDRSS S-band return services, most likely the SMA return service. No additional cost is then involved, although the required MPRTS contacts may adversely affect ATDRSS user services. MPRTS ground segment and operations costs were previously estimated at $19.1 million; here, an estimate of $20 million is obtained where the difference is due to the change from 1988 to 1987 dollars, the extension of operations from 10 to 15 years, and other minor variations.

Assuming an S-band beacon is already part of the baseline ATDRSS space segment costs, the additional cost due to use of the PRTS signal structure in MPRTS is estimated to be $10.9 million. This cost was not previously estimated for MPRTS and reflects the need for additional channels and the associated hardware to support the multichannel PRTS signal structure. The resultant total cost of MPRTS is then shown to be $30.9 million, representing an increase of 0.9 percent to the ATDRSS reference architecture as of April 1989.

If a dedicated MPRTS return channel is provided, the associated costs in both the ATDRSS space and ground segments increase. The dedicated MPRTS return channel is assumed to be supported by a receiver diplexed on the beacon antenna, with additional down converters and receiver chains provided at the ground segment. The increased costs result in a total MPRTS cost of $45.7 million, a 1.3 percent increase above the reference architecture's cost.

Additional supporting data for the ATDRSS study group's MPRTS cost estimates are shown in Figures E-2 through E-5. Figure E-2 gives the incremental space segment weight, power consumption, and costs associated with the two MPRTS options; Figure E-3 summarizes the incremental ground segment costs associated with support of a dedicated MPRTS return channel; Figure E-4 documents the MPRTS operational costs; and Figure E-5 summarizes the ATDRSS spacecraft subsystem costs using the cost estimation relationships (CERs) of the U.S. Air Force's Space and Missile Systems Organization (SAMSO) unmanned spacecraft cost model (USCM).

E.2 AKuRS LIFE-CYCLE COSTS

Cost estimates for AKuRS have been determined by the ATDRSS study group through comparison with MPRTS. As discussed in Section 3 of this study, the AKuRS ground stations are roughly comparable to those of MPRTS: both systems rely

	ADDED WT (LBS)	ADDED PWR (W)	FY87 ($M) NREC	REC
ALTERNATIVE 1:				
0 MPRTS NAV BEACON	32	53	0.7	1.7
		1ST ATDRS	-	2.4
		REC X 5 ADD'L ATDRS	-	8.5
		TOTAL		10.9
ALTERNATIVE 2:				
0 MPRTS NAV BEACON	32	53	0.7	1.7
0 MPRTS RETURN CHANNEL	9	17	0.5	0.7
		S/TOTAL	1.2	2.4
		1ST ATDRS	-	3.6
		REC X 5 ADD'L ATDRS	-	12.0
		TOTAL		15.60

Figure E-2. Space Segment Cost Overview

		FY87 ($M) NREC	REC
0	ASGLT COSTS*		
	- DOWN CONVERTERS	.3	.3
	- PMMSCS EXPANSION	.1	.1
	- P/R MPRTS RCVR CHAINS (DESPREAD/DEMOD)	1.0	.1
	- DIS EXPANSION & LOCAL CABLE EXTENSION	.1	.2
	- CDCN EXPANSION	1.2	.1
		2.5	1.9
	1ST ASGLT		4.4
	REC X 3 ADDN'L		5.7
	ASGLT TOTAL		10.1
0	MPRTS STATION COSTS		14.7
			24.8

* THIS COST IS APPLICABLE FOR ALTERNATIVE 2 ONLY.

Figure E-3. Ground Segment Cost Overview

	FY87 ($M) NREC	REC
MPRTS STAFFING (6 PERSONS/YR. @ 50K/PERSON)	.3	4.5
MPRTS CONSUMABLES (.054/YR)	.054	.8
	.354	5.3

[NO ADDITIONAL OPERATIONS COST PER ASGLT FOR MPRTS ALTERNATIVE 2]

Figure E-4. Operations Cost Detail

S/C SUBSYSTEM ROM COST ESTIMATES
USING USCM ('87 $K) - REVISED CER'S

MPRTS
02/01/89

SUBSYSTEM	WEIGHT (LBS)	POWER (W)	COMPLEXITY FACTORS NR	REC	NONRECUR COST	RECURRING COST
TT&C	105	53	1	1	5601.1	5759.6
ATTITUDE CONTROL	163	114	1	1	9397.2	16603.1
STRUCTURE	1149		1	1	13698.2	3532.5
THERMAL	101	570	1	1	2358.6	2104.1
POWER	1210	50	1	1	9922.0	15467.5
PROPULSION (DRY) *	150	1	1	1		
TELECOM: ELECTRONICS	820	2088	1.15	1.16	37685.7	63825.7
TELECOM: ANTENNAS	532	125	1.05	1.22	24659.4	23619.9
SUBTOTAL	4230	3001	PLATFORM		103322.2	130912.4
MARGIN/LOSSES	141	181				
TOTALS	4371	3182	PROGRAM LEVEL		32537.3	46045.1
			S/C SUBTOTAL		135859.5	176957.5
BOL POWER	4100 WATTS					
			FEE (15%)		20378.9	26543.6
			TOTALS		156238.4	203501.1
* PROPULSION COSTS INCLUDED WITH ACS			1st UNIT COST			359739.5
			RECURRING UNIT COST			203501.1

Figure E-5. Spacecraft Subsystem ROM Cost Estimates for MPRTS

upon two-way measurements and require the development of new transponders. MPRTS transceivers would involve more signal processing hardware, but, in general, the two systems are roughly equivalent. Figure E-6 summarizes the AKuRS life-cycle cost estimates, where the ATDRSS study group has used the same ground segment and operations costs for AKuRS as for MPRTS, assuming that AKuRS uses a dedicated return channel. Unlike the situation with MPRTS, the ATDRSS reference architecture does not include the costs associated with a beacon suitable for use in AKuRS. Accordingly, space segment costs for AKuRS shown in Figure E-6 reflect the full cost of the AKuRS Ku-band beacon, estimated to be $67.0 million. The total incremental cost of AKuRS is estimated to be $97.1 million, representing an increase of 2.7 percent above the cost of the reference architecture.

Supporting data for the AKuRS cost estimates are shown in Figures E-7 through E-10. As with MPRTS, details of the space segment, ground segment, operations, and spacecraft subsystem costs are shown.

FY 87 ($M)

	SPACE SEGMENT	GROUND SEGMENT	15 YEAR OPS	UST	TOTAL	% Δ TO REF. ARCH.
REFERENCE ARCHITECTURE Z-BAND = Ka	2,600.6	440.7	584.6	--	3,625.9	--
Δ TO REF. ARCH.						
AKuRS	67.0*	24.8	5.3	--	97.1	+ 2.7%

20QM3/AJ/022/5-19-89

* INCLUDES FULL COST OF Ku-BAND BEACON

Figure E-6. ATDRSS Ku-Band Ranging System (AKuRS) LCC Impact Summary

		ADDED WT (LBS)	ADDED PWR (W)	FY 87 ($M) NREC	REC
0	AKuRS BEACON	121	350	4.7	9.6
0	AKuRS RETURN CHANNEL	9	20	0.5	0.7
		130	370	5.2	10.3
			1ST ATDRS	-	15.5
			REC X 5 ADD'L ATDRS	-	51.5
			TOTAL		67.0

Figure E-7. Space Segment Cost Overview

	FY87 ($M)	
	NREC	REC
0 ASGLT COSTS		
- DOWN CONVERTERS	.3	.3
- PMMSCS EXPANSION	.1	.1
- P/R RCVR CHAINS (DESPREAD/DEMOD)	1.0	.1
- DIS EXPANSION & LOCAL CABLE EXTENSION	.1	.2
- CDCN EXPANSION	1.2	.1
	2.5	1.9
1ST ASGLT		4.4
REC X 3 ADDN'L		5.7
ASGLT TOTAL		10.1
0 AKuRS STATION COSTS*		14.7
		24.8

* ASSUMED TO BE SAME AS MPRTS STATION COST

Figure E-8. Ground Segment Cost Overview

	FY87 ($M) NREC	REC
AKuRS STAFFING (6 PERSONS/YR. @ 50K/PERSON)	.3	4.5
AKuRS CONSUMABLES (.054/YR)	.054	.8
	.354	5.3

Figure E-9. Operations Cost Detail

S/C SUBSYSTEM ROM COST ESTIMATES
USING USCM ('87 $K) - REVISED CER'S

AKURS
04/11/89

SUBSYSTEM	WEIGHT (LBS)	POWER (W)	COMPLEXITY FACTORS NR	REC	NONRECUR COST	RECURRING COST
TT&C	105	53	1	1	5601.1	5759.6
ATTITUDE CONTROL	163	114	1	1	9397.2	16603.1
STRUCTURE	1149		1	1	13698.2	3532.5
THERMAL	101	570	1	1	2588.8	2324.1
POWER	1210	50	1	1	10890.0	16919.5
PROPULSION (DRY) *	150	1	1	1		
TELECOM: ELECTRONICS	820	2258	1.15	1.16	37685.7	64751.6
TELECOM: ANTENNAS	532	125	1.05	1.22	24659.4	23619.9
SUBTOTAL	4230	3171	PLATFORM		104520.4	133510.3
MARGIN/LOSSES	141	181				
TOTALS	4371	3352	PROGRAM LEVEL		32729.0	46330.9
BOL POWER	4500 WATTS		S/C SUBTOTAL		137249.4	179841.2
			FEE (15%)		20587.4	26976.2
* PROPULSION COSTS INCLUDED WITH ACS			TOTALS		157836.8	206817.4
			1st UNIT COST			364654.2
			RECURRING UNIT COST			206817.4

Figure E-10. Spacecraft Subsystem ROM Cost Estimates for AKuRs

REFERENCES

E-1. K. Cunningham, Precise Ranging and Timing System (PRTS): Life Cycle Costing, STI/TR880123, September 1988.

E-2. K. Cunningham, Modified Precise Ranging and Timing System (MPRTS): Life-Cycle Costing, STI/TR880124, September 1988.

GLOSSARY

ACN	Ascension Island (tracking station)
AGT	ATDRSS Ground Terminal
AKuRS	ATDRS Ku-Band Ranging System
AMS	American Samoa (tracking station)
ATDRS	Advanced Tracking and Data Relay Satellite
ATDRSS	Advanced Tracking and Data Relay Satellite System
AUS	Australia (tracking station)
bps	bits per second
BRTS	Bilateration Ranging Transponder System
C/A	clear acquisition
CDP	Crustal Dynamics Project
CEI	connected element interferometer
cm	centimeter
CONUS	continental United States
C_R	solar radiation pressure coefficient
CSNR	coherent signal-to-noise ratio
dB	decibel
dBW	decibel watts
DVLBI	differenced very long baseline interferometry
EIRP	effective isotropic radiated power
f	frequency
FDF	Flight Dynamics Facility
FET	field effect transistor
FTE	full-time equivalent
Gbits	gigabits
GEM	Goddard Earth model
GHz	gigahertz
GM	gravitational constant

GPS	Global Positioning System
GSFC	Goddard Space Flight Center
GSTDN	Ground Spaceflight Tracking and Data Network
GT	ground terminal
G/T	gain/noise temperature
GWM	Guam (tracking station)
HAW	Hawaii (tracking station)
HOW	handover word
HPA	high-power amplifier
Hz	hertz
IF	intermediate frequency
I-O	interoperability
k	degrees kelvin
kB	kilobyte
kbps	kilobits per second
kg	kilogram
km	kilometer
KSA	Ku-band single access
LNA	low-noise amplifier
m	meter
MA	multiple access
Mb	megabits
MB	megabytes
Mbps	megabits per second
MHz	megahertz
MIL	Merritt Island (tracking station)
mm/sec	millimeters per second
MPRTS	Modified Precise Ranging and Timing System
MTTR	mean time to repair
mu	µsec
NASA	National Aeronautics and Space Administration
Nascom	NASA Communications Network
NCC	Network Control Center
NRAO	National Radio Astronomy Observatory

NRZ	nonreturn to zero
ns	nanosecond
OD	orbit determination
ORAN	Orbit Analysis Program
OSC	Optimal 21-Satellite Constellation
phasecal	phase calibration
PN	pseudorandom noise
PPS	Precise Positioning Service
PRTS	Precise Ranging and Timing System
ps	picosecond
PSC	Primary Satellite Constellation
REY	Reykjavik, Iceland (tracking station)
RF	radio frequency
rms	root mean square
SA	single access
SBIR	Small Business Innovative Research
sec	second
SGL	space-to-ground link
SMA	S-band multiple access
SNR	signal-to-noise ratio
SQPN	staggered quadriphase pseudonoise
SPS	Standard Positioning Service
SSA	S-band single access
STGT	Second TDRSS Ground Terminal
STI	Stanford Telecommunications, Inc.
TBS	to be supplied
TDAS	Tracking and Data Acquisition System
TDRS	Tracking and Data Relay Satellite
TDRSS	Tracking and Data Relay Satellite System
TLM	telemetry
TR	trajectory recovery
TT&C	Telemetry, Tracking, and Command

TWTA	traveling wave tube amplifier
USNO	U.S. Naval Observatory
VAN	Vandenberg AFB, CA (tracking station)
VLA	Very Large Array
VLBA	Very Long Baseline Array
VLBI	very long baseline interferometry
W	watt
WAS	Richland, Washington (tracking station)
WHS	White Sands, New Mexico (tracking station)
WSGT	White Sands Ground Terminal
ZA	zenith angle